ERDC/CHL TR-03-X

Coastal and Hydraulics Laboratory

DRAFT

US Army Corps of Engineers®
Engineer Research and Development Center

Savannah Harbor Entrance Channel: Nearshore Placement of Dredged Material Study

July 2003

By: Joseph Z. Gailani, S. Jarrell Smith, Layla Raad, Bruce A. Ebersole

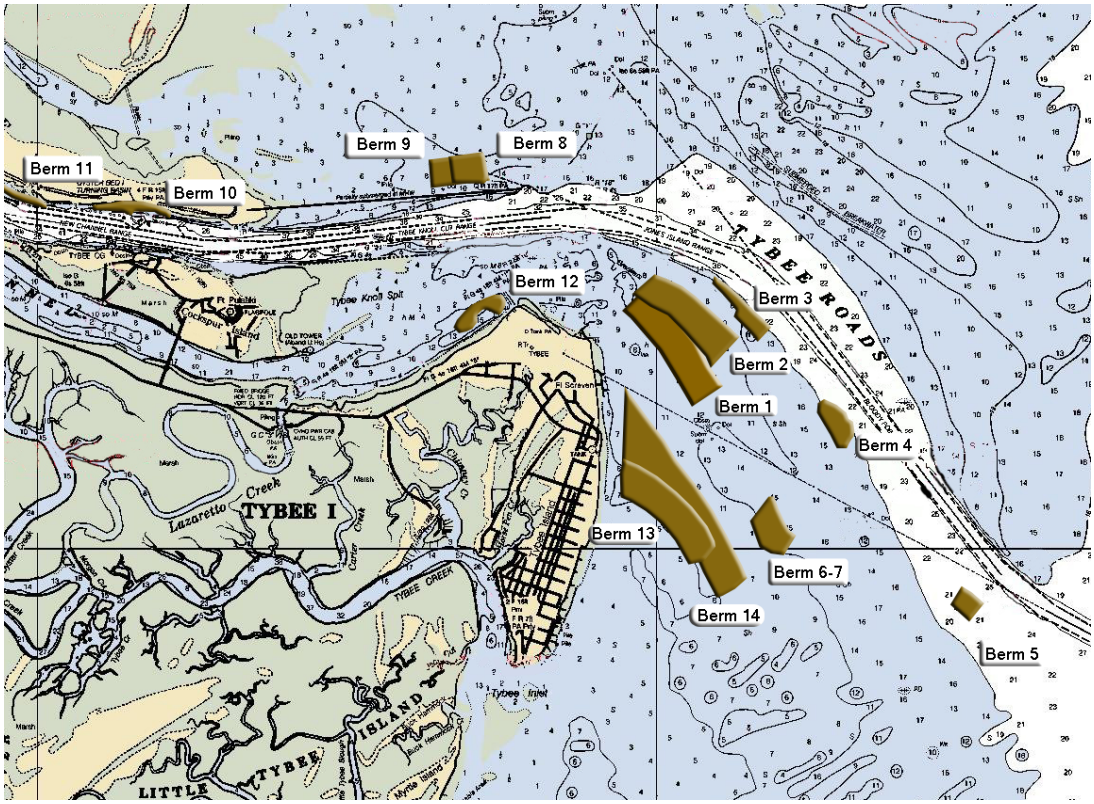

~~Approved for public release; distribution is unlimited~~.

Contents

1 Introduction

Background

The Savannah River serves as the boundary between South Carolina and Georgia for much of their common border. Much of the lower River is divided into north and south channels. The river flows directly into the Atlantic Ocean, not into a bay or sound. The Savannah River Entrance is an important commercial waterway. Nearest the coast, the main navigation channel is in the river's north channel (Figure 1).

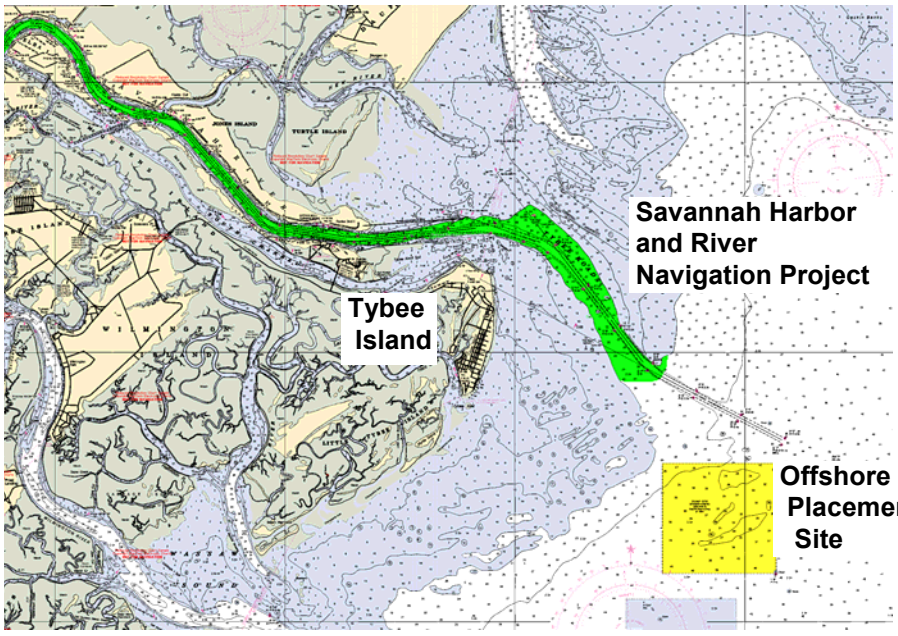

Figure1. Map of Savannah River Entrance, Lower Portions of the Federal Navigation Project, and Tybee Island

The coast and ebb shoal complex at the Savannah River Entrance is a network of rivers, creeks, marshlands and islands. Significant wetting and drying of the marsh occurs during the approximately 2 m tidal range. The wetlands and associated creeks add additional sources of sediment and energy to this complex ebb shoal system. Contributions to the ebb shoal are made not only by the Savannah River, but also by Tybee Creek, which borders Tybee Island on its south side, the creeks draining Turtle and Daufuskie Islands to the north, and

Calibogue Sound, which has its main entrance channel north of the Savannah River Entrance (visible at the top of the figure). The community of Tybee Island is on the south side of the river mouth and unpopulated Oyster Bed Island is on the north side of the River, immediately adjacent to the river.

The area between the coast and ebb shoal is broad and relatively flat. Water depths are generally less than 4 m except near the channel. The south attachment bar of the ebb shoal intersects Tybee Island approximately half way down the island, south of the channel. The north attachment bar is on Hilton Head Island, SC well north of the channel. Evolution of the ebb shoal attachment bar at Tybee Island over the last century is provided in Oertel et al (1995) and reviewed briefly in Chapter 4.

The Savannah River Entrance Channel (or Bar Channel) dredged through the river's ebb shoal is approximately 19 km long, starting in a west/northwest direction offshore of the Savannah River ebb shoal, turning northwest as it cuts through the ebb shoal and Tybee Roads and then turning west at the entrance to the River. At the River mouth, the entrance channel is protected from shoaling by a north jetty that protects it from longshore transport. The north jetty/training wall is slightly less than 4 km long. The partially submerged south jetty is approximately 2.5 km long and protects the channel from shoaling generated by sediment exiting the south channel of the river. Fort Pulaski, which includes a tide gage, is near the land terminus of the south jetty. From the landward end of the north jetty, it is over 20 km to the city of Savannah and Savannah Harbor. A review of the development of the channel over the past century is provided in the Draft Savannah Harbor Beach Erosion Study (ATM, 2001).

Dredging is required annually to maintain the Bar Channel to the Federally authorized channel depth of 44 ft. Much of the dredging occurs on Tybee Roads, where longshore transport from the north fills the channel with a predominately sandy material. This is mixed with fine-grained sediment transported by the river. The U.S. Army Engineer District, Savannah (SAS), which oversees the Savannah Harbor and River Federal Navigation Project, has been investigating alternate disposal locations to place the estimated 500,000 yd^3/yr dredged annually from the ebb shoal navigation channel. This material is predominately sand, but is not considered beach quality because of the 12-30% fine content. In addition, SAS is preparing to dredge $1.3x10^6$ yd^3 of advance maintenance material that will be almost all pure sand.

Typical dredging practice has included offshore placement of ebb channel material. This process isolates the material from the regional sediment system. Placement within the littoral zone would keep some of the material within the coastal sediment system and could provide benefit to adjacent beaches. The goal of this study is to identify and evaluate nearshore placement alternatives that represent reasonable cost alternatives while providing benefit to the littoral system. Included among the disposal site options are several sites between the ebb shoal channel and Tybee Island shoreline. All ebb shoal dredged material is considered acceptable for open-ocean placement without management according to the procedures outlined in the "Evaluation of Dredged Material Proposed for Ocean Disposal – Testing Manual".

At the request of SAS, the U.S. Army Engineering Research and Development Center, Coastal and Hydraulics Laboratory (CHL) conducted studies that involved use of numerical models to characterize water level, current, and wave conditions in areas being considered for nearshore placement; and using the models, identified sediment pathways around the Savannah Harbor Entrance Channel and the surrounding ebb shoal. Specifically, CHL was tasked with preparing recommendations for nearshore placement of dredged material. Of specific interest is nearshore placement that maximizes benefit to the littoral system and the beaches along Tybee Island. Concerns with nearshore placement include increased nearshore turbidity during and after placement, movement of the dredged material back into the navigation channel, and influence of a nearshore berm on adjacent shorelines. The conclusions of this study will assist SAS in developing a Dredged Material Management Plan (DMMP) for the Savannah Harbor and River Federal Navigation channel and will assist the district in developing methods for utilizing dredged material beneficially within the context of a Regional Sediment Management (RSM) plan for the Savannah River/north Georgia coastline.

Study Objectives

The primary objectives of this study are:

1. Develop, calibrate, and apply a fine-grid hydrodynamic model of the Savannah River Entrance Channel and the surrounding ebb shoal and coast.
2. Develop and apply a fine-grid wave model to simulate transformation of offshore waves over the entire ebb shoal.
3. Simulate dredged material mound movement in the nearshore and lower river regions
4. Develop methods for assessing sediment pathways in the region between Tybee Island and the channel
5. Predict magnitude of turbidity during the dredging and placement operations
6. Provide guidance and recommendations for nearshore placement for feeding sand to the littoral system and beach, while minimizing re-handling (dredged material re-entering the channel), and minimizing any adverse impact on adjacent shorelines

Study Approach

Meetings between ERDC and SAS staff were used to develop project goals and an initial scope of work (SOW) covering areas of interest to the district. The original SOW included study of offshore placement sites and a few nearshore mound locations. As the study progressed, goals were modified to meet evolving questions and the focus was placed on nearshore placement for maintaining dredged material in the littoral zone/beach area.

Current and wave conditions expected during placement operations, i.e., typical non-storm wave and tidal conditions, and active high-energy (storm) periods are critical for evaluating all locations being considered for placement. Therefore, as part of this project, SAS requested a comprehensive review and

modeling of current and wave conditions across the ebb shoal as well as current conditions in the river and around the jetties. In addition, sediment properties of the dredged material must be assessed for transport predictions. The dredged material is a mixture of sand, silt, and clay. Some of these mixed sediments will behave as non-cohesive sand, but some material will display cohesive properties. Erosion, transport and dispersion properties of cohesive material depends on multiple factors, including grain size distribution, mineralogy, pore water chemistry, organic content, bulk density, and other factors. Although these bulk properties are easily assessed, there are no theoretically valid methods available to accurately quantify sediment transport processes based on the sediment properties for mixed cohesive sediments. Therefore, a second part of this study was laboratory testing of sediments collected on site to quantify the erodability and transport characteristics of the dredged material (expected maintenance material). The third part of this study was assessing placement options for maintaining the material in the littoral system. The final part addresses turbidity due to dredging and placement operations.

The remainder of this section briefly describes each of the study components.

a. ADCIRC modeling of tidal circulation, wind-driven currents, and storm surge. The ADvanced CIRCulation (ADCIRC) model (Luettich et al, 1992) was used to generate tidal currents, wind driven currents and storm surges needed for the for the sediment transport and wave models. ADCIRC is a two-dimensional, depth-integrated, finite element, ocean circulation model that has been proven to accurately simulate tidal and storm conditions in near-shore regions. ADCIRC-predicted velocities and water levels were used to develop storm and non-storm hydrodynamic conditions in the river and on the ebb shoal. The ADCIRC modeling effort is described in Chapter 2. The accuracy of the model was evaluated using available tidal data at Fort Pulaski, in Tybee Creek, and offshore. In addition, current data provided by ATM, which were collected using an Acoustic Doppler Current Profiler (ADCP) (ENSR, 1999) were used to evaluate the model.

b. STWAVE modeling of wave transformation over the ebb shoal. Databases exist for offshore wave conditions near Savannah (Brooks and Brandon, 1995), produced by the U.S. Army Corps of Engineers Wave Information Studies (WIS). These data reflect conditions well offshore of Tybee Island, in deeper water, and do not accurately reflect conditions in shallower water. Also, wave transformation over a complex channel/ebb shoal region cannot be predicted using simple refraction and shoaling equations because the bottom bathymetry is so irregular. Therefore, the STWAVE model was applied over the entire ebb shoal to predict wave refraction and shoaling, and to characterize wave conditions at the potential nearshore placement sites and along Tybee Island. The offshore WIS wave data were used to define the offshore boundary conditions needed as input by STWAVE. A two-step STWAVE modeling approach was adopted, using nested grids, in light of the wide shelf seaward of the ebb shoal and the complexity of the bathymetry. The STWAVE model was also used, along with the GENESIS shoreline change model, to investigate the potential impacts of a nearshore berm on local wave transformation, longshore sand transport processes, and shoreline change.

c. Sediment properties analysis. Historical data available from dredging records and previous studies were used to estimate grain size distributions, dredging volumes, and ebb shoal evolution. These data provide significant information on the ebb shoal and channel processes which can be used as input to transport models and to verify transport model results. As stated previously, site-specific cohesive sediment erosion tests were required to understand critical stresses for initiation of transport and transport rates of mixed dredged material. These experiments involved applying an erosion-testing flume, SEDFLUME (McNeil et al, 1996), to examine erodability of dredged material collected from various stretches of the channel. The erosion data are then used to develop site-specific erosion algorithms that are incorporated into the sediment transport models. The algorithms define sediment erosion rates as a function of bulk density, shear stress, and depth of burial. Algorithms were developed for each stretch of channel, for which sediments were acquired and tested.

d. Modeling of mound erosion and sediment pathways. The GTRAN model was used to simulate mound erosion at each proposed nearshore and riverine mound during storm and normal hydrodynamic conditions. The cohesive sediment erosion algorithms were incorporated into GTRAN and erosion from various mound configurations was simulated. In addition, a mesh of points was established between the channel and Tybee Island. Sand erosion magnitude and direction time series were developed at each point to assist in determining sediment pathways. This provided needed information for assessment of various nearshore placement locations. Hydrodynamic and wave time series required to estimate transport were developed from ADCIRC and STWAVE simulations.

e. Modeling of dispersion of material during dredging and placement operations. A significant amount of fine material is stripped from the sediment/water mixture during dredging and placement. This material is free to move through the water column. Transport of material released during the dredging process was modeled using the SSFATE model (Clarke ****). Various dredging methods, sediment types, dredging rates, and loss rates were simulated to provide a comprehensive understanding of sediment plume concentration and migration. In addition, the D-CORMIX model was used to predict loss of sediment during a pipeline placement operation. Placement is especially a concern in the nearshore where released sediment could migrate toward the beach.

2 Wave Transformation Modeling

Waves influence sediment transport along the Tybee Island shoreline and also over the ebb shoal where nearshore placement of dredged material is being evaluated. The sediment transport models described in Chapter 4 require temporal and spatial descriptions of the nearshore wave climate to make sediment transport estimates. Representative and long-term wave conditions were extracted from the Wave Information Study (WIS) 1976-1995 hindcast (Brooks and Brandon, 1995) and these conditions were transformed from the offshore hindcast station to the nearshore through the STeady-state spectral WAVE model (STWAVE). Nearshore wave conditions were extracted for point sediment transport modeling and shoreline change modeling described in Chapter 4.

STWAVE

STWAVE (Resio 1987, 1988a, 1988b; Smith et al. 2001) is a half-plane, phase-averaged, spectral wave transformation model. STWAVE simulates depth-induced refraction and shoaling, current-induced refraction and shoaling, depth- and steepness-induced wave breaking, wave growth from wind input, non-linear wave-wave interactions, and energy dissipation due to white capping. Assumptions applied in the governing equations include 1) mild bottom slope and negligible wave reflection, 2) spatially homogeneous offshore wave conditions, 3) steady-state waves, currents, and winds, 4) linear refraction and shoaling, 5) depth-averaged current, and 6) bottom friction is neglected.

STWAVE has been successfully compared to field and laboratory measurements of wave transformation over ebb shoals and near tidal inlets (Smith and Smith 2002, Smith and Harkins 1997, and Cialone and Kraus 2002.)

Model Application Near Savannah River Entrance

Waves were transformed from WIS sta 33 to the nearshore through a nested grid approach. Support of grid nesting in STWAVE was recently developed as described by Smith and Smith (2002). Waves are transformed from the offshore over a typically coarse “parent” grid and the transformed wave spectra are saved along the offshore boundary of the more finely resolved “nested” grid. Nested grid simulations begin with the saved conditions from the parent grid and transform these waves over a more finely resolved grid towards shore.

The parent and nested grids for the present study are presented in Figure 2-1. The parent grid has dimensions of 36 km x 67 km with a resolution of 200 m. The nested grid covers a smaller area with dimensions of 15 km x 30 km but with finer resolution of 50 m. Bathymetry for both grids was developed from the National Geophysical Data Center's (NGDC) coastal relief model which is constructed from the National Ocean Service (NOS) hydrographic database. The coastal relief model compared favorably to the November 1997 NOAA Navigation Chart 11512 and to available survey data obtained from the Savannah District.

Winter Month Simulations

Offshore wave conditions were developed from the 20-year (1976-1995) WIS hindcast at sta 33 (Figure 3-1). For the requirements of the sediment transport study, the hindcast record was analyzed to identify statistically representative wave conditions during the winter dredging season (defined as the months of November to March). The hindcast record was analyzed to identify a mean winter month and a winter month with a two-year return interval. As the focus of the sediment transport study was on movement of mounds placed in the nearshore, a measure of wave properties more directly related to sediment transport in the nearshore was sought. Wave energy (proportional to H^2) is more directly related to bottom shear stresses and was evaluated instead of wave height. Wave energy density is given by

$$\overline{E} = \frac{\rho g H^2}{8} \tag{2-1}$$

where,
ρ = density of water
g = gravitational acceleration
H = wave height.
Table 2-1 presents the monthly mean wave energy density for the 20-year hindcast.

To represent the wave conditions during dredging operations and frequently recurring wave conditions, two months of wave information were selected from the WIS hindcast (1976-1995). Operational conditions were selected as the month with average wave energy density nearest the median value for the dredging season (considered October through March). The median of average monthly wave energy density during the dredging season is 2080 J/m^2, corresponding to the month of January 1992. Similarly, the 2-year return month based on wave energy density was November 1979. Offshore wave conditions for these two months are presented in Figures 2-3 and 2-4.

Parametric spectra of TMA form (Bouws 1985) were developed for the conditions of the January 1992 and November 1979 WIS hindcast. These wave spectra were then applied to the offshore boundary of the parent grid and transformed shoreward and saved at the position of the offshore boundary of the nested grid. The spectra saved at the offshore boundary of the nested grid then served as input conditions for each berm scenario simulated in the sediment transport study (Chapter 4). Water level for the winter month simulations was obtained from simulations of the same period of time in the hydrodynamic model (Chapter 3) at a position on the offshore boundary.

Long-Term Wave Climate Simulations

For the evaluation of longshore transport and shoreline change effects resulting from nearshore placement of dredged material, a longer-term simulation was required. For this purpose, statistics were developed from the 20-year wave hindcast to define the wave climate at WIS station 33. The wave climate was characterized by "binning" the offshore wave conditions by wave height, wave period, and wave direction. Bin boundaries are presented in Table 2-2 and a summary of the analysis is presented in Appendix 2A. The analysis resulted in the population of 277 unique wave height, wave period, and wave direction bins.

The tide range (high-mesotidal) at the site and the shallow, complex shoal structure at the Savannah River Entrance require that water-level be considered in wave transformation. Figures 2-5 and 2-6 illustrate the influence of water level on nearshore wave conditions. Identical wave conditions were applied to the offshore boundary of the parent grid, but significant differences in nearshore wave height and wave direction are evident over the ebb shoal and the nearshore. Each of the 277 wave conditions were simulated with 3 water levels: average low tide (-1.05 m Mean Tide Level (MTL)), mean tide (0.00 m MTL), and average high tide (+1.05 m MTL). The resulting 831 wave and water-level conditions were simulated on the parent grid and saved at the offshore boundary of the nested grid. These saved spectra were then transformed across the nested grid for each of the ocean-side berm scenarios presented in Chapter 4.

Summary

To support sediment transport studies of nearshore placement of dredged material, a numerical wave transformation model was applied. The offshore wave climate was analyzed from the WIS hindcast record at station 33 offshore of the Savannah River entrance. Statistically significant months of wave conditions were selected from the 20-year hindcast record and simulated to provide nearshore wave conditions for the sediment transport study. In addition, for long-term simulations, the wave climate was binned into unique wave height, wave period, wave direction, and water level combinations to characterize the nearshore wave climate. These wave conditions were then applied to sediment transport models as described in Chapter 4.

REFERENCES

Bouws, E., Gunther, H. , Rosenthal, W., and Vincent, C.L. 1985. "Similarity of the wind wave spectrum in finite depth waves; 1. Spectral form." J. Geophys. Res., 90(C1), 975-986.

Brooks, R.M. and Brandon, W.A. (1995) "Hindcast Wave Information for the U.S. Atlantic Coast: Update 1976-1993," WIS Report 33, U.S. Army Corps of Engineers Waterways Experiment Station, Vicksburg, MS.

Cialone, M. A. and Kraus, N. C. 2002, Wave Transformation at Grays Harbor, WA with Strong Currents and Large Tide Range. Proc 4th Waves Conf., ASCE, 794-803.

Resio, D. T. 1987. ''Shallow-water waves. I: Theory.'' *Journal of Waterway, Port, Coastal, and Ocean Engineering*, ASCE, 113(3), 264–281.

Resio, D. T. 1988a. ''Shallow-water waves. II: Data Comparisons.'' *Journal of Waterway, Port, Coastal, and Ocean Engineering*, ASCE, 114(1), 50–65.

Resio, D. T. 1988b. ''A steady-state wave model for coastal applications.'' *Coastal Engineering*-1998, ASCE, New York, 929–940.

Smith, J. M., and Smith, S. J. 2002. "Grid nesting with STWAVE," ERDC/CHL CHETN I-66, U.S. Army Engineer Research and Development Center, Vicksburg, MS. http://chl.wes.army.mil/library/publications/chetn/

Smith, J. M., Sherlock, A. R., and Resio, D. T. 2001. "STWAVE: Steady-State Spectral Wave Model, user's guide for STWAVE Version 3.0," ERDC/CHL SR-01-01, U.S. Army Engineer Research and Development Center, Vicksburg, MS. http://chl.wes.army.mil/research/wave/wavesprg/numeric/wtransformation/downld/erdc-chl-sr-01-11.pdf

Smith, S.J. and Harkins, G.S. 1997. "Numerical wave model evaluations using laboratory data." *Proc., Ocean Wave Measurement and Analysis, Waves'97*, Virginia Beach, Va., ASCE, Reston, Va., 271-285.

Smith, S.J. and Smith, J.M 2001. "Numerical Modeling of waves at ponce de leon inlet, Florida." *Journal of Waterway, Port, Coastal, and Ocean Engineering*, ASCE 127 (3), 176-184.

TABLES

Table 2-1 Monthly Averaged Wave Energy Density (kJ/m^2)

Year	Jan	Feb	Mar	Apr	May	Jun	Jul	Aug	Sep	Oct	Nov	Dec	Avg
1976	2.43	2.21	1.80	1.55	1.70	1.53	0.49	2.34	0.99	2.60	1.64	2.58	1.82
1977	1.86	1.89	2.43	2.44	1.16	0.49	0.54	0.87	0.70	2.02	3.03	2.14	1.63
1978	3.32	2.09	2.06	1.31	1.33	0.94	0.80	1.00	1.95	1.89	2.24	3.00	1.83
1979	3.62	3.33	3.11	2.98	1.97	1.87	1.44	1.08	5.05	1.75	3.46	2.28	2.66
1980	2.32	1.93	3.49	2.11	0.83	1.09	0.68	1.75	1.92	2.19	2.29	2.90	1.96
1981	1.29	4.69	2.35	1.85	1.25	1.01	0.83	1.38	1.78	1.83	1.61	1.57	1.79
1982	1.18	2.86	1.81	1.68	0.78	0.83	0.64	0.62	1.22	1.78	1.92	2.16	1.46
1983	2.71	3.54	3.27	1.92	1.54	1.21	0.96	0.91	1.38	2.29	2.15	3.68	2.13
1984	3.06	2.99	2.29	1.96	1.29	0.51	1.05	0.61	4.65	1.81	4.29	1.52	2.17
1985	1.78	2.11	2.24	1.78	1.16	0.67	1.31	0.99	4.39	3.55	2.98	1.55	2.04
1986	2.42	1.30	2.61	1.16	0.92	1.27	0.68	1.07	1.85	1.65	2.86	2.95	1.73
1987	2.92	2.97	2.31	1.26	1.33	1.03	0.76	0.85	1.07	1.39	1.91	1.48	1.61
1988	1.85	1.34	1.23	0.76	0.93	0.84	1.08	1.17	1.96	1.50	1.83	0.90	1.28
1989	2.17	1.92	1.79	1.44	1.00	1.11	1.01	1.37	6.93	2.23	1.74	1.32	2.00
1990	1.53	2.72	2.02	2.25	1.27	1.10	1.48	0.95	1.62	2.53	1.51	2.46	1.79
1991	1.61	1.58	2.34	1.93	1.65	1.44	0.76	0.92	2.65	2.42	1.42	1.70	1.70
1992	2.08	1.56	2.04	1.28	0.88	0.68	0.61	0.98	1.17	1.46	2.58	1.77	1.42
1993	3.60	1.86	3.23	1.60	1.18	0.88	0.55	1.29	0.87	1.95	3.13	1.58	1.81
1994	2.06	2.30	1.94	1.27	1.20	0.79	0.71	0.87	0.78	2.27	2.31	2.72	1.60
1995	2.56	1.35	1.44	1.07	0.93	1.06	0.56	2.16	1.95	2.34	1.61	1.43	1.54
Avg	2.32	2.33	2.29	1.68	1.21	1.02	0.85	1.16	2.25	2.07	2.33	2.08	1.80

Table 2-2. Wave Climate Definition

Bin	Wave Height (m)	Wave Period (sec)	Wave Direction (deg true)
1	0.0 to 0.5	3 to 6	50.5 to 65.5
2	0.5 to 1.0	6 to 8	65.5 to 80.5
3	1.0 to 1.5	8 to 10	80.5 to 95.5
4	1.5 to 2.0	10 to 12	95.5 to 110.5
5	2.0 to 2.5	12 to 14	110.5 to 125.5
6	2.5 to 3.0	14 to 16	125.5 to 140.5
7	3.0 to 4.0	16 to 18	140.5 to 155.5
8	> 4.0	> 18	155.5 to 170.5

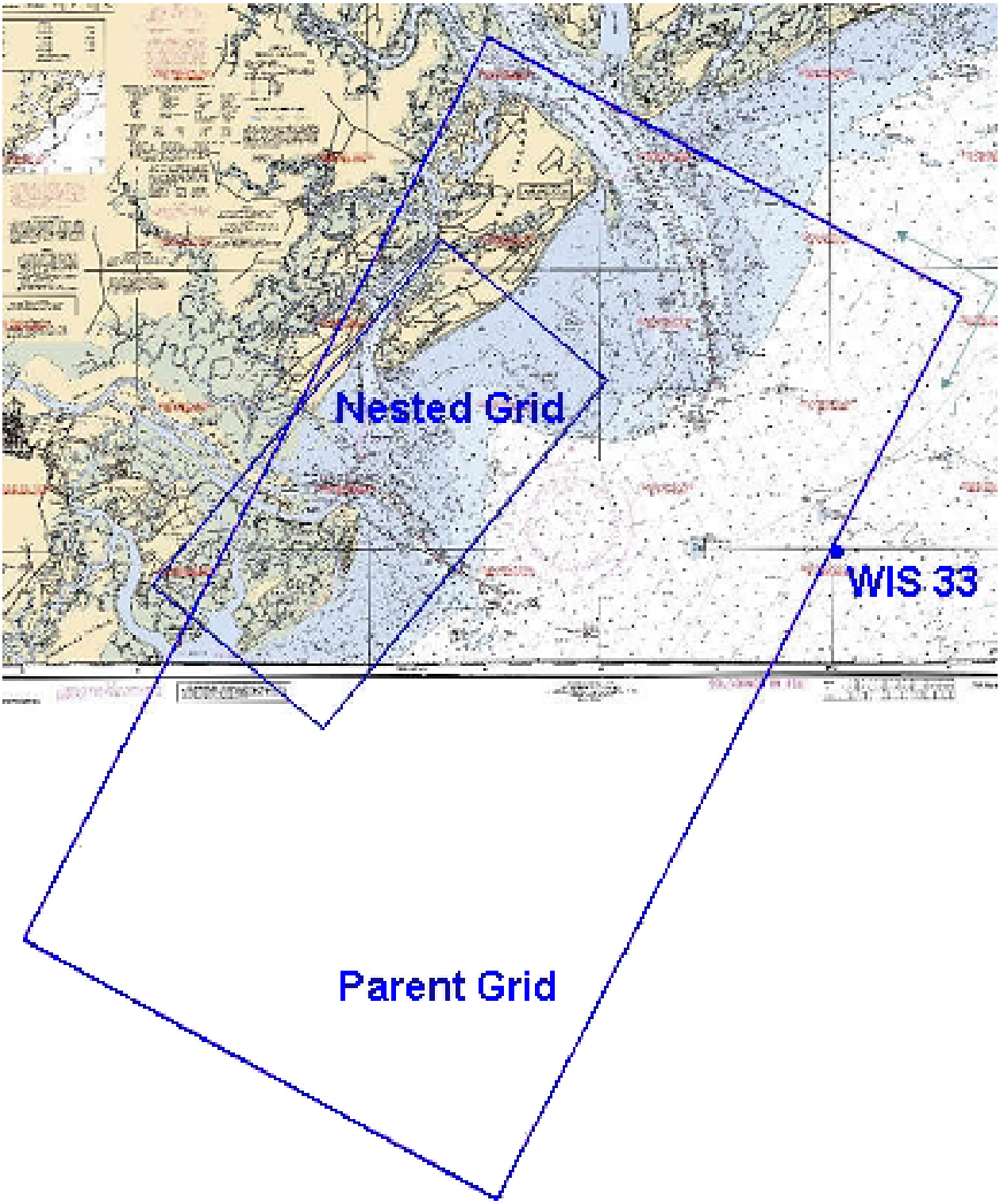

Figure 2-1. STWAVE parent and nested grid model boundaries.

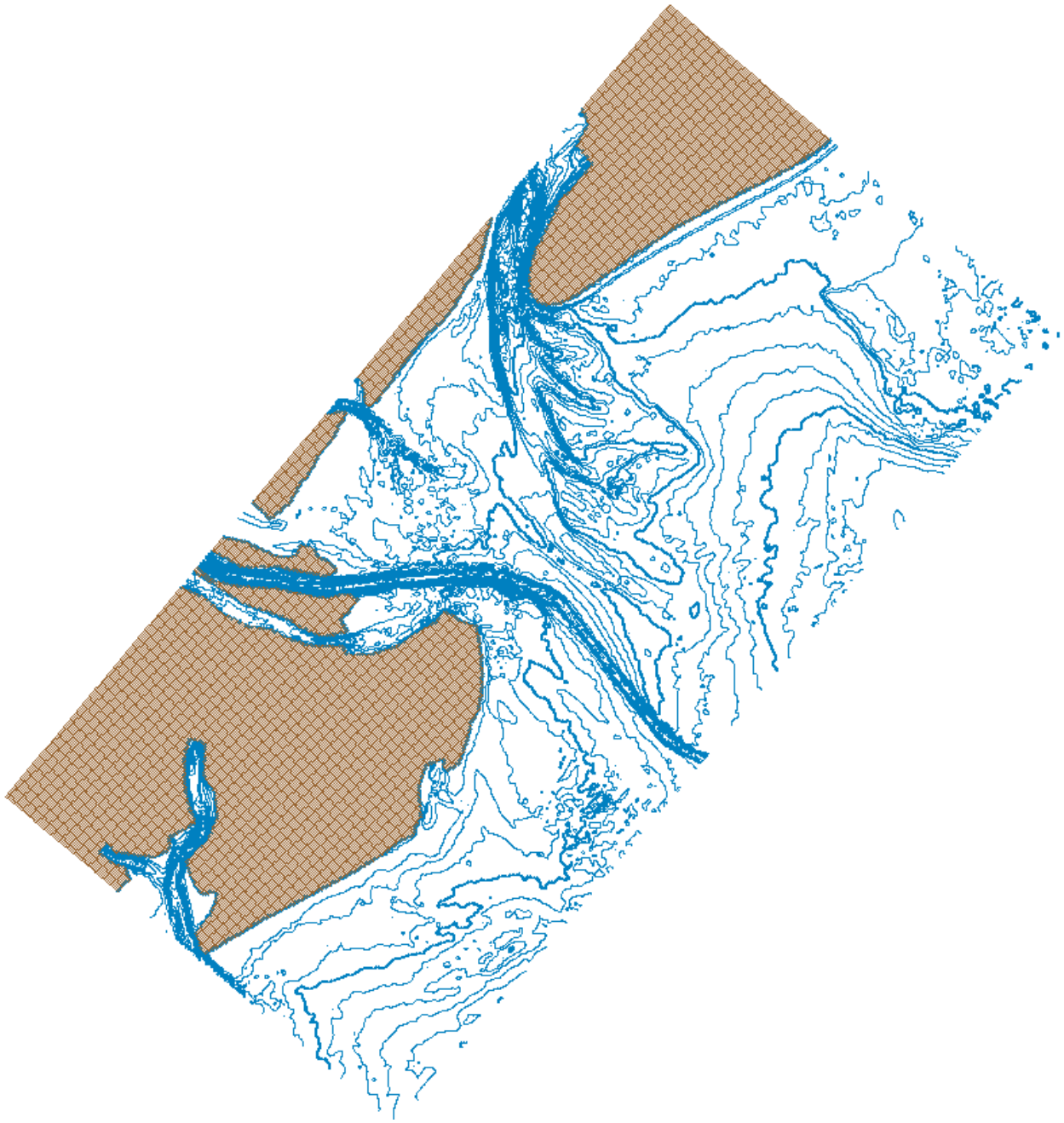

Figure 2-2. STWAVE nested grid bathymetry. Depths relative to Mean Sea Level (MSL). Contour interval 1 m and bold contours at 5 and 10-m depth.

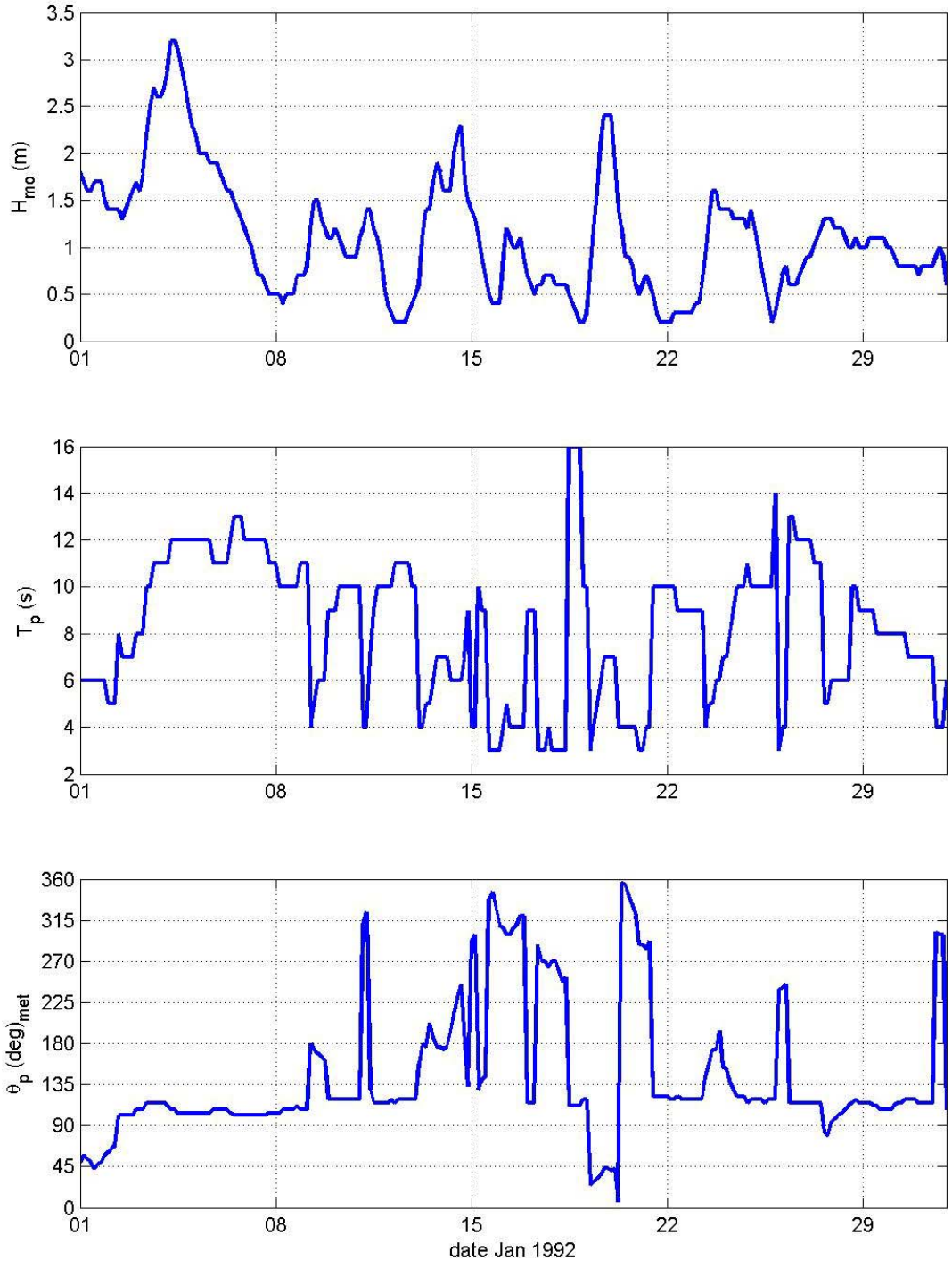

Figure 2-3. Offshore wave conditions for month of January 1992 at WIS sta 33. H_{mo} is energy-based wave height, T_p is the spectral peak period, θ_p is the meteorological-convention wave direction (direction from which waves are approaching).

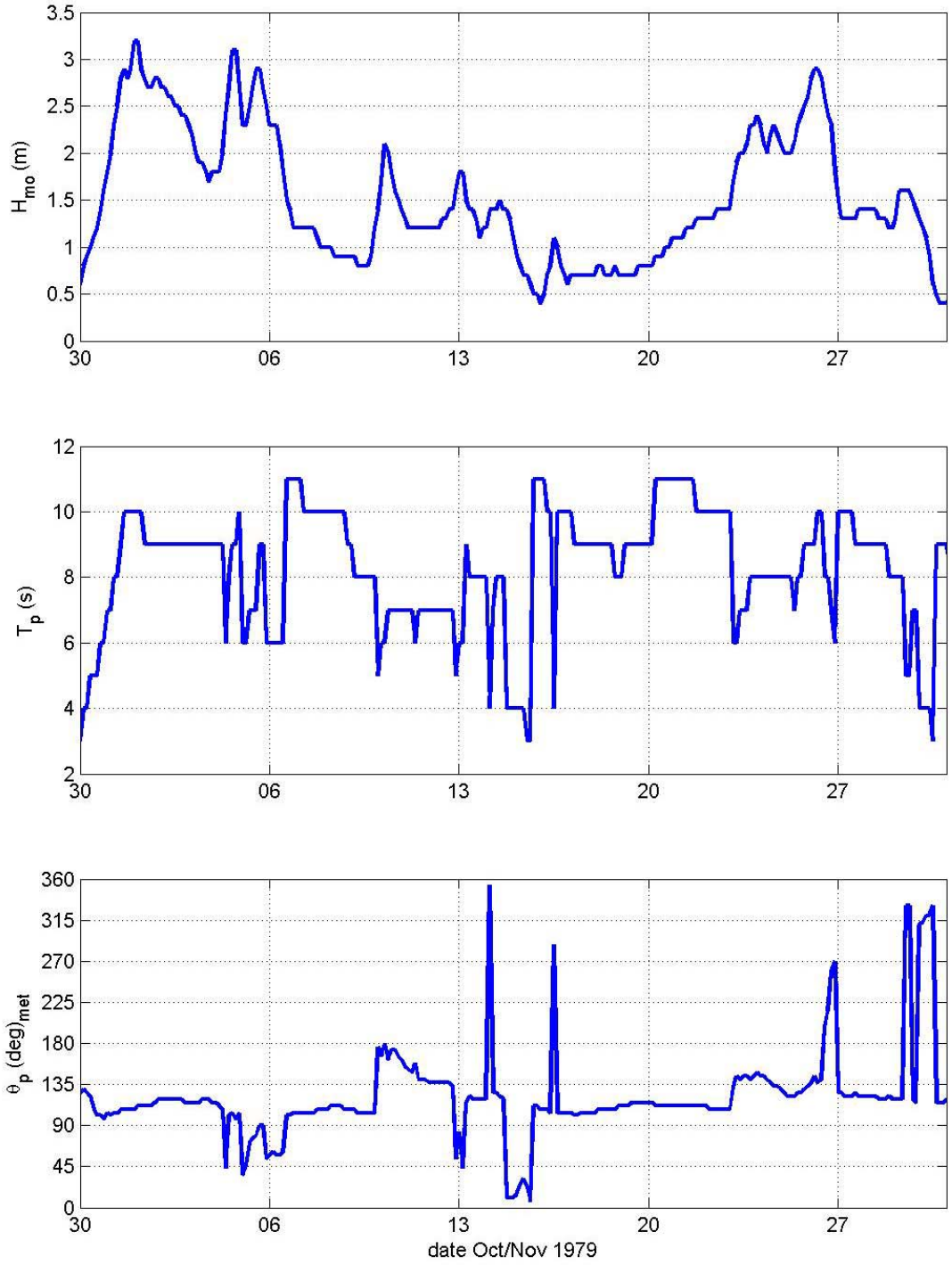

Figure 2-4. Offshore wave conditions for month of November 1979 at WIS sta 33. H_{mo} is energy-based wave height, T_p is the spectral peak period, θ_p is the meteorological-convention wave direction (direction from which waves are approaching).

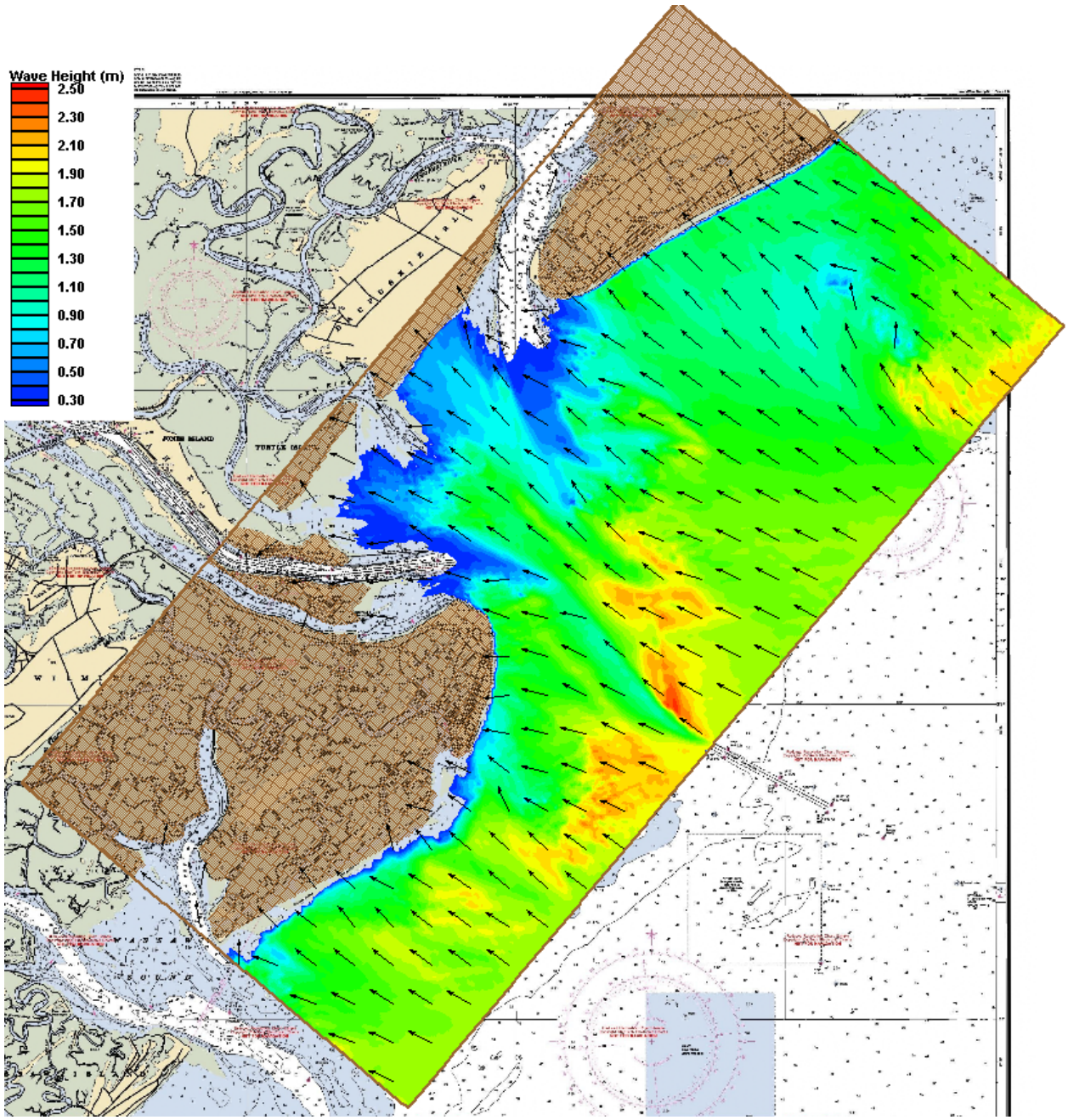

Figure 2-5. Wave transformation at mean low water over the nested grid for a frequently occurring energetic wave condition (Offshore wave conditions: H_{mo} = 1.75, T_p = 9 sec, θ_p = 118 deg true)

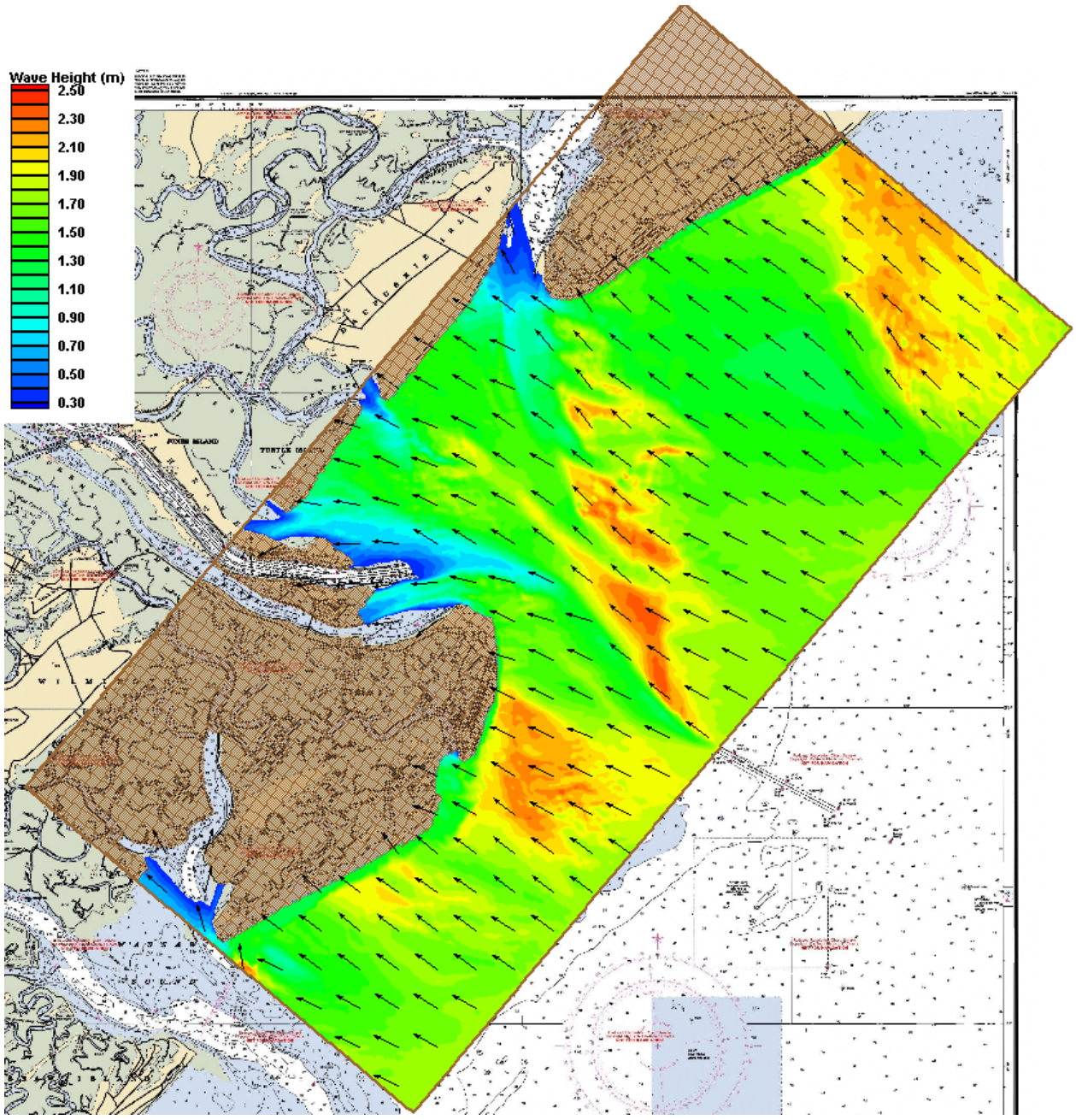

Figure 2-5. Wave transformation at mean high water over the nested grid for a frequently occurring energetic wave condition (Offshore wave conditions: H_{mo} = 1.75, T_p = 9 sec, θ_p = 118 deg true)

3 Circulation Modeling

Currents from wind, tides, and flow from the Savannah River strongly influence sediment transport near the Savannah River Entrance. Sediment transport models described in Chapters 4 and 5 require accurate representation and high spatial and temporal resolution of circulation within the study area. Because the study area is influenced by numerous, complex tidal inlets, marshes, structures, and shoals, a high-resolution finite-element mesh was developed for application with the Advanced CIRCulation (ADCIRC) model. Representative time periods for environmental conditions were selected as described in Chapter 2 and these periods were simulated with wind, astronomical tide, and river flow boundary conditions on the calibrated mesh. The resulting hydrodynamics were supplied to the sediment transport models described in Chapters 4 and 5. The areas of interest for this study are indicated in Figure 1 and defined as follows:
Nearshore disposal sites off Tybee Island: sites 1,3,4 and 5
Near Oysterbed Island and along northern jetty: site 2
Near Jones Island: site 6
Site 7 is located between the main navigation channel and Hilton Head.

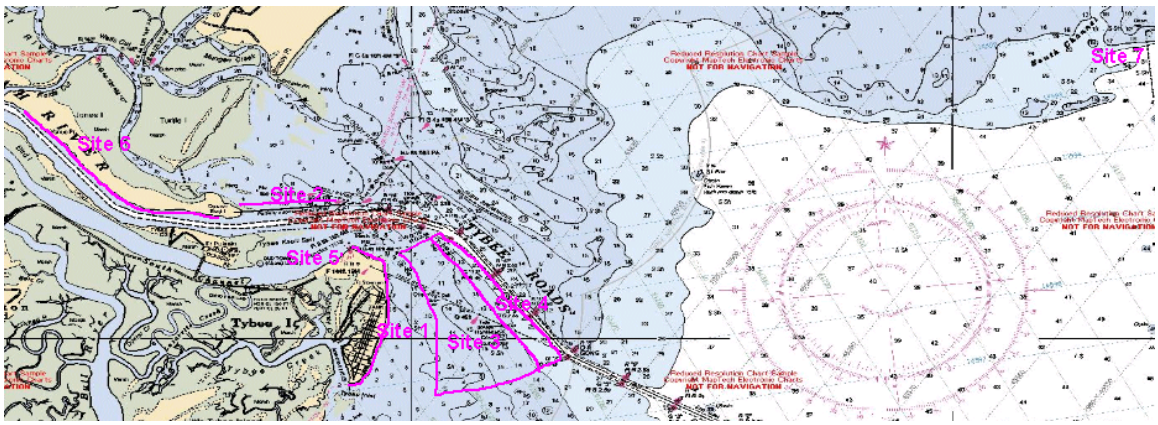

Figure 1. Potential sites for sediment placement

This task mainly consisted of applying the hydrodynamic model Advanced CIRCulation (ADCIRC) to calculate water-surface and current in the study area (Luettich, Westerink, Scheffner 1992). ADCIRC is a system of computer programs for solving time dependent, free surface circulation and transport problems in two and three dimensions. These programs utilize the finite element method in space and therefore can be run on highly flexible, irregularly spaced grids. Fine resolution can be specified in the area of interest and coarse resolution can be

specified in areas distant from the region of interest. The ADCIRC hydrodynamic model was used to simulate:

1- December 1999. December 1999 was chosen as the model calibration period. Specifications for simulations of hydrodynamics at the study area included forcing with tidal constituents, river flow, and wind.

2- One extreme storm. Hurricane Hugo, which occurred during September 14-22 1989, was chosen to represent the extreme storm. An atmospheric model was applied to compute wind and pressure fields from Hurricane Hugo.

3- One-month active period characterizes by a number of more frequent storms. November 1979 was chosen as the active period month. Specifications for simulations of hydrodynamics at the study area included forcing with tidal constituents, river flow, and wind.

4- One-month operational period that represents a typical dredging window. January 1992 was chosen as the operational month. Specifications for simulations of hydrodynamics at the study area included forcing with tidal constituents, river flow, and wind.

5- One-month summer period. July 1999 was chosen as the summer month. Specifications for simulations of hydrodynamics at the study area included forcing with tidal constituents only.

ADCIRC Domain Extent

The model domain extent was selected based on several types of information. The first consideration is the area of interest for a particular application. The domain boundaries must be sufficiently far from the area of interest so that localized inaccuracies near boundaries do not influence calculations in the study area. A second consideration for domain extent is the conditions under which the model will be run. In representing hurricanes, storm surge may be underpredicted if the domain is not sufficiently large to simulate the large-scale storm-driven processes (Militello, 1998).

The circulation model will be used to simulate extreme storm. Therefore, the study area was centered within a coastline which extended about 200 miles to accurately simulate extreme storm conditions. The coastline was chosen in a geographic range defined by longitude of 82°-79° W and latitude of 30.5°-33.5° N. Two coastlines were extracted using the National Oceanic and Atmospheric Administration (NOAA) Coastline Extractor. The first coastline is defined by longitude of 82°-79° W and latitude of 30.5°-33.5° N and its digitized shoreline coordinates were obtained from the World Vector Shoreline. To obtain more details in the study area, a refined coastline defined by longitude of 81.3°-80.7° W and latitude of 31.85°-32.6° N was obtained from the Medium Resolution Coastline. The two coastlines were merged together to represent the land boundary of the domain. The ocean boundary is created by connecting the end points of the land boundary with a half circle shape.

ADCIRC was forced with normal flow boundary at the upstream of the Savannah River where no tidal influence was detected. The tidal influence along the river was observed by examining the U S geological Survey (USGS) stations along the Savannah River and no tidal

influence was detected at the USGS Savannah Near Clyo Station. Therefore the normal flow was forced at the Savannah Near Clyo Station which is about 60 miles inland. Figure 2 shows the model domain and its boundaries.

ADCIRC Grid

The quality of the bathymetric data in grid generation plays a significant role in the accuracy of the hydrodynamic calculations. Because the bottom topography can change significantly over a relatively short time, bathymetric data collected closest to the simulation time should be incorporated in grid generation (Militello, 1998).

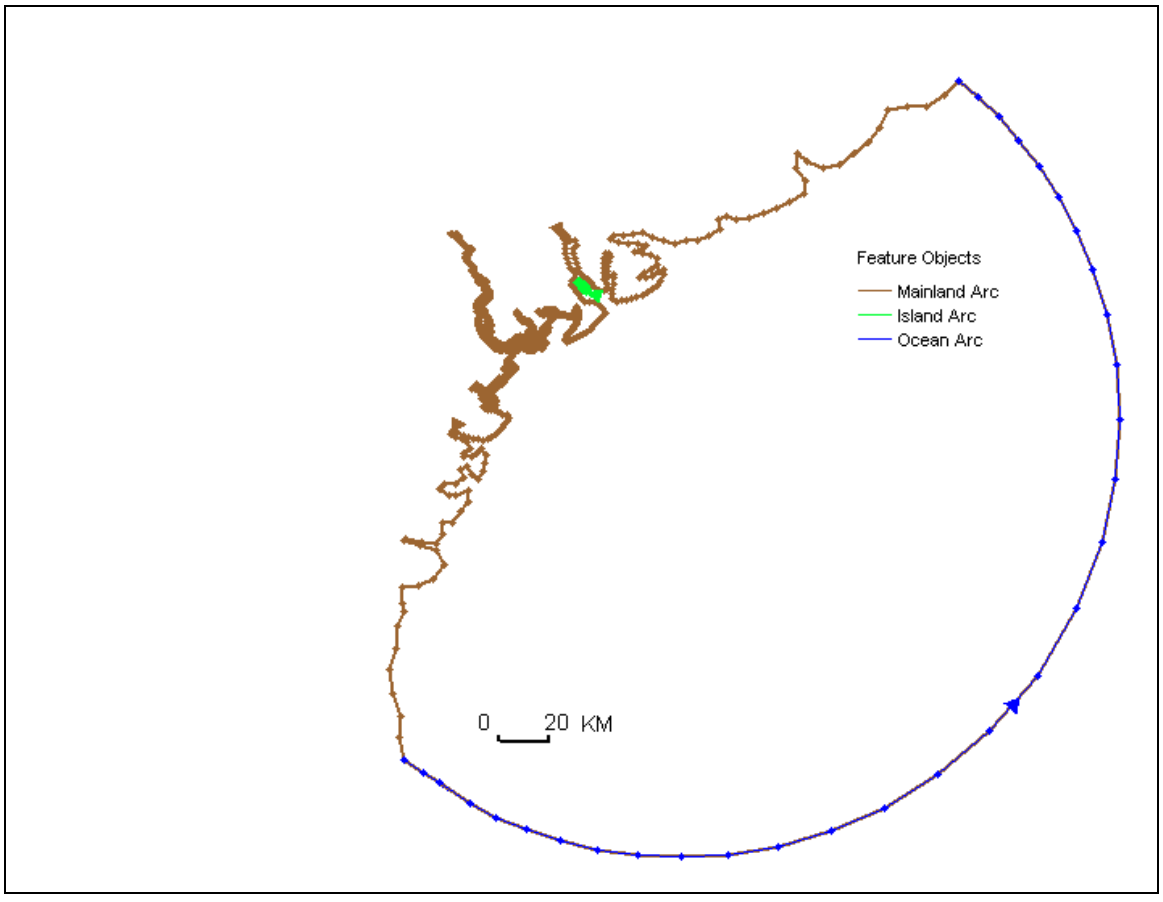

Figure 2. ADCIRC domain and its boundaries

Bathymetric data was obtained from different sources. The bathymetric data for the region defined by 31° - 40° N latitude (US Southeast Atlantic Coast) is obtained from GEOphysical Data System (GEODAS) developed by National Geophysical Data Center. GEODAS contains area

survey data from the National Ocean Service (NOS), the National Imagery & Mapping Agency (NIMA), and international sources. The GEODAS data includes bathymetric data from different time periods and some data was collected since 1930. Detailed sea and land data was obtained in the region defined by longitude of 81.3°-80.7° W and latitude of 31.85°-32.6° N. The grid cell was chosen as 6 seconds and the data was referenced to Mean Sea Level (MSL). Coarser sea bathymetric data was obtained for the region defined by longitude of 81.3°-80.7° W and latitude of 31°-32.6° N. The grid cell was chosen as 1 minute and the data was referenced to MSL.

More detailed bathymetric data collected closest to the calibration period of December 1999 were used. The bathymetric data for the main channel, south channel and Savannah River were obtained from (SAS) and the data was adjusted to the MSL vertical datum and to the NAD83 horizontal datum. The district bathymetric data was chosen closest to December 1999. The upstream portions of the Savannah River, which were not covered by SAS surveys, were extracted from NOAA Charts 11512 and 11514. The location and the elevation of the main channel jetties were extracted from NOAA Chart 11512. NOAA Chart 11512 was the 56th edition of 1999. The partially submerged northern jetty elevation was set to Mean High Water (MHW) and the southern submerged jetty was set to Mean Low water (MLW).

The region of the mesh not covered by the GEODAS data was obtained from:

- Local surveys collected between 1954 and 2000.
- NOAA Navigation Chart number 11503 for areas not covered by the local surveys.
- The Eastcoast 2001 tidal database and grid.

Grids should be coarse in the open ocean and fine resolution should be specified in the direct areas of interest. Grid resolution must be sufficient to distinguish major channels from adjacent shallower areas. Navigational channels should usually be modeled with one to three elements across the channel, depending on the level of interest in the calculated velocities within the channel. Higher resolution within the channel can be specified if details of the flow field are of interest (Militello, 1998).

Grid resolution can vary spatially, and grading between coarse and fine resolution should be done with regard to transition between element areas. A general rule is that adjacent elements should not differ in size by more than 50 percent (Donnell et al. 1996).

Areas having fine resolution in relatively deep water often dictate the maximum time-step that can be applied to achieve stability. Stability depends on the Courant number Cr given by:

$$\mathrm{Cr} = \frac{\Delta t\sqrt{gh}}{\Delta s}$$

where,

Δt = time-step
Δs = grid spacing
g = gravity acceleration
h = ambient depth

Model stability requires that Cr < 1.

Highest resolution is within the study sites and minimum node spacing is approximately 40 m in a depth of about 15 m. Therefore a time step of 2.0 sec was chosen in compliance to the Courant number. The regional grid is shown in Figure 3 with coarse resolution over the open ocean and increasing resolution toward the shore. Details of the grid for the study area and the tidal marshes around it are shown in figure 4. The adjacent elements did not change in size by more than 50 percent and the number of nodes and elements of the mesh were 29767 and 57066 respectively.

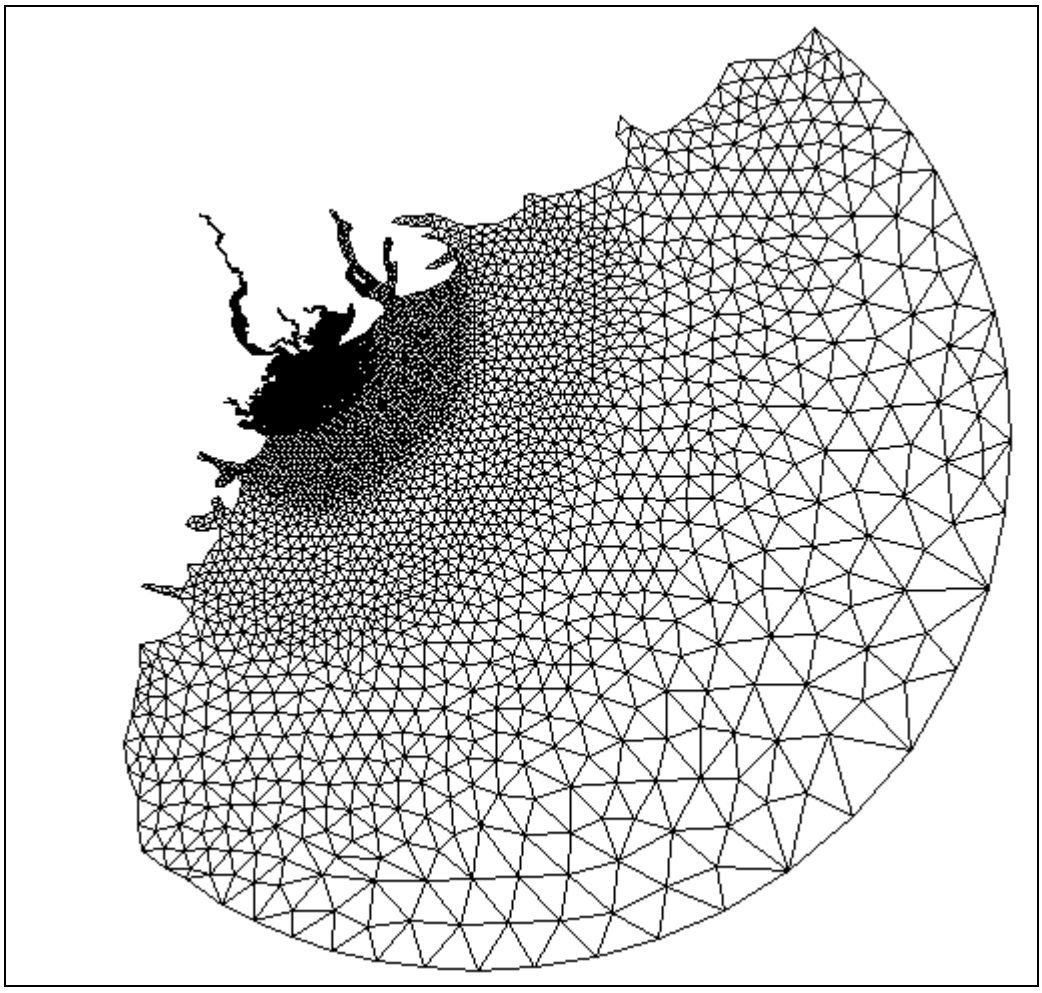

Figure 3. Regional ADCIRC grid

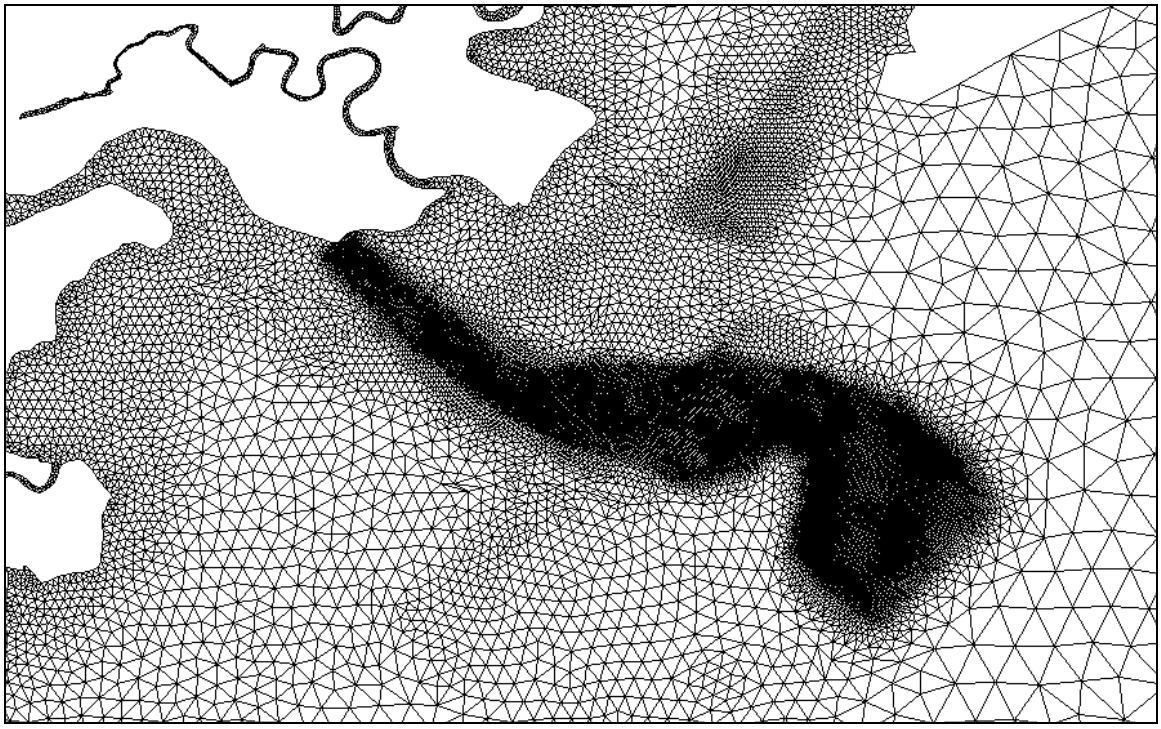

Figure 4. Details of ADCIRC grid for the Savannah area

ADCIRC Forcing Boundaries

Hydrodynamic forcing at the study area includes forcing with two types of boundaries. The first applies time series of water-level forcing constructed from astronomical tidal constituents at the open ocean boundary obtained from the Eastcoast 2001 tidal database (Mukai, Westerink, Luettich 2002). The control file specifies values corresponding to different parameters used by ADCIRC. For tidal Forces the following options were used in the control file:

- Tidal potential was set on.
- Hyperbolic tangent ramp was set on.
- K1, O1, M2, N2, S2, K2, and Q1 minor constituents were used to simulate the semi-diurnal tide.

The second applies river flow at the upstream of the Savannah River. The river flow was obtained from the USGS Savannah Near Clyo Station. Daily river flow was assumed constant during the calibration period and was distributed over the nodes along the normal flow string.

Meteorological forcing of wind speed and direction was entered to a longitude, latitude grid and interpolated in space onto the ADCIRC for the three months of December 1999, November 1979 and January 1992. Fleet numeric wind format was set on and the NWS (the parameter controlling whether wind velocity or stress, wave radiation stress and atmospheric pressure are used to force ADCIRC) was set to 3.

For Hurricane Hugo, wind velocity and atmospheric pressure were interpolated in space onto the ADCIRC grid and in time to synchronize the wind and pressure information with the model time step. The NWS was set to 6 in the control file.

Simulation of December 1999

The time interval for calibration of the model was December 1999.

Model forcing

Water-level forcing constructed from astronomical tidal constituents at the open ocean boundary for December 1999 was obtained from Eastcoast 2001 tidal database (. River flow was obtained from the USGS Savannah Near Clyo Station. Figure 5 shows the daily discharge river flow for December 1999. Wind data during December 1999 was obtained from global National Centers for Environmental Prediction (NCEP) winds.

Model calibration

Initial calculations by the circulation model overpredicted the water level values during low tide. The model was calibrated by:

- Smoothing the irregularities in the marshes.
- Adjusting the values of NODEDRYMIN and NODEWETMIN in the model control file. NODEDRYMIN is the minimum number of time steps after a node dries that it must remain dry before it can wet again. This parameter helps to keep nodes/elements from repeatedly turning on and off during wetting process. NODEWETMIN is the minimum number of time steps after a node wets that it must remain wet before it can dry again. A value of 150 for NODEDRYMIN and 0 for NODEWETMIN produced good agreement between the measured and calculated water level values.
- Adjusting the friction factor. The friction coefficient was adjusted until good agreement between measured and calculated water levels was achieved. A friction factor of 0.05 was set to marshes with elevations more than 0.5 m (MSL) which represents the densely vegetated marshes. A friction factor of 0.0025 was set throughout the rest of the model domain.

Model verification

The circulation model was verified by comparing measured and calculated water level at nine monitoring stations. Measured and calculated current data were compared for a flood and ebb tides.

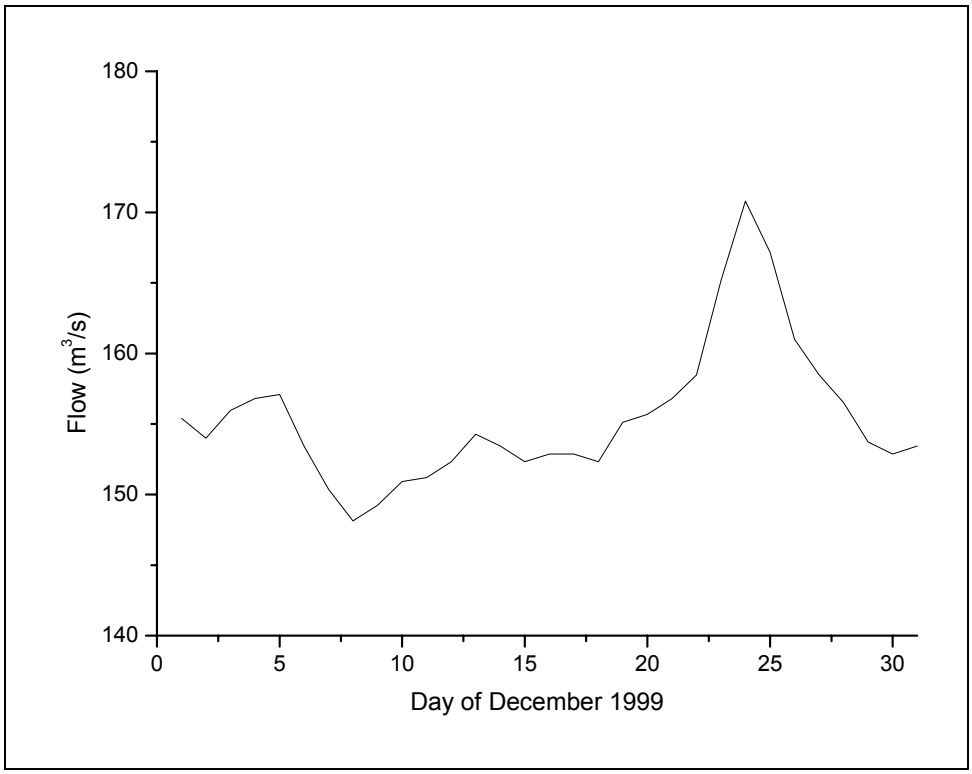

Figure 5. Daily discharge river flow for December 1999

Comparison of measured and calculated water level

The mean error and percent error calculations were used to quantify the comparison of measured and calculated water level at stations shown in figure 6.

The water level data collected in the open ocean was obtained from the South Atlantic Bight Offshore Observational Network (SABSOON) station (R2 Tower) operated by the NAVY. The station is located at 31.375 N and 80.5665 W and at a depth of 26.2 m. The data is obtained from a pressure sensor attached to the tower at a mean depth of 5.69 m below the surface. The data measured by SABSOON was collected in millibar every 6 minutes.

The water level data in the main channel was collected by NOAA station of Fort Pulaski, Savannah River, GA. The station is located at 32.033 N and 80.902 W and hourly data referenced to MSL was used in the comparison with model data.

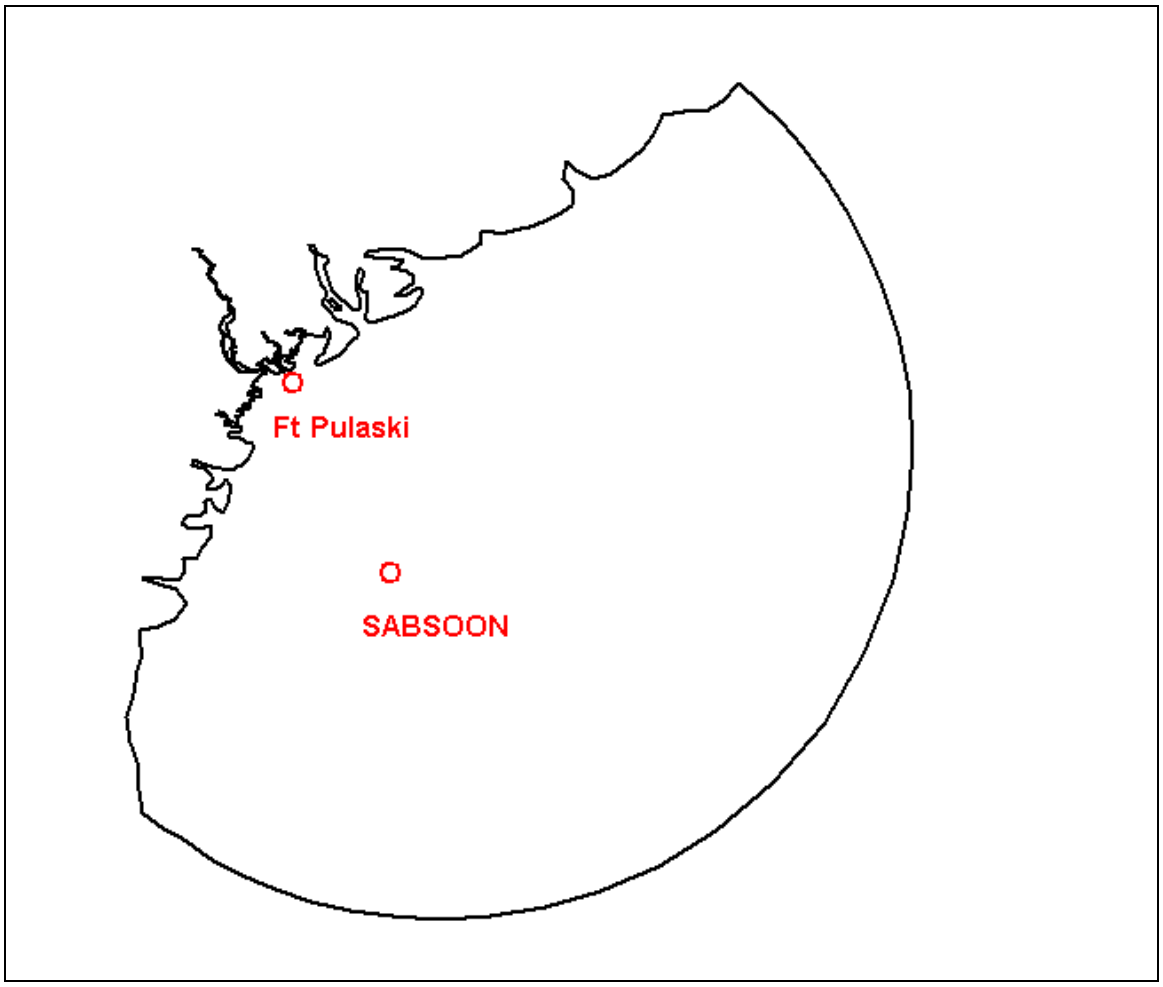

Figure 6. Location of stations for comparison of measured and calculated water level

The rms error E_{rms} provides an absolute measure of error and is given by:

$$E_{rms} = \sqrt{\frac{\sum_{i=1}^{N} X_c - X_m)^2}{N}}$$

where X_c is the calculated value of a variable X, X_m is the measured value of the variable, and N is the number of points.

Percent error E_{pct} is defined in terms of rms error as:

$$E_{pct} = 100 \frac{E_{rms}}{R}$$

where R is a representative range of values for the variable X. For percent error calculations of water level, the difference between MHHW and MLLW at a specified NOS station within the

study area is taken as R. Percent error of less than 10 are considered acceptable (Militello and Kraus, 2001).

To retain nontidal motion, time series of the measured water level were low-pass filtered using cutoff frequency of 0.5 cpd to eliminate motion with 2-day or shorter period. The calculated water level was corrected by adding the filtered data. The percent error at SABSOON was 8 and was 6.0 at Ft Pulaski.

Comparison of measured and calculated water level at SABSOON station, and FT Pulaski are shown in figures 7 and 8 respectively.

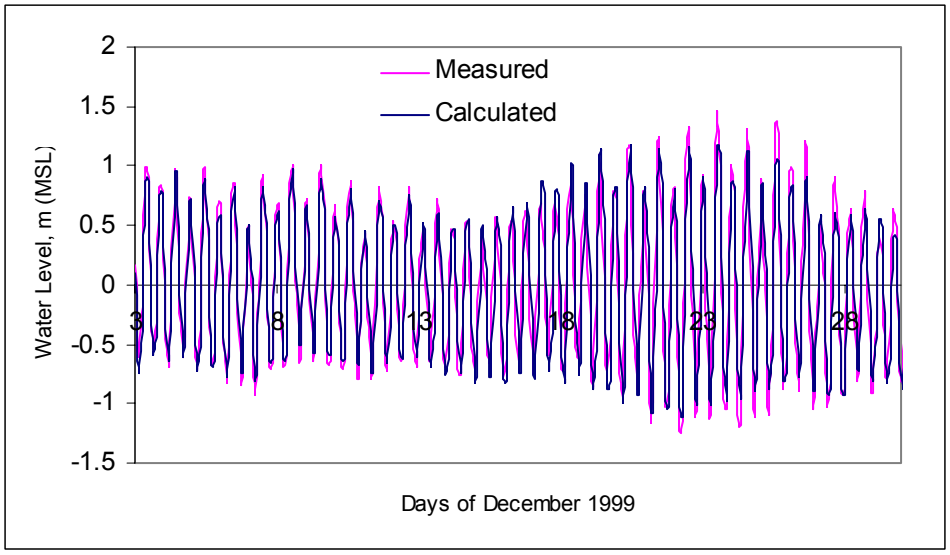

Figure 7. Comparison of measured and calculated water level at SABSOON

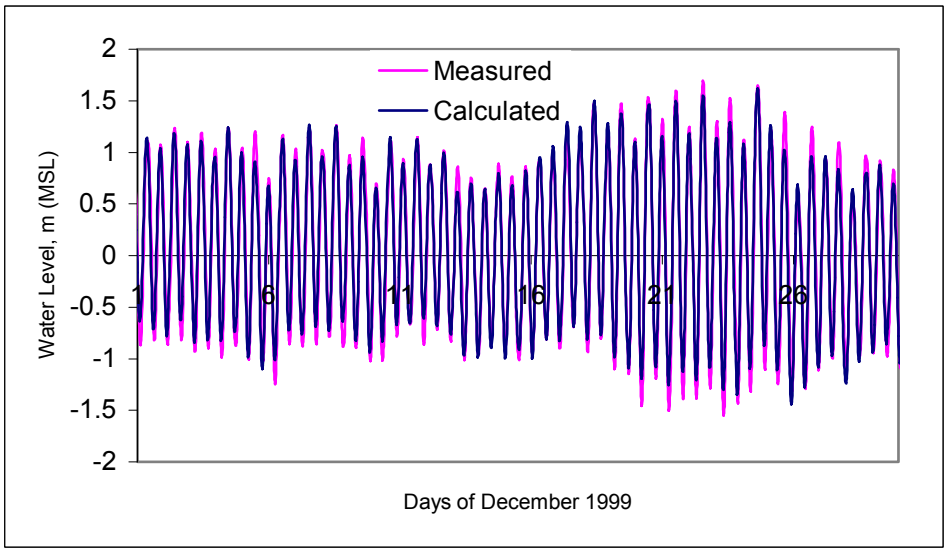

Figure 8. Comparison of measured and calculated water level at Ft Pulaski

Verification of the circulation model was also conducted by comparing measured and calculated water level at seven subordinate stations in the study area (Figure 9). The publication of fully daily tide predictions is limited to small number of stations referred to as “reference stations”. Tide prediction at other locations can be obtained by applying time and height differences and ratios to daily tide predictions for the reference stations. Ft Pulaski was the reference station used to predict the tide at six subordinate stations. Figures 10 through 15 show the comparison of measured and calculated water level at the subordinate stations. It can be seen from the figures that calculated water level is in good agreement with measurements.

At Ft Jackson the measured and calculated spring tidal range is compared because no tidal data was found at the reference station of Savannah during December 1999. The ratio of the calculated mean tidal range to the measured one is 0.87 which shows good agreement with measurements.

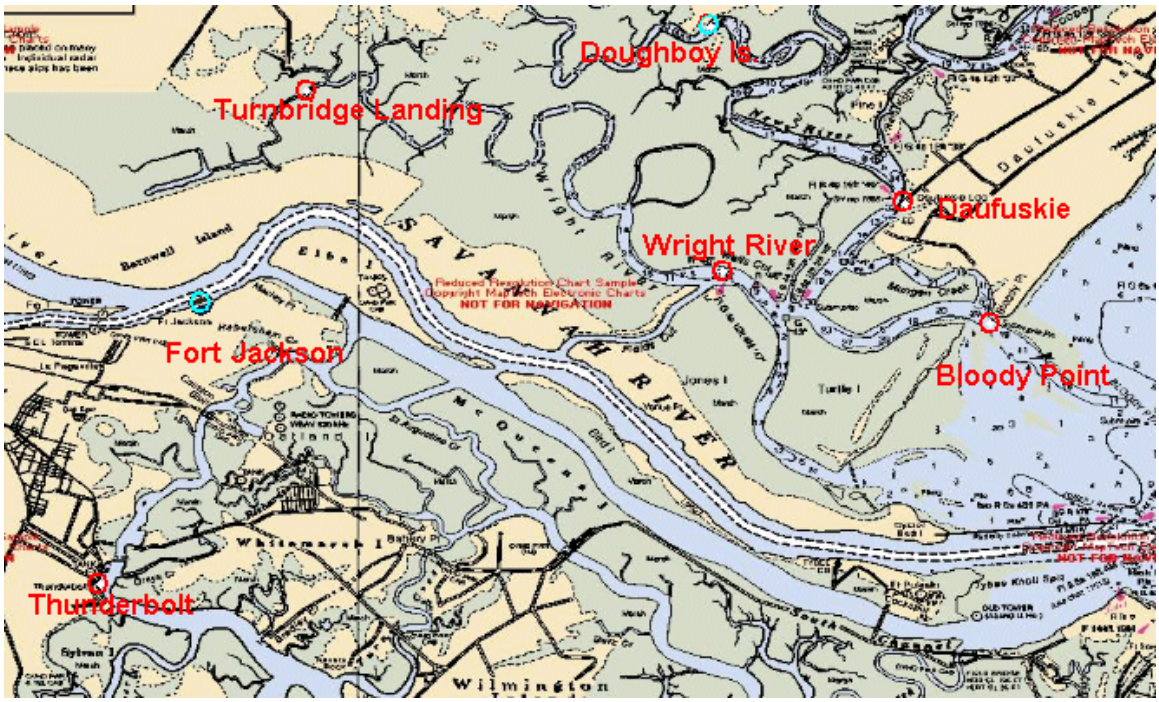

Figure 9. Location of subordinate stations for comparison of measured and calculated water level

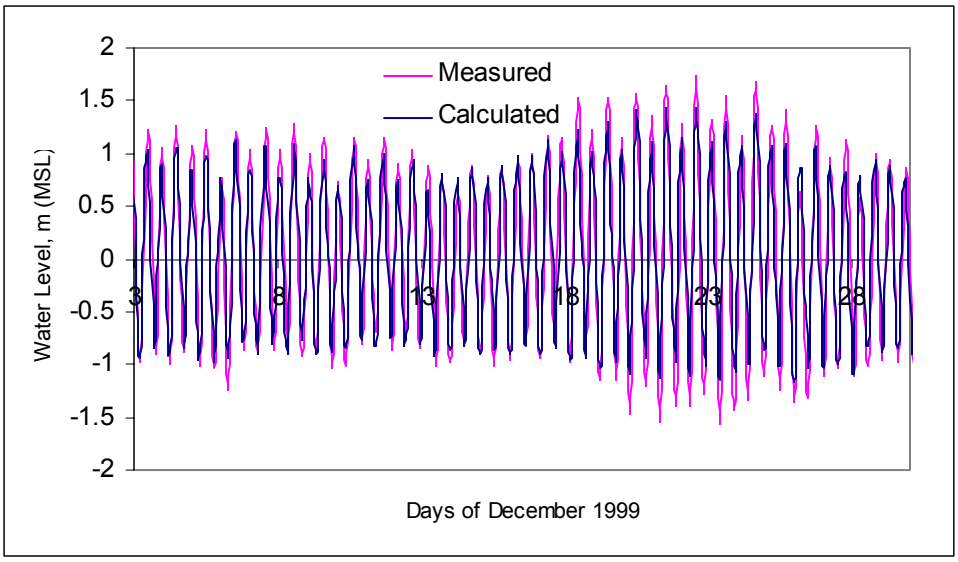

Figure 10. Comparison of measured and calculated water level at Daufuskie

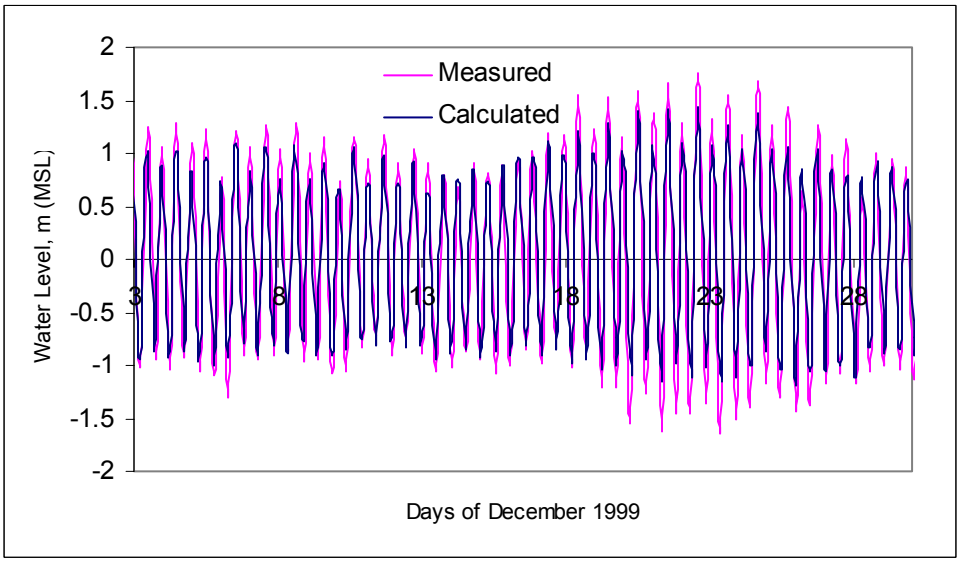

Figure 11. Comparison of measured and calculated water level at Wright River

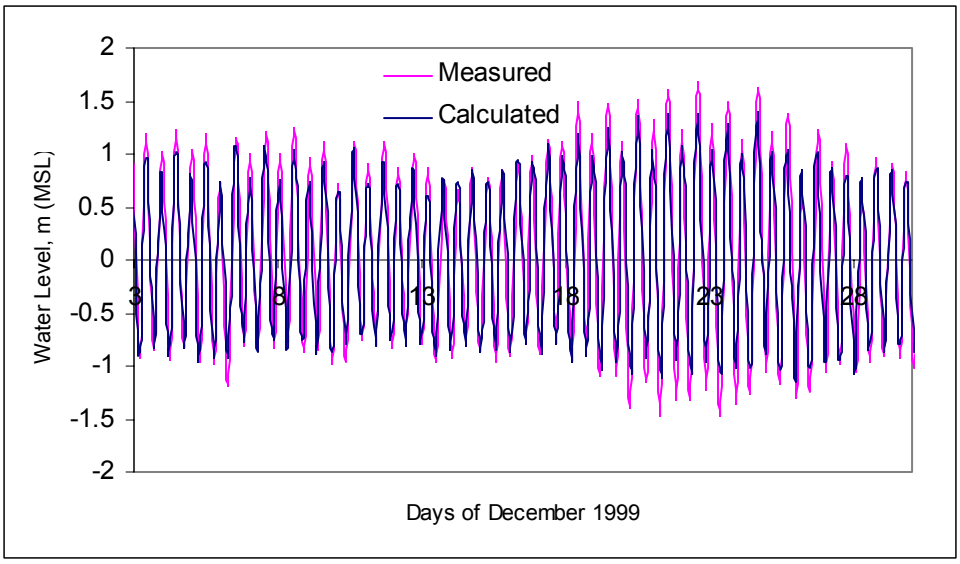

Figure 12. Comparison of measured and calculated water level at Bloody Point

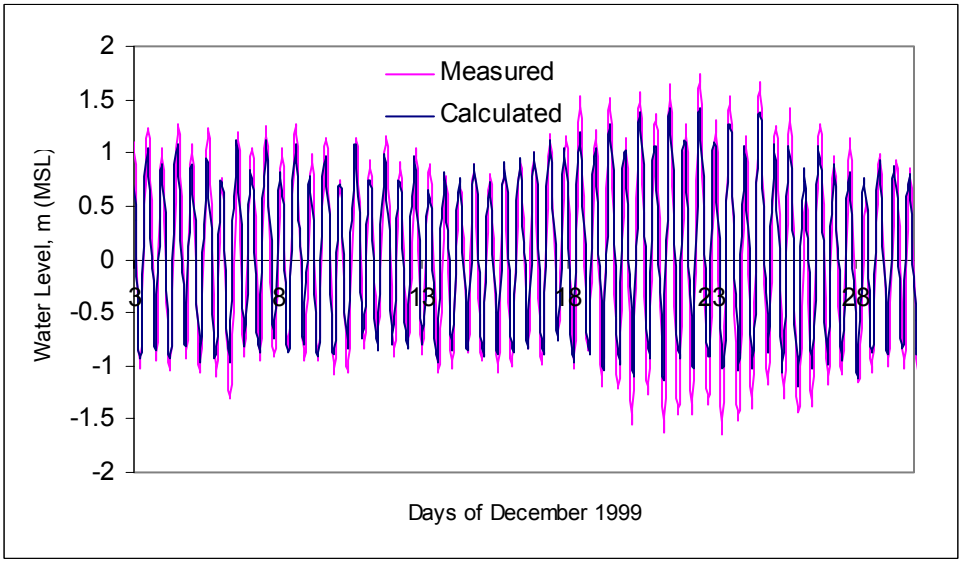

Figure 13. Comparison of measured and calculated water level at Doughboy

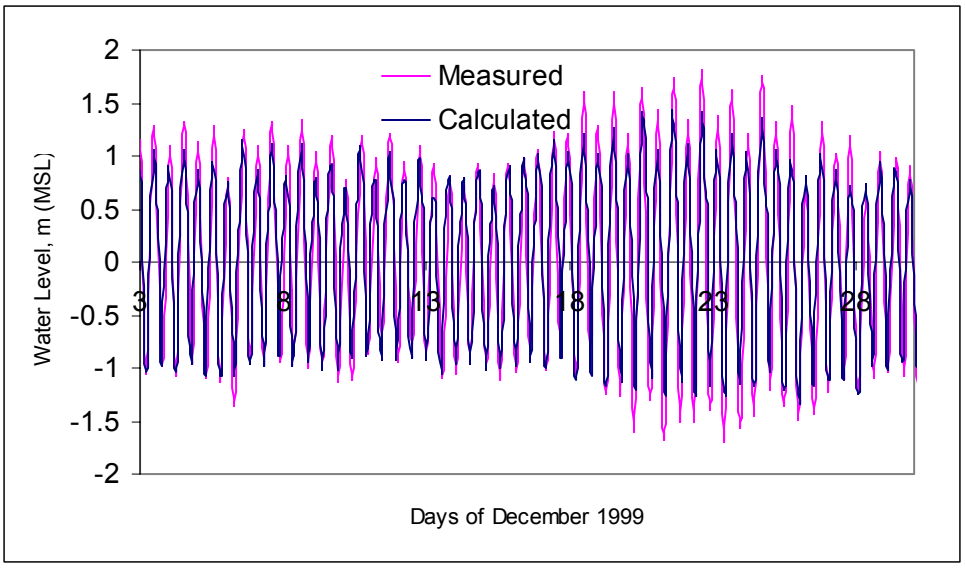

Figure 14. Comparison of measured and calculated water level at Turnbridge Landing

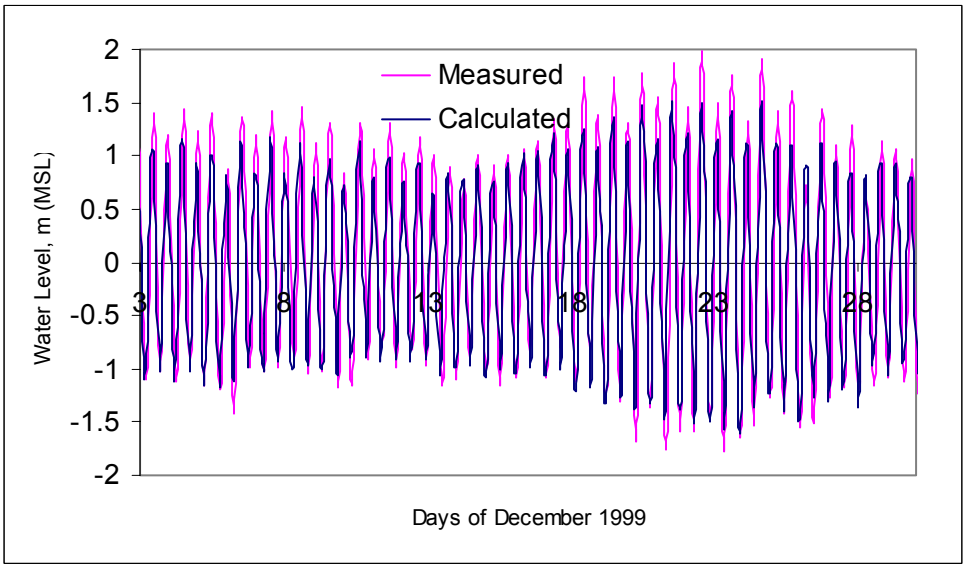

Figure 15. Comparison of measured and calculated water level at Thunderbolt

Comparison of measured and calculated current data

Current data collected by the Applied Technology & Management Inc. was compared to the model on flood and ebb tides as shown in figures 16 and 17 respectively.

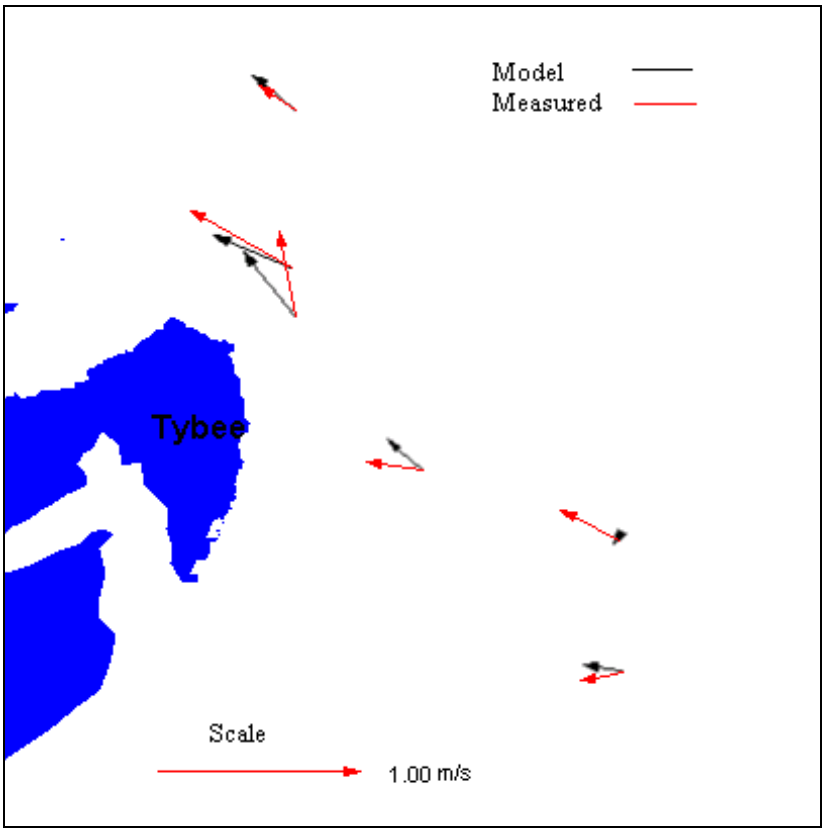

Figure 16. Comparison of measured and calculated current data during flood flow on December 9, 1999

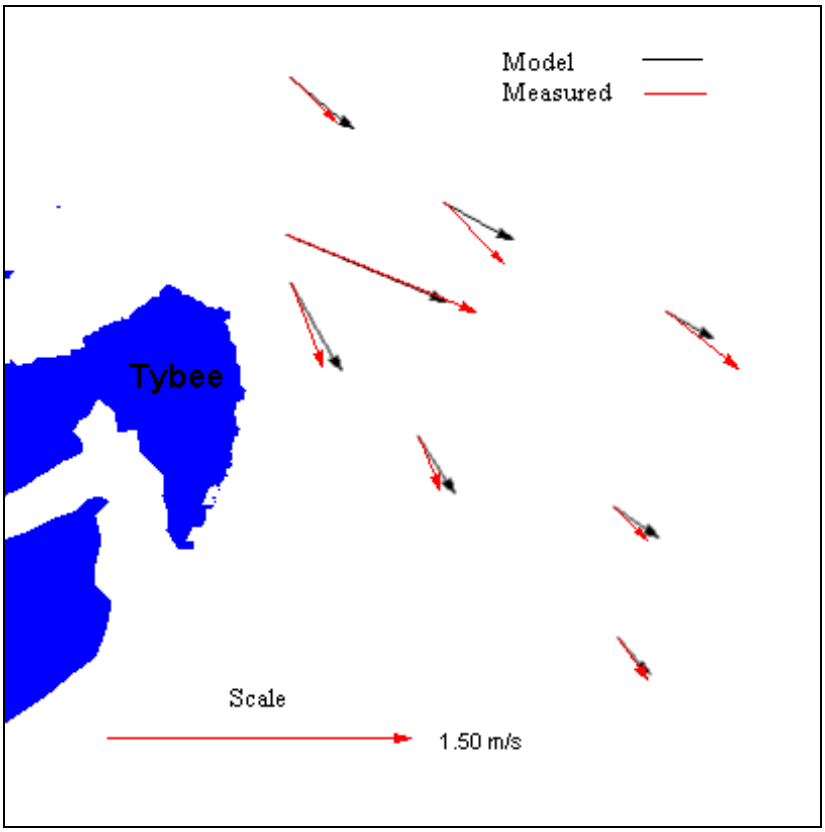

Figure 17. Comparison of measured and calculated current data during ebb flow on December 9, 1999

The measured data was collected on December 9, 1999 from 10:45 to 12:58 (EST) for the flood flow and from 16:16 to 17:00 (EST) for the ebb flow as shown in figure 18. The current data was collected using an Acoustic Doppler Current Profiler (ADCP). The current measurements were depth averaged and averaged over 1-minute.

The comparison between the measured and calculated data shows good agreement during the flood and ebb flows. In general the model is able to reproduce the measured currents. The comparison between the measured and calculated currents for the flood tide shows better agreement than for the ebb case. The measurement time during the flood tide extended for longer period (1.75 hr) compared to the ebb tide (0.75 hr). The flood tide case represents a peak flood and the ebb case was close to slack flow and does not represent peak ebb.

For the ebb case, and close to slack flow, the change in current direction occurs during short period of time. The model results were obtained every 15 minutes. Therefore, the deviation in current direction might be due to mismatching the exact measurement time.

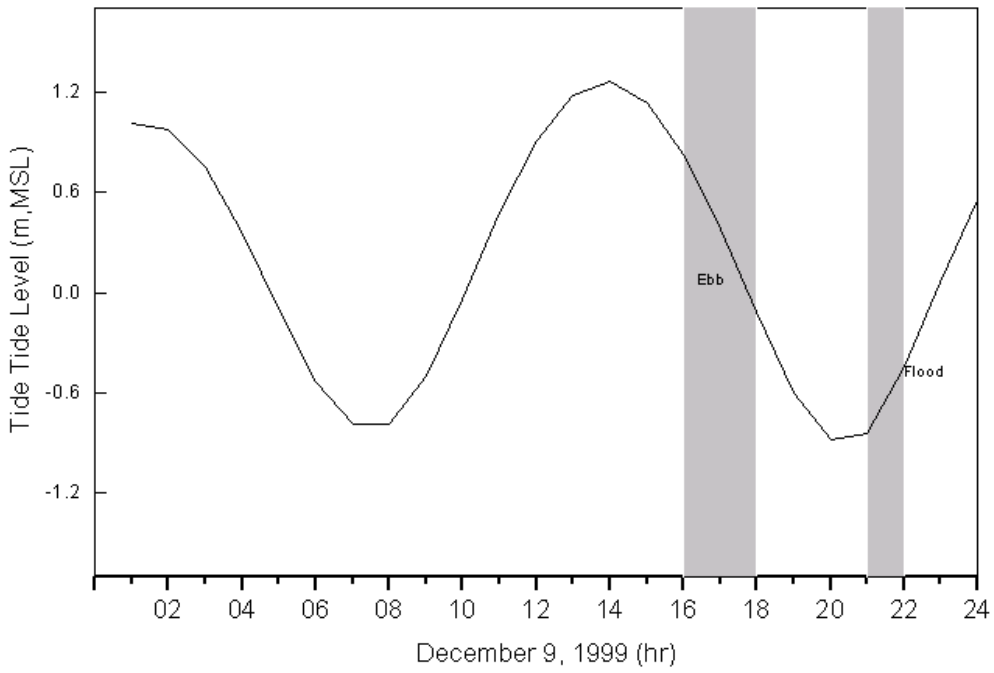

Figure 18. Duration of flood and ebb flow during December 9, 1999

Simulation of One Extreme Storm

Hurricane Hugo was chosen to represent the extreme storm. Hurricane Hugo occurred during September 14-22 1989 and it struck Charleston, South Carolina on September 21 as a category 4 storm. Hugo ranked as the eleventh most intense hurricane at time of landfall to strike U.S. this century and is rated as the second costliest hurricane with over $7 billion in damages. Hurricane Hugo weakened from its peak intensity by the time it smashed the U.S. Virgin Islands on Sept. 17, and then struck a glancing blow to Puerto Rico with winds gusting to 160 mph the next day. Weakened temporarily by its Caribbean island assault, Hugo intensified significantly prior to landfall as it crossed the Gulf Stream off the Southeast U.S. coast. Hugo blew into Charleston, S.C., on the evening of Sept. 21, the autumnal equinox, with winds of 138 mph and a 20 foot storm surge on top of astronomically high tides.

An atmospheric model was applied to compute wind and pressure fields from Hurricane Hugo during the period from September 14 at hour 12 GMT to September 22 at hour 12 GMT. Actual intensity parameters were used, but the locations of the storm for 22/00, 22/06 and 22/12 have been shifted to strike Savannah Harbor. Figure 19 shows the actual and the retracked Hurricane Hugo track. Wind and pressure fields for the "retracked" Hurricane Hugo 1989 were hindcasted every 15 minutes. Figures 20 through 22 show the pressure fields for the “retracked” Hurricane Hugo on 22/00, 22/06 and 22/12 respectively.

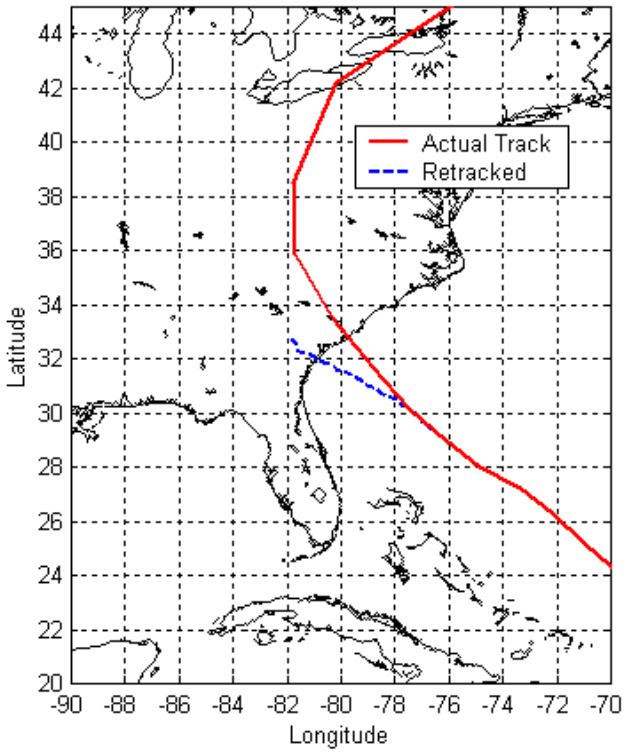

Figure 19. Actual and retracked Hurricane Hugo track

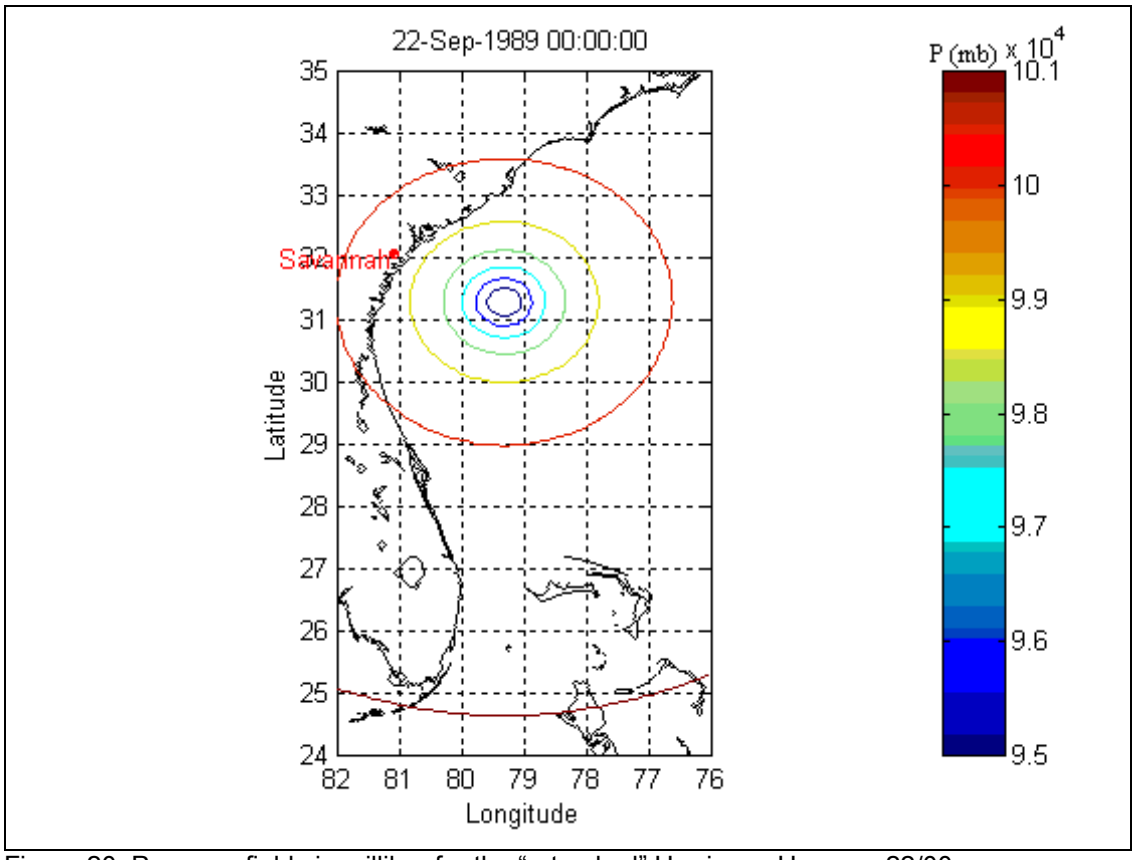

Figure 20. Pressure fields in millibar for the “retracked” Hurricane Hugo on 22/00

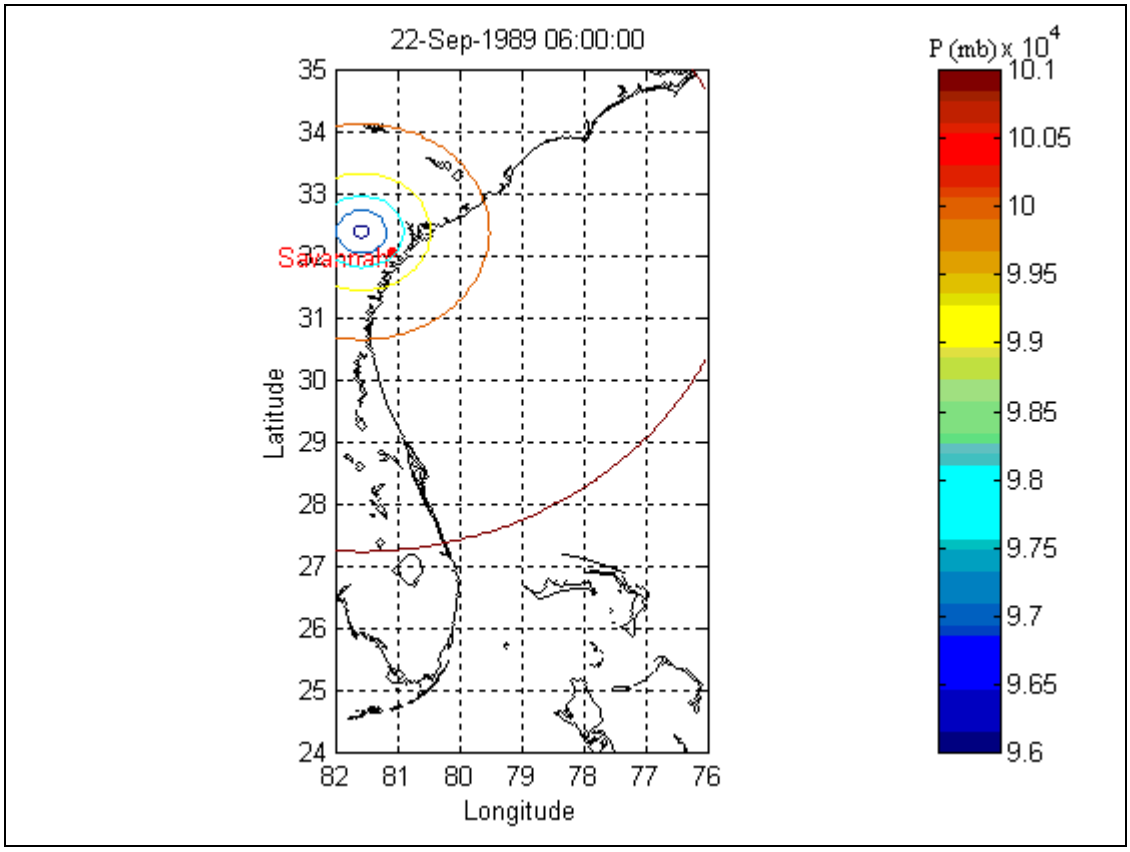

Figure 21. Pressure fields in millibar for the “retracked” Hurricane Hugo on 22/06

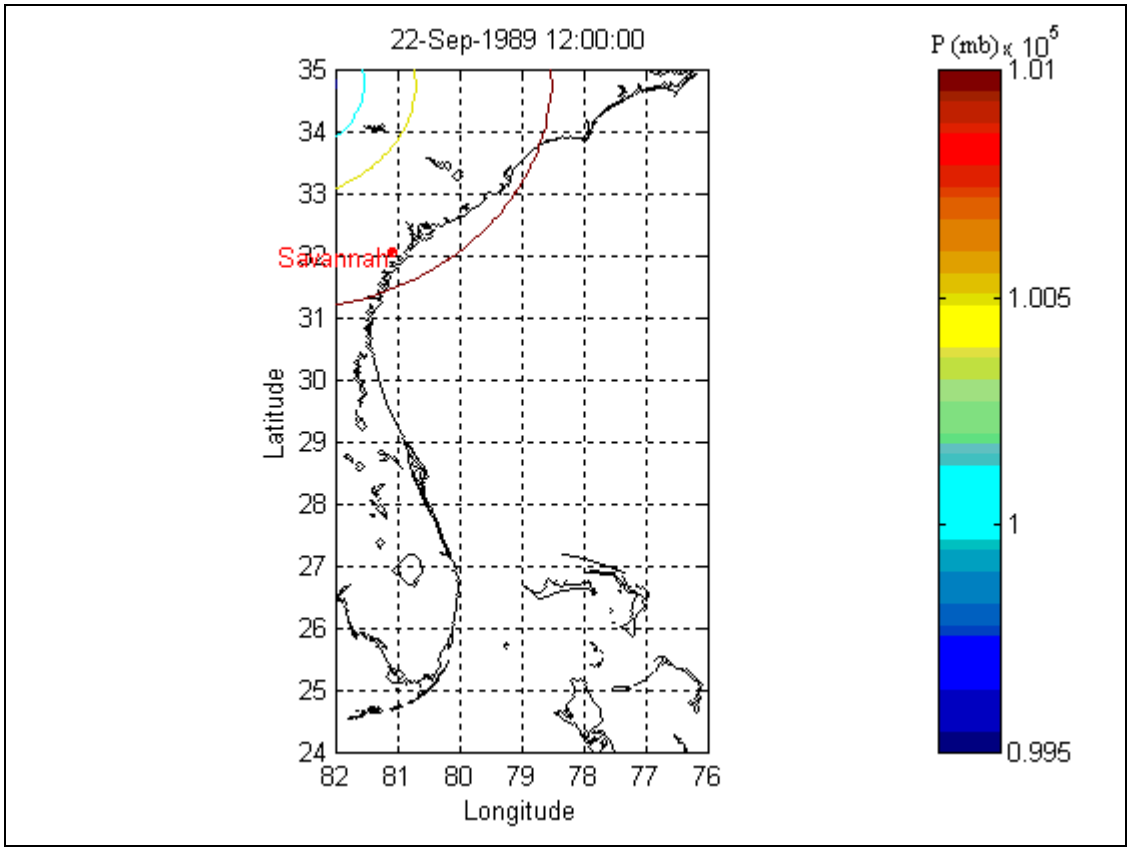

Figure 22. Pressure fields in millibar for the “retracked” Hurricane Hugo on 22/12

The ADCIRC model was forced with water level, river flow and wind and pressure fields. Water-level forcing constructed from astronomical tidal constituents at the open ocean boundary for September 1989 was obtained from the Eastcoast 2001 tidal database. The NODEDRYMIN was set to 30 to reduce the time that the node must remain dry before it can wet again. Daily river flow during the Hurricane at Clyo Station is shown in figure 23. The retracted wind and pressure fields from Hurricane Hugo were converted into an ADCIRC single meteorological input file. Wind velocity and atmospheric pressure are read in for a rectangular grid in Longitude- Latitude. This information is interpolated in space onto the ADCIRC grid and in time to synchronize the wind and pressure information with the model time step.

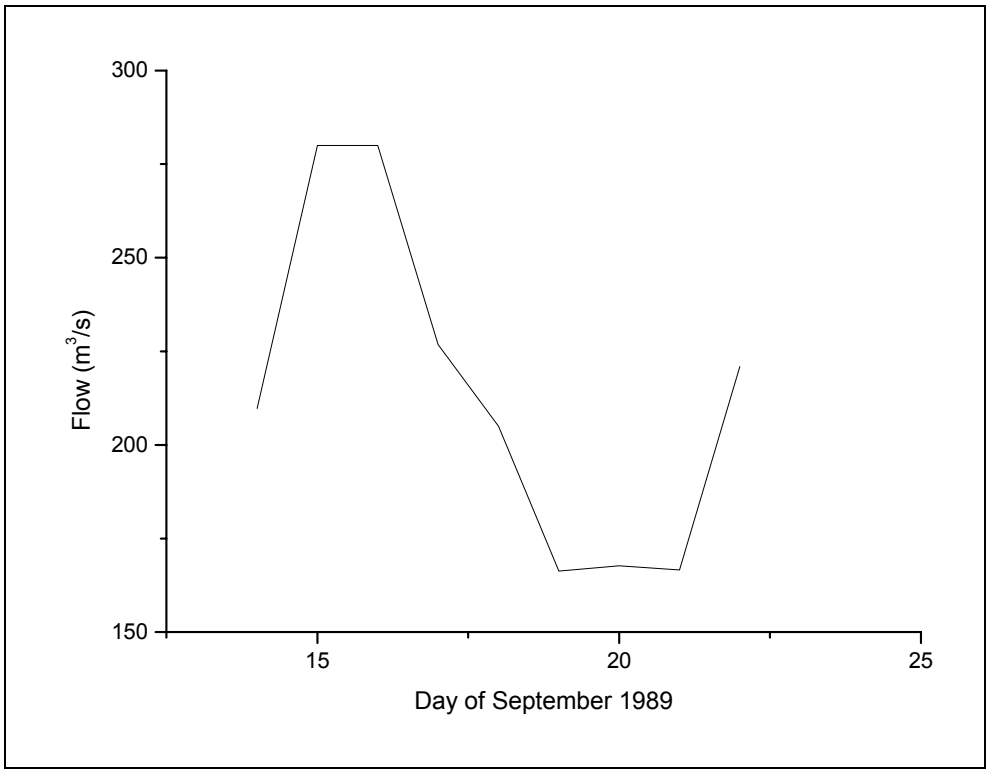

Figure 23. Daily discharge river flow for September 1989

The calculated water level at Ft Pulaski is shown in figure 24. A peak value of 3.1 m was calculated at Ft Pulaski. The circulation pattern during the peak water level at Ft Pulaski is shown in figure 25.

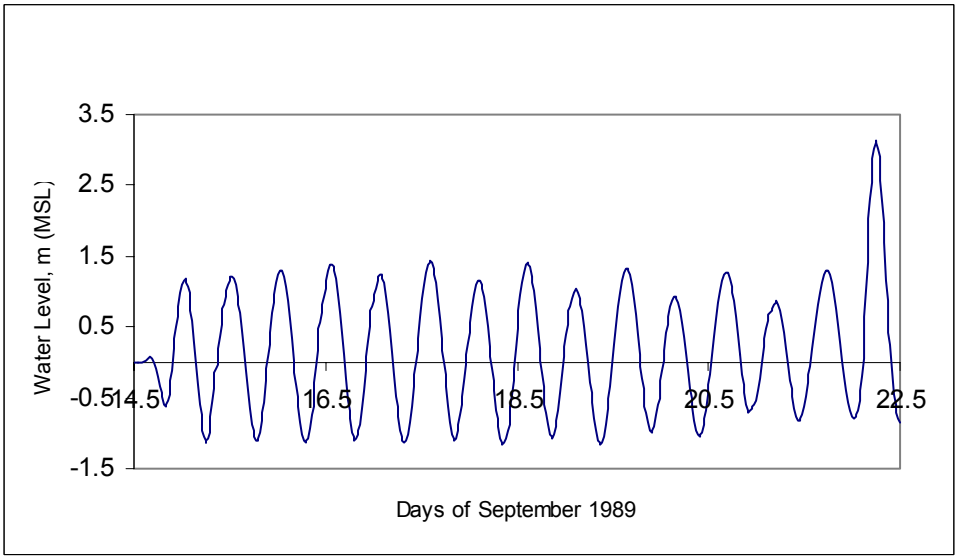

Figure 24. Calculated water level at Ft Pulaski

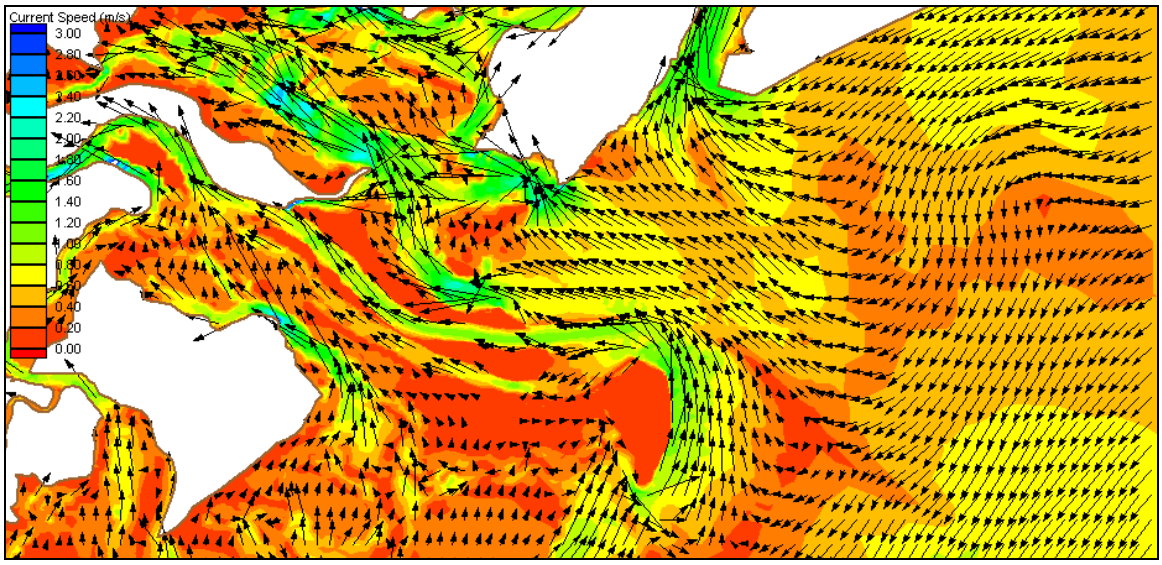

Figure 25. Circulation pattern in the study area during peak water level at Ft Pulaski

Current speed and direction at the seven proposed study sites are shown in figures 26 through 32 during the storm.

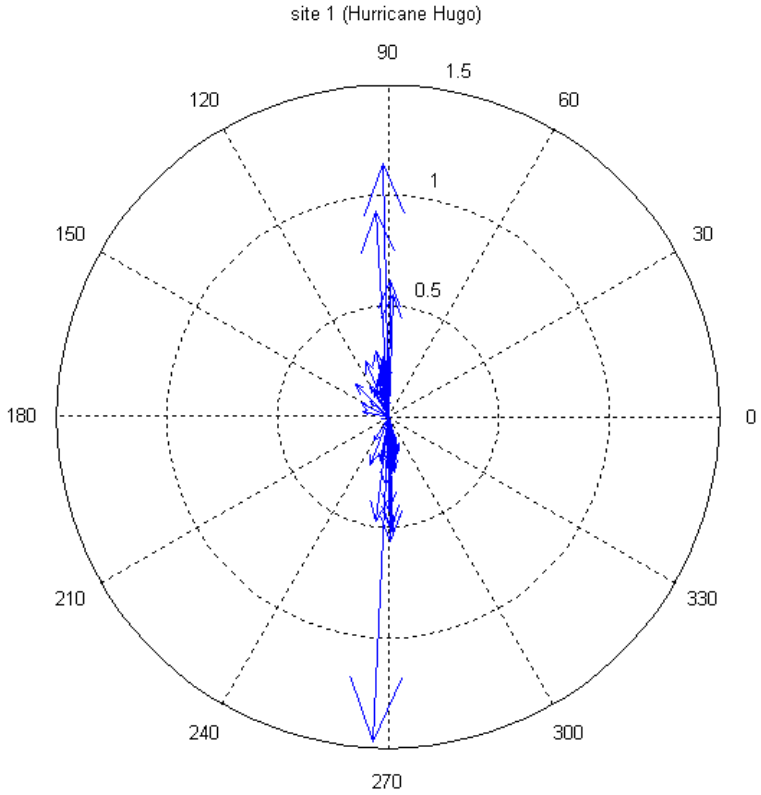

Figure 26. Current vectors at site 1 (current speed in m/s)

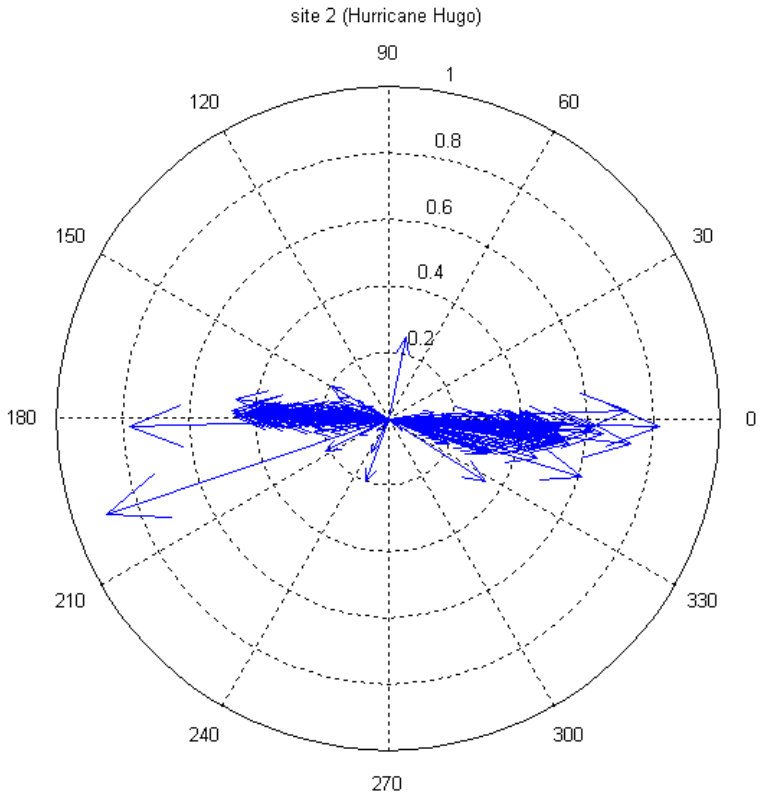

Figure 27. Current vectors at site 2 (current speed in m/s)

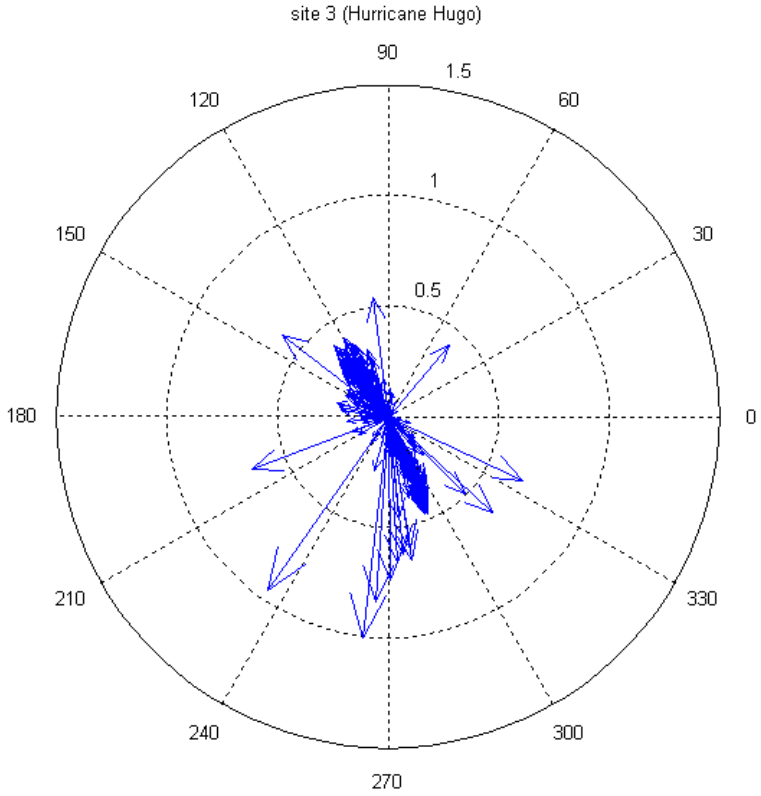

Figure 28. Current vectors at site 3 (current speed in m/s)

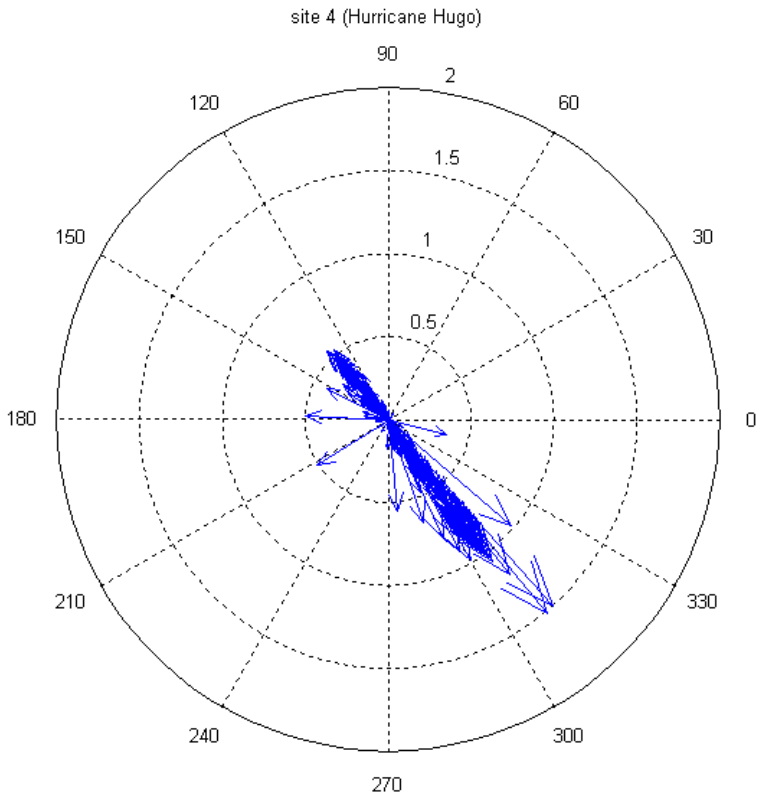

Figure 29. Current vectors at site 4 (current speed in m/s)

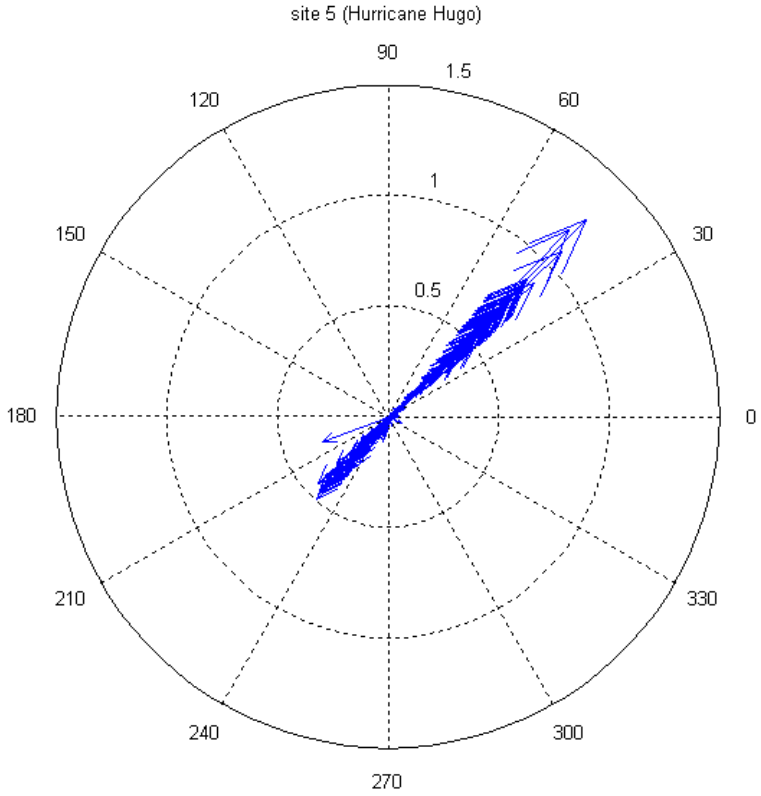

Figure 30. Current vectors at site 5 (current speed in m/s)

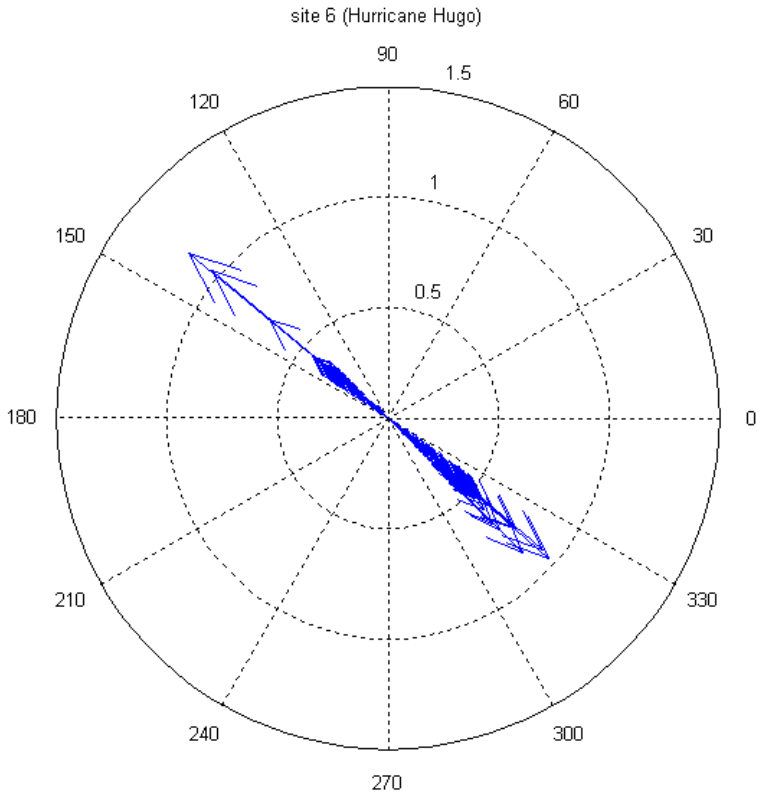

Figure 31. Current vectors at site 6 (current speed in m/s)

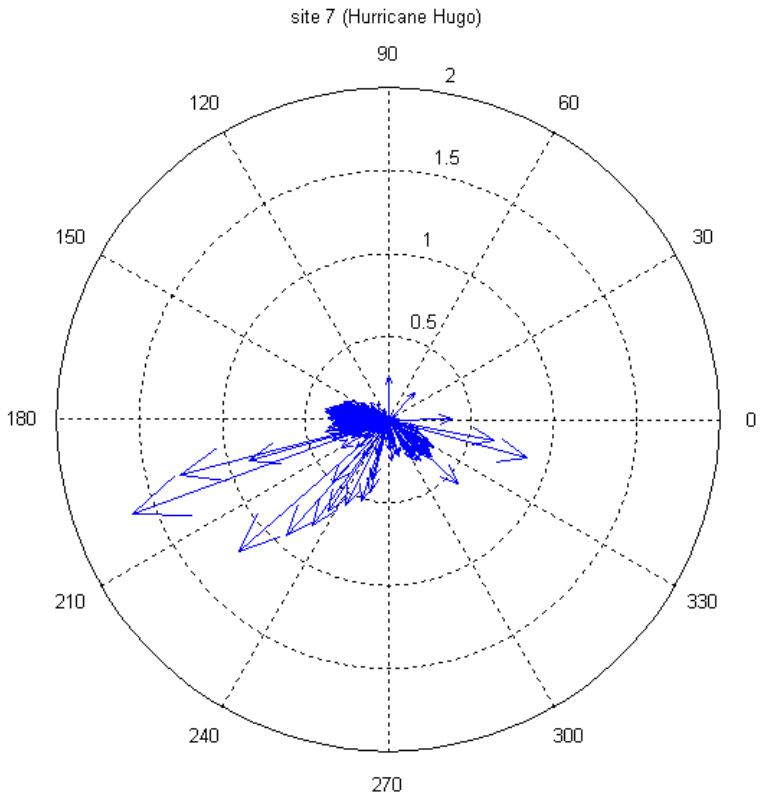

Figure 32. Current vectors at site 7 (current speed in m/s)

At site 1, the current is approximately parallel to the shoreline with maximum current speed of about 1.5 m/s. At site 2 the current is moving approximately parallel to the jetty with maximum speed of about 0.8 m/s. At site 3 the current is shows influence by the tide (toward northeast and southwest), but strong current of about 1.0 m/s moved toward Tybee Island. At site 4 the current is mainly influenced by the tide, the net direction was toward the southeast with maximum current speed of 1.5 m/s. At site 5 the current is parallel to the shore with net direction toward the northeast and with maximum speed of about 1.3 m/s. At site 6 the current is parallel to the shore with net direction toward the southeast and with maximum speed of about 1.2 m/s. At site 7 the current direction is influenced by the tide, but strong currents of about 1.5 m/s were moving toward the shore (northeast).

Simulation of One-Month Active Period

ADCIRC was run for November 1979 as the one-month active period characterizes by a number of more frequent storms. Figure 33 shows the energy-based zero-moment wave height (Hmo) and peak period and direction during November 1979.

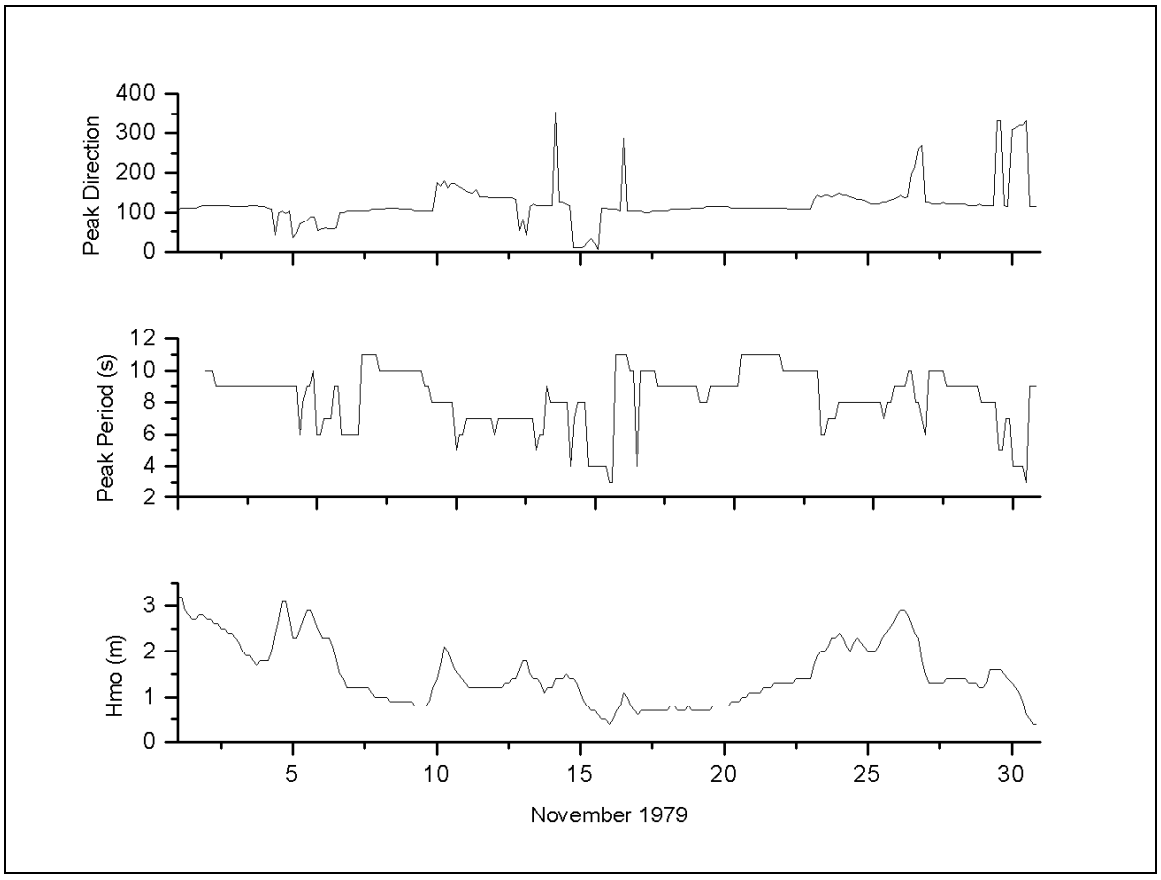

Figure 33. Wave height, period and direction during November 1979

The ADCIRC model was forced with water level, river flow and wind. Water level forcing constructed from astronomical tidal constituents at the open ocean boundary for November 1979 was obtained from the Eastcoast 2001 tidal database. Daily river flow for November 1979 is shown in figure 34. Wind speed and direction was entered to a longitude, latitude grid and interpolated in space onto the ADCIRC grid.

The percent error between measured and calculated water level at Ft Pulaski was 5.

Comparison of measured and calculated water level at Ft Pulaski is shown in figure 35.

Circulation patterns in the study area during peak flood and peak ebb flows are shown in figures 35 and 36 respectively.

Current speed and direction at the seven proposed study sites are shown in figures 38 through 44.

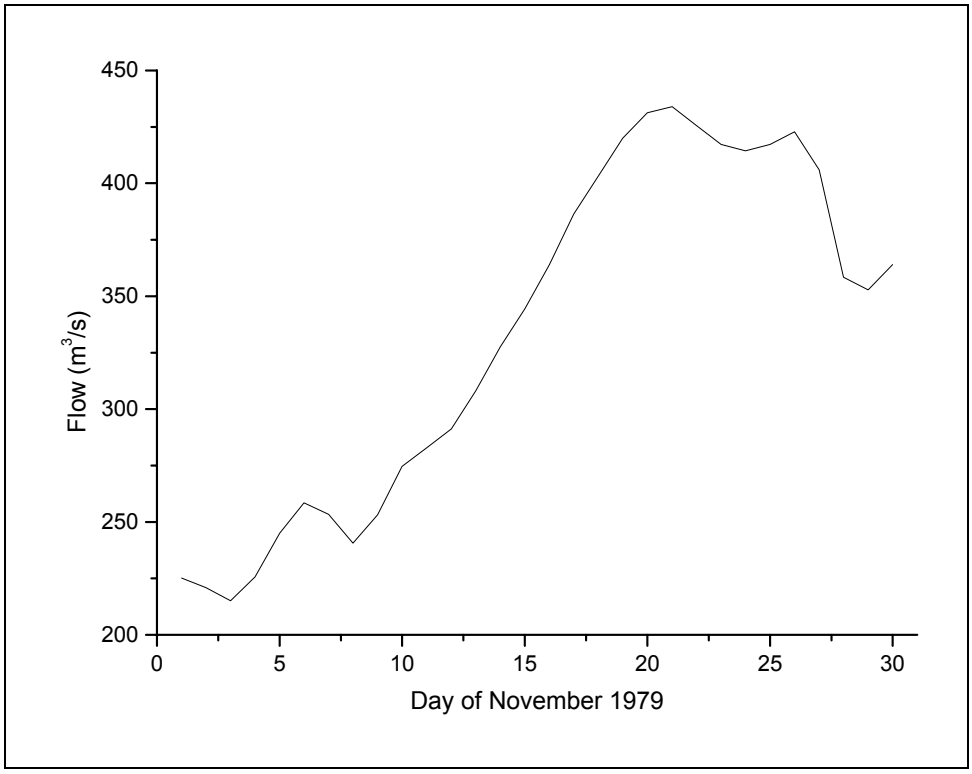

Figure 33. Daily discharge river flow for November 1979

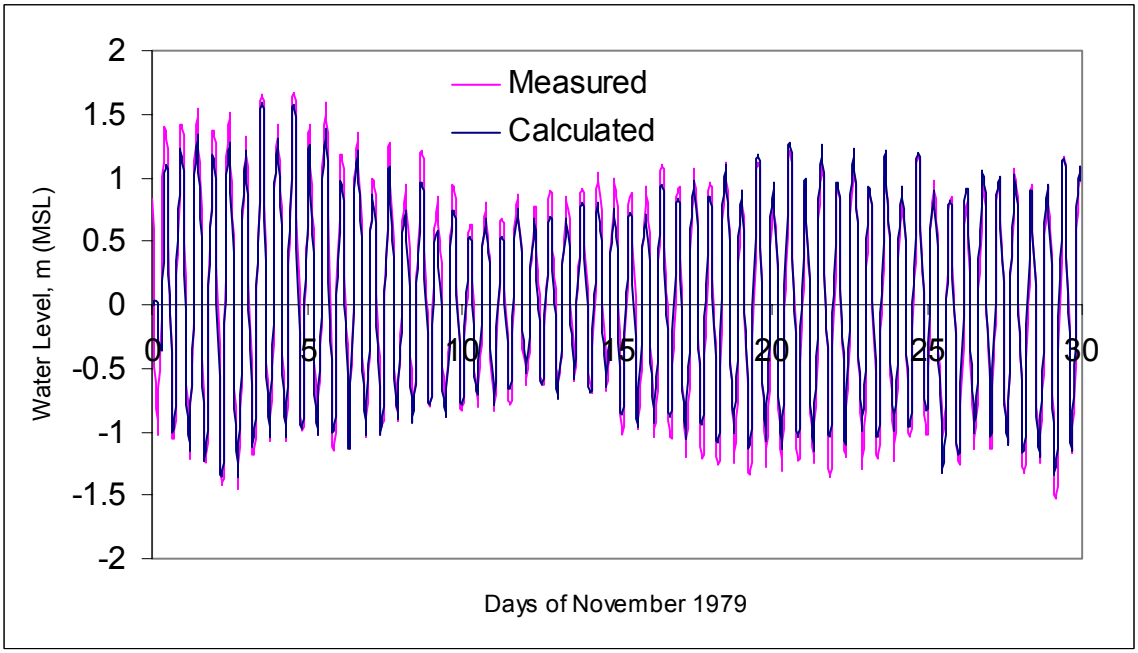

Figure 34. Comparison of measured and calculated water level at Ft Pulaski

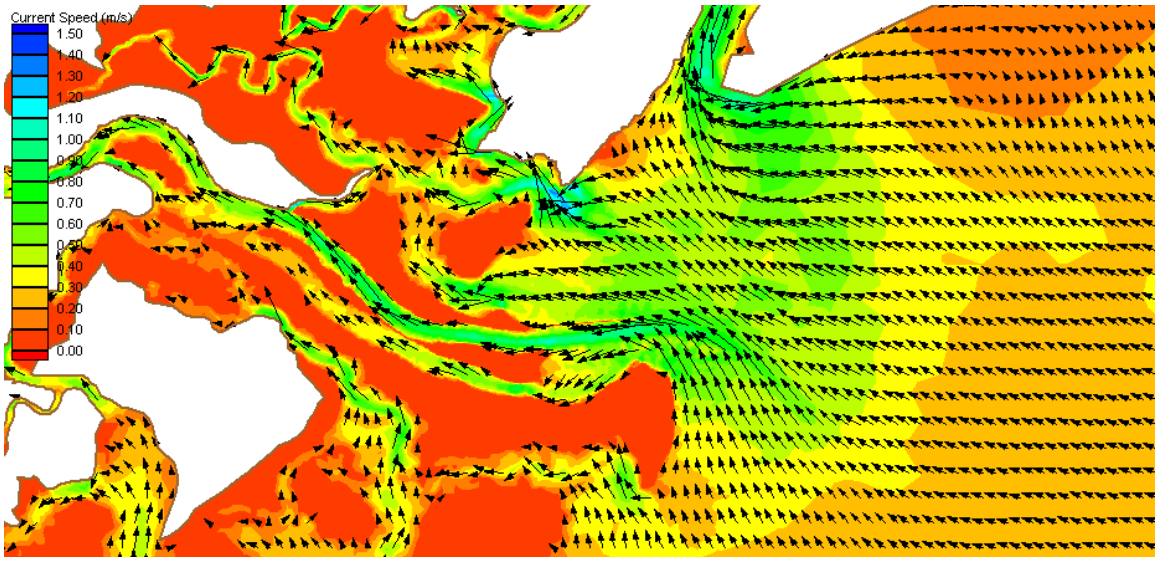

Figure 37. Circulation pattern in the study area during peak flood flow

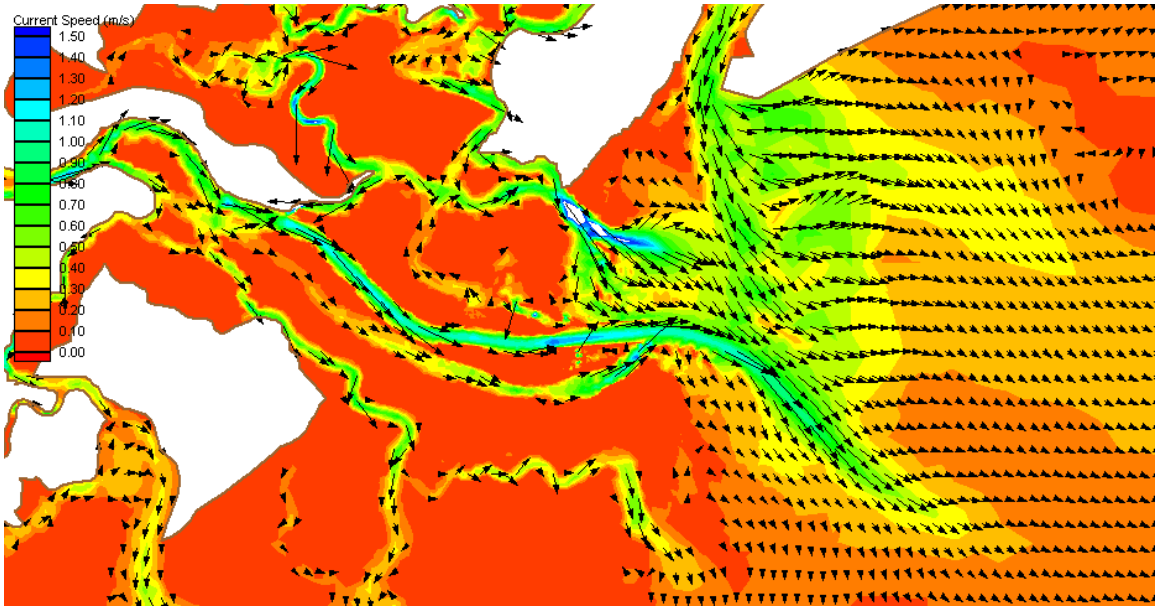

Figure 37. Circulation pattern in the study area during peak ebb flow

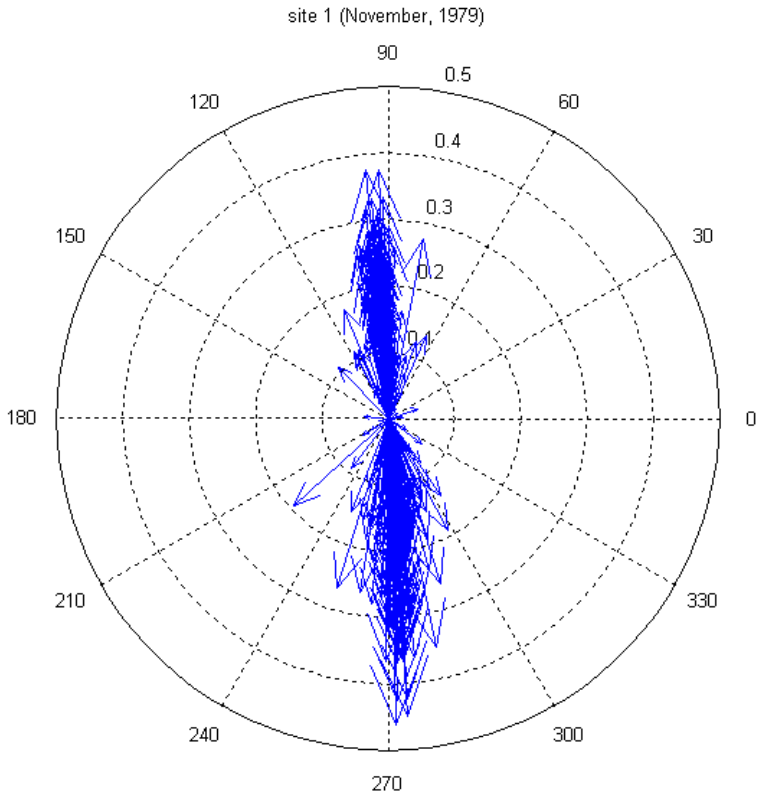

Figure 38. Current vectors at site 1 (current speed in m/s)

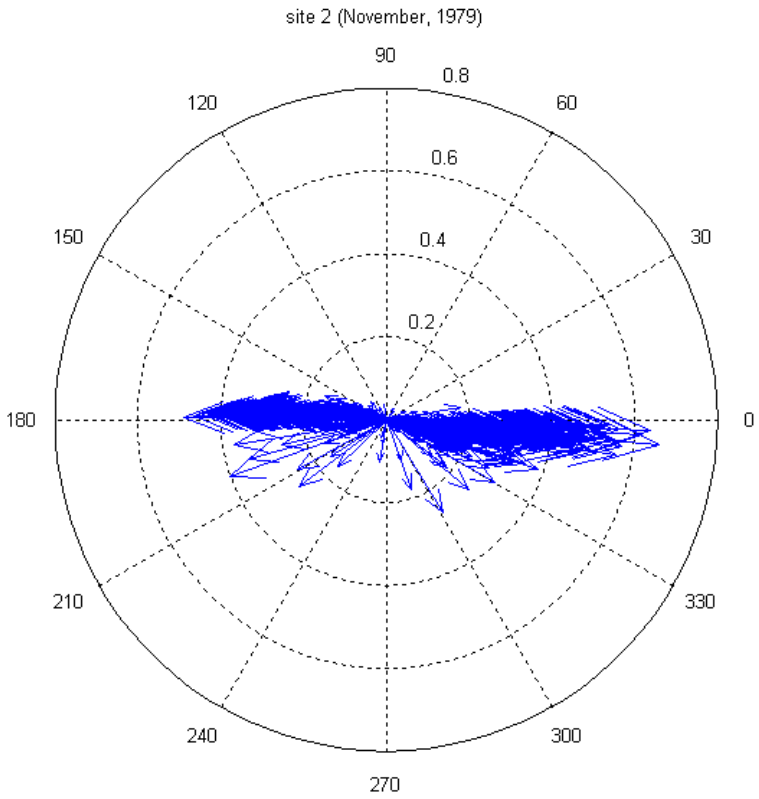

Figure 39. Current vectors at site 2 (current speed in m/s)

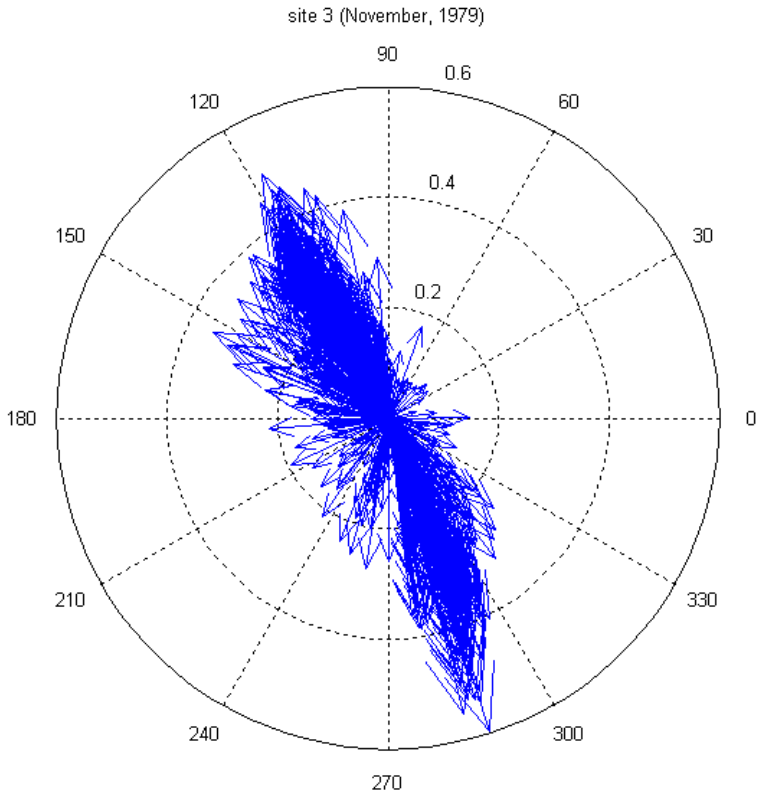

Figure 40. Current vectors at site 3 (current speed in m/s)

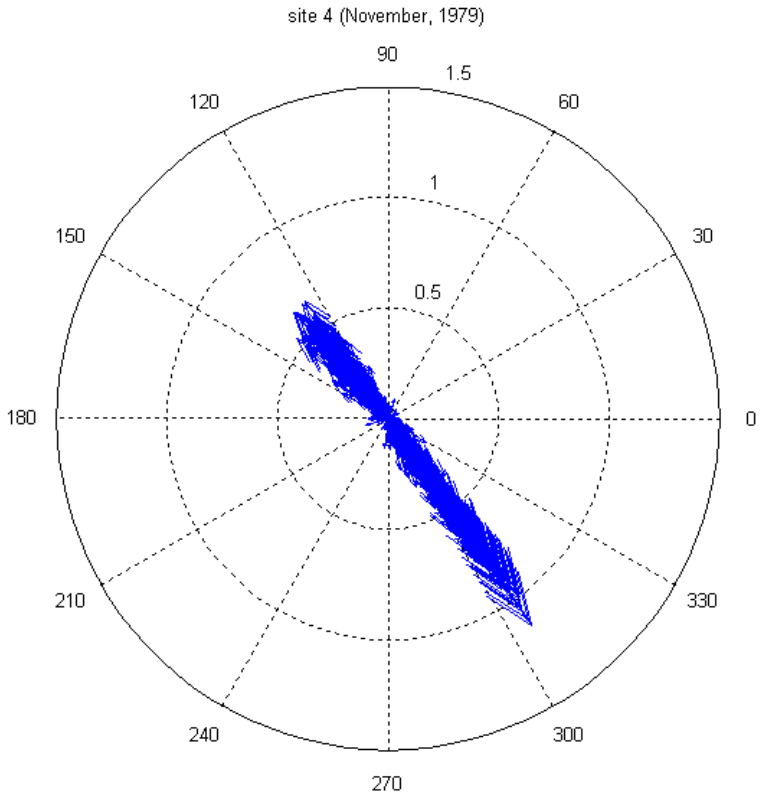

Figure 41. Current vectors at site 4 (current speed in m/s)

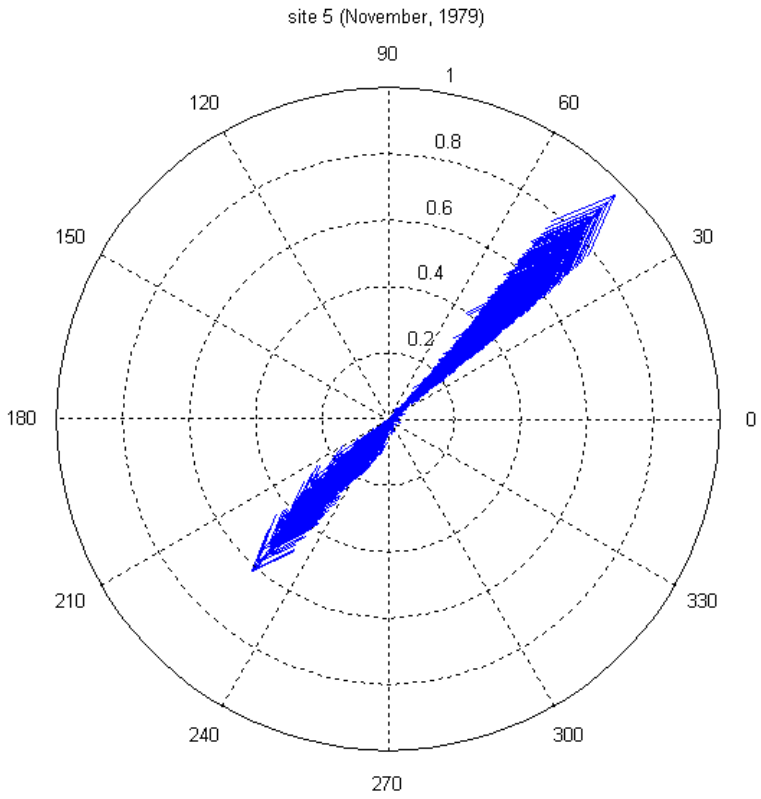

Figure 42. Current vectors at site 5 (current speed in m/s)

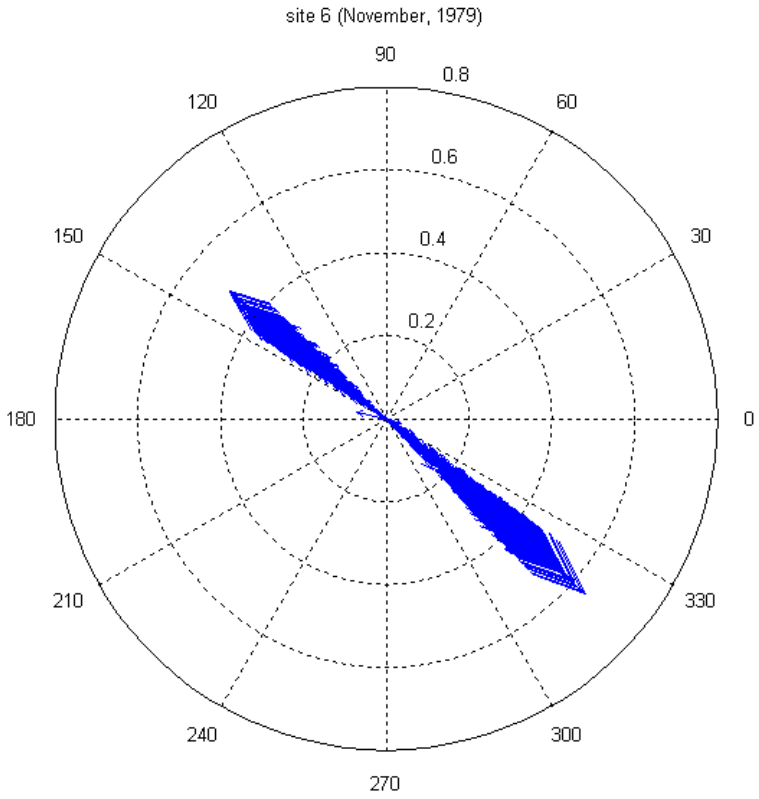

Figure 43. Current vectors at site 6 (current speed in m/s)

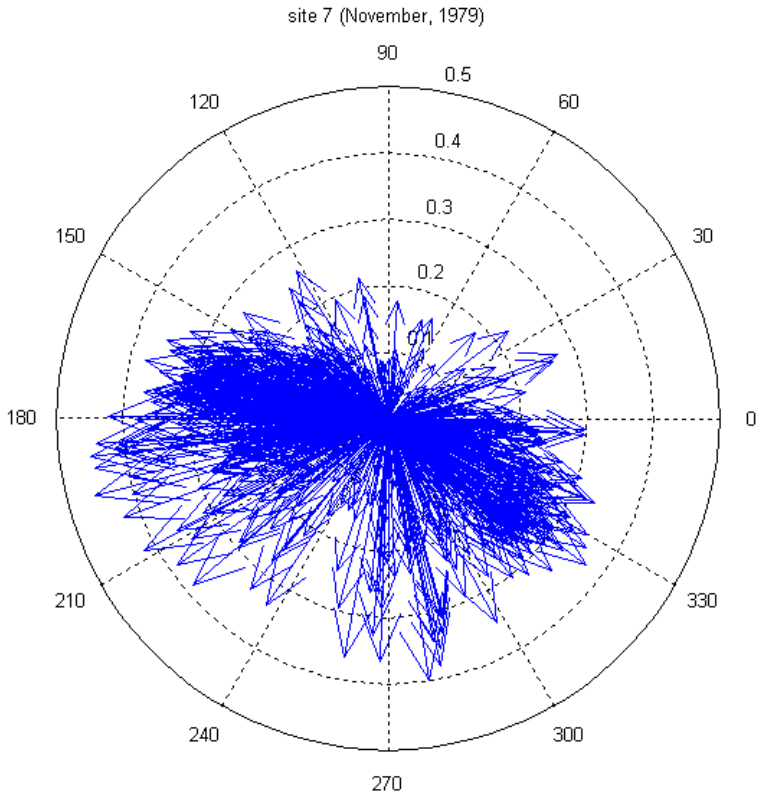

Figure 44. Current vectors at site 7 (current speed in m/s)

It can be seen from the figures that at site 1, the current is approximately parallel to the shoreline with maximum current speed is about 0.4 m/s. At site 2 the current is moving approximately parallel to the jetty with maximum speed of about 0.6 m/s. At site 3 the current is influenced by the tide (toward northeast and southwest) with maximum speed of about 0.6 m/s. Currents with magnitudes of 0.2-0.3 m/s moved toward Tybee Island. At site 4 the current is mainly influenced by the tide with maximum speed of about 1.2 m/s and with net direction toward the southeast. At site 5 the current is parallel to the shore with net direction toward the northeast and with maximum speed of about 1.0 m/s. At site 6 the current is parallel to the shore with net direction toward the southeast and with maximum speed of about 0.65 m/s. At site 7 the current direction is influenced by the tide with maximum speed of about 0.45 m/s, but shows strong tendency for current movement toward the shore (northeast).

Simulation of One-Month Operational Period

ADCIRC was run for January 1992 as the one-month operational period that represents a typical dredging window. Figure 45 shows the energy-based zero-moment wave height (Hmo) and peak period and direction during January 1992.

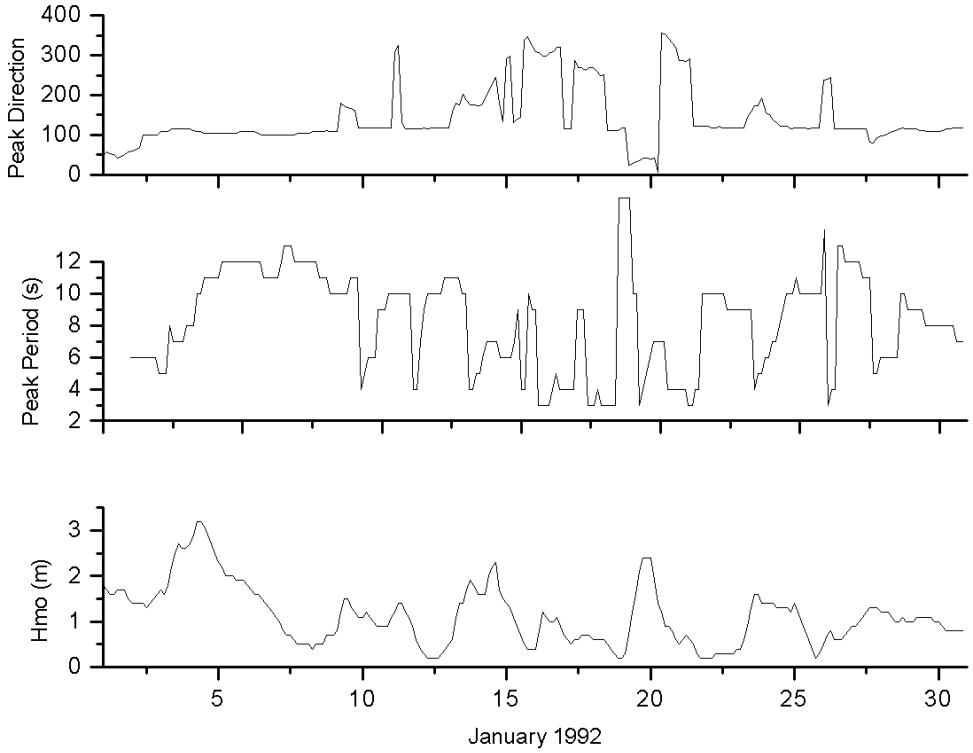

Figure 45. Wave height, period and direction during November 1979

The ADCIRC model was forced with water level, river flow and wind. Water level forcing constructed from astronomical tidal constituents at the open ocean boundary for January 1992 was obtained from the Eastcoast 2001 tidal database. Daily river flow for January 1992 is shown in figure 46. Wind speed and direction was entered to a longitude, latitude grid and interpolated in space onto the ADCIRC grid.

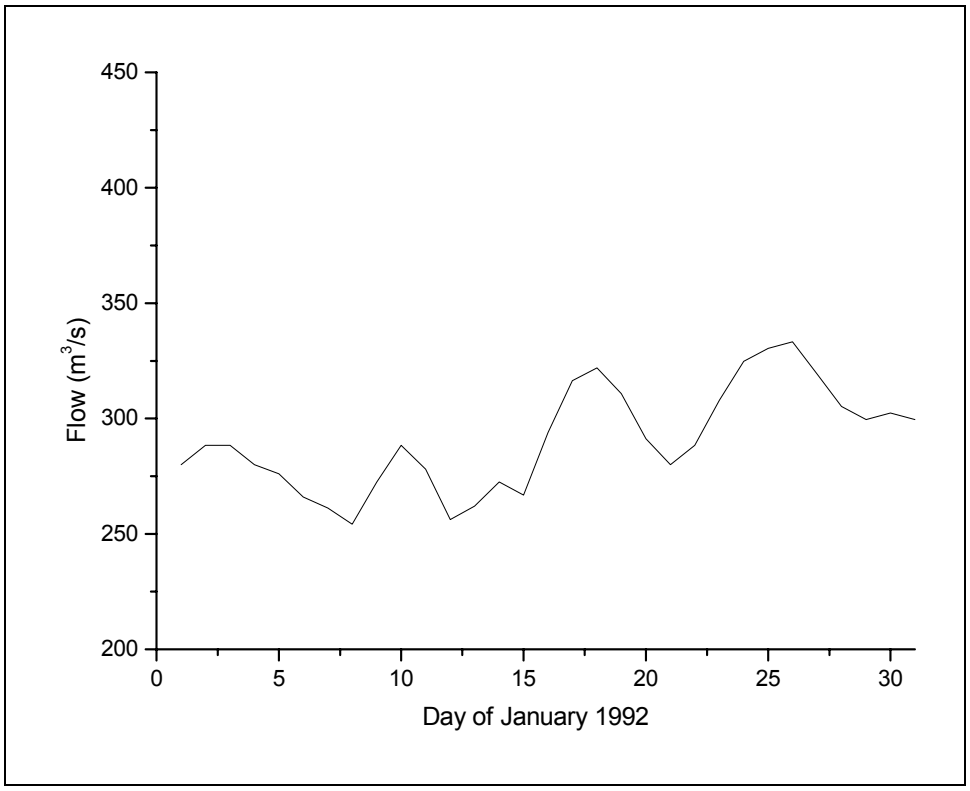

Figure 46. Daily discharge river flow for January 1992

The percent error between measured and calculated water level at Ft Pulaski was 7.

Comparison of measured and calculated water level at Ft Pulaski is shown in figure 48.

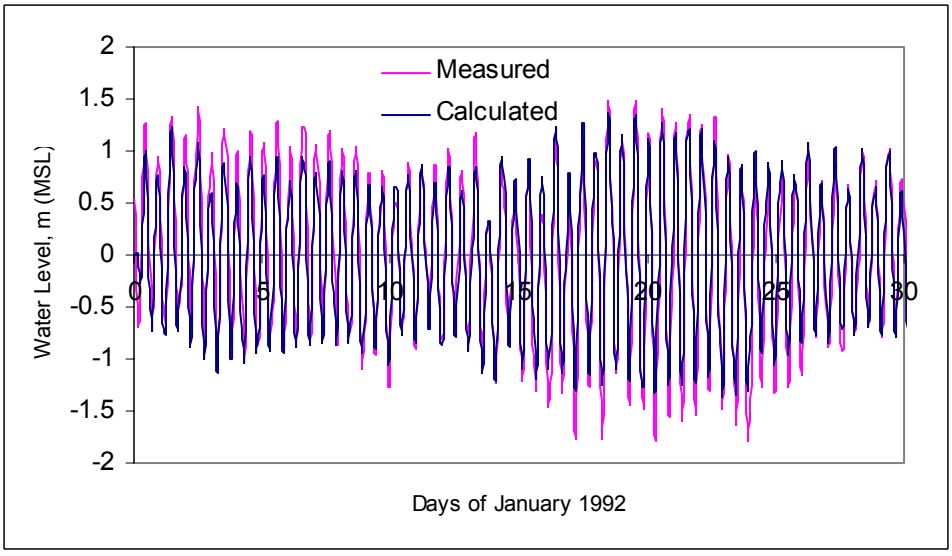

Figure 48. Comparison of measured and calculated water level at Ft Pulaski

Circulation patterns in the study area during peak flood and peak ebb flows are shown in figures 49 and 50 respectively.

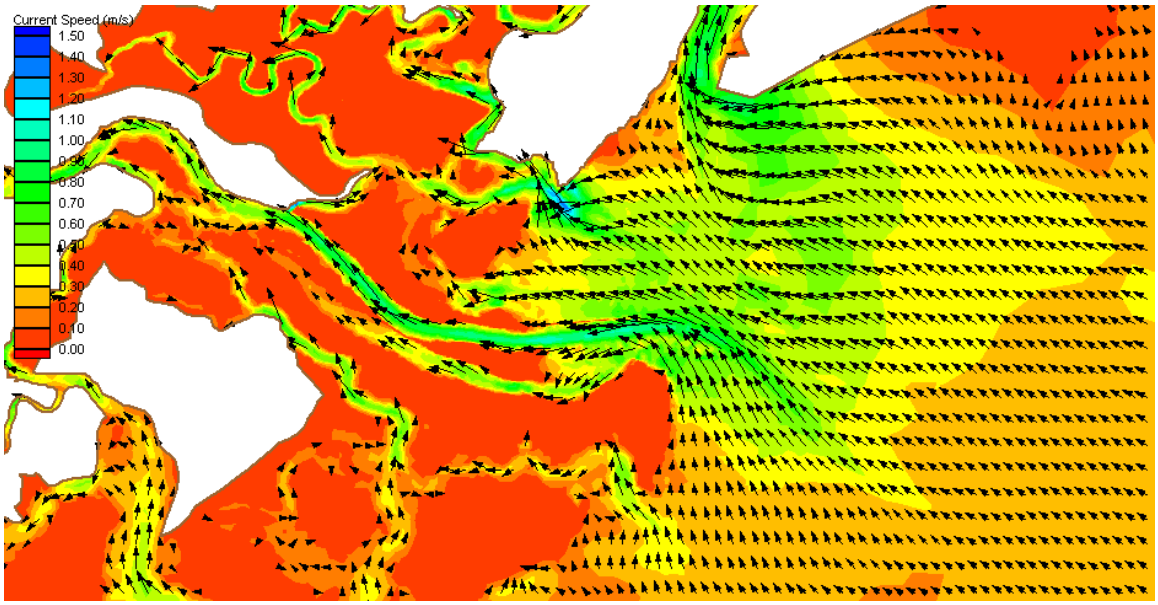

Figure 49. Circulation pattern in the study area during peak flood flow.

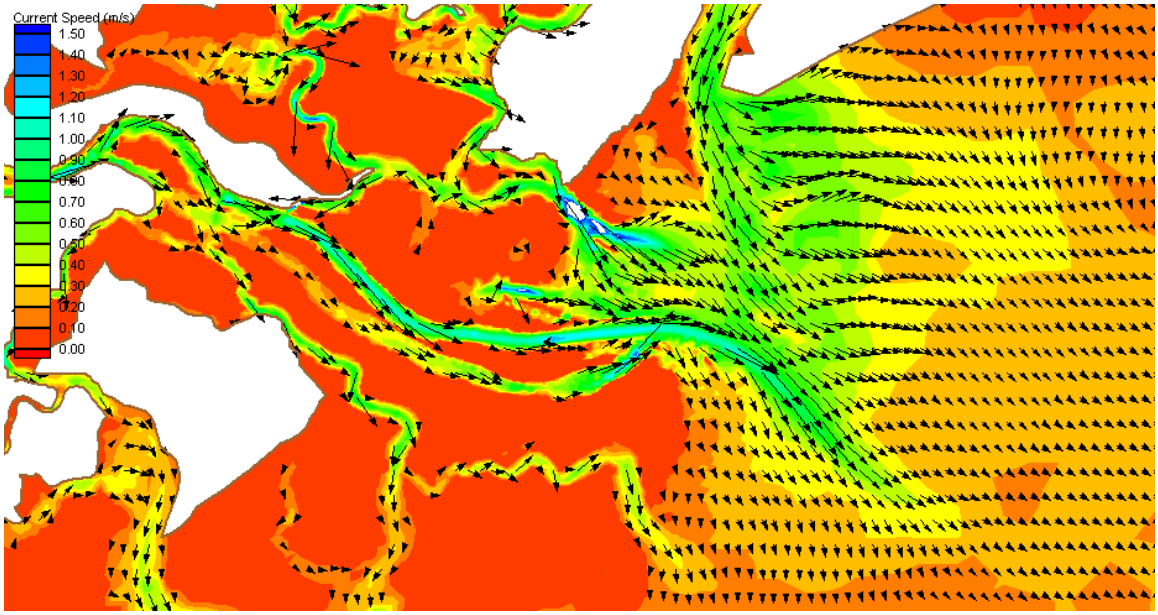

Figure 50. Circulation pattern in the study area during peak ebb flow.

Current speed and direction at the seven proposed study sites are shown in figures 51 through 57.

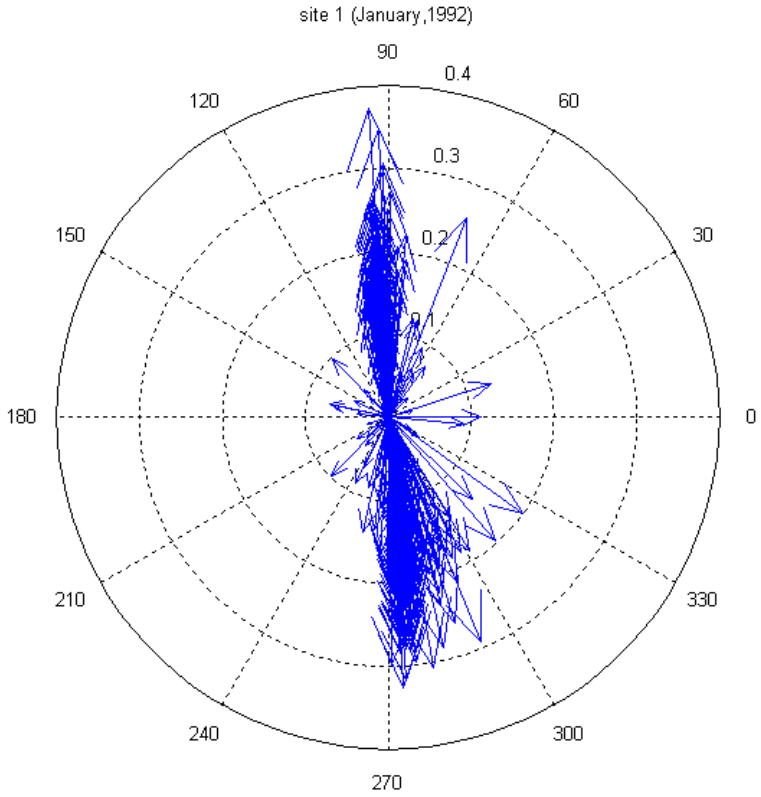

Figure 51. Current vectors at site 1 (current speed in m/s)

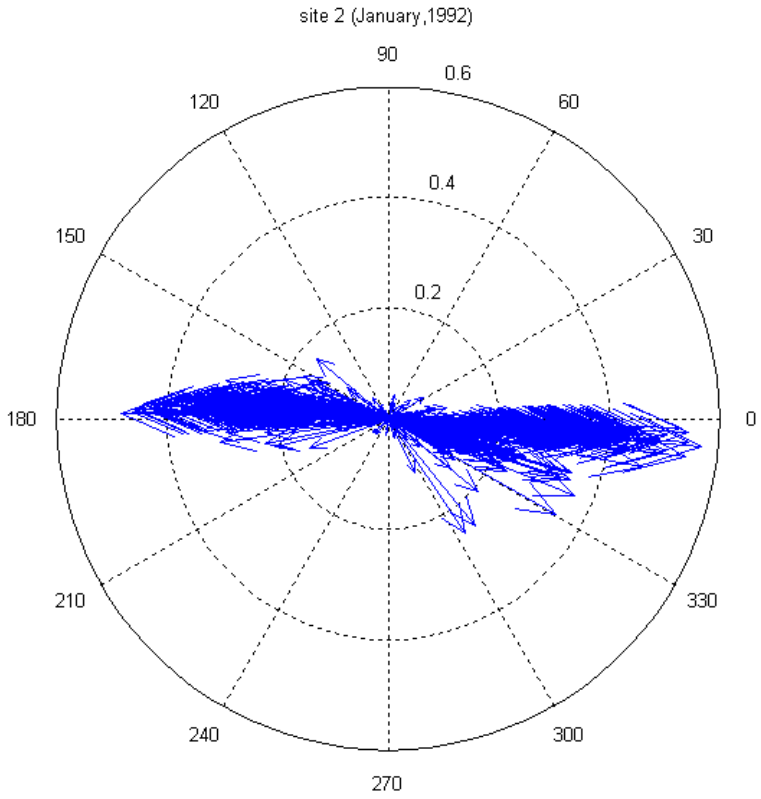

Figure 52. Current vectors at site 2 (current speed in m/s)

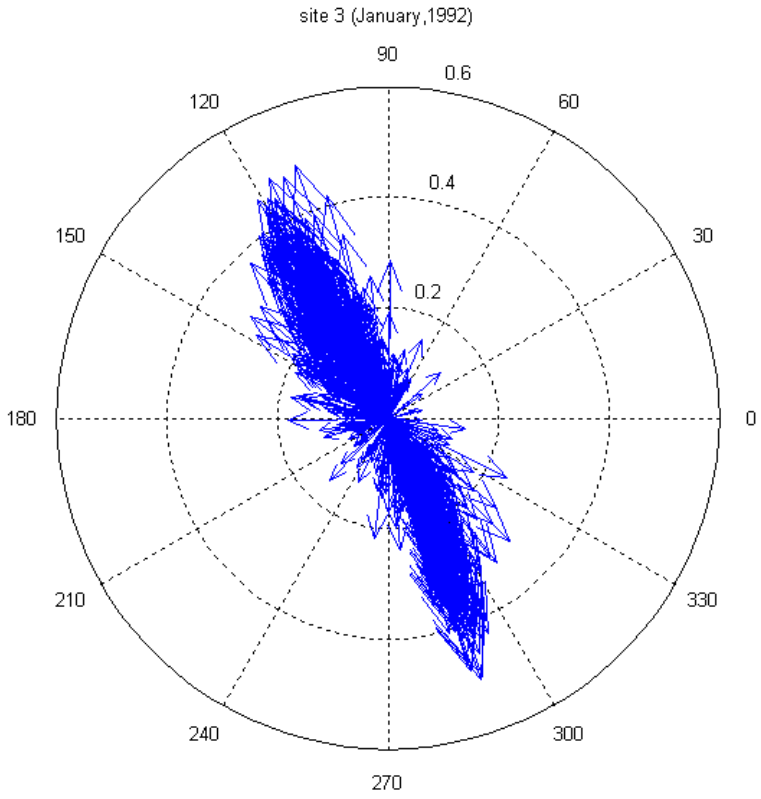

Figure 53. Current vectors at site 3 (current speed in m/s)

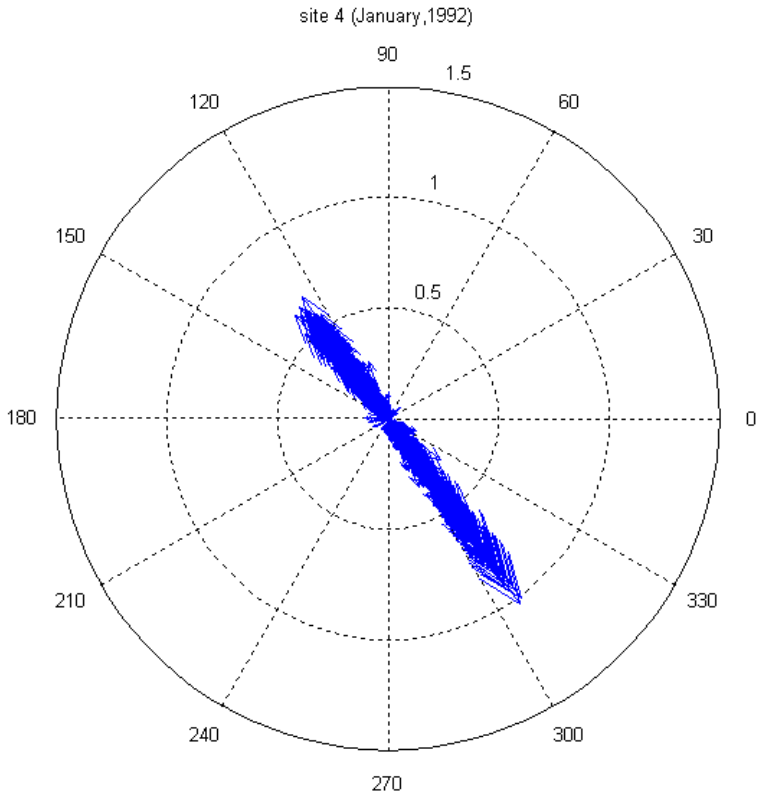

Figure 54. Current vectors at site 4 (current speed in m/s)

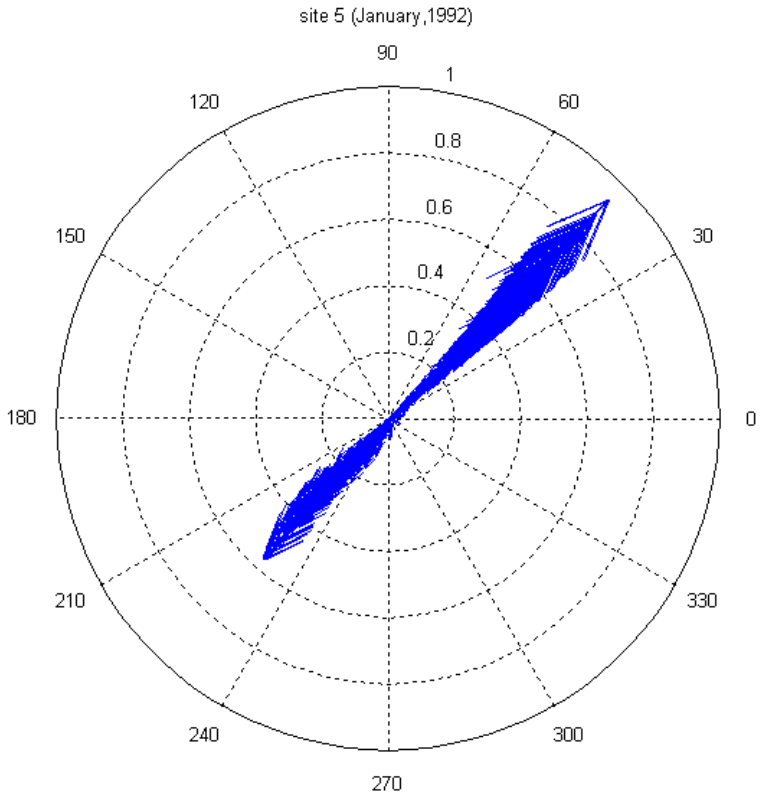

Figure 55. Current vectors at site 5 (current speed in m/s)

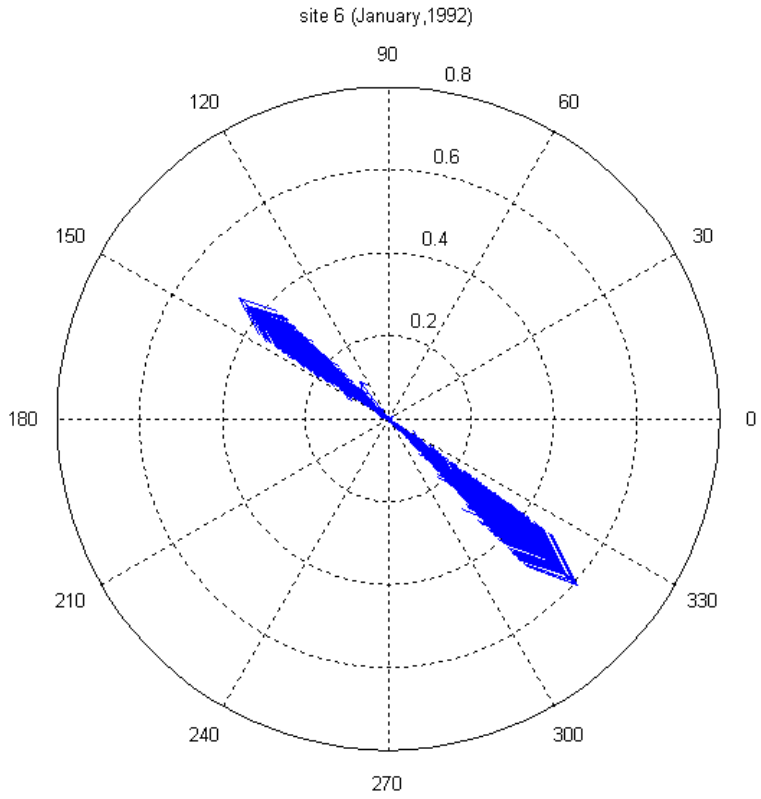

Figure 56. Current vectors at site 6 (current speed in m/s)

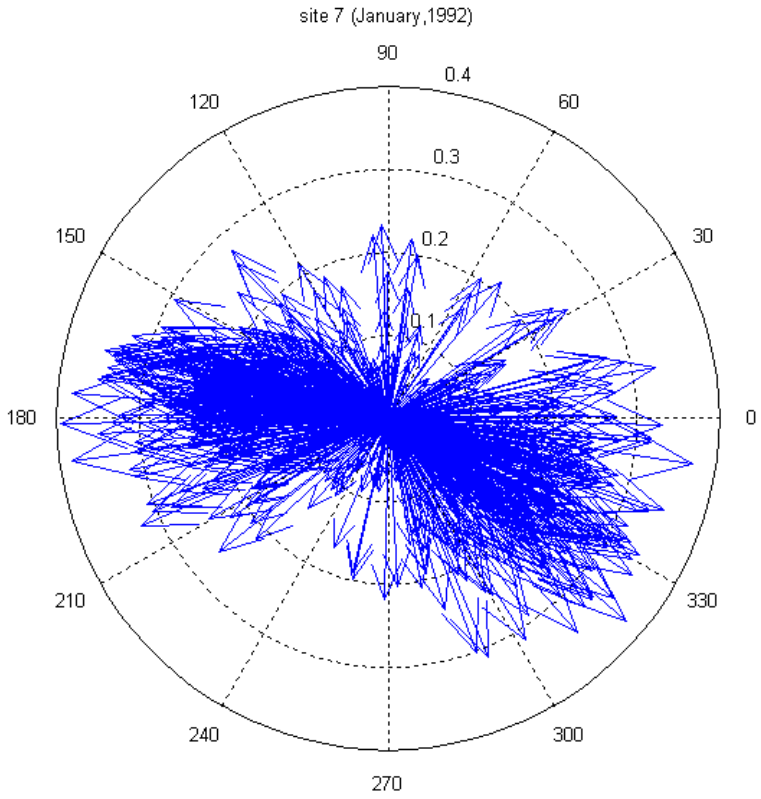

Figure 57. Current vectors at site 7 (current speed in m/s)

At site 1, the current is approximately parallel to the shoreline with maximum current speed of about 0.4 m/s. At site 2 the current is moving approximately parallel to the jetty with maximum speed of about 0.5 m/s. At site 3 the current is influenced by the tide (toward northeast and southwest) with maximum speed of about 0.5 m/s. At site 4 the current is mainly influenced by the tide with maximum speed of about 1.0 m/s and with net direction toward the southeast. At site 5 the current is parallel to the shore with net direction toward the northeast and with maximum speed of about 1.0 m/s. At site 6 the current is parallel to the shore with net direction toward the southeast and with maximum speed of about 0.6 m/s. At site 7 the current direction is influenced by the tide with maximum speed of about 0.4 m/s, but shows tendency for current movement toward the shore (northeast).

Simulation of One-Month Summer Period

ADCIRC was run for July 1999 as the one-month summer period. The ADCIRC model was forced with water level only. Water level was constructed from astronomical tidal constituents at the open ocean boundary for July 1999 obtained from the Eastcoast 2001 tidal database.

The percent error between measured and calculated water level at Ft Pulaski was 5.

Comparison of measured and calculated water level at Ft Pulaski is shown in figure 58.

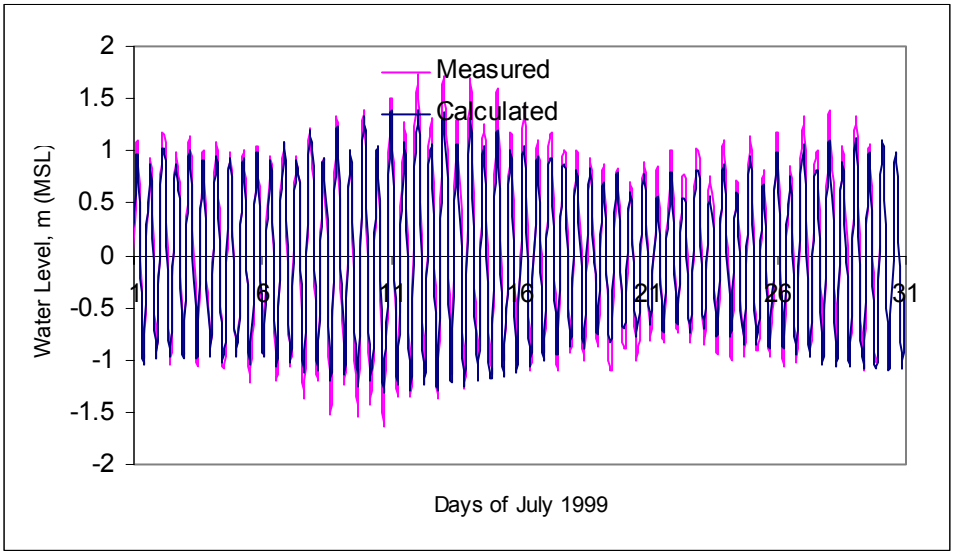

Figure 58. Comparison of measured and calculated water level at Ft Pulaski

Circulation patterns in the study area during peak flood and peak ebb flows are shown in figures 59 and 60 respectively.

Current speed and direction at the seven proposed study sites are shown in figures 61 through 67.

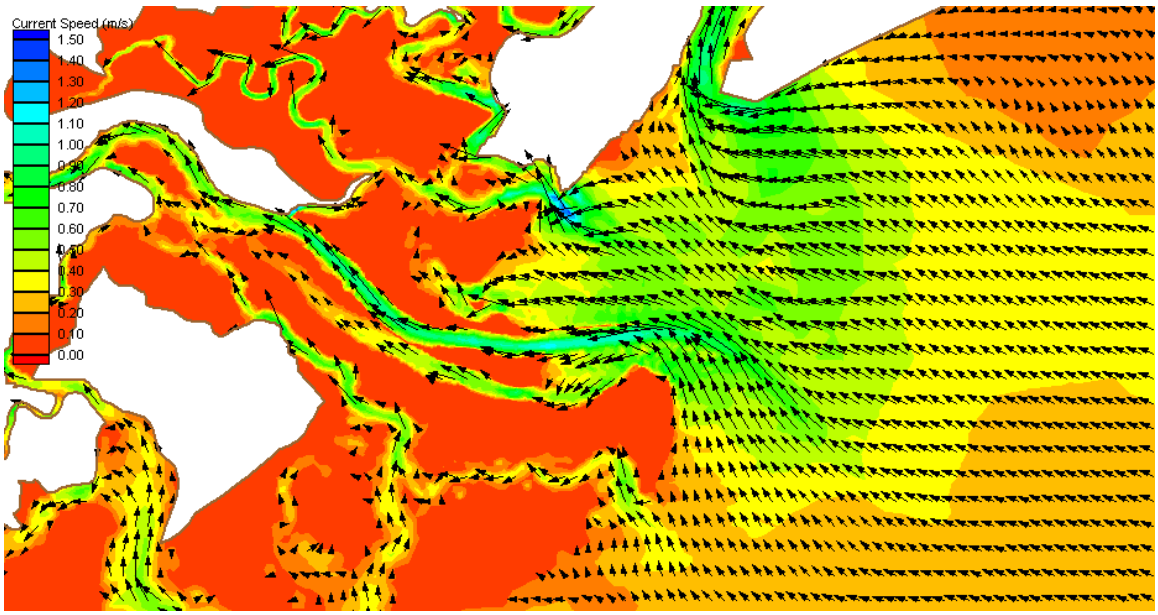

Figure 59. Circulation pattern in the study area during peak flood flow

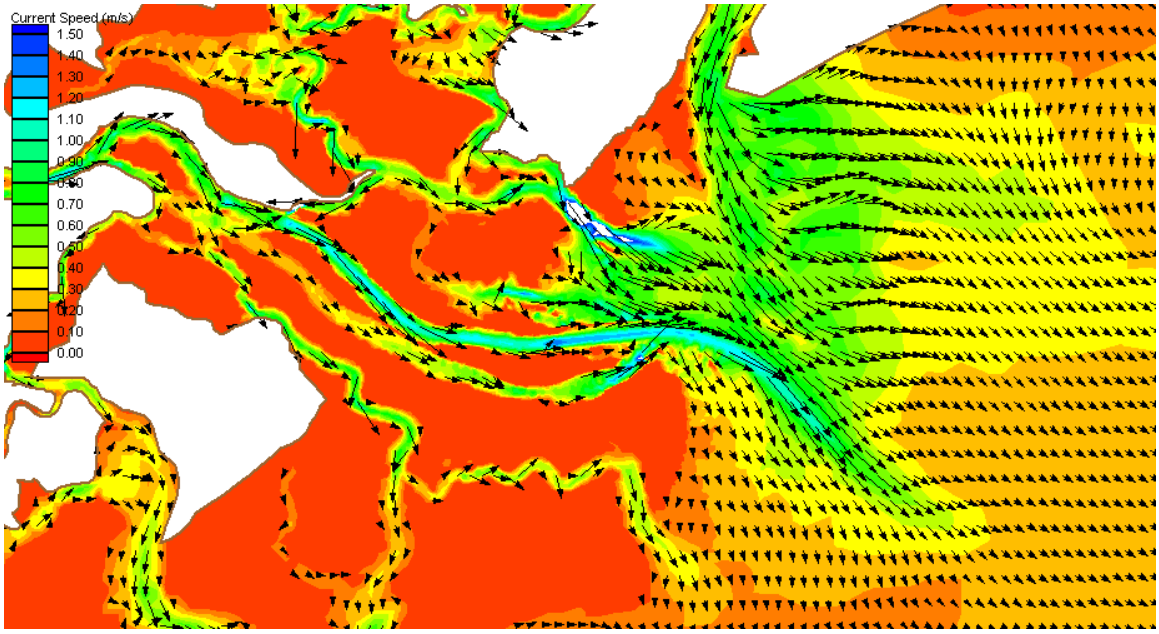

Figure 60. Circulation pattern in the study area during peak ebb flow

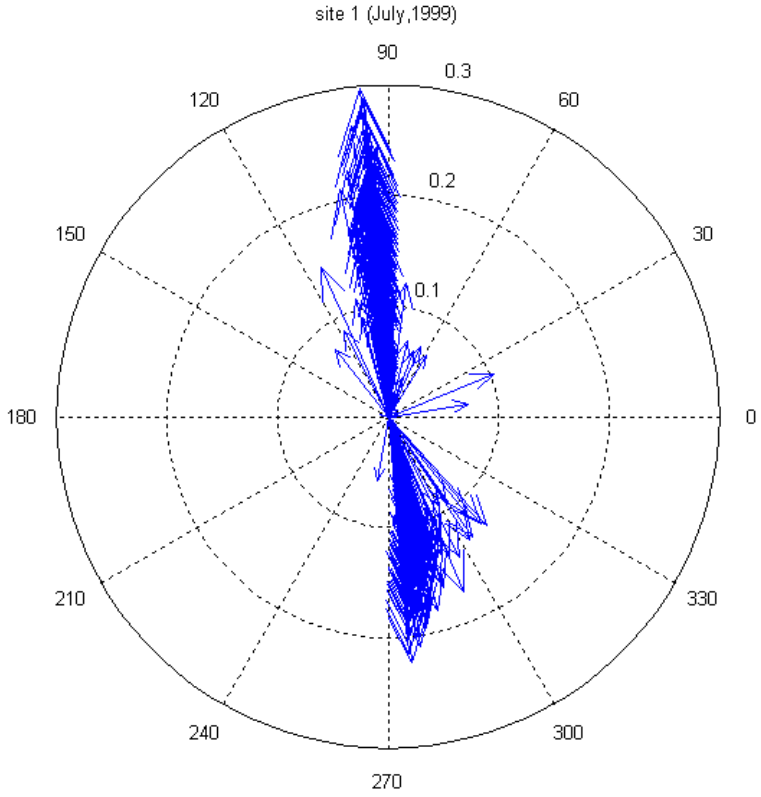

Figure 61 Current vectors at site 1 (current speed in m/s)

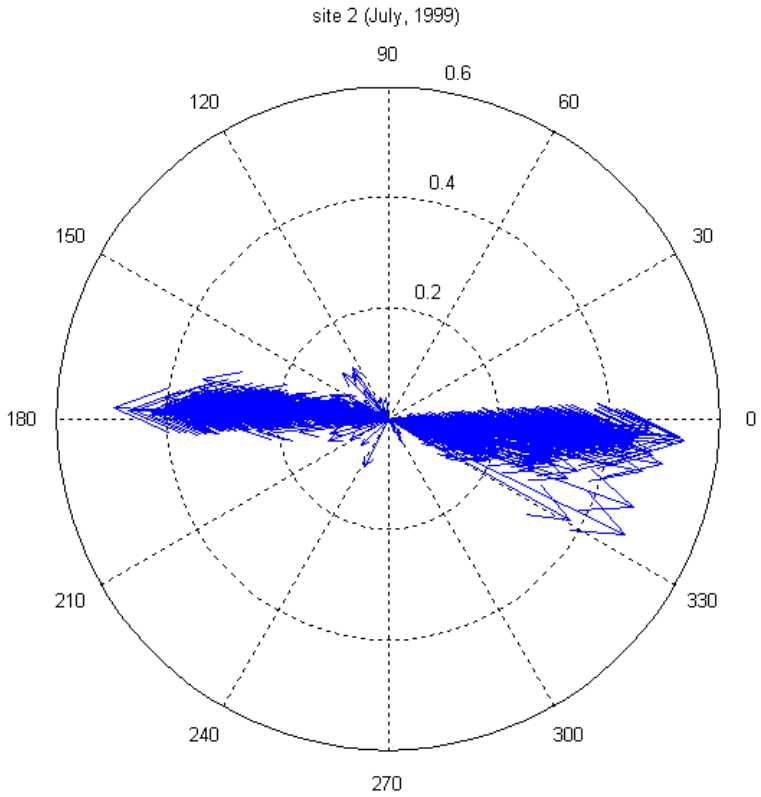

Figure 62. Current vectors at site 2 (current speed in m/s)

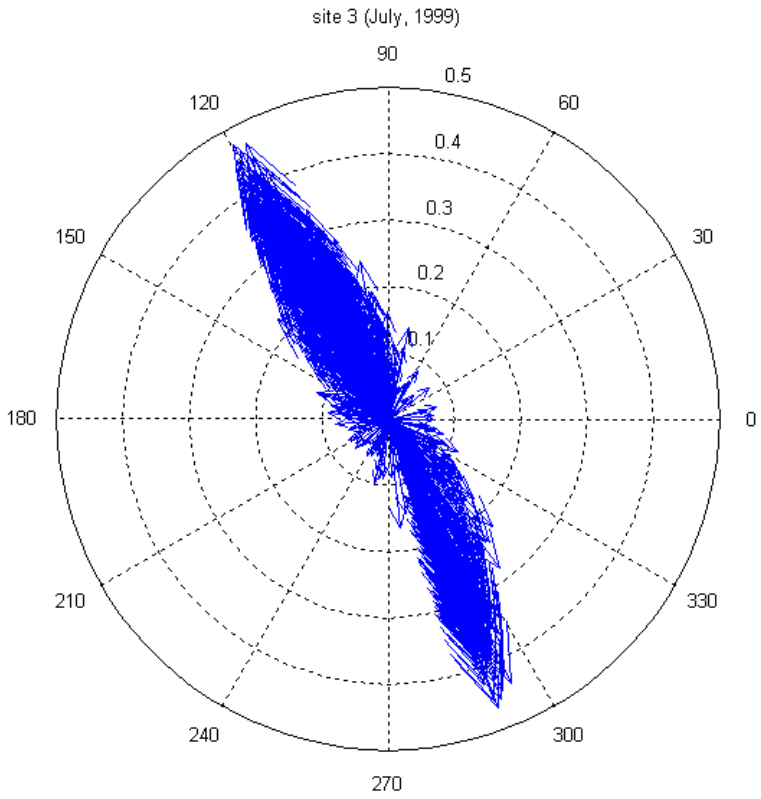

Figure 63. Current vectors at site 3 (current speed in m/s)

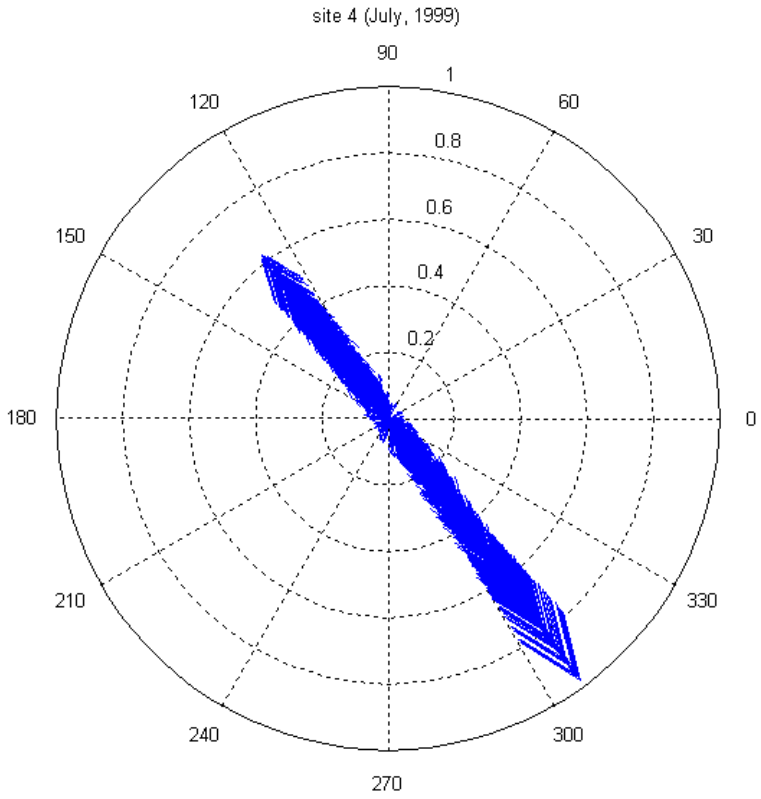

Figure 64. Current vectors at site 4 (current speed in m/s)

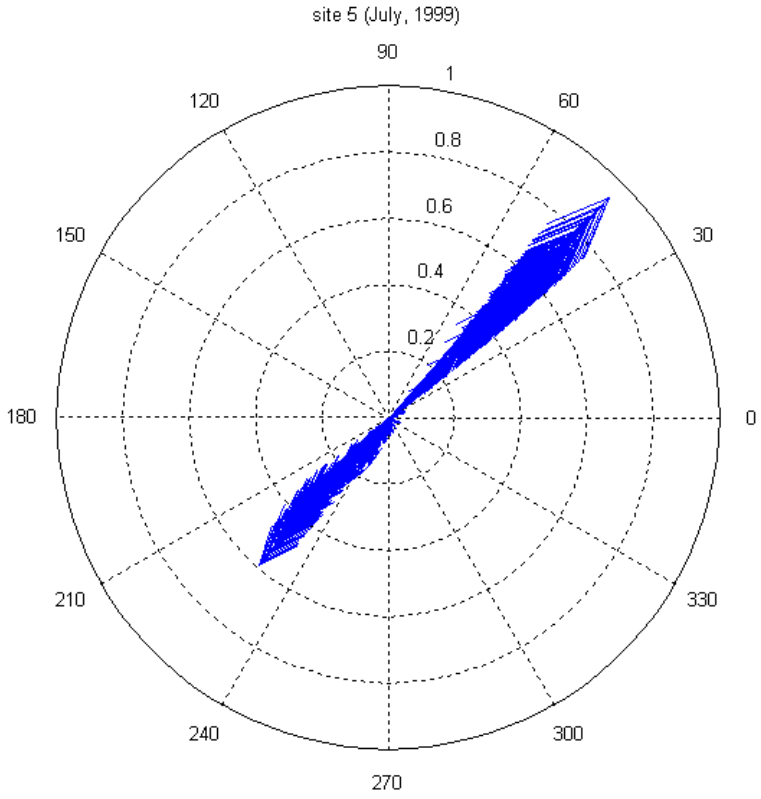

Figure 65. Current vectors at site 5 (current speed in m/s)

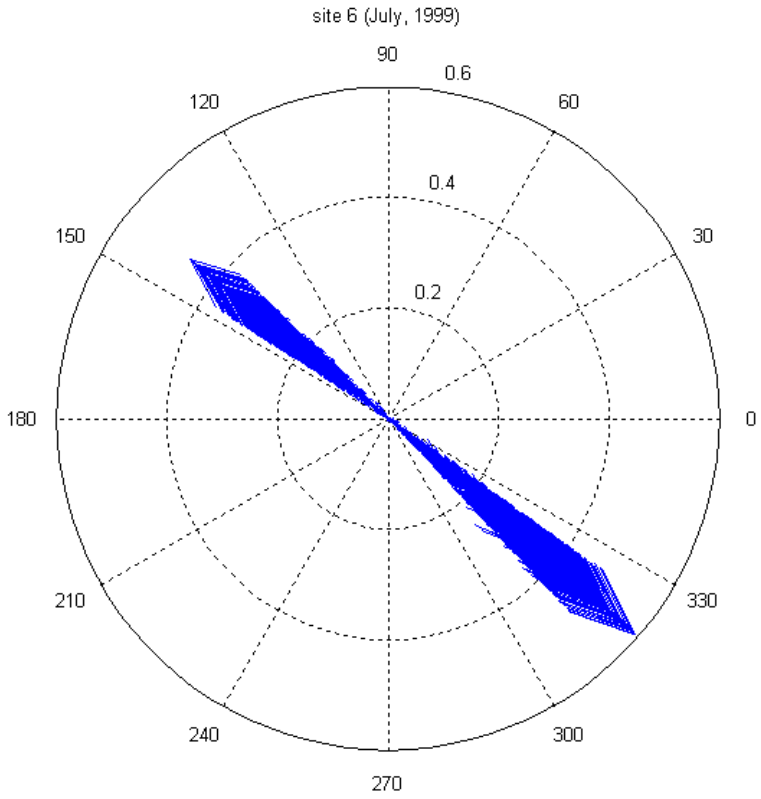

Figure 66. Current vectors at site 6 (current speed in m/s)

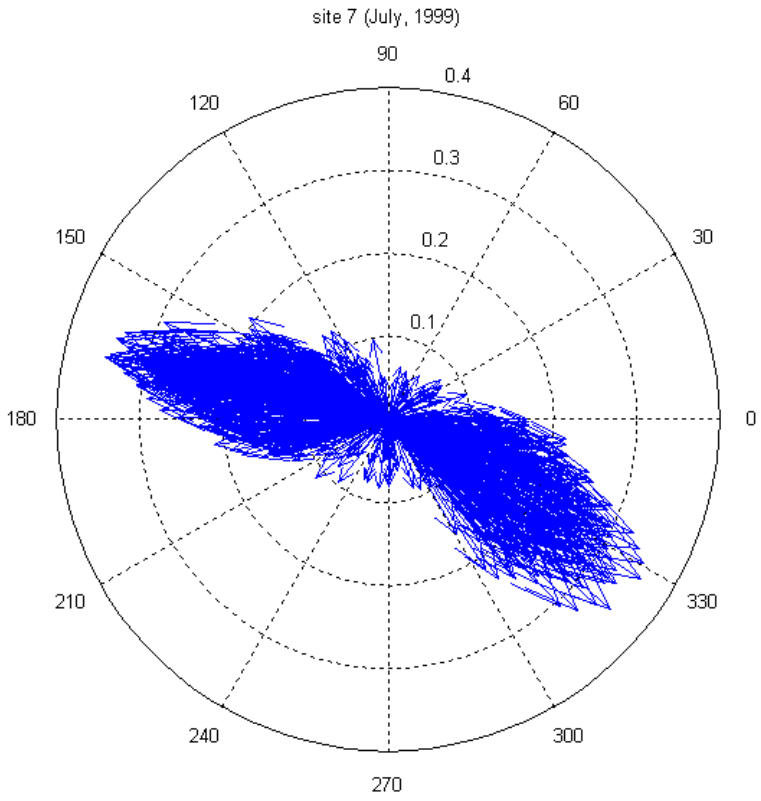

Figure 67. Current vectors at site 7 (current speed in m/s)

At site 1, the current is approximately parallel to the shoreline with maximum current speed of about 0.3 m/s. At site 2 the current is moving approximately parallel to the jetty with maximum speed of about 0.5 m/s. At site 3 the current is influenced by the tide (toward northeast and southwest) with maximum speed of about 0.5 m/s. At site 4 the current is mainly influenced by the tide with maximum speed of about 1.0 m/s and with net direction toward the southeast. At site 5 the current is parallel to the shore with net direction toward the northeast and with maximum speed of about 1.0 m/s. At site 6 the current is parallel to the shore with net direction toward the southeast and with maximum speed of about 0.6 m/s. At site 7 the current direction is mainly influenced by the tide with maximum speed of about 0.35 m/s.

Summary of ADCIRC Results

ADCIRC was calibrated for the period of December 1999. The model was used to simulate the flow during one extreme storm (Hurricane Hugo, 1989), one-month active period (November, 1979), one-month operational period (January, 1992) and one-month summer period (July, 1999).

Table 1 shows the percent error between measured and calculated water level at Ft Pulaski during the above mentioned simulation periods. Measured data was not available at Ft Pulaski during the Hurricane case and therefore the percent error was not calculated. The model shows good agreement between measured and calculated water level during all the simulations.

Table 1
Error in Calculated Water Level

Simulation	Percent Error
November 1979	5
January 1992	7
July 1999	5

Tables 2 through 8 show the maximum current speed and the predominant direction at the seven proposed study sites during each simulation period.

Table 2
Maximum Current Speed and Predominant Direction at Site 1

Simulation	Maximum Current Speed (m/s)	Predominant Direction
Hurricane Hugo	1.5	Parallel to shoreline
November 1979	0.4	Parallel to shoreline
January 1992	0.4	Parallel to shoreline
July 1999	0.3	Parallel to shoreline

Table 3
Maximum Current Speed and Predominant Direction at Site 2

Simulation	Maximum Current Speed (m/s)	Predominant Direction
Hurricane Hugo	0.8	Parallel to jetty
November 1979	0.6	Parallel to jetty
January 1992	0.5	Parallel to jetty
July 1999	0.5	Parallel to jetty

Table 4
Maximum Current Speed and Predominant Direction at Site 3

Simulation	Maximum Current Speed (m/s)	Predominant Direction
Hurricane Hugo	1.0	Influenced by the tide with strong current moving toward Tybee Island
November 1979	0.6	Influenced by the tide with current of 0.2-0.3 m/s moving toward Tybee Island
January 1992	0.5	Influenced by the tide
July 1999	0.5	Influenced by the tide

Table 5
Maximum Current Speed and Predominant Direction at Site 4

Simulation	Maximum Current Speed (m/s)	Predominant Direction
Hurricane Hugo	1.5	Influenced by the tide with net direction toward southeast
November 1979	1.2	Influenced by the tide with net direction toward southeast
January 1992	1.0	Influenced by the tide with net direction toward southeast
July 1999	1.0	Influenced by the tide with net direction toward southeast

Table 6
Maximum Current Speed and Predominant Direction at Site 5

Simulation	Maximum Current Speed (m/s)	Predominant Direction
Hurricane Hugo	1.3	Parallel to shore with net direction toward northeast
November 1979	1.0	Parallel to shore with net direction toward northeast
January 1992	1.0	Parallel to shore with net direction toward northeast
July 1999	1.0	Parallel to shore with net direction toward northeast

Table 7
Maximum Current Speed and Predominant Direction at Site 6

Simulation	Maximum Current Speed (m/s)	Predominant Direction
Hurricane Hugo	1.2	Parallel to shore with net direction toward southeast
November 1979	0.65	Parallel to shore with net direction toward southeast
January 1992	0.6	Parallel to shore with net direction toward southeast
July 1999	0.6	Parallel to shore with net direction toward southeast

Table 8
Maximum Current Speed and Predominant Direction at Site 7

Simulation	Maximum Current Speed (m/s)	Predominant Direction
Hurricane Hugo	1.5	Tidal with strong current moving toward northeast
November 1979	0.45	Tidal with strong current moving toward northeast
January 1992	0.4	Tidal with some current moving toward northeast
July 1999	0.35	Tidal

Highest current speed occurred during the hurricane case at the seven sites as expected. Lowest current speed values were observed during the calm period of July where the model was forced with water level only. The tendency for current to move toward the shore increased during the storm and the active period at sites 3 and 7.

References

Donnell, B. P., Letter, J. V., McAnally, W. H., and Roig, L. C. 1996. “User’s guide for RAMA2 Version 4.3, ”U S Army Engineer Waterways Experiment Station, Vicksburg, MS.

Luettich, R. A., Westerink, J. J., and Scheffner, N. W. 1992. “ADCIRC: An advanced three-dimensional circulation model for shelves, coasts, and estuaries; Report 1, Theory and methodology of ADCIRC-2DDI and DCIRC-3DL,” Technical Report DRP-92-6, U.S. Army Engineer research and Development Center, Vicksburg, MS.

Militello, A. 1998. “Grid Development for Modeling Two-Dimensional Inlet Circulation,” ERDC/CHL CETN IV-14, U S Army Engineer research and Development Center, Vicksburg, MS.

Militello, A. and Kraus, N. 2001. “Shinnecock Inlet, New York, site Investigation, Report 4, Evaluation of Flood and Ebb Shoal Sediment Source Alternatives for the west of Shinnecock Interim Project, New York,” U S Army Corps of Engineers, Coastal Inlets Research Program.

Mukai, A. W., Westerink J. J., Luettich, R. A. 2002. “Guidelines for Using Eastcoast 2001 Database of Tidal Constituents within Western North Atlantic Ocean, Gulf of Mexico and Caribbean Sea,” ERDC/CHL CETN IV-40, U S Army Engineer research and Development Center, Vicksburg, MS.

4 Sediment Transport

A primary component of the Savannah Harbor study is assessing various placement locations. Specifically of interest is Tybee Island littoral zone placement of dredged material. The goal of this effort would be to nourish the nearshore profile and the associated potential for beach nourishment. Additional issues include re-handling of dredged material placed near the channel and separation of fine from coarse material after nearshore placement. This chapter describes laboratory experiments and modeling efforts to estimate erosion and transport rates of dredged material placed in the region between Tybee Island and the ship channel. The simulations of sediment transport described in this chapter rely heavily on the estimated environmental conditions at the site, specifically the STWAVE wave simulations (Chapter 2) and the ADCIRC circulation simulations (Chapter 3) presented earlier.

This chapter is divided into five sections. The first section describes available field data on ebb shoal evolution and dredging history from the ship channel. This section includes description of laboratory experiments performed to estimate erosion rates of dredged material. These sediments are a mixture of sand, silt, and clay. Therefore, their behavior cannot be described using routines for sand transport and site-specific erosion experiments are required. The second section describes proposed placement sites for analysis developed by SAS and ERDC. The third section describes the effects of these berms on nearshore placement. GENESIS (Hansen and Kraus 1989, Gravens et al. 1992) model simulations predict longshore transport at the Tybee Island surf zone and the resulting surf zone transport changes due to nearshore mound placement. The fourth section describes sediment transport modeling from proposed berms and in the nearshore region using the GTRAN model. The first part of this section describes GTRAN simulations for possible mound configurations in the river, near the channel, and between Tybee Island and the channel. The second part describes GTRAN simulations of sediment transport patterns over the entire nearshore Tybee region. The original scope of work required simulation of operational and storm one-month periods. However, further analysis of data from the selected months indicated that they may not be representative of long-term conditions. Therefore, additional 24-year simulations of waves and tidal currents only (no wind-driven current) were added to this section. . The final section provides analysis of model results and recommendations for nearshore placement based on the historical data and modeling.

Historical Data

SAS provided ERDC data on ebb shoal evolution from 1852-present, dredging records from 1998-2001, and placement records for the existing offshore placement site. In addition, sediment grain size distributions were provided and this effort included sediment erosion analysis. These data are described in this section because of their relevance to proposed nearshore placement of dredged material.

Dredging records

SAS provided ERDC with dredging records from the base of the north jetty out to the end of the channel for the years 1998-2001. Information provided in this section is reported in English, not metric, units so it remains consistent with the SAS data files and navigation charts. Dredging volumes for these four years were divided into five sections (Figure 4-1): channel stations 0-14 (0-14,000 ft from the base of the north jetty); stations 14-20; stations 20-30; stations 30-40, and stations 40-60. Figure 4-2 provides the dredging volume from each reach for each year. Between 500,000 yd^3 and 1,200, 000 yd^3 were dredged each year. Approximately 3.4 million yd^3 was dredged during the four years, or an average of 850,000 yd^3 annually. Excluding 1998, average annual dredging was approximately 500,000 yd^3.Over 40% of the dredging during the four years was between stations 30-40. Over 1.5 million yd^3 was dredged from this section during the four years. Virtually no dredging occurred beyond station 40. The high volume of dredging in this reach is probably caused by a combination of factors, the two most dominant being longshore transport from the north and deposition of material flowing through the channel as the current velocities decrease (see Chapter 2, ADCIRC simulations). Station 0-14 channel infilling is dominated by river sediment. Stations 14-30 are a combination of river sediment and longshore transport.

Long-term analysis of dredging records performed by ATM (Applied Technology Management Inc., 2001) for the Georgia Port Authority indicated that the annual average dredging from the ebb shoal to maintain navigable depth is approximately 510, 000 yd^3. Volume of maintenance material dredged in the bar channel was large (2M yd^3) for the first year of 44 ft maintenance (1995), but averaged approximately 500,000 yd^3 between 1996 and 1998. This would indicate that the 1998-2001 record described here is similar to findings of ATM. The sediment processes influencing the first four reaches (Figure 4-2) will be described in more detail later in this chapter.

Sediment Bed

The dredged material at the Savannah site can be generally classified into two types, cohesive and non-cohesive. The cohesive bed material has erosion resistance greater than the simple self-weight of larger, non-cohesive sediments. Cohesive sediments are a mixture of both cohesive and non-cohesive particles.

Definition of cohesive particles is dependent on water and sediment properties such as chemistry and mineralogy, but a general definition that can be applied is that sand-size particles are non-cohesive, clay-size particles are cohesive, and silt-size particles may or may not be cohesive. As will be described later, whether a sediment mixture of sand/silt/clay behaves cohesive is also dependent on many factors.

Non-Cohesive Sediments. Non-cohesive, or sand, erosion is characterized by a particle-by-particle nature. Transport potential of non-cohesive sediments is a function of the mass of the particles in the bed and the applied bottom shear stresses. Most of the particles roll or move by saltation along the bottom. Only under high-energy conditions is there a significant amount of suspension. Even under high wave energy, the majority of suspended sand re-deposits over each wave cycle during the backward velocity under the trough. The mechanics of non-cohesive sediment transport results in a phenomenon called armoring. Armoring starts with the winnowing of fine-grained particles (silt and clay) out of the sediment bed and into suspension. These fine-grained particles cannot deposit because of the high-energy due to waves and are carried away by currents. This leaves a layer of sand, moving as bedload, behaving as a sheet of sand protecting the bed underneath. As wave/current energy increases, more fine sediments are winnowed from the underlying stable bed.

Cohesive Sediment. Cohesive sediment transport potential is not solely a function of particle size. Rather, the inter-particle electro-chemical forces control the behavior of transport. These forces, and thus transport rate and mechanism, is a function of many factors, including grain size distribution, bulk density, chemistry, organic content, and mineralogy. Under some conditions, electro-chemical bonds influence predominately sand beds if sufficient fine material lies between the sand particles. These fine particles behave as a cementing agent for the sand particles. Depending on mineralogy and other factors, a predominately clay bed can be much more resistant to erosion than sand. However, the mechanisms of transport between fine-grained particles and sands also differ. The fine-grained clay and silt moves as suspended load, while the sand moves as bedload or combined bedload and suspended load. The clay and silt are not in frequent contact with the bed once suspended. Therefore, they do not armor the bed like sand particles moving as sheet flow.

Sediment grain size and spatial distribution

Several data sets describing grain size distribution on the ebb shoal and in the channel have been collected in recent years. ATM (2001) provides a detailed discussion of grain size distributions over the entire ebb shoal, including the channel. All data sets indicate that the majority of material in the channel is sand. However, the study described below (and included in the ATM study) indicates that the material is far from uniform. Rather it is stratified, with layers of mud intermingled with the sand.

In 1998, Law Engineering Inc. sampled surface sediments between the jetty and the offshore terminus of the channel. Forty locations were sampled. Table 4-1 summarizes the percent sand and mean grain size for each core sample. These

samples indicate that most locations are predominately sand. These samples also indicate that little of the material would be classified as beach quality (greater than 88% sand). Placing this material at offshore disposal sites would isolate the sand fraction from the littoral system. One concept discussed in this section is that placement in the nearshore will emulate processes under a non-controlled river. Specifically, mixed material will move into and deposit in the nearshore during calm conditions. A combination of wave and tidal forces during higher energy events will winnow the fine material, which will then move offshore.

In winter 2001, shallow core samples were collected at six locations in the navigation channel. The sample locations are indicated in Figure 4-3. Approximately 50 gallons of sediment were extracted from each site. Table 4-2 summarizes the sediment grain size distributions and percentile diameters from sample slurry analysis. Figure 4-4 provides the complete distribution for each sample. These are the sediments that were used for erosion experiments described in the next section. It can be seen that the percent sand for the Law Engineer studies differ somewhat from those performed in this study. This is not unexpected for samples of channel infilling material, where the grain size distribution is a function of many time varying factors, including time history of prior hydrodynamics and river loadings. However, in general, the samples collected between station 17 and 62 will be predominately sand and therefore may be utilized in nourishing the littoral zone.

Erosion rate data

The balance of gravity forces and drag forces on individual particles governs mobilization and transport of non-cohesive sediments. With silt and clay (cohesive sediment), the interparticle forces become important to sediment bed erosion resistance, particularly for the case of well-consolidated sediments with tightly packed particles. There exists a fraction (by weight) of fine particles at which a mixed sand/silt/clay bed will behave cohesively. This fraction is variable, dependent on particle and bed conditions. There are no established relationships between the physical properties and mineralogy of cohesive sediments and sediment mobility. The erosion resistance of silt and clay is highly variable, site-specific, and typically varies with erosion of the bed below the water-sediment interface due either to stratification or increasing bulk density, which increases the interparticle forces. To address the site-specific nature of sediment mobility of the mixed sediments filling the navigation channel, a sediment erosion study was conducted. This study is required to determine the mobility of dredged material placed in the nearshore.

SEDFLUME is a false-bottom flume that allows the determination of shear-stress/erosion relationships of minimally disturbed sediment samples. Figure 4-5 presents a schematic that indicates the fundamental operating principles of SEDFLUME. A vertical core collected from the sediment bed is inserted into the false bottom of the flume and is positioned such that the sediment surface is flush with the channel bottom. A pump-and-valve system on the flume allows the operator to control the flow rate and corresponding bottom shear stress across the surface of the sediment core. This shear stress is applied for a length of time and

the sediment core is advanced such that the sediment surface remains flush with the channel bottom. The distance that the core was advanced divided by the time that the shear stress was applied indicates the erosion rate at a given level in the sediment core. As the sediment core is eroded, this procedure is repeated with a stair-stepped approach that results in erosion rates over a range of shear stresses and depths. For these experiments, an additional segment of test section was attached to the exit of SEDFLUME. This addition included bottom traps that collect sediment traveling as bedload. These bedload samples, collected after each shear stress test, permit evaluation of separation of fine from coarse sediment as the mixed sediment bed erodes. Sediment bulk property samples were collected from a comparable core consolidated in the same manner as the erosion core. Data from the erosion and bulk property cores are then used to relate sediment properties and the erosion rate data. A detailed description of the SEDFLUME study is presented in Appendix A.

Sediment samples were collected at the locations labeled in Figure 4-3. The samples were individually slurried and poured into coring tubes. Six cores were poured for each site. These cores were then permitted to consolidate. Consolidation periods were 4 days, 20 days, and 120 days. After seven days, two of the cores were removed from the refrigerator. One was eroded in SEDFLUME and shear-stress/erosion relationships were determined for each core. The other core was used to develop bulk density profiles for the sediment core. Data from the two cores were combined to develop relationships between erosion rate, shear stress, and bulk density. The final equations are of the form:

$$E = A\tau^n \rho^m \tag{4-1}$$

where A, n, and m are site-specific parameters resulting from data regression, E is the erosion rate (cm/s), τ is the shear stress (dynes/cm^2) and ρ is the sediment bed bulk density (g/cm^3). The second core is used to develop values for bulk density values at intervals below the original sediment/water interface This equation is coupled with these bulk density values within GTRAN to estimate erosion rates under specified wave-current shear stress and the change in these erosion rates with depth below the mound surface. The erosion rate data served to represent the erosion resistance and transport reduction caused by the cohesive nature of the dredged material sediment mounds.

Figure 4-6 presents the erosion-rate/bulk density relationships developed for SEDFLUME analysis of site 78s sediments. The impact of bulk density on erosion rate is seen here by the parallel lines, which relate bulk density to erosion. A 10% change in bulk density caused an order of magnitude change in erosion rate for a specified shear stress for sediments at this site. Coupled with bulk density profiles measured from the cores, sufficient data exist to define erosion of mound material as a function of surface shear stress and distance between the existing surface layer and the original surface layer. Other cohesive samples behaved the same way, although the exact relationship is site specific. Cores that behave non-cohesively do not show any relationship between bulk density and erosion rate. The erosion rate is similar at any bulk density and the parallel lines in Figure 4-6 would have near zero slope. Sediments behaved as a non-cohesive bed at locations 17 and 62 (Figure 4-3).

The bedload traps attached to SEDFLUME for these experiments indicate that separation of fine from coarse material occurs almost instantaneously with erosion of the ebb shoal channel dredged material. Table 4-3 shows example grain size distribution for the eroded core and the material collected in the bedload traps. This table also shows percent of total material eroded that was trapped. It can be seen that for material collected outside the jetties (not including site 38N), the modest fraction of fine material less than .08 mm was reduced significantly. The trapped material from the offshore sites is 4-20% less silt/clay than the original material. The percent of fine material remaining in the traps ranged from 2-21% in the traps verses 6-41% in the cores. The core at 38N (in the river) eroded as small aggregates and the grain size distribution of trap material is similar to core sediment. This indicates no separation of fine and coarse material during the erosion process.

A general guideline for beach fill (beach quality material) is 88-90% sand (*****). All tested offshore channel sediments showed a smaller percent fine material in the bedload trap than in the original core. This indicates that fine and coarse grains are separated during erosion of the mixed sediment bed. Fine material moved in suspension and coarse material as bedload. These experiments also indicated that erosion, and therefore release of fine material, will occur at moderate rates. Specifically, the bed will not experience mass failure at one time. This type of mass failure could cause turbidity plumes of unacceptable magnitude. The steady release of fines from the bed will result in modest turbidity plumes during storm events. Quantification of turbidity plumes would require a complex modeling application beyond the scope of this project. However, it should be noted that turbidity, even in nearshore regions, is elevated during storms in most East Coast locations. Sources of the sediment include nearby inlets and rivers, and offshore deposits.

Potential Sites for Nearshore Placement of Dredged Material

Early in the study, 12 potential sites for dredged material placement were identified, primarily from the perspective of economic and convenient dredged material placement. The initial placement alternatives are referred to as Berms 01-12 in Figure 4-7a. Following initial assessment of Berms 01-12 and general transport trends over the ebb shoal, Berms 13 and 14 were added to the group of alternatives. Figure 4-7b presents mean lower low water (MLLW) crest elevation, surface area of the mound footprint, and volume of material contained within the mound. The mound volume given is the maximum capacity of the mound with the given footprint, crest elevation, and existing bathymetry.

Three candidate placement locations (Berms 10-12) are considered estuarine environment. Berms 10 and 11 are long, narrow areas near the channel and represented as uniform, 1-m thick veneers of dredged material. Berm 12, near the north tip of Tybee Island was approximated as a mound with 3.0-m MLLW crest elevation placed over a natural depression in the existing bathymetry.

Two candidate placement locations (Berms 8 and 9) are located adjacent and immediately north of the north jetty. Berm 8 is a smaller but thicker placement extending 480 m west of the north jetty tip. Berm 9 covers a larger area with a smaller thickness, extending 770 m west of the north jetty tip.

Candidate placement locations in the nearshore region of Tybee Island include Berms 01 through 07 and Berms 13 and 14. Berm 01 and 02 are large berms, with capacity of 766,000 and 451,000 m^3 of dredged material, respectively. Berm 01 is located closer to shore (approximately 750-1300 m from the north Tybee shoreline) and is placed on top of the ebb shoal platform in 3-4 m ambient water depths MLLW. Berm 02, located 900-1700 m from the north Tybee shoreline is in 3-4 m ambient depths.

Berms 03 through 05 are channel-adjacent alternatives and are attractive from the perspective of low dredged material handling costs. Berms 03, 04, and 05 would contain between 237,000-412,000 m^3 of dredged material and are located in 4-7 m ambient water depths MLLW distributed along the outer reaches of the navigation channel.

Berms 06 and 07 share the same footprint, with variation only in crest elevation and capacity. These berms are located offshore of central Tybee Island in ambient depths of 4-5 m. It is assumed that a shallow draft split-hull scow or hopper dredge could potentially place material economically in this site as it is located 1800-2200 m from the navigation channel. Anticipated advantages of this placement location are the reduction of the potential for sediment rehandling, and proximity to the shoreline where sediment may feed the littoral system and benefit the Tybee Island shoreline.

Berms 13 and 14 are placed 2700-3700 m from the channel immediately offshore of central Tybee Island, adjacent to and merging with the existing transverse attachment bar. The primary difference between the two berms is the variation in footprint size and site capacity. Concerns of such nearshore placement are cost (because of the longer transport distance for a pipeline dredge) and potential negative impacts to the Tybee Island shoreline arising from wave refraction over the nearshore feature. Potential benefits include a more effective sediment source for Tybee Island.

With this wide range of alternatives for nearshore placement defined, sediment transport modeling simulations were performed to 1) evaluate the effects of nearshore berms on shoreline change, 2) assess the likelihood of dredged material re-entering in the navigation channel, and 3) determine the relative potential of dredged material serving as a source of sand to the Tybee Island littoral zone.

Effects of Nearshore Berms on Shoreline Change

The placement of dredged material in the nearshore is proposed as a potential benefit to the Tybee Island shoreline by supplying sediment to the littoral system. However, there are potentially negative impacts to shoreline change arising from wave refraction patterns produced by the nearshore berms of dredged material.

The morphological shape of Tybee Island's ocean shoreline is significantly influenced by refraction of waves over the ebb shoal present offshore. Changes in bathymetry on this ebb shoal (through dredged material placement) may introduce changes to the Tybee Island shoreline. Evaluation of this potential is addressed through application of wave refraction and shoreline change models on 9 scenarios of dredged material placement.

Wave refraction over depressions or mounds in the nearshore bathymetry may produce amplification or reduction in nearshore wave height and changes in nearshore wave direction. Mounds introduced onto shallow, relatively flat bathymetry tend to focus wave energy in a zone behind the mound with lateral lobes of lower wave energy as depicted in Figure 4-8. Figure 4-9 illustrates the simulated change in wave refraction patterns produced by the introduction of Berm 01 to the nearshore bathymetry for a single wave condition. The wave conditions for this simulation were the most frequently occurring conditions from the 20-year simulation (H_{mo} = 0.75 m, T_p = 7 sec, and wave direction from ESE). Note that wave breaking at low tide reduces wave height over and in the lee of the berm. At mid-tide, the water depth allows waves to pass over the berm, resulting in a wave focusing pattern in the lee of the berm. The modification of the nearshore wave climate as illustrated in Figure 4-9 is sufficient to modify longshore sand transport and consequently may modify trends in shoreline evolution. The trends in longshore sand transport and shoreline change resulting from changes in the nearshore wave climate will be quantified through application of a shoreline change model.

GENESIS

The GENEralized Model for SImulating Shoreline Change (GENESIS) (Hanson and Kraus, 1989) is a one-line numerical model for simulating longshore sand transport and shoreline change. The model assumes that beach profile shape is constant and all alongshore transport is produced by the action of breaking waves. (Note: The version of GENESIS applied in this study neglects tidal currents; a recently released version of the model has this capability. The ramifications of neglecting tidal currents will be addressed later.). The governing partial differential equation for shoreline change is derived from conservation of sand volume (Eq. 4-2).

$$\frac{\partial y}{\partial t} + \frac{1}{\left(D_B + D_C\right)}\left(\frac{\partial Q}{\partial x} - q\right) = 0 \qquad (4\text{-}2)$$

where,
x = longshore position,
y = shoreline position,
t = time,
D_B = berm height,
D_C = depth of closure,
Q = longshore sand transport,
q = source/sink term.
The empirical estimate for longshore sand transport, Q, is given by

$$Q = \left(H^2 C_g\right)_b \left(a_1 \sin 2\theta_{bs} - a_2 \cos\theta_{bs} \frac{\partial H}{\partial x} \right)_b \quad (4\text{-}3)$$

where,
H = wave height, m
C_g = wave group speed from linear wave theory, m/s
b = subscript denoting breaking wave condition
θ_{bs} = angle of breaking waves to the local shoreline

and nondimensional parameters a_1 and a_2 are given by

$$a_1 = \frac{K_1}{16(S-1)(1-p)(1.416)^{5/2}} \quad (4\text{-}4)$$

$$a_2 = \frac{K_2}{8(S-1)(1-p)\tan\beta\,(1.416)^{7/2}} \quad (4\text{-}5)$$

where
K_1 = empirical coefficient
S = specific gravity of sand
p = porosity of sand on the bed (taken as 0.4)
K_2 = empirical coefficient
$\tan\beta$ = average bottom slope from the shoreline to depth of active transport

Additional details on the development, assumptions, and application of GENESIS are provided by Hanson and Kraus (1989) and Gravens, Kraus, and Hanson (1991).

Approach

STWAVE (Chapter 3) and GENESIS were applied to evaluate the impact of nearshore placement of dredged material on wave refraction, longshore sand transport, and shoreline change. The approach taken in this study was to apply GENESIS with no representation of structures along the Tybee shoreline. Neglecting structures in this application is justified in that the objective is to identify changes in the longshore transport and shoreline change resulting from nearshore placement of dredged material. This GENESIS application did not include contributions to longshore transport from tidal currents (which are likely important near the northern tip of Tybee Island). This model limitation is accepted, keeping in mind that the objective of this evaluation is to identify potential impacts from the nearshore placement of dredged material.

Figure 4-10 presents the positioning of the GENESIS baseline (x-axis), the nearshore reference line (where waves are given from the wave transformation model), and candidate berm locations. The grid in the figure represents the resolution of the STWAVE grid. The GENESIS baseline extends 4150 m from the north end of Tybee Island near the north terminal groin to the southern tip of the island with a shoreline resolution of 50 m.

The nearshore reference line was established in a nominal depth of 3 m at the north end of Tybee Island but transitioned into depths of 1.5 m. The nearshore reference line was placed in these relatively shallow water depths to represent the refractive effects of the ebb shoal and the dredged-material berms under evaluation. The Tybee Island beach profile is perched upon the offshore ebb shoal platform at a depth of 3 m. Depth of closure is defined as the depth at which the native sediment ceases to be influenced by the largest waves of the wave climate. The depth of closure offshore of Tybee Island is significantly deeper than 3 m, however the substantial width of the ebb shoal platform and the protection the platform offers the Tybee Island shoreline causes shoreline change at Tybee Island to be controlled more by the depth of the ebb shoal platform than the depth of closure. To represent the Tybee Island shoreline change potential, the GENESIS depth of closure was set to the 4-m platform depth and the subaerial berm height was set to 2 m. Calibration of the GENESIS model was performed to yield reasonable longshore transport rates at the north tip of Tybee Island. Little published data were found regarding the net longshore transport rates at Tybee Island. Posey and Seyle (1980) report a net volume loss between Center St. and the north terminal groin of 420,600 m^3 (550,000 yd^3) between May 1976 and March 1979. Averaged over the 43-month period, this amounts to an annual loss rate along the northern half of the island of 117,000 m^3/yr. GENESIS was calibrated to this volume loss rate by adjusting the K_1 and K_2 coefficients of Equations 4-4 and 4-5 and simulating the period between May 1976 and March 1979 and comparing annual average net transport during this period. The calibrated net transport rate at north Tybee (for the period May 1976 to March 1979) was 114,000 m^3/yr to the north. The calibrated value of K_1 used in evaluating each scenario was 0.06 and K_2 was set to the recommended value of 0.5 times the K_1 value. The coefficient K_2 Simulations with K_2 set to 2.0 times K_1 were performed for sensitivity analysis.

Twenty-year simulations of shoreline change were performed for the without berm condition and for each of the berm cases shown in Figure 4-10. The 20-year offshore wave record (1976-1995) was transformed to the nearshore reference line through wave transformation indices from the 831 STWAVE simulations characterizing the nearshore wave environment (See Chapter 3). These wave transformation simulations represent changes in wave transformation over the ebb shoal resulting from variation in wave height, wave period, wave direction, and water level. Differences in shoreline change between the no-berm scenario and those including nearshore berms were evaluated to determine the effect on the Tybee Shoreline. The wave transformation simulations assumed that the berms were a permanent feature in the bathymetry. In practice, the berms are expected to erode and disperse when placed in the active, nearshore environment. The static treatment of these features in the wave transformation and sediment transport simulations is likely to overstate the impact of the nearshore berms on shoreline change.

Analysis of Results

The 20-year average annual net longshore transport estimated by GENESIS is presented in Figure 4-11. The solid line indicates the average annual net

longshore transport rate along the shoreline and the dashed lines represent the north-bound and south-bound longshore transport rates. (Note, negative net longshore transport indicates transport to the north and positive net longshore transport indicates movement to the south.) The 20-year average net longshore transport at the north terminal groin is 87,000 m^3/yr to the north and at the south end of the island the net longshore transport is 33,000 m^3/yr to the south. Notice that between 0 and 1500 m south of the north terminal groin, the transport is nearly exclusively to the north.

The gradient in the average annual net longshore transport indicated in Figure 4-11 suggests that the entire Tybee Island shoreline is in an erosive configuration. A nodal point (or reversal) in net longshore transport direction is evident at approximately 2700 m from the GENESIS origin, corresponding to approximately 9th St. The net longshore transport gradient suggests a tendency for erosion along the entire Atlantic shoreline of Tybee Island, but the magnitude of the transport gradient (and the corresponding shoreline erosion tendency) is stronger north of the nodal point than south of the nodal point. The modeled gradient in transport suggests that the Tybee shoreline would experience average shoreline erosion rates of 3 to 7 m/yr. Average shoreline change rate between 1920 and 1972 was approximately 1 to 2 m/yr (Posey and Seyle, 1980), somewhat less than predicted by this GENESIS application. One likely explanation for the higher predicted erosion rates by GENESIS (and a point of consideration for evaluating these model results) is that the model neglects any supply of material from the offshore ebb-shoal platform. Nearshore placement of dredged material will introduce substantial quantities of sand into the littoral system that may mitigate a portion or all of the negative impacts introduced by the nearshore berms. Whether or not a nearshore mound of dredged material causes erosion of the shoreline depends on the relative magnitude of the gradients in longshore transport and the quantity of sand introduced to the littoral system.

Berm 01 located north-east of northern Tybee Island produces a relative change in shoreline position as indicated in Figure 4-12. Relative shoreline change indicates the difference in shoreline position between the with- and without-berm simulations after 20 years of simulation. Positive values of relative shoreline change indicate decreasing erosional trends and negative values indicate increasing erosional trends attributed to the dredged material mound. The solid and dashed lines in the figure indicate the range of valid solutions resulting from varying the coefficient K_2. The dotted lines indicate the envelope of relative shoreline change over the 20-year simulation. The sheltering effect of Berm01 on the waves at the northern tip of Tybee Island results in a reduction in erosion rate from the north terminal groin to approximately 1000 m south of the groin. The reduction in erosion rate amounts to a relative shoreline change of 8 to 25 m over the 20-year simulation. Refraction patterns further to the south result in a slight increase in erosional trend amounting to approximately 0 to -3 m of relative shoreline change over the 20-year simulation. The positioning of Berm 01 is such that longshore transport (and that by tidal currents) will not carry material along the northern Tybee shoreline and will not likely feed the Tybee littoral system.

Berm 02, positioned just offshore of Berm 01, produces (Figure 4-13) a smaller accretional trend at the north end of Tybee Island, but produces a larger zone of erosional tendency with a maximum of 3 to 5 m of relative shoreline change over the 20-year simulation. As with Berm 01, Berm 02 is not regarded as a promising location for feeding of littoral material to Tybee Island.

Berms 03 through 05 are located in deeper water depths and further from the shoreline and consequently produced only slight changes in longshore transport and relative shoreline change. The maximum relative shoreline change produced by these scenarios is approximately 3 m of accretional tendency and 2 m of erosional tendency. Placement of material in these regions is not expected to measurably impact the Tybee shoreline.

Berm 06 is positioned offshore of central Tybee Island and produces relative shoreline change indicated in Figure 4-13a. Moderate erosional tendencies are found near central Tybee Island with adjacent lobes of moderate accretional tendency. Berm 07 is placed at the same location as Berm 06, but with higher crest elevation. The relative shoreline response to Berm 07 is indicated in Figure 4 –13b. A mixed erosional/accretional trend is indicated, with moderate to small magnitude. Erosional and accretional trends do not exceed 5 m over the 20-year period. Placement of dredge material at Berms 06 and 07 is not expected to introduce significant changes in the present shoreline change rate.

Berm 13 is positioned just offshore of central Tybee Island and adjacent to the existing shore-attached transverse bar. The wave refraction patterns produced by this modification to the ebb shoal reduce the erosion potential in the central portion of the island, but increase the erosional potential to the southern third of the island (Figure 4-14). The maximum increase in erosion potential after 20 years is approximately 6-8 m along the southern third of the island. Recall that these results neglect the additional sediment introduced to the littoral system through cross-shore transport processes.

Berm 14 is positioned just offshore of central Tybee Island, and is essentially a larger version of Berm 13, extending further offshore and to the north of the existing shore-attached, transverse bar. Being larger and extending further offshore, Berm 14 produces a greater signature in the relative shoreline change as seen in Figure 4-15. Maximum reduction in erosion trends between 25 to 30 m over 20 years is centered about the shoreline 1600 m south of the north jetty (3rd St.). Two zones of increased erosional tendency are estimated at the north and south ends of the island: a 700-m wide zone at the northern tip and a 1400-m wide zone at the southern tip, with a maximum erosional tendency of –10 m over 20-year simulation. Again, these model simulations neglect the effect of a large quantity of sand available for feeding the littoral system.

Sand released from dredged material placed at Berms 13 and 14 will be in a zone of predominantly north-bound longshore sediment transport (refer back to Figure 4-11). Although most of the sand released from the Berm 13/14 position is expected to be transported north, the placement location is in a region where longshore transport is also directed to the south. Therefore, benefits to the shoreline through littoral feeding are expected both north and south of Berms 13 and 14.

Sediment Transport from Dredged Material Placement Sites

In addition to the assessment of shoreline change effects from the nearshore placement of dredged material, sediment transport at the placement sites was evaluated. The two primary issues addressed through sediment transport modeling at the placement site are 1) dredged material re-entering and depositing in the navigation channel and 2) dredged material as a source of material to the Tybee Island littoral system. The following section will describe the development and application of a numerical sediment erosion model, GTRAN (Jensen et al, 2002), to estimate sediment transport in the nearshore. The model results will then be presented and reviewed to address the channel infilling and littoral feeding issues.

Nearshore Sediment Transport Model

To estimate the transport of dredged sediment placed in the nearshore, predictive techniques must be applied with available knowledge of the environmental conditions and sediment properties. The sediment transport model GTRAN was supplied a blend of field and modeled data to predict mound erosion and transport pathways in the Tybee nearshore region. GTRAN includes effects of wave and current on transport of non-cohesive sediment. Although the sediment transport represented in the model is purely non-cohesive, a cohesive sediment bed algorithm is included which represents site-specific erosion resistance from the Sedflume erosion data. Wave conditions and tidal and wind-generated circulation are provided to GTRAN through the external models STWAVE and ADCIRC. Sediment properties for the dredged material mounds were determined from the sediment sampling and laboratory erosion rate experiments described earlier. From input wave, hydrodynamic, and sediment bed conditions, GTRAN calculates sediment transport through a collection of sediment transport methods. A detailed description of the GTRAN sediment transport methods, including sediment transport equations, is provided in Appendix 4B.

In order to numerically estimate sediment transport, certain simplifying assumptions and representations of the natural processes must be developed. Making such approximations is standard practice in the field of numerical modeling and is not unique to sediment transport models. The following discussion of the approximations developed for estimating transport rates will be limited to general statements and descriptions of the approximations applied.

Wave-Generated Current and Transport.

ADCIRC simulations include currents from tidal, wind, and river discharge and do not include currents generated by wave action. The presence of surface waves in the nearshore region produces stresses and near-boundary effects that were not represented in the ADCIRC hydrodynamics. Wave-generated currents

(longshore currents and undertow) and asymmetry in the wave orbital motions are a significant or dominant factor in nearshore hydrodynamics at many sites and must be considered in nearshore transport studies. This section will address the treatment of wave-induced hydrodynamics included in this study and the implications of neglecting certain components of the hydrodynamic forcing on model results.

Longshore Current. Longshore transport is defined as the quantity of nearshore sediment transport generated along the coast by the effects of breaking waves and the associated longshore currents. At Savannah, the shore parallel tidal and wind-driven currents augment this transport. The distinction between transport in the nearshore region and offshore (deep water) region is primarily in the transport processes of the two regions. In offshore transport, waves produce additional bottom shear stresses and increase turbulence that suspends sediment near the bottom. Surface waves contribute little to transport direction. Ocean circulation currents transport the suspended sediment (and sediment near the bed). In the most general terms, the waves act as a stirring mechanism, and the currents transport the sediment. In the case of nearshore transport, breaking waves also impart an increased shear stress and turbulence on the bottom sediments. In addition, breaking waves exert a stress that generates longshore currents and transport along with tidal and wind-driven currents. Wave-generated longshore currents are difficult to estimate over straight beaches, and become quite complex and non-linearly coupled with the tidal and wind-generated circulation. Because of these complexities, wave-generated longshore current and transport are not represented in the GTRAN sediment transport calculations.

The impact of the missing longshore transport can be qualitatively evaluated through assessment of longshore transport estimated by GENESIS. The GENESIS simulations described above indicate a northerly net longshore transport direction north of central Tybee Island. The longshore transport estimated by GENESIS at the north terminal groin is 84,000 m^3/yr north-directed. These same GENESIS simulations indicated south-directed transport south of the attachment bar. These longshore transport rates are due to the wave-generated component not included in GTRAN and neglect the effects of tidal and wind-generated currents on longshore transport. Later analysis in this chapter will discuss the implications of these rates on GTRAN predictions.

Undertow. In addition to longshore currents, waves generate an offshore-directed current or 'undertow' to balance the shoreward mass flux that occurs above wave troughs. Undertow is a primary factor in offshore sediment transport during storms (Miller et al. 1999, Smith and Miller, in review). Undertow exists in the lower water column, influencing the sediment bed and is therefore a strong mechanism for offshore sediment transport during large wave events.

A simple estimation of undertow derived through mass balance was implemented in the GTRAN simulations. The undertow estimate (called stokes velocity), U_{Stokes} as described Nielsen (1992) is:

$$U_{stokes} = \frac{-gH^2}{8cD} \tag{4-6}$$

where,

g = gravitational acceleration
H = wave height
c = wave celerity
D = water depth

Wave Asymmetry. Wave asymmetry is the imbalance of forward (onshore) and backward (offshore) components of the bottom orbital velocities resulting from the non-linear behavior of surface waves in shallow water. Wave asymmetry becomes a mechanism for shoreward sediment transport primarily during milder wave conditions (when undertow is small). In deep water, waves have a sinusoidal form and generate equal backward and forward bottom velocities. As the waves approach shallow water, wave crests become short and steep, while the troughs become long and flat. Near the bottom, orbital velocities include short-bursts of fast, forward velocity under the steep wave crest and slow, longer duration backward velocity under the trough. These forward bursts generally move more sand than the longer-duration, lower-magnitude offshore velocities. The transport methods in GTRAN include the effect of wave asymmetry on transport.

Transport and Erosion of Simulated Mounds

Twelve possible dredged material mound placement sites were assessed in the initial phase of this study. Nine of these sites, with an assumed maximum crest elevation are mapped in Figure 4-16. Two locations are riverine, long narrow areas near the channel (these do not have crest elevations, but rather are 1 m thick placements). Two locations are north of the north jetty at the entrance channel. One location is in the south channel. Seven locations are near Tybee Island, five close to the channel and two mid-way between the channel and island. In addition to wave orbital velocities, tidal currents, and wind driven currents; the coastal sites are exposed to the effects of breaking storm waves, asymmetric wave motion in shallow water, and wave generated longshore currents. As previously stated, of these three coastal conditions, only wave asymmetry is accounted for in the mound sediment transport simulations.

The GTRAN model, described above and in Appendix 4B was used for the nearshore mound simulations. GTRAN is a point model which does not account for incoming sediment transport, i.e. it is a gross transport and not net transport model. However, of interest in the mound simulations is net transport magnitude and direction, which is more representative of mound migration. To address this interest, GTRAN was applied at the mound crest and at the base of the mound in the direction of current. The difference of sediment transport at the base (assumed to be entering the mound configuration) and sediment transport at the crest (assumed to represent material exiting the mound configuration) was used to develop net transport direction and magnitude from the mound.

It is unlikely that any of these sites would be completely filled in one dredging cycle. Dredging practice would call for minimizing pipeline pumping or barge transport. Therefore, several sites would be used in any given year. To assess this situation, various mound configuration and orientation combinations

were modeled at each site. Three mound orientations were simulated for each configuration (Figure 4-17). Mound configurations were 75x250 m, 150x150 m, and 250x250 m. Each configuration's mound crest elevation was set at the maximum condition shown in Figure 4-16. Dimensions and orientation were chosen such that the mounds remained completely within the proposed locations outlined in Figure 4-17. In addition, mound location within each site was varied within the larger sites. Figure 4-18 provides mound crest and base locations processed in the GTRAN model for mounds at sites 1-7. Each berm site includes 1-3 mound locations. Multiple locations were considered necessary at some berm sites because hydrodynamic and wave conditions vary significantly over the site.

The periods of simulation were January 1992 and November 1979, the operational period and two-year return period, respectively. Multiple mound configuration and sediment type simulations were performed. The patterns of transport, however, were similar at a site because the initial mound crest elevation at any designated site was constant for all simulations (Figure 4-17). As an example, the range of crest erosion for 75x250 m mounds at each location is provided in Table 4-4 This table includes results for multiple initial sediment conditions from the Sedflume results, and three mound orientations (Figure 4-16). It can be seen from this table that all mounds in the nearshore are dispersive during the winter months. The amount of mound erosion is highly sensitive to mound orientation. Mounds perpendicular to main current direction experienced more erosion. The amount of erosion is not sensitive to initial sediment type because typically there is an armored sheet flow layer of sand atop the cohesive base. Table 4-4 can be used to provide a relative comparison of the different locations. Clearly, the mound at site 5 will experience the most erosion. This is due to a combination of strong tidal currents and high wave energy. Wave energy at sites 1-3 is much less than at site 5 because a significant amount of breaking occurs on the shoals seaward of these locations. Site 5 has much less protection. Similarly, it can be seen that erosion at site 1 and 2 is very sensitive to location. Again, this is due to the complex shoals and channel that change rapidly at these sites.

Figure 4-18 shows transport rose plots for an example offshore mound at berm locations 1, 5, and 7 for the active month (November 1979). Each rose plot was constructed by summing the GTRAN sediment transport directed into bins with 15-degree resolution. The area of each wedge represents the sum of the hourly transport in each bin. Each wedge protrudes from the GTRAN calculation point in the direction of transport. It can be seen from the rose plots in Figure 4-18 that the directions of transport from berms 1 and 5, which are near the channel, are almost exclusively in the direction of tidal currents, i.e. the direction of the channel. This indicates that there is a strong possibility that sediment from these berms will re-enter the channel. Large amounts of sediment moving on the channel slope would be biased toward moving down-slope into the channel. The small components of onshore transport indicated in the along-channel sites suggests that placement of dredged material at berms 1 through 5 would have negligible impact on beach or littoral zone nourishment. Placement at these locations would result in significant re-handling of the material.

Transport at berms 6 and 7 (Figure 4-18), which are further from the channel, is dominated by shore-parallel components of the hydrodynamics. In addition, transport at these berms includes a modest component toward shore (due to wave asymmetry). Under most storm conditions, undertow would counteract wave asymmetry, but undertow will not impact the mound crest. It should be noted that although material moving off the mound has a toward-shore bias, once a sand particle leaves the mound, it will be exposed to undertow and may start moving offshore. However, the general trend of mound migration is longshore spreading with a slight onshore bias during the time when the mound remains an identifiable feature. Berms 6 and 7 will be dominated by shore-parallel transport. It is expected that most of the transport will be predominately parallel to shore because of the strong shore parallel tidal currents on the Tybee Island coast. The mound would be dissipated long before it attaches with the beach. This modest onshore bias is important for nearshore placement because it indicates that some sediment will migrate toward the beach. Although the mound will spread out during winter months, and there is an offshore bias to non-mound storm transport, this will reverse during summer periods and winter non-storm periods. Low energy onshore movement can be seen from the typical winter and summer beach profiles. Summer (and other non-storm periods) will move this material toward shore. This is a gradual process and the benefit of nearshore placement will provide a new sediment source for onshore migrations. These processes will be discussed further in the next section.

Although berms 6 and 7 would provide sand for littoral zone nourishment, the main impact will be on south Tybee, not the north Tybee area of concern. Once material leaves the mound in the north direction, it will become part of the attachment bar of the ebb shoal. As will be demonstrated in the next section, material moving onto the south side of the ebb shoal does not benefit north Tybee. The next section reviews sediment pathways for the entire region between Tybee and the channel.

Besides the nearshore locations, five river or jetty placement sites were also assessed (Figure 4-17). Three of these were existing depressions that would be filled (Berms 08, 09, and 12). The remaining two sites (Berms 10 and 11) are placement of material along the north side of the channel off of Jones Island. These locations would not be significantly affected by wave action. Therefore GTRAN simulations included current only. Material type input for the riverine placement sites came from SEDFLUME sample 38N, the only riverine sample collected. 38N consolidated material eroded as a combination of individual particles and aggregates (see Appendix A). The aggregates move as bedload and are sensitive to slope.

As described in Chapter 2, riverine hydrodynamics are strongly influenced by tidal current, with an ebb bias from river flow contributions. This can be seen for the near-channel placement site transport rose plot (Figure 4-19) which has both ebb and flood components, but a larger ebb component. There is little detectable transport in the cross-channel direction. However, the point simulations assumed a flat-crested mound. The channel slopes would influence material that moves as bedload off of the mound. This may introduce much of the aggregate erosion back into the channel due to the steep side slopes.

Approximately 50% of the material erodes as individual particles in suspension. The majority of this material will be transported out of the river before re-deposition or will deposit in the low-energy near-bank areas.

The ADCIRC simulations were two-dimensional and therefore do not represent the vertical stratification in tidal estuaries. However, the direction of transport is clearly biased toward ebb flow. The proposed mound locations are in 1-4 m water depth and therefore would be influenced more by the fresh-water surface flow than the ocean water tidal currents in the channel. Therefore, if the hydrodynamic modeling were three-dimensional, the transport direction ebb bias at these placement sites may be greater than indicated in these GTRAN simulations.

Berm 12 is on the northwest side of Tybee Island in a natural depression at the mouth of the south channel. The transport pattern is clear and unidirectional (Figure 4-19). Material moves toward the northeast. This is in the direction of the shoal forming off of the north tip of Tybee Island. This shoal is believed to be a source for channel infilling. Material placed at Berm 12 will erode at a high rate. The depression at this location is due to shoaling on the north side of the south channel, which diverts flow to the south, producing higher shear stresses and sediment transport to the south side of the channel. High currents at this depression are one of the reasons it has not filled in. It is claimed by some (Eric Olsen, personal communication), that this depression is a remnant of a previous channel. Therefore, the depression may not be a scour hole, but the high currents at the site does not permit deposition or infilling.

The Berm 08 and 09 site, on the north side of the north jetty, is also positioned over an active channel with depths up to 4.5 m. Transport from this site is tide dominated with a strong offshore bias. The channel probably exists due to the high velocities in this area from tidal drainage of the marshes around Daufuskie Island. It should be assumed that material placed at this site would disperse and move offshore from the site. Some of the coarser material will likely move into the navigation channel.

General Trends in Nearshore Transport

The mound erosion study described in the previous section, centered on consideration of specific pre-defined sites, was the main transport analysis defined in the original scope of work. However, the results of this analysis indicated a need to understand transport direction and magnitude throughout the nearshore region. This is specifically required to assess optimum placement of dredged material to benefit the beach and nearshore profiles. Berms at sites 1-5 in the original study will have very little impact on nearshore nourishment. Most of the material will move parallel to the channel, with strong indications that the material will re-enter the channel. These locations (1through 5) were originally selected for assessment because of the low-cost of pipeline or barge placement. Sites 6and 7 were selected because light-loaded barges could place material there. Assessment of sites 6 and 7 indicated that material placed further from the channel has more potential for littoral zone nourishment and less potential for rehandling. Therefore, a second phase was added to the sediment transport study.

This phase uses the recently developed GTRAN model applied over an array of points in the nearshore region to assess sediment pathways and aid in placement site selection that will most benefit the beach with minimal sediment rehandling.

Figure 4-20 shows a distribution of points selected for GTRAN simulations of general transport over the ebb shoal. Ambient bathymetry (no mounds) was used for transport simulations at these points and undertow was included. The following analyses and discussions are intended to estimate dominant sediment transport processes and sediment pathways for material placed in the nearshore region and are not intended to simulate erosion from a mound.

Winter conditions. GTRAN transport simulations were performed for two winter months of varying wave conditions: the operational (January 1992) and storm (November 1979) months. Figure 21a-f provides time-history of waves, currents, and transport at GTRAN points 60, 70, 75, 80, 83, and 90 (Figure 4-20) for November 1979. These time series can be utilized to assess relative activity at various locations. The transport magnitude variation is an order of magnitude, with greatest transport rates near the channel (Figure 4-21d-f) and more modest near the coast of Tybee Island (Figure 4-21a-c). In addition, the majority of transport over the month is during the two wave/wind-driven current events centered on November 3 and November 25. These time series demonstrate the episodic nature of sediment transport.

Relative to offshore placement, transport in most of the nearshore region is significant due in part to the strong tidal currents. Figure 22 provides time history of waves, currents and transport at the present offshore disposal site. It can be seen that transport in the nearshore regions is several times greater than at the present disposal site. Therefore, while dredged material remains in place at the offshore disposal site for long durations, this is not expected to occur at nearshore placement sites.

The net transport direction and relative magnitude at each node in the fine mesh are provided for the operational (Figure 4-23) and storm (Figure 4-24) periods. Rose plots of transport magnitude and direction are provided in Figure 4-25 for the storm month. The remainder of this sub-section will describe the results in these two figures and their implications for nearshore transport of dredged material.

Review of transport (Figure 4-23) at points 32-48 (from Figure 4-20) reveals that net transport is seaward along the navigation channel. These locations are also where the greatest magnitude of transport occurs. This is due to the strong tidal currents that dominate transport in this area. The offshore bias of transport shown in the rose plots is due to the addition of river flow to the tidal currents and stronger ebb currents for purely tidal conditions. This figure also indicates a gradient in transport magnitude suggesting a depositional zone in the channel. This depositional zone corresponds to the location of increased dredging volume between Stations 30 and 40 shown in Figure 4-2. It should be noted that transport magnitude and direction on the outer edge of the ebb shoal (around channel stations 40-45) may not be accurate because wave-generated longshore currents not included in the GTRAN simulations may be significant here, particularly during storms with wave direction from the northeast.

Net transport vectors in the nearshore region of north Tybee Island generally indicate north-directed net transport with some offshore component. The offshore component is expected during a storm month when undertow is strongest. The rose plots indicate that there are periods of onshore transport even during this stormy month. The shoreward transport components (Figures 4-25 and 4-27) are greatest in 5-10 ft water depth and then decrease in the surf zone (<5 ft water depth). The decrease is due to the increased impact of undertow and decreased wave height (wave breaking) in the surf zone. . Sediment transport north of the ebb shoal is in the tidal current directions, with a bias toward the north direction (flood cycle). This net north-direction of transport for both the January 1992 and November 1979 periods provides some explanation for migration of the ebb shoal to the south over the past decades. The attachment bar is located at a nodal point in net transport during these two periods. North of the attachment bar, sediment moves northward. While the south directed transport indicated in the rose plots will nourish the ebb shoal, the north directed component erodes the ebb shoal. Since the north directed component is slightly larger, the net effect will be net sediment movement from the attachment bar of the ebb shoal toward the north (Figure 4-24). This does not, however, imply that the ebb shoal is disappearing. There are other sources of sediment to the attachment bar, which will be described later. It does, however, indicate that the ebb shoal will move south as offshore and southerly sources nourish the shoal. It should be emphasized that these are one-month simulations. Other months may be different. This is the reason that the 24-year wave simulation described in Chapter 3 were applied in the GTRAN model, as will be described later in this section.

Net transport on the attachment bar of the ebb shoal during the active and operational periods is generally offshore. This is due to the effect of strong undertow during winter storms. Less wave energy and weaker tidal currents exist over the nearshore portion of the attachment bar compared to the nearshore region to the north of the attachment bar. Consequently, transport magnitudes are smaller for locations close to shore on the attachment bar (points 8-10) than for similar locations north of the bar (points 3-6)..

Locations south of the attachment bar indicate a net offshore and southward transport during both the operational and active months. The net southward transport is stronger during the active month because of wind-generated southerly currents during the first week in the period. The net southerly direction coupled with the net northerly direction on the north side of the attachment bar does not necessarily imply risk to the bar stability. Both of the active and operational months included strong northerly winds. In addition, the time series transport data (Figure 4-21) indicate that transport during different periods of the month will be in different directions, including strong northerly and northeast components south of the attachment bar. These transport periods would feed the bar.

Long-Term Simulations. Net transport direction vectors and rose-plots for the 24-year wave hindcast are provided in Figures 4-26 and 4-27, respectively. It should be noted that wind-generated currents are not included in these simulations. Wind generated currents included in the ADCIRC one-month

simulations are not computationally feasible for the 24-year wave hindcast period. Therefore, ADCIRC 30-day tidal cycle simulations were repeated to provide currents for the 24-year simulation. Comparison of one-month sediment transport simulations for tide-only and tide-plus-wind forcing indicate that wind forcing may contribute significantly to transport magnitude and net transport direction in the nearshore regions, particularly for areas further removed from the Savannah River entrance channel. The 24-year wave hindcast was originally performed for GENESIS simulations. Application to GTRAN is representative of low-wind conditions where wind-generated currents are negligible, but wave conditions represent the actual 24-year hindcast.

Long-term transport directions and relative magnitudes are similar to those for the one-month simulations except on and south of the attachment bar. Without the strong, south-directed, wind-generated currents experienced in the one-month simulations, nearshore currents south of the attachment bar are dominated by tidal flow from Savannah River. Therefore, there is an indicated net northerly transport direction (flood flow bias) for most locations south of the attachment bar. The November 1979 and January 1992 simulations indicated a net south-directed transport in this area. This indicates that low-wind conditions will favor transport towards the attachment bar from the south while high-wind conditions from the northeast will favor net transport off the south edge of the attachment bar. In addition, there is a noticeably stronger north-directed component to transport over the ebb shoal attachment bar. Long-term hydrodynamic simulations including wind forcing would assist in estimating the overall impact of wind-generated currents in the Tybee nearshore region. However, this effort is beyond the scope of this study.

Uncertainty in Transport Estimates

Uncertainty in the sediment transport estimates is difficult to quantify, site-specific, and would require significant field data. This is particularly true for estimating erosion volumes from mounds. These erosion estimates can, however, be used to compare various placement locations and options, as has been described in this chapter. The sediment pathways on the fine grid are logical, given what is known about morphologic evolution, wave/current patterns, and dredging volumes in the area. Therefore, relative magnitude and direction of transport are relevant and can be used for assessing the benefit of various placement options. However, treatment of undertow and wave asymmetry has significant influence on transport direction and present understanding limits predictive capabilities over complex bathymetry. In addition, longshore currents are not treated in these estimates. This process will also influence longshore transport, especially during storms.

Recommendations

Recommendations on nearshore placement of dredged material from the Savannah River Navigation channel are developed from knowledge of sediment

transport processes near inlets and model simulations. Key issues addressed include 1) the effects of nearshore berms of dredged material on wave refraction and consequently on shoreline change at Tybee Island, 2) the likelihood that dredged material will re-enter the navigation channel and increase maintenance dredging volumes, and 3) the potential of nearshore-placed dredged material to provide sand to the littoral system of Tybee Island.

The recommended location for nearshore placement of dredged material is adjacent to the transverse, shore-attached bar just offshore of central Tybee Island (Berms 13 and 14). The dominant transport direction from these berms will be north, with some material moving shoreward, especially during low-wave conditions. This process will enhance the normal shoreline accretion experienced during mild conditions. Net movement will be offshore during storm conditions. However, even during these periods, this material will benefit and nourish the littoral system, thus reducing shoreline erosion. Any nearshore placement at north Tybee will result in some material eventually moving to the shoal north of the island. Some of this material will re-enter the channel. The likelihood of significant increases in maintenance dredging for nearshore placement along central Tybee Island is less than other alternatives for nourishing the north Tybee littoral system. Berms 13 and 14 are the furthest locations from the north shoal and channel that will still provide littoral and beach nourishment to north Tybee. Adverse impacts to the shoreline (as predicted by GENESIS) are small relative to the present rate of shoreline change and are likely to be offset by the addition of sand to the Tybee Island littoral system.

Berms 06 and 07 are other promising locations for nearshore placement of dredged material. Model predictions made assuming that the mound relief eliminates undertow indicate an onshore bias of the migrating mound. Berm migration is dominated by tidal current direction, but the onshore bias in direction is the important factor. Placement at these locations will reduce shoreline erosion because the health of the beach is directly tied to the sediment quantity in the littoral zone. The transport roses at these mound locations initially created the interest in 2-3 m water depth placements, eventually leading to the development of Berms 13 and 14.

Placement of dredged material adjacent to the channel (Berms 03 through 05) will likely result in significant quantities of dredged material re-entering the channel and increasing maintenance dredging volumes. Transport patterns over the ebb shoal indicate that although some of this material could re-enter the littoral system along the outer margin of the ebb shoal, little of this material would directly benefit the Tybee Island littoral system.

Dredged material placed on the ebb shoal platform offshore of the northern portion of Tybee Island (Berms 01 and 02) provide some benefit to northern Tybee Island in the form of wave sheltering, but material transported from these locations is likely to re-enter the channel and increase maintenance dredging volumes. As much of the transport from these locations is directed toward the channel and then offshore, relatively little of the dredged material is expected to directly benefit the Tybee Island littoral system.

Placement of material in Berm 12 at the northeast end of Tybee Island is not recommended. Sediment transport from this site is unidirectional towards the shoals off north Tybee, which are suspected to contribute significantly to channel infilling at that location. Little lasting benefit to the ocean or river-facing shorelines is expected from dredged material placement at this location.

Dredged material placement at Berms 08 and 09 is not recommended for similar reasons as Berm 12. The placement zone is in an active channel fed by salt marsh backing Daufuskie Island and Turtle Island. Dredged material placed here would likely be eroded from the placement zone and transported into the navigation channel.

Material placed in shallow water near the river banks (Berms 10 and 11) will move in a net seaward direction. Some of the material will likely re-enter the channel. However, the majority of suspended material will either deposit in low energy nearshore regions or move offshore via the channel.

Summary and Conclusions

Regional considerations of sediment management have expanded traditional viewpoints of dredged material handling to include nearshore placement of dredged material containing significant fractions of sand. The focus of this study was to identify favorable locations for nearshore placement of dredged material. Issues considered in the study include 1) the effects of nearshore berms of dredged material on wave refraction and consequently on shoreline change at Tybee Island, 2) the likelihood that dredged material will re-enter the navigation channel and increase maintenance dredging volumes, and 3) the potential of nearshore-placed dredged material to provide sand to the littoral system of Tybee Island.

Shoreline Change.

Effects of nearshore berms of dredged material on wave refraction, longshore transport, and shoreline change were assessed through application of the shoreline change model, GENESIS. Nine nearshore berm scenarios were represented on the ambient bathymetry. Wave transformation simulations representing the long-term wave climate were preformed over the ambient bathymetry and each of the dredged material berm scenarios. The resulting nearshore wave climate was then passed to GENESIS to simulate changes in the shoreline change response of Tybee Island. Berms placed in deeper water and further from the shoreline produced little change in shoreline change trends. Berms placed closer to or immediately offshore produced moderate changes in the shoreline evolution trends. Berms 01 and 02, offshore of the northern tip of Tybee Island resulted in a decreased erosional trend at the northern tip of the island, but increased the erosional trend along the central portion of the shoreline. Berms 13 and 14, placed adjacent to the transverse bar attached to the central island shoreline produced a reduction in erosion rates along the central third of the island and relatively weak erosional trends on the northern and southern

thirds of the island. The influence of sediment supply to the littoral zone and the influence of tidal currents were neglected in the GENESIS simulations.

Maintenance Dredging Requirements.

A point sediment transport model for combined wave and current environments was applied to estimate transport and erosion of nearshore-placed dredged material mounds. One issue of concern is an increase in maintenance dredging requirements resulting from the nearshore placement of dredged material. One conclusion from the sediment transport simulations is that placement of dredged material in the nearshore will likely lead to some increase in maintenance dredging requirements over placement of material in the offshore disposal site. However, not all nearshore placement sites were equal in the likelihood of significant increases in maintenance dredging volumes. Simulated transport over the ebb shoal indicates that a significant portion of dredged material placed adjacent to the offshore channel, adjacent to the north jetty, and at the northeastern tip of Tybee Island is likely to re-enter the channel. Dredged material placed offshore of central Tybee Island is least likely to produce significant quantities of channel infilling.

Littoral Feeding

The point sediment model was also used to assess the potential for benefits to the Tybee Island shoreline through feeding of sand to the littoral system. The balance of undertow and wave asymmetry have been shown to play a strong role in shoreward sediment transport. By placing dredged material in shallow water, the stronger influence of wave asymmetry allows sand to be transported toward shore. Sediment transport simulations at the offshore disposal site indicate that significantly lower transport rates occur there compared to the more energetic nearshore environment. Nearshore sediment transport simulations indicate that placement of dredged material near the central Tybee Island shoreline adjacent to the present transverse, shore-attached bar is most likely to introduce sand to the littoral system and provide a benefit to the north Tybee shoreline. Trends in nearshore transport over the ebb shoal suggest that dredged material placed in deeper water near the navigation channel will either be transported back to the channel, or will re-enter the littoral system along the margins of the ebb shoal, providing little direct benefit to the Tybee shoreline. Transport offshore of the northern tip of Tybee Island is predominantly directed to the north from both tidal and longshore transport influences. This predominant direction of transport is likely to transport dredged material there back to the channel instead of benefiting the Tybee Island littoral system.

Recommendations

The recommended location for nearshore placement of dredged material is adjacent to the transverse, shore-attached bar just offshore of central Tybee Island. The impacts to the shoreline at this location are similar to those of other

extreme-nearshore placement options, but these impacts are likely to be offset by the potential of sand to be transported shoreward to benefit the littoral system. Figure 28 presents a schematic of the mechanisms delivering sediment from the nearshore placement zone to the beach at north Tybee Island. The large arrow indicates the dominant transport direction, and the smaller arrows indicate the onshore component that will benefit the beach. The figure is not to suggest that the material will not disperse in other directions under the complex forcing at this site. This location has the least potential for increasing maintenance dredging while providing benefit to Tybee Island.

References

Gravens, M.B., Kraus, N.C., and Hanson, H. 1991. "GENESIS: Generalized Model for Simulating Shoreline Change, Report 2, Workbook and System User's Manual," Technical Report CERC-89-19, Coastal Engineering Research Center, US Army Engineer Waterways Experiment Station, Vicksburg, MS.

Hanson, H. and Kraus, N.C. 1989. "GENESIS: Generalized Model for Simulating Shoreline Change, Report 2, Workbook and System User's Manual," Technical Report CERC-89-19, Coastal Engineering Research Center, US Army Engineer Waterways Experiment Station, Vicksburg, MS.

Jensen, R., Scheffner, N., Smith, S.J., Webb, D., and Ebersole, B.A. 2002. Engineering studies in support of Delong Mountain Terminal project. Technical Report ERDC/CHL TR-02-26. US Army Engineer Research and Development Center, Vicksburg, MS.

Madsen, O.S., and Wikramanayake, P.N., 1991. Simple models for turbulent wave-current bottom boundary layer flow. Contract Report DRP-91-1, U.S. Army Engineer Waterway Experiment Station, Vicksburg, MS, USA.

Meyer-Peter, E., and Müller, R., 1948. Formulas for bed-load transport. Second International Association of Hydraulic Engineering and Research (IAHR) Congress, Stockholm, Sweden. IAHR, Delft, Netherlands.

Nielsen, P., 1992. *Coastal Bottom Boundary Layers and Sediment Transport.* World Scientific Publishing, Singapore, Advanced Series on Ocean Engineering, vol. 4.

Posey, F.H. and Seyle, F.W. 1980. Unpredicted rapid erosion, Tybee Island, Georgia. Proceedings of the Symposium on Coastal and Ocean Management. 1869-1882.

Soulsby, R.L., 1997. *Dynamics of marine sands.* Thomas Telford, London.

Taylor, J.R. 1997. *An introduction to error analysis.* 2nd ed., University Science Books, Sausolito, CA.

Van Rijn, L.C., 1984. Sediment Transport: part I: bedload transport; part ii: suspended load transport: part iii: bed forms and alluvial roughness, *Journal of Hydraulic Engineering* 110(10): 1431-1456; 110(11): 1613-1641, 110(12): 1733-1754.

Vincent, C.E. and Green, M.O., 1990. Field measurements of the suspended sand concentration profiles and fluxes and of the resupsension coefficient over a rippled bed. Journal of Geophysical Research, 95(C7): 11591-11601.

Wikramanayake, P.N., and Madsen, O.S., 1994a. Calculation of suspended sediment transport by combined wave-current flows. Contract Report DRP-94-7, U.S. Army Engineer Waterway Experiment Station, Vicksburg, MS, USA.

Wikramanayake, P.N., and Madsen, O.S., 1994b. Calculation of movable bed friction factors. Contract Report DRP-94-5, U.S. Army Engineer Waterway Experiment Station, Vicksburg, MS, USA.

Station	Location (N=North S=South C=Center)	% Sand	d_{50} (mm)	Observations
16	S	59.7	0.684	Fine sand and shale
17	S	33.9	0.231	Medium sand, mud rip-ups
18	S	55.4	2.630	Coarse sand, gravel, shale
33	N	72.4	0.212	Medium sand and black high water mud
33	C	73.2	0.277	Medium sand and mud rip-ups
33	S	71.8	0.386	Medium sand and black high water mud
34	C	77.4	0.260	Medium sand and mud rip-ups
36	N	66.3	0.165	Medium sand with minor mud
40	S	74.0	0.157	Fine sand
42	N	62.7	0.150	Olive mud, rip-ups, minor sand and shale
42	C	68.8	0.292	Medium sand and shell with mud rip-ups
44	S	74.5	0.195	Find sand and shell
45	S	48.1	0.115	Black mud under fine thick sand
49	S	78.3	0.495	Medium sand and shell with mud rip-ups
50	N	74.3	0.426	Medium sand and shell on top of muddy sand
51	N	73.6	0.198	Find, muddy sand
51	C	79.9	0.639	Coarse, slightly muddy sand
51	S	79.4	0.192	Fine sand on top of olive high water mud
52	S	50.0	0.185	Find sand on top of sandy mud
53	N	62.3	0.207	Black high water mud with 1 inch sand on top
54	S	40.6	0.153	Dark olive high water mud with 1 inch fine sand on top
55	S	54.6	0.135	Dark gray high water mud with 1 inch fine sand on top
55	N	61.4	0.109	Tan high-water mud
56	N	47.6	0.121	Black high water mud with 1 inch sand on top
56	S	55.9	0.123	Black high water mud with 1 inch sand on top
57	S	37.5	0.105	Dark gray high water mud with 1 inch fine sand on top
58	N	57.5	0.115	Dark gray high water mud with 1 inch fine sand on top
59	N	64.2	0.115	Dark gray high water mud with 1 inch fine sand on top
59	C	66.6	0.119	Dark gray high water mud with 1 inch fine sand on top
59	S	52.6	0.112	Dark gray high water mud with 1 inch fine sand on top
60	S	67.1	0.111	Dark gray high water mud with 1 inch fine sand on top
61	N	47.3	0.108	Dark gray high water mud with 1 inch fine sand on top
61	S	65.1	0.110	Dark gray high water mud with 1 inch fine sand on top
61	N	47.3	0.108	Dark gray high water mud with 1 inch fine sand on top
62	N	67.8	0.110	Very dark sand and dark gray mud, separate layers
62	S	55.5	0.110	Dark gray high water mud with 1 inch fine sand layer on top
63	S	45.4	0.110	Dark gray high water mud with 1 inch fine sand on top
63	N	52.7	0.117	Dark gray high water mud with 1 inch fine sand layer on top
63	S	45.4	0.110	Dark gray high water mud with 1 inch fine sand layer on top
66	S	67.1	0.112	Tan high-water mud
66	N	70.5	0.106	Tan high-water mud

Table 4-1: Law Engineering bar channel sediment samples

	38n	17s	33s	52s	62s	78s
Percent < 4 micron	8.9	1.5	1	2.7	2.5	7
Percent < 20 micron	23.1	4.8	2.5	10.3	6.1	20.5
Percent < 80 micron	47.7	14.3	8.2	35.9	23	50.7
Percent < 400 micron	96.3	63.2	55.7	98.4	100	99.1
D10 (micron)	5	52	96	20	45	7
D50 (micron)	90	290	350	115	120	80
D90 (micron)	280	1000	850	270	200	205

Table 4-2 Sedflume sediment sample grain size distributions

Site	Bedload (%)	Mean Particle Size Trap (mm)	Mean Particle Size Core (mm)	Silt Component Trap (%)	Silt Component Core (%)
38N	70	0.136	0.136	37	40
17S	62	1.226	0.51	3.1	11
33S	65	0.868	0.584	1.8	6
52S	40	0.205	0.144	23	27
62S	20	0.19	0.147	1.8	14
78S	50	0.2	0.112	21	41

Table 4-3: Mean particle size and silt component of eroded and bedload samples

Location (berm/point)	1/92 Erosion (min/max) (cm)	11/79 Erosion (min/max) (cm)
01-7481	14-42	27-47
01-7482	17-38	27-48
01-7483	13-31	25-26
02-7587	23-37	31-39
02-7588	21-39	15-27
02-7589	14-32	22-85
03-7593	16-45	14-54
03-7594	12-28	14-75
04-7597	9-28	8-26
05-7599	25-68	67-92
06-7601	5-26	26-71
06-7602	13-51	27-58
07-7601	15-41	38-58
07-7602	17-33	35-40

Table 4-4. Mound crest erosion range (cm).

FIGURES

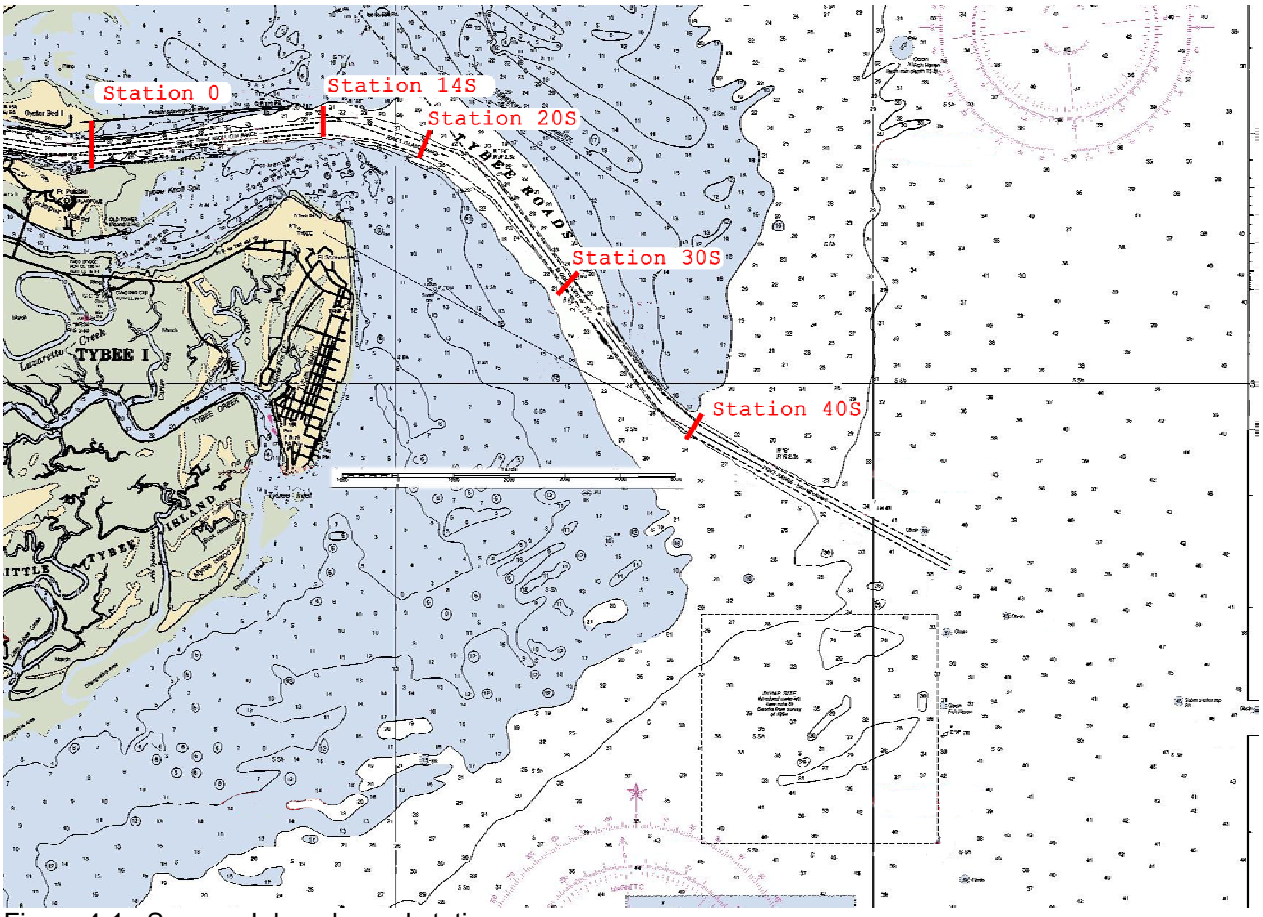

Figure 4-1. Savannah bar channel station map.

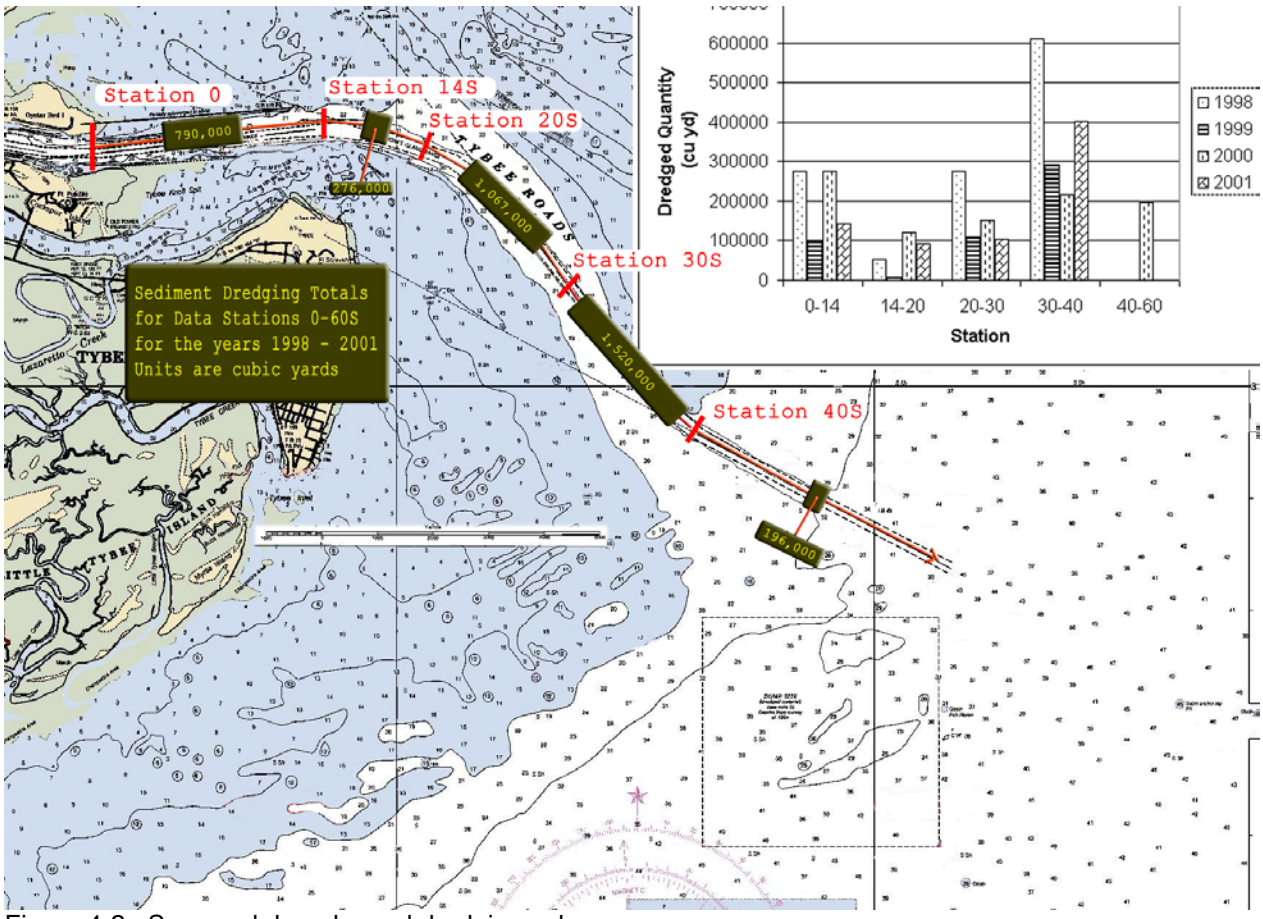

Figure 4-2. Savannah bar channel dredging volumes.

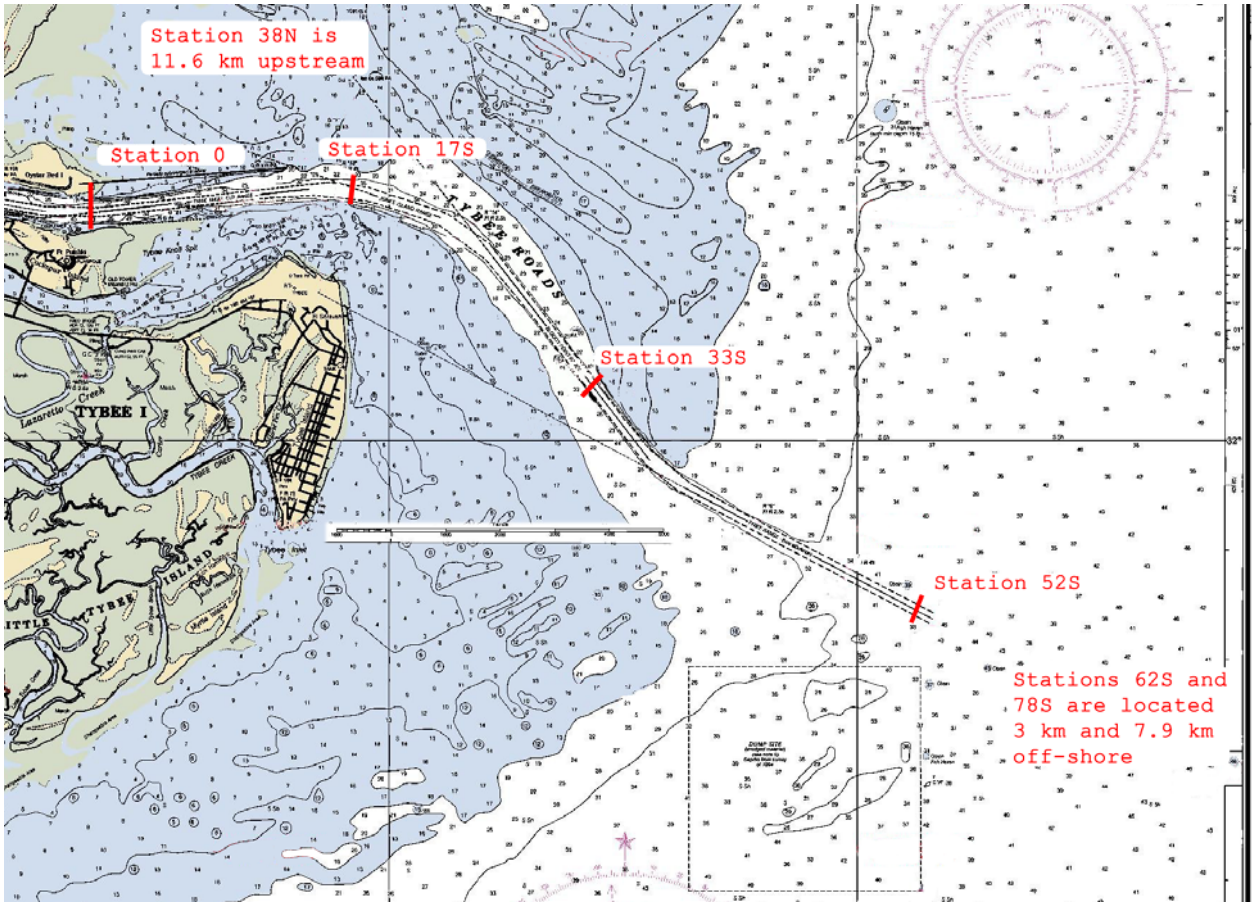

Figure 4-3. Savannah bar channel Sedflume sample locations.

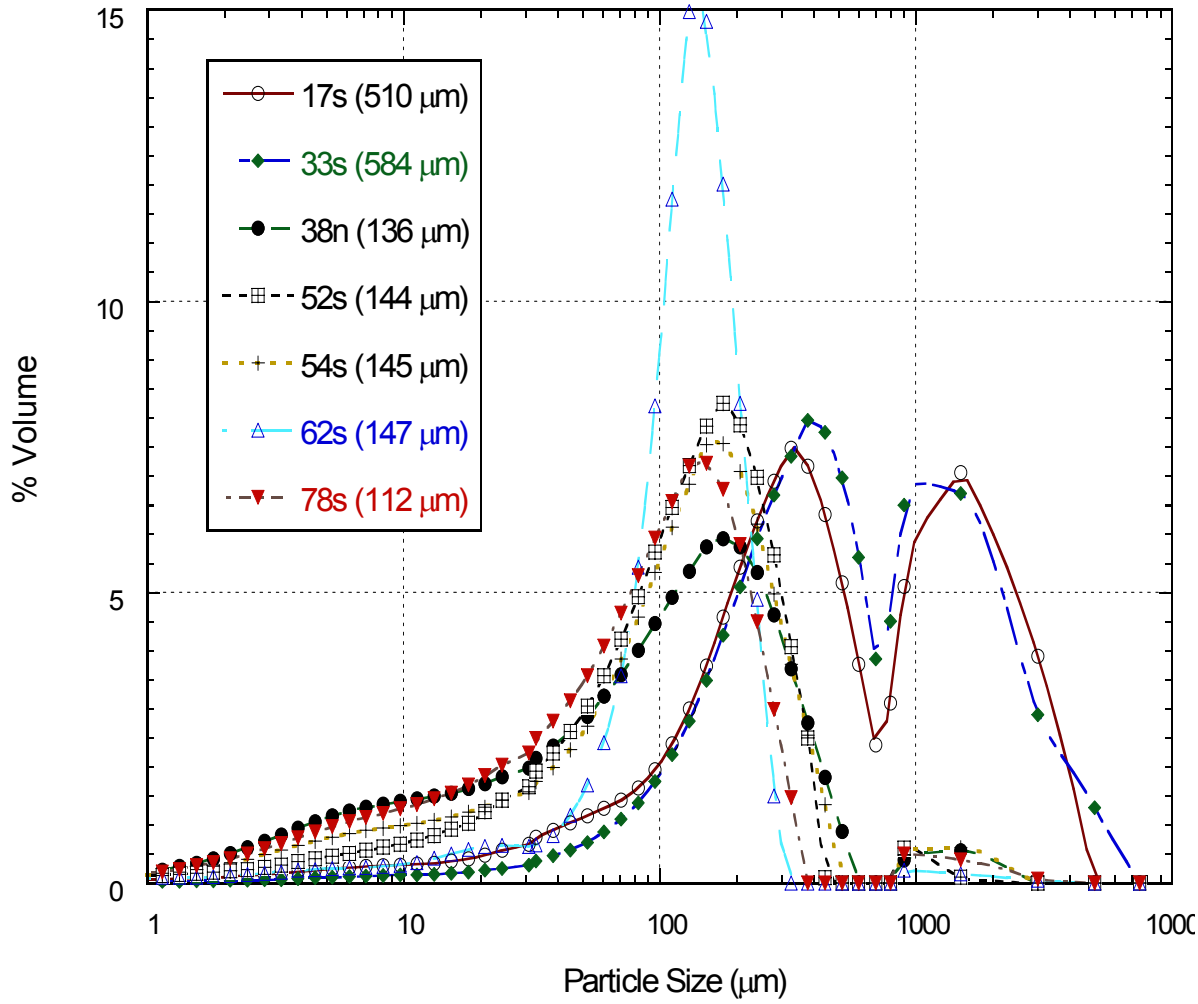

Figure 4-4. Particle size volume distribution for six Sedflume sample sites.

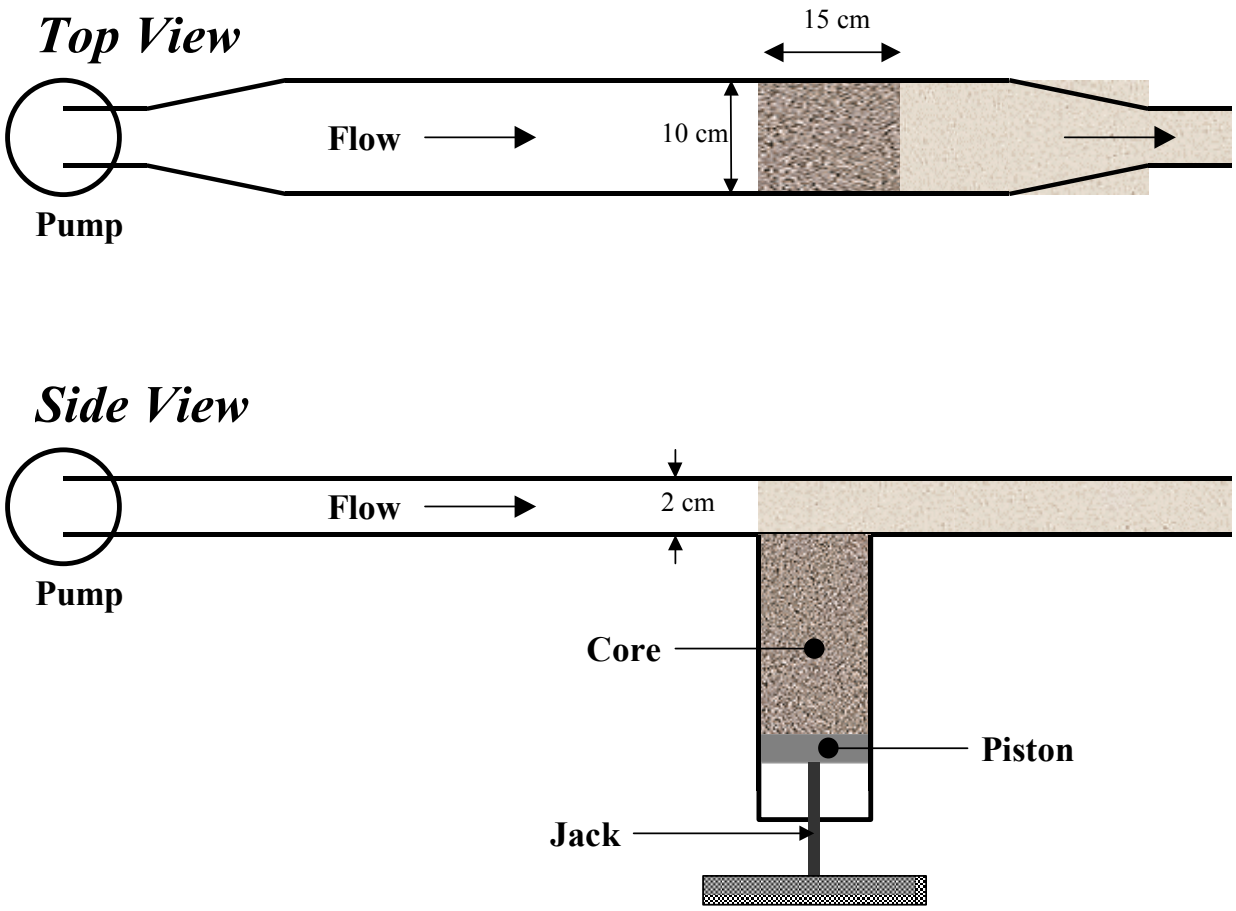

Figure 4-5. Schematic of Sedflume.

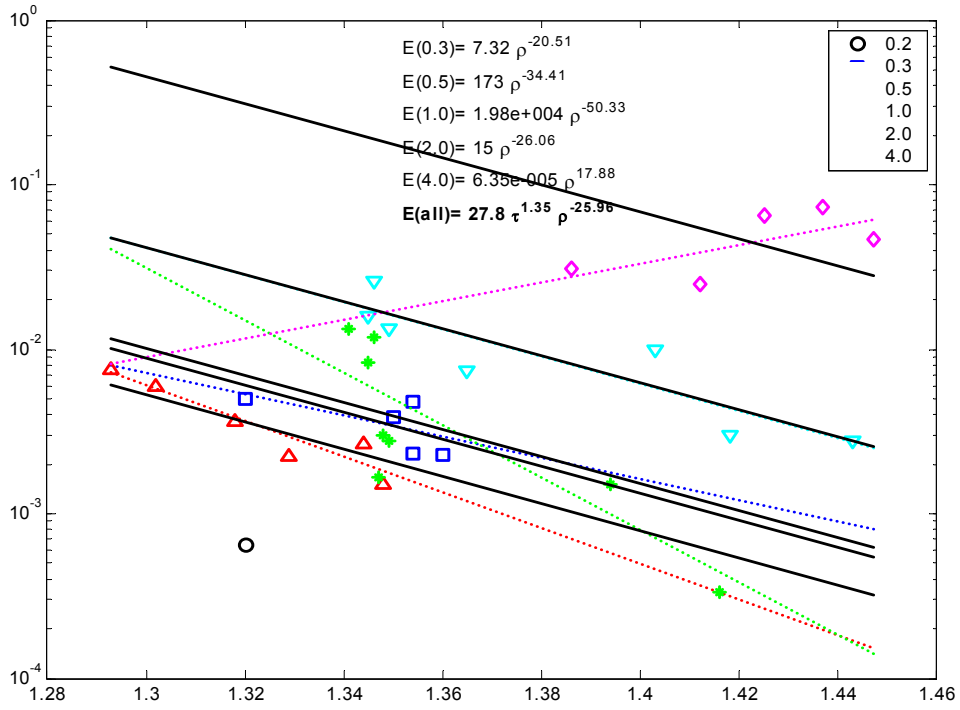

Figure 4-6. Erosion data and equation at Site 78S.

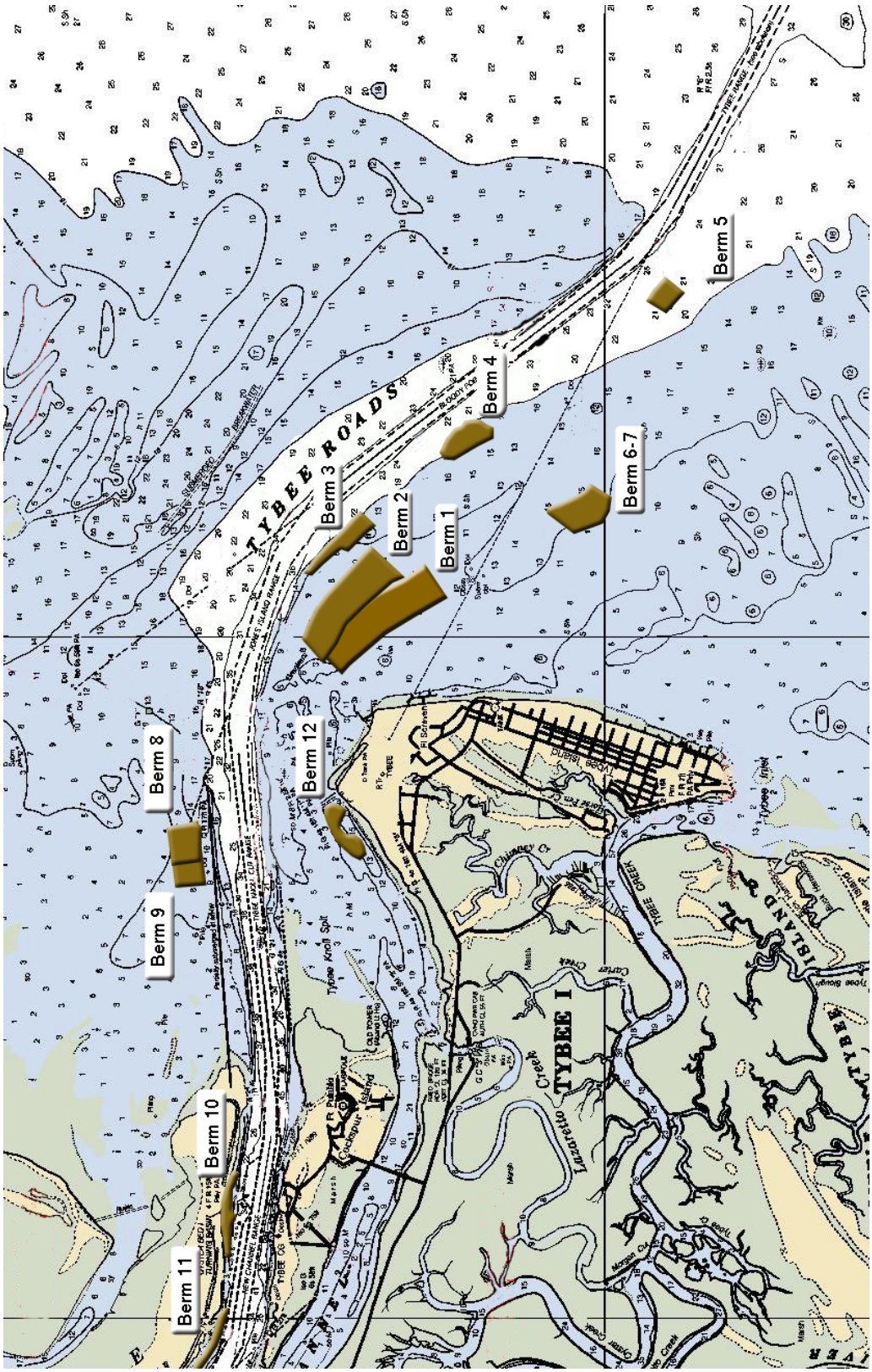

Figure 4-7a. Original mound locations analyzed.

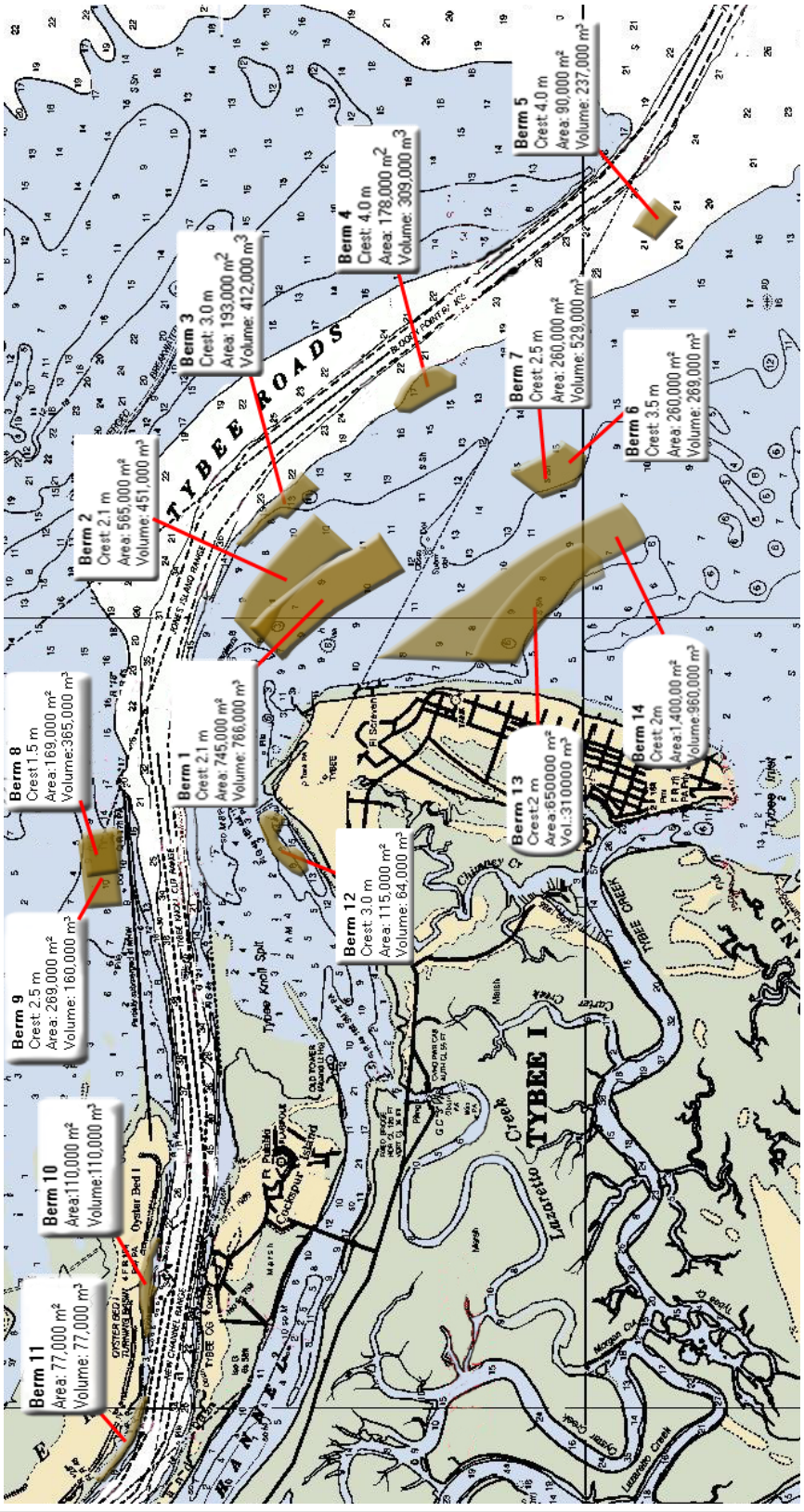

Figure 4-7b. Mound water depth (MLW), area, and maximum capacity.

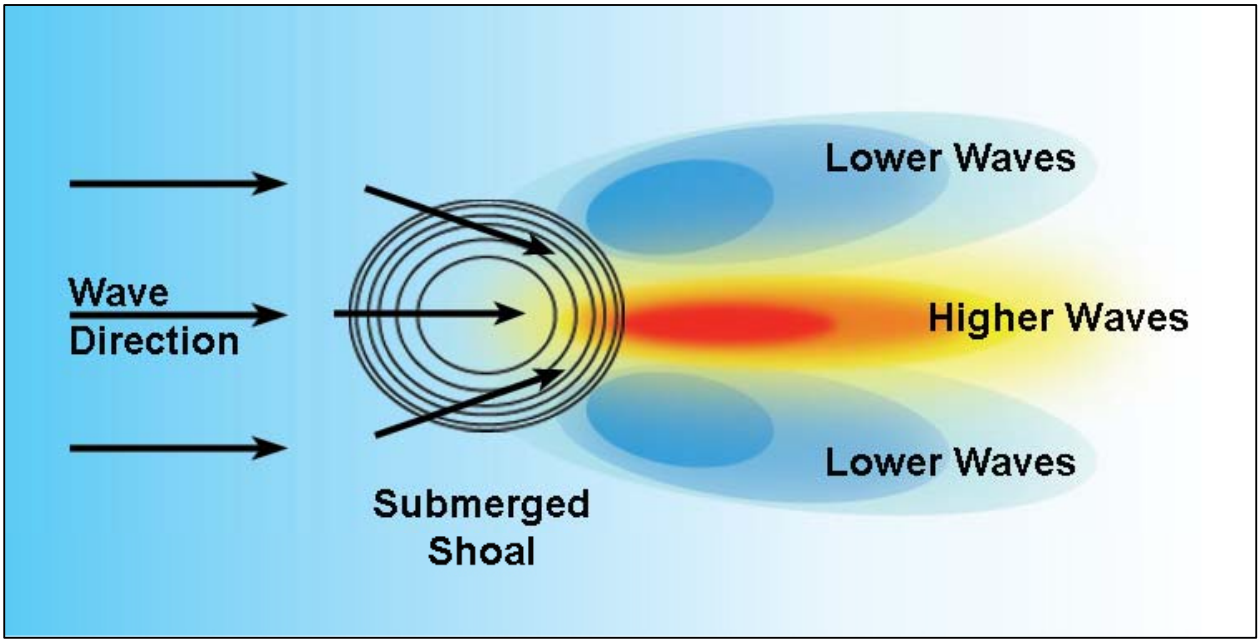

Figure 4-8. Schematic of effect of submerged shoal on wave refraction.

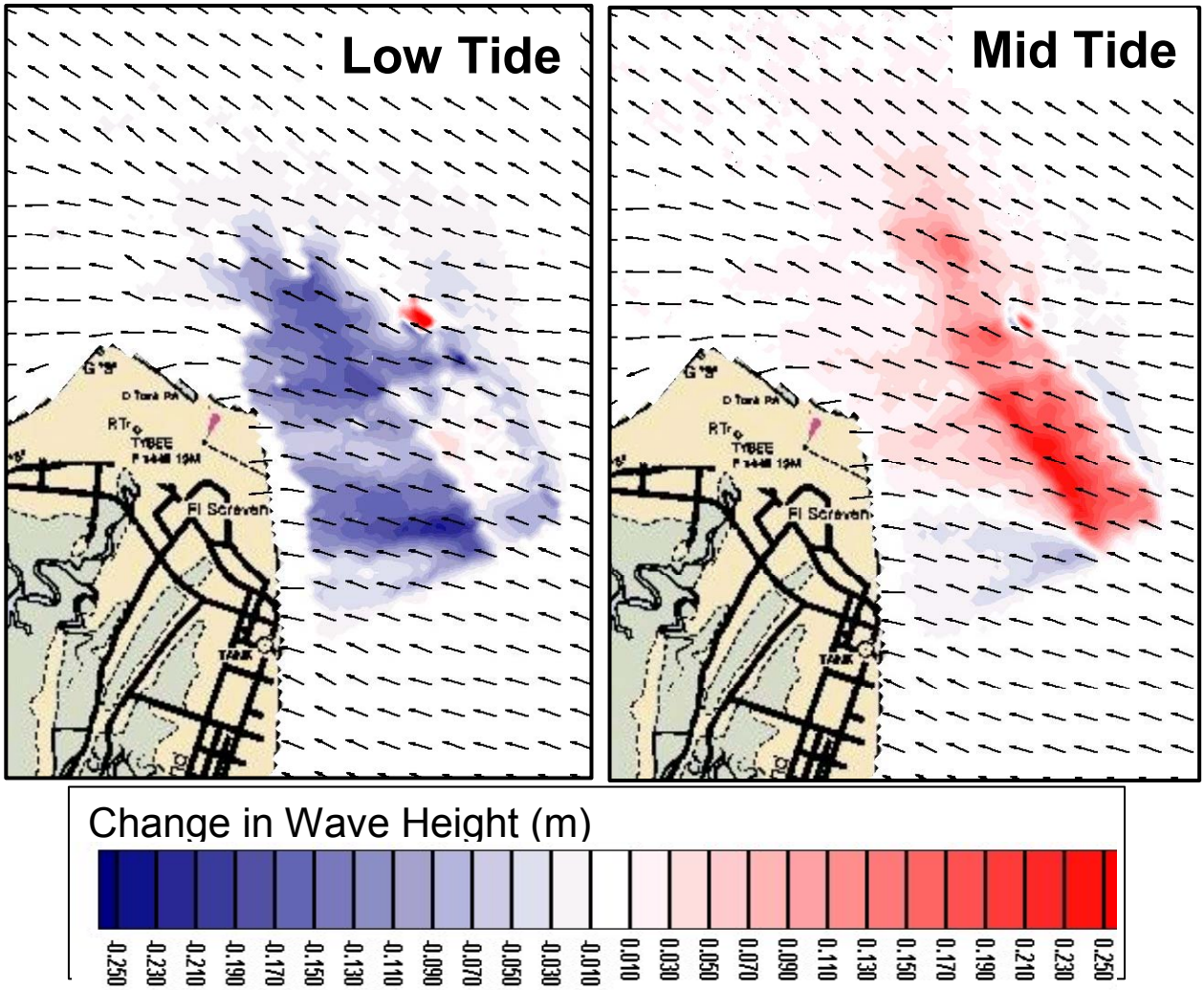

Figure 4-9. Change in wave transformation over Berm 01 at low- and mid-tide. Offshore wave conditions: H_{mo} = 0.75 m, T_p = 7 sec, wave direction: from ESE.

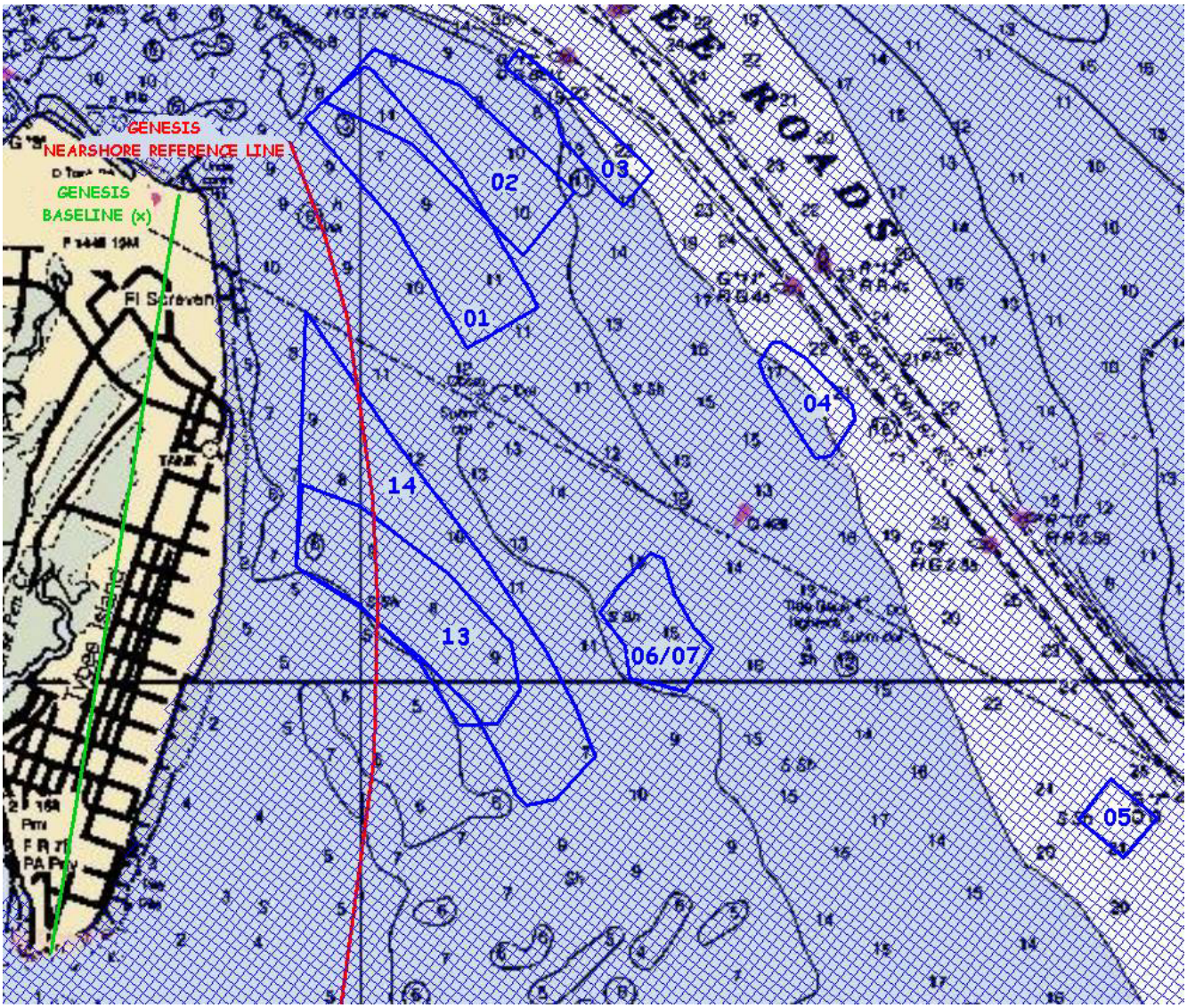

Figure 4-10. GENESIS domain, nearshore reference line, and candidate configurations for nearshore placement berms.

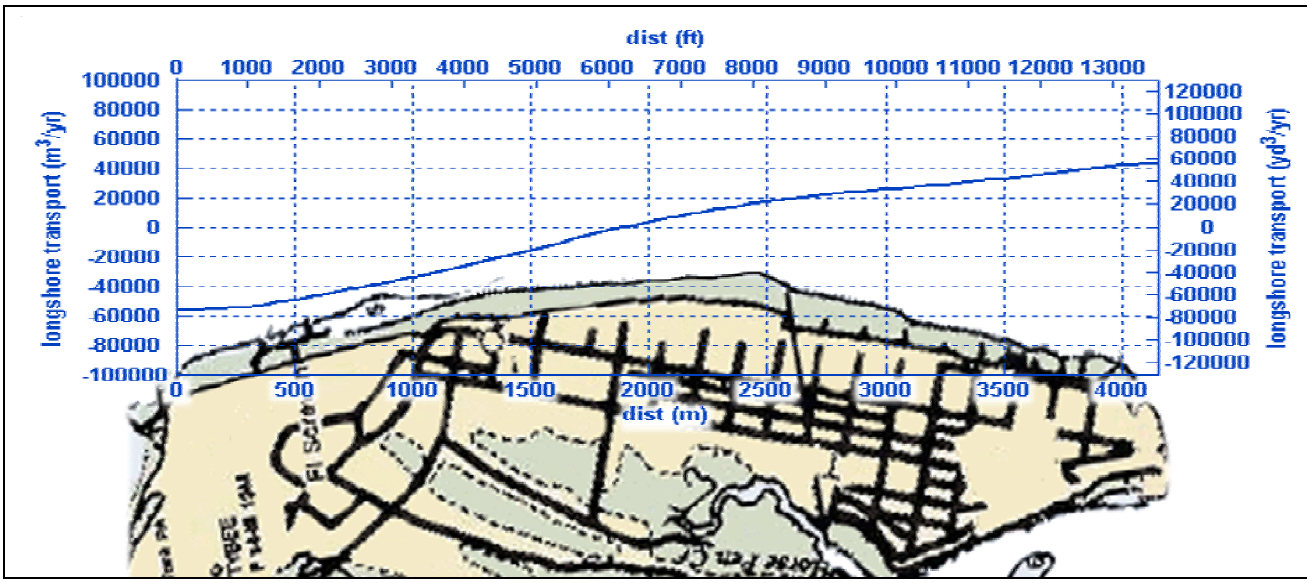

Figure 4-11. Average annual net longshore sediment transport rate estimated by GENESIS along Tybee Island shoreline for 1976-1995 simulation.

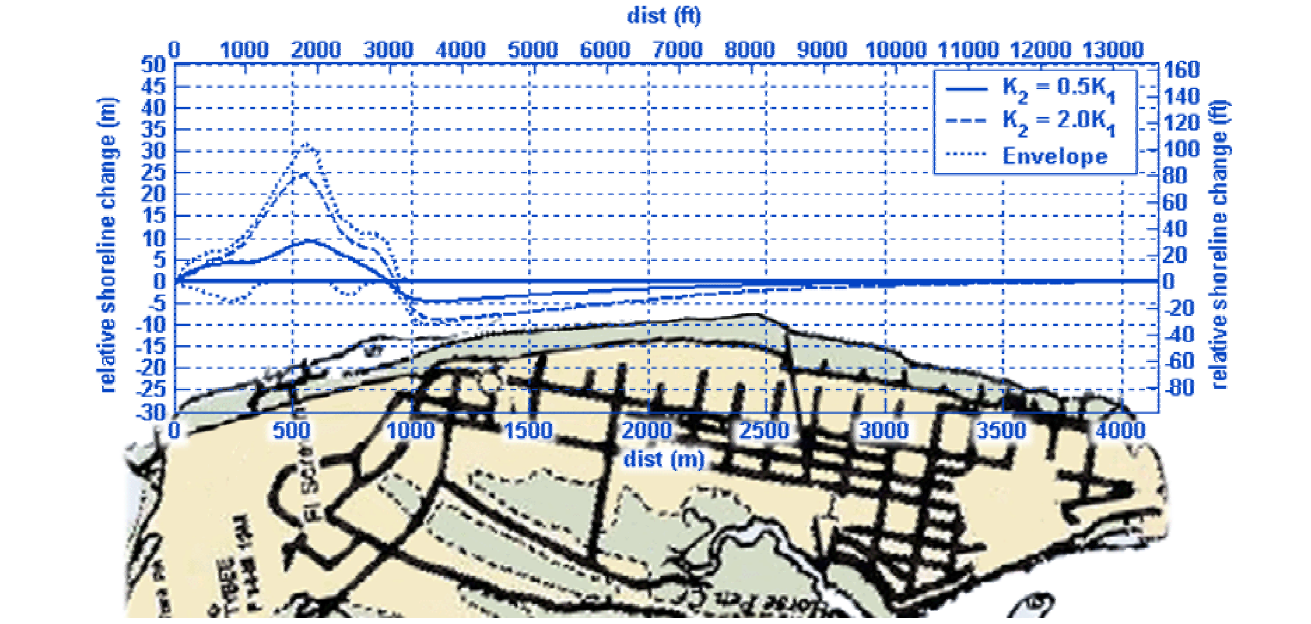

Figure 4-12. Relative change in shoreline between the Berm01 and base case. Solid line represents range in solutions within the uncertainty in the value of K_2. Dotted line indicates range of relative shoreline change over the 20-year simulation.

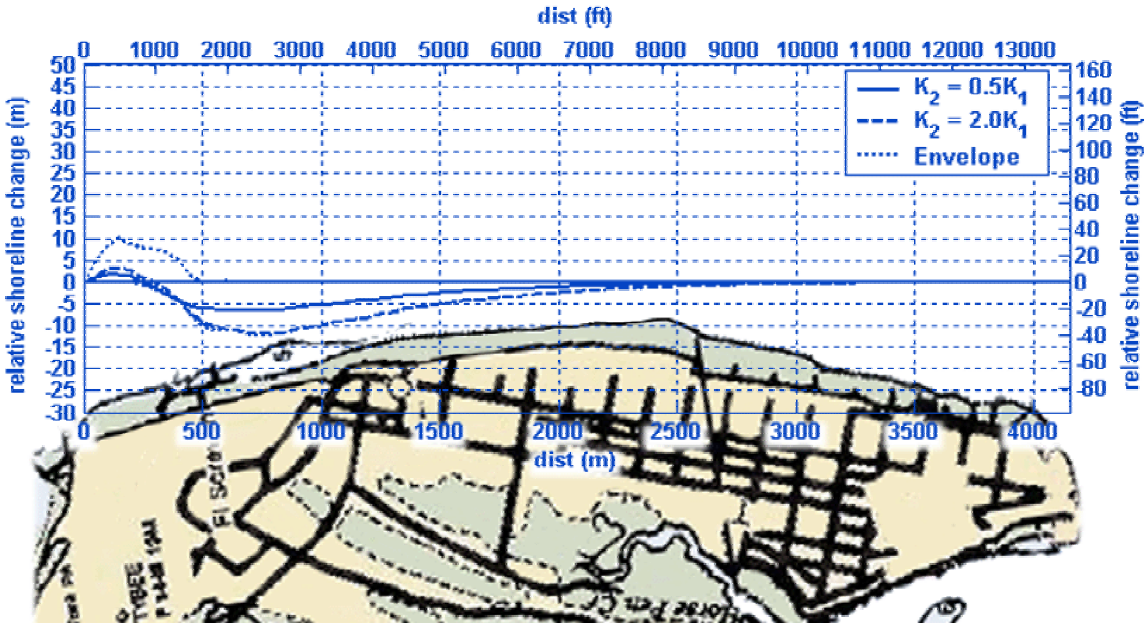

Figure 4-13. Relative change in shoreline between the Berm02 and base case. Solid line represents range in solutions within the uncertainty in the value of K_2. Dotted line indicates range of relative shoreline change over the 20-year simulation.

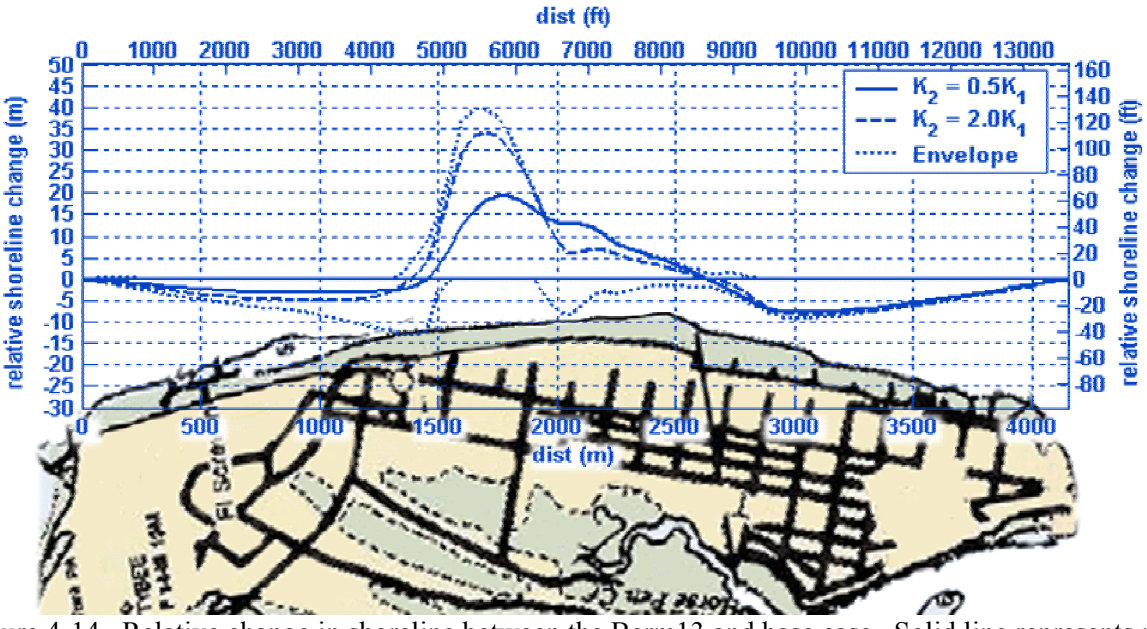

Figure 4-14. Relative change in shoreline between the Berm13 and base case. Solid line represents range in solutions within the uncertainty in the value of K_2. Dotted line indicates range of relative shoreline change over the 20-year simulation.

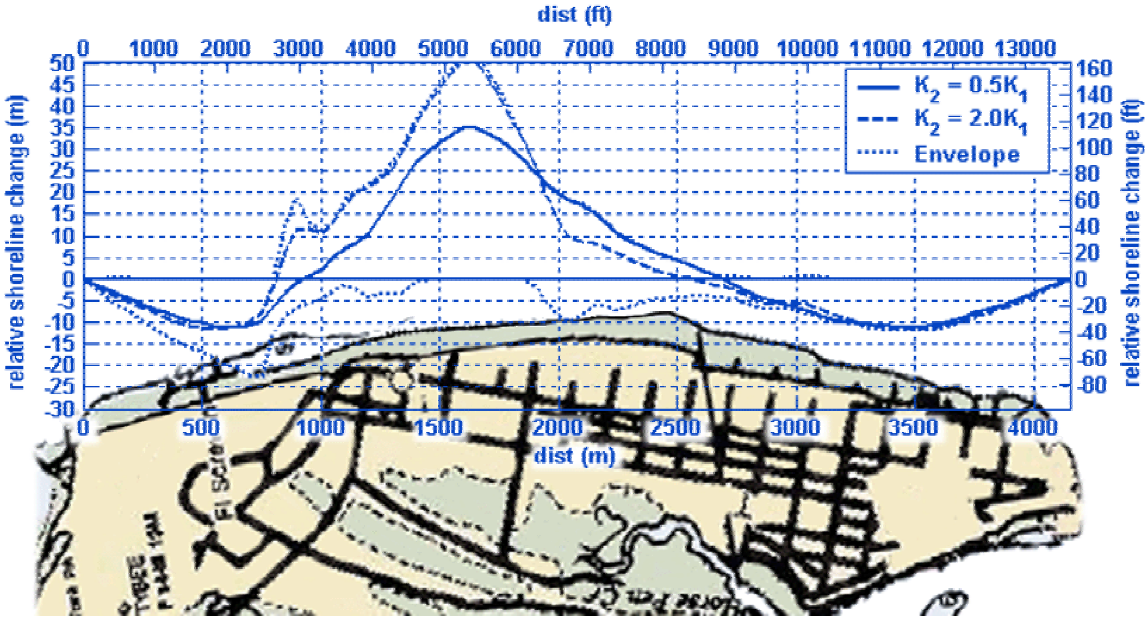

Figure 4-15. Relative change in shoreline between the Berm14 and base case. Solid line represents range in solutions within the uncertainty in the value of K_2. Dotted line indicates range of relative shoreline change over the 20-year simulation.

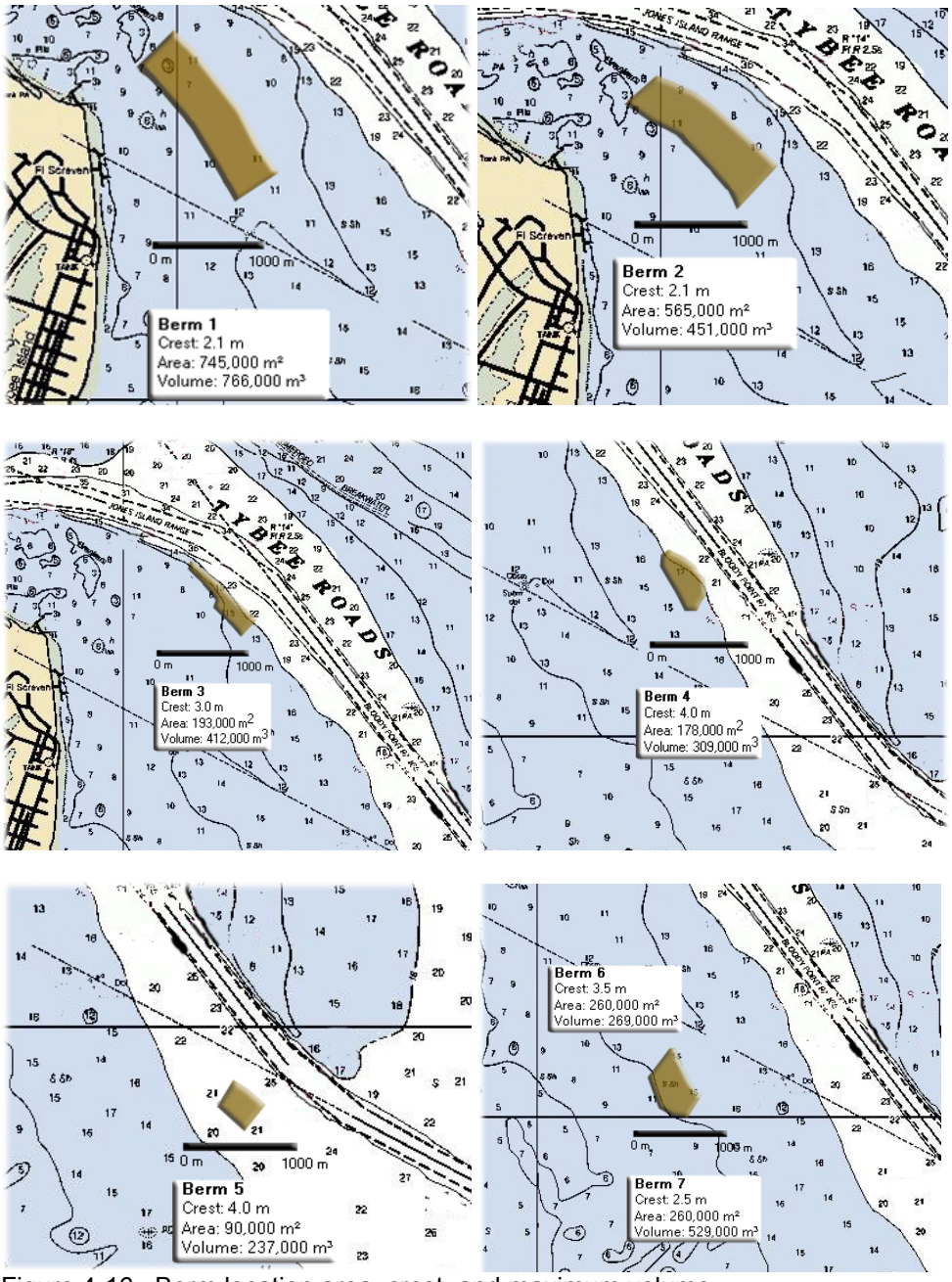

Figure 4-16. Berm location area, crest, and maximum volume

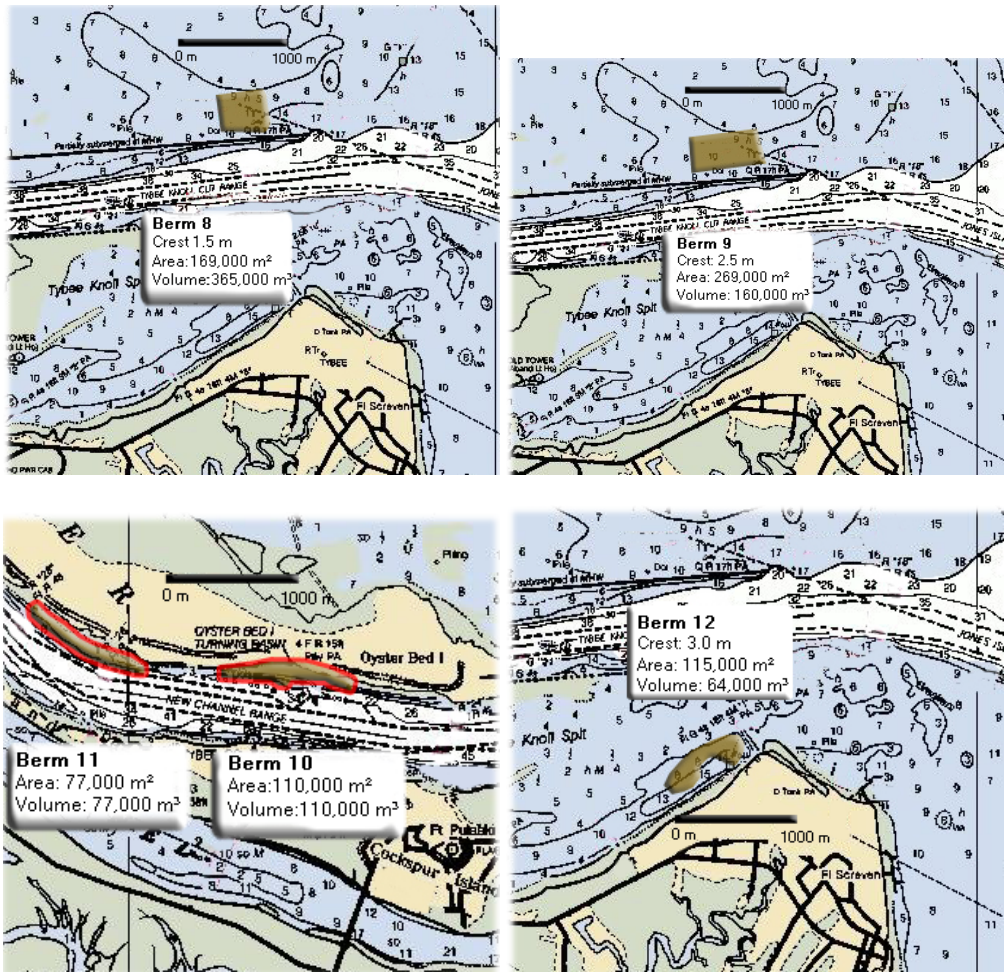

Figure 4-16. Berm location area, crest, and maximum volume

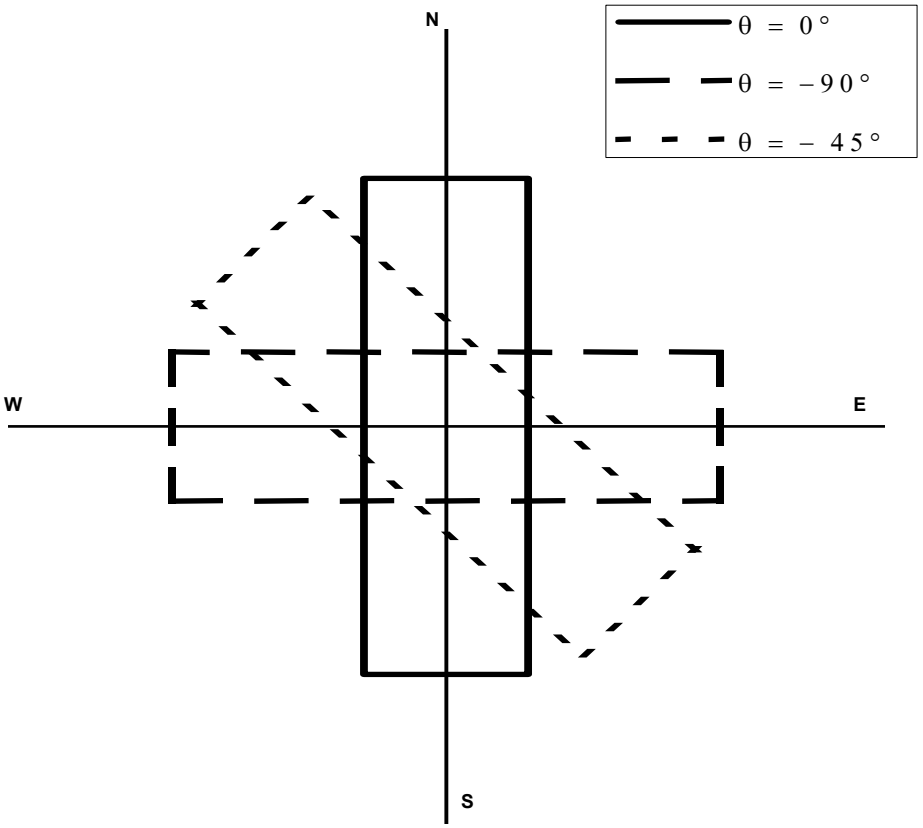

Figure 4-17. Mound orientations

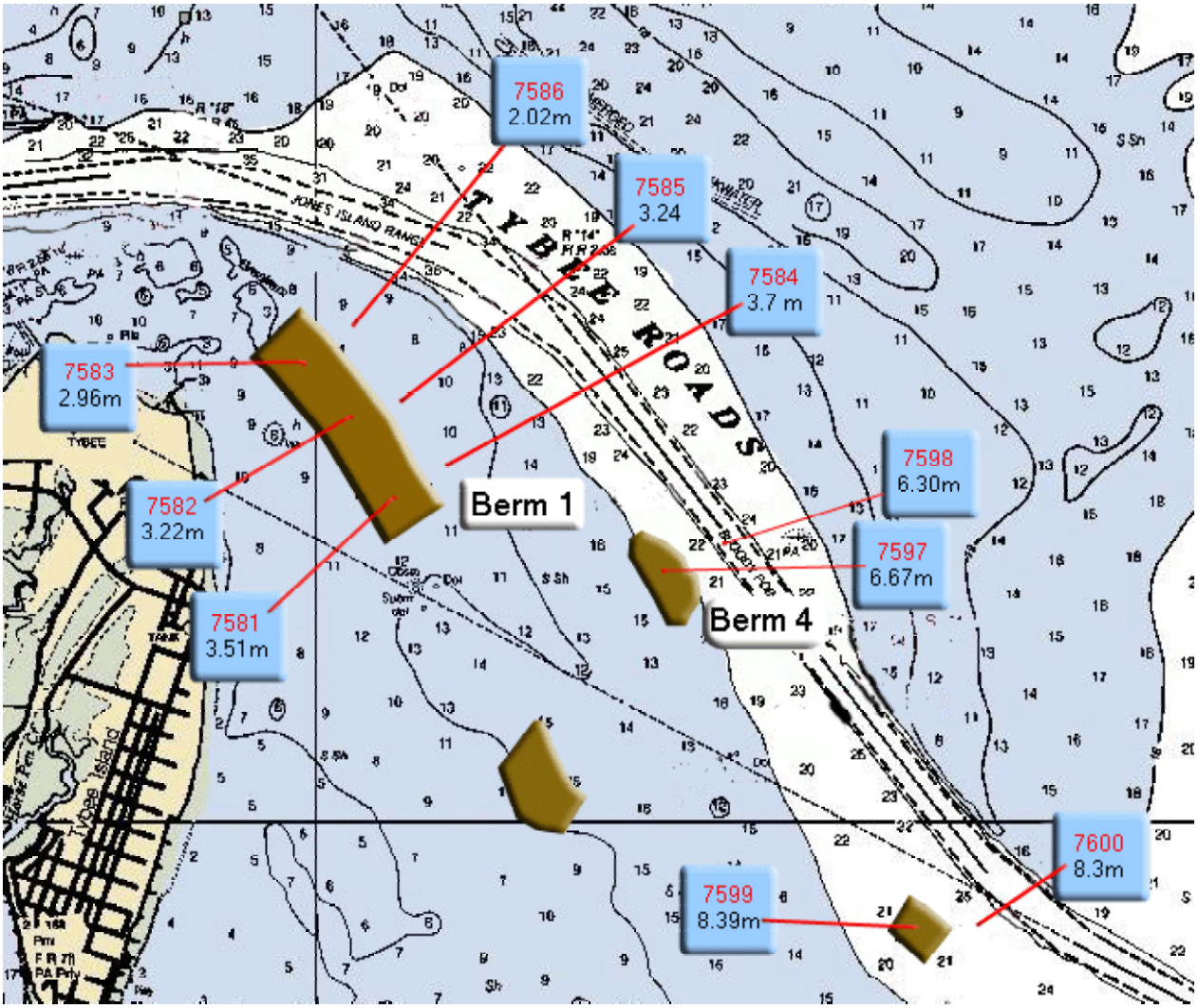

Figure 4-18. Locations for GTRAN erosion calculation: mounds 1,4,5.

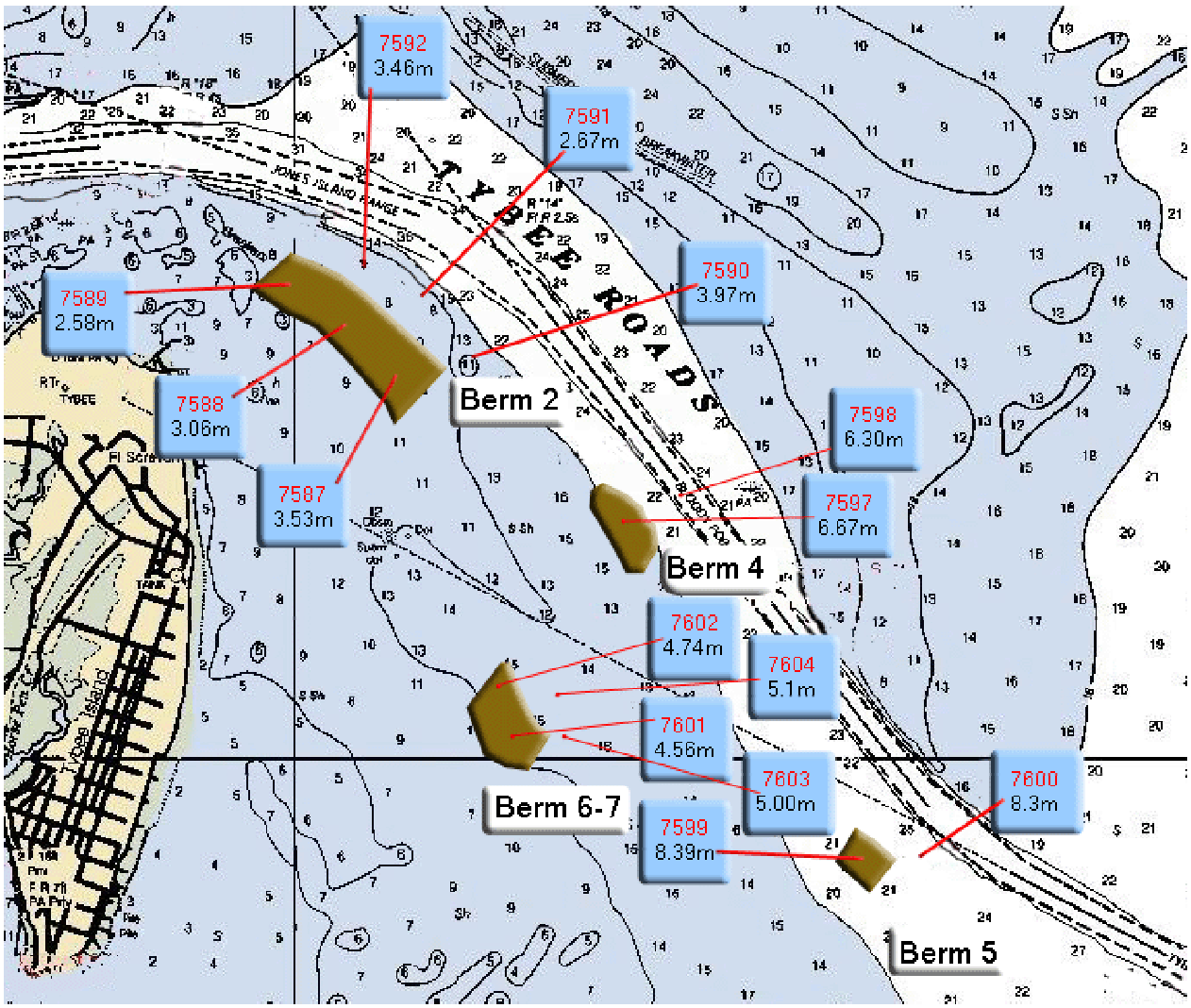

Figure 4-18. Locations for GTRAN erosion calculation: mounds 2,4-7.

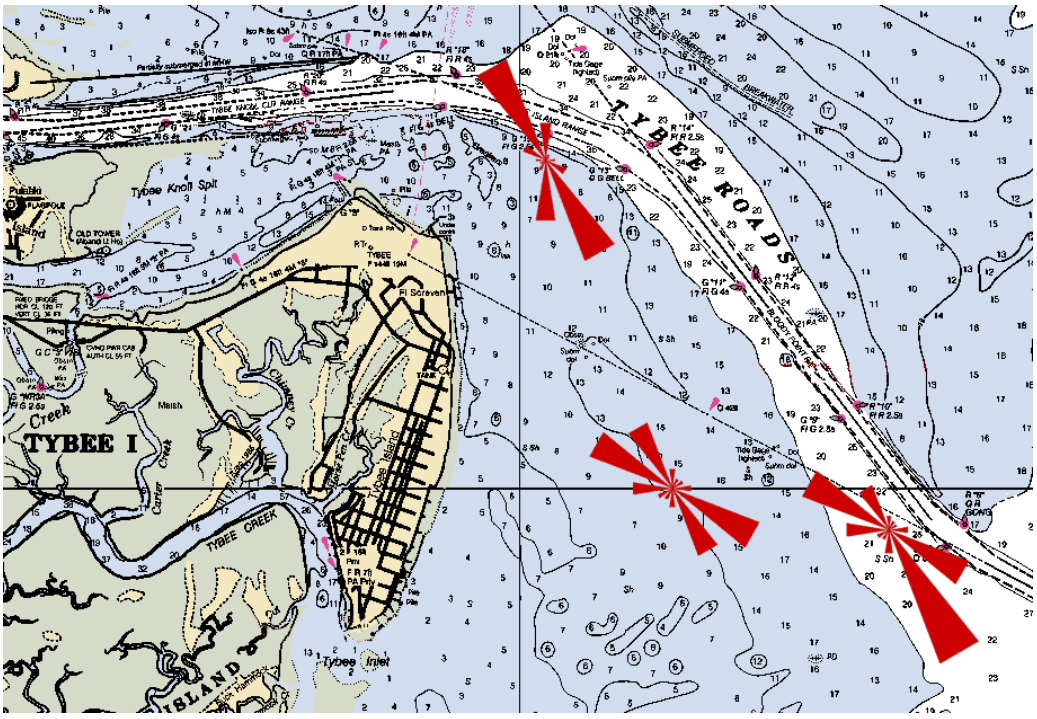

Figure 4-18. Sample rose plot of erosion magnitude and direction at berms 1,5,7

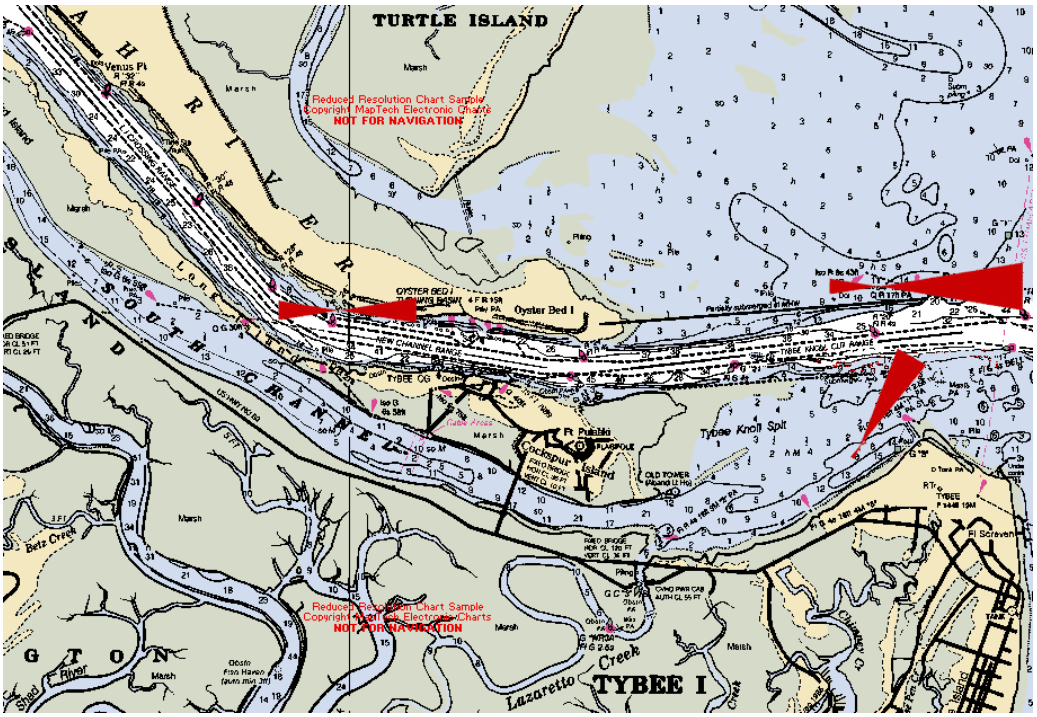

Figure 4-19. Sample rose plot of erosion magnitude and direction at berms 8, 10, 12

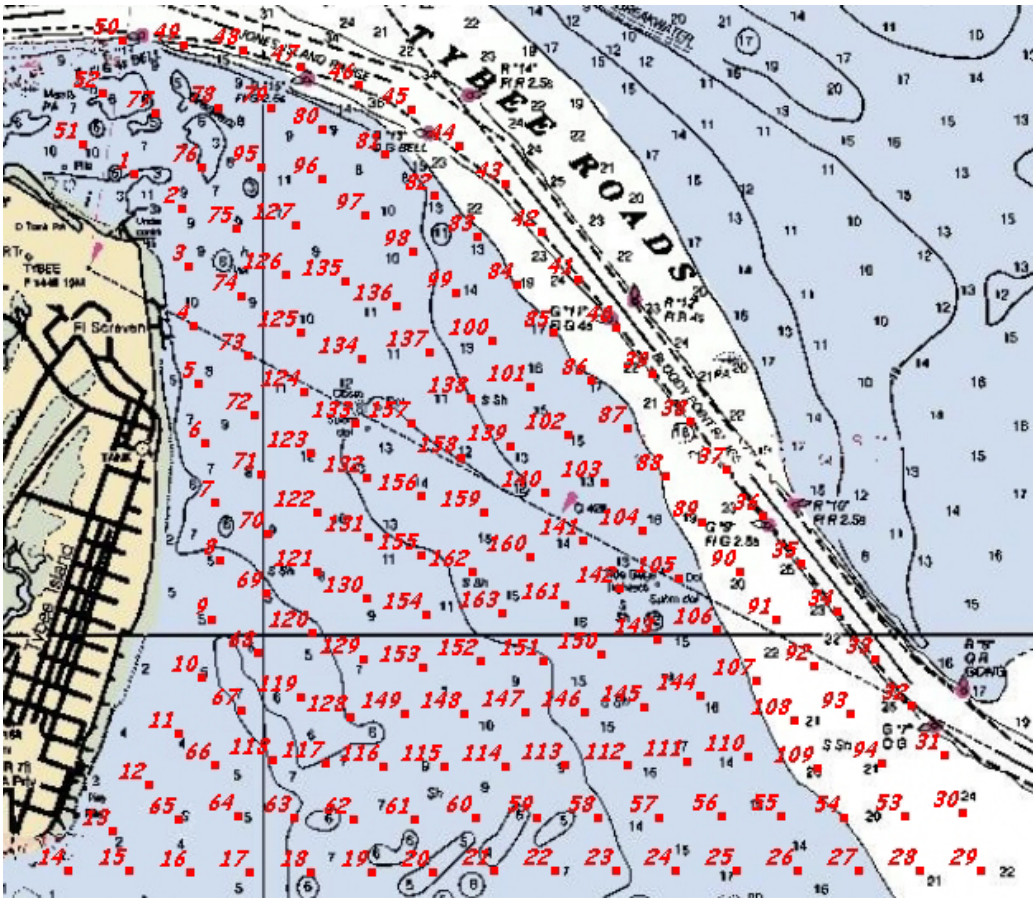

Figure 4-20. Distribution of GTRAN calculation points.

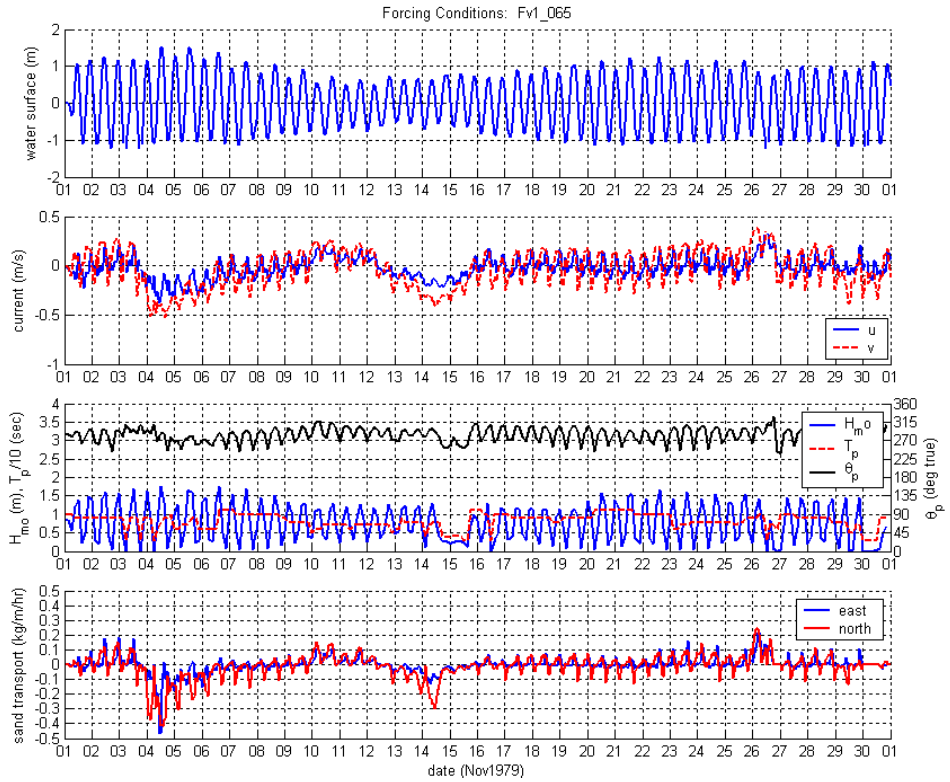

Figure 4-21a Time-series of water level, current, waves, and transport for November 1979 at Point 65 (Figure 4-20)

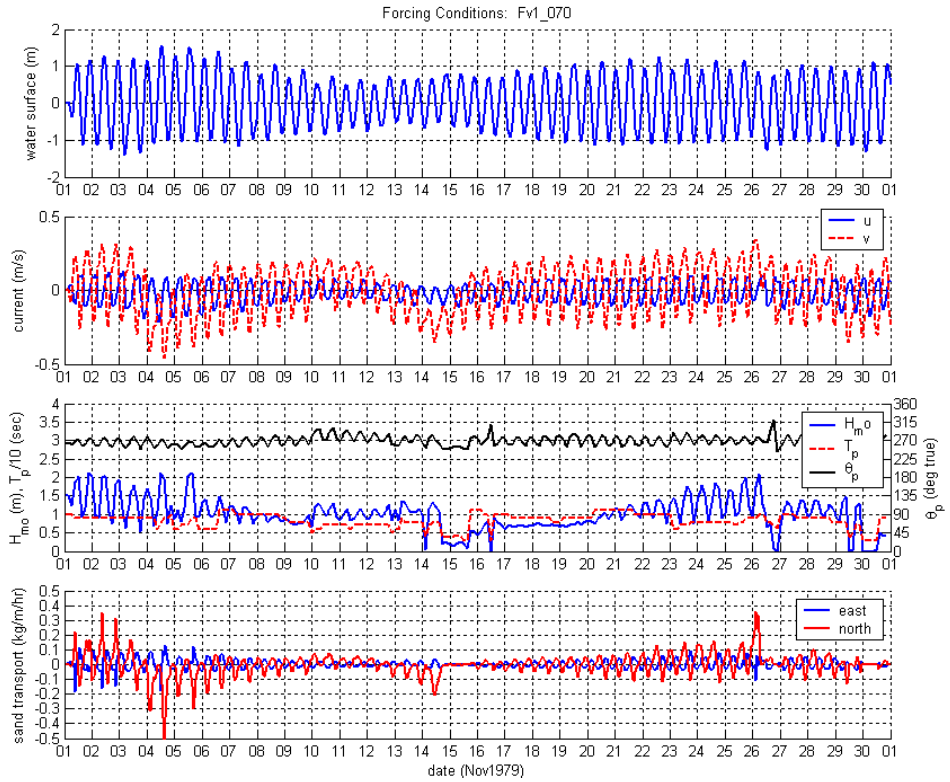

Figure 4-21b Time-series of water level, current, waves, and transport for November 1979 at Point 70 (Figure 4-20)

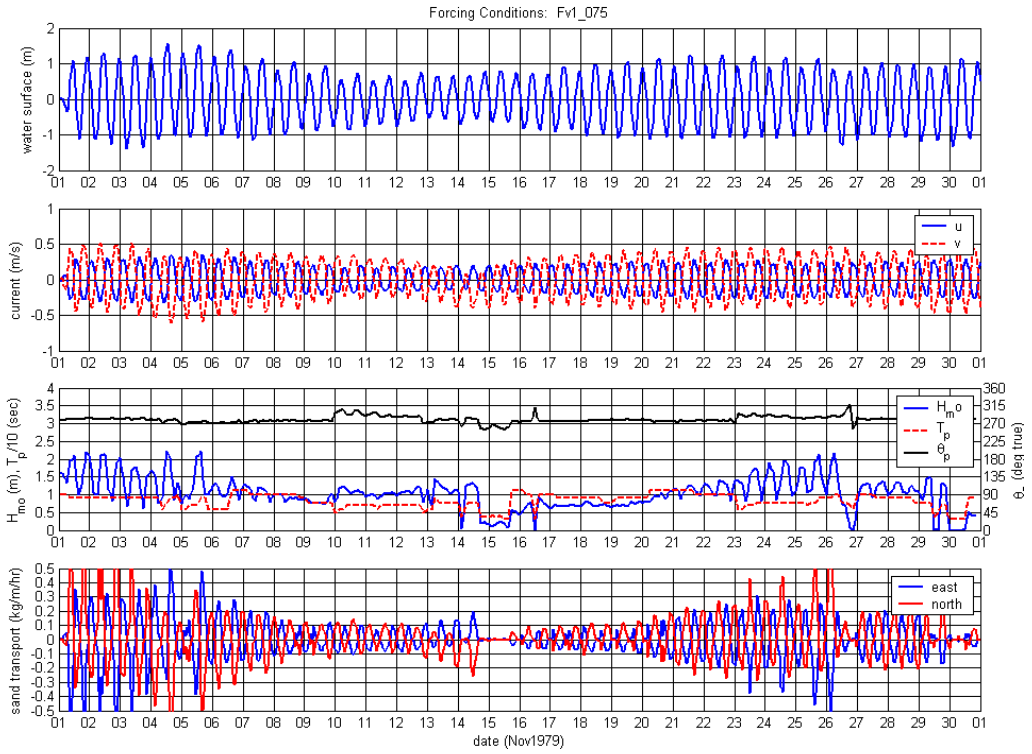

Figure 4-21c Time-series of water level, current, waves, and transport for November 1979 at Point 75 (Figure 4-20)

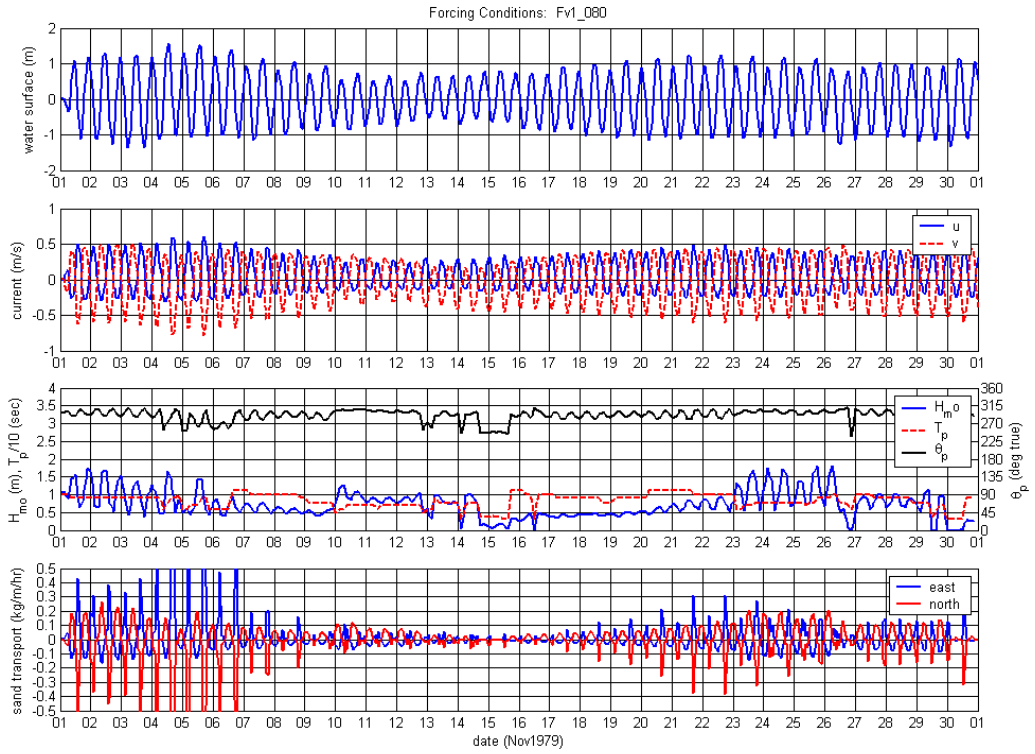

Figure 4-21d Time-series of water level, current, waves, and transport for November 1979 at Point 80 (Figure 4-20)

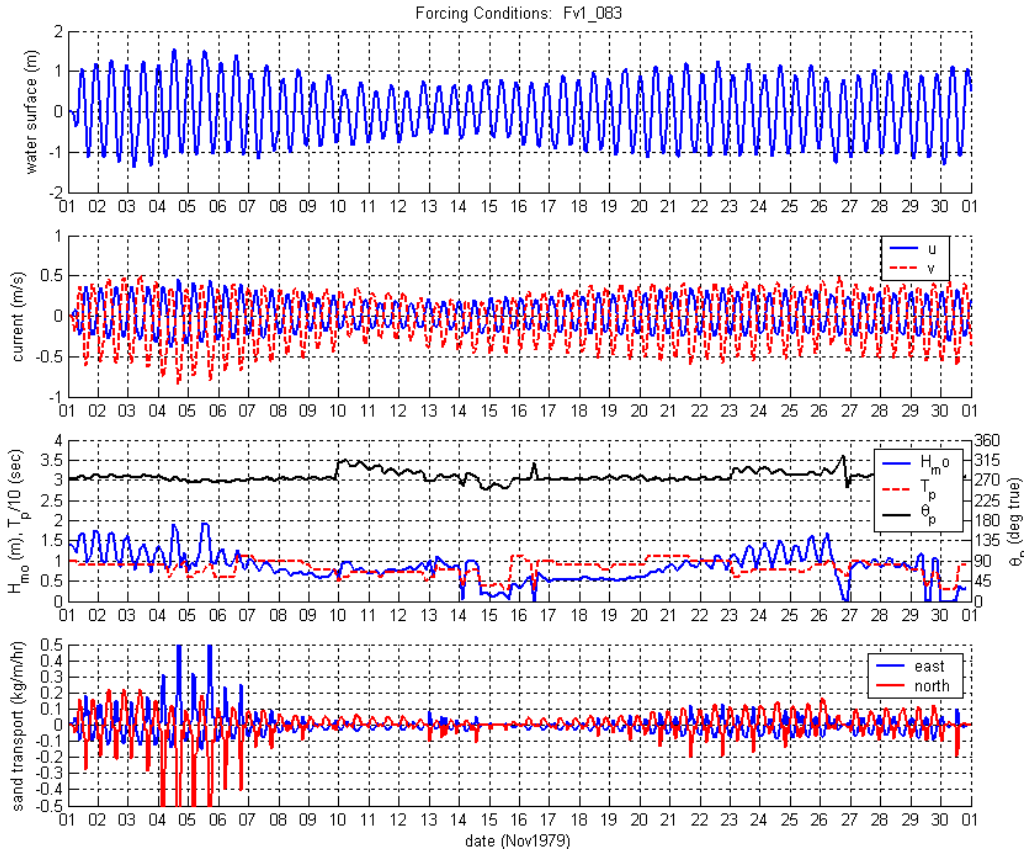

Figure 4-21e Time-series of water level, current, waves, and transport for November 1979 at Point 83 (Figure 4-20)

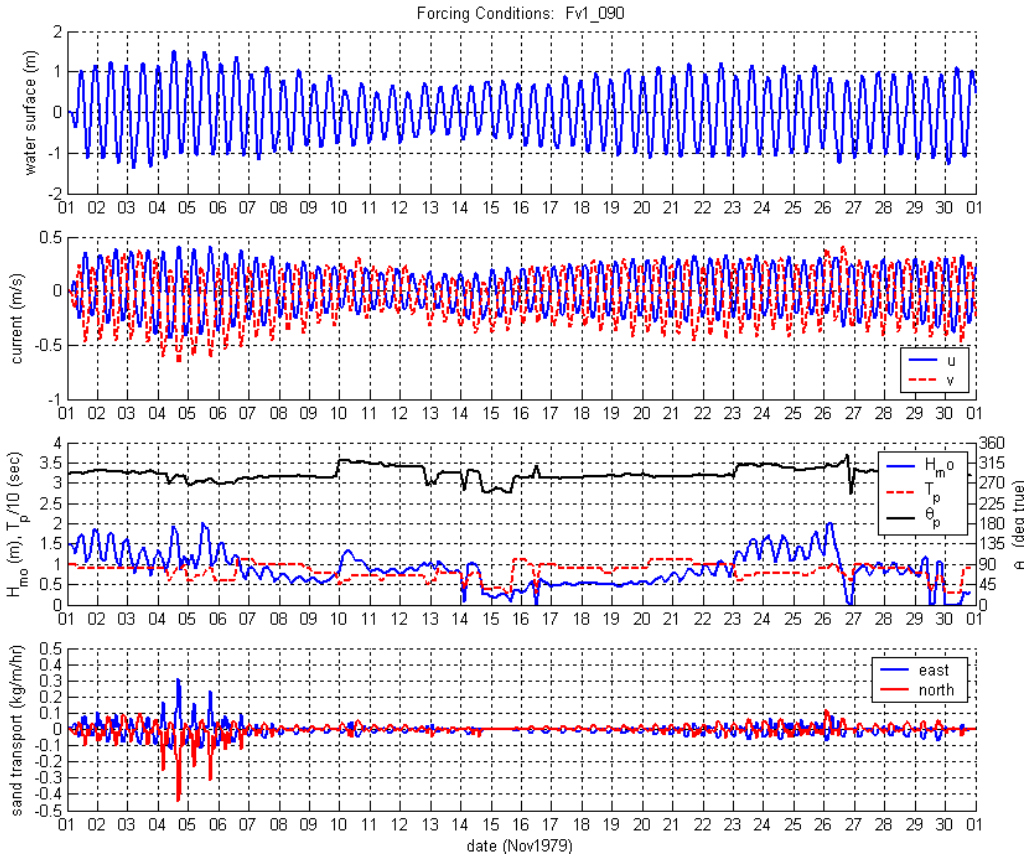

Figure 4-21f Time-series of water level, current, waves, and transport for November 1979 at Point 90 (Figure 4-20)

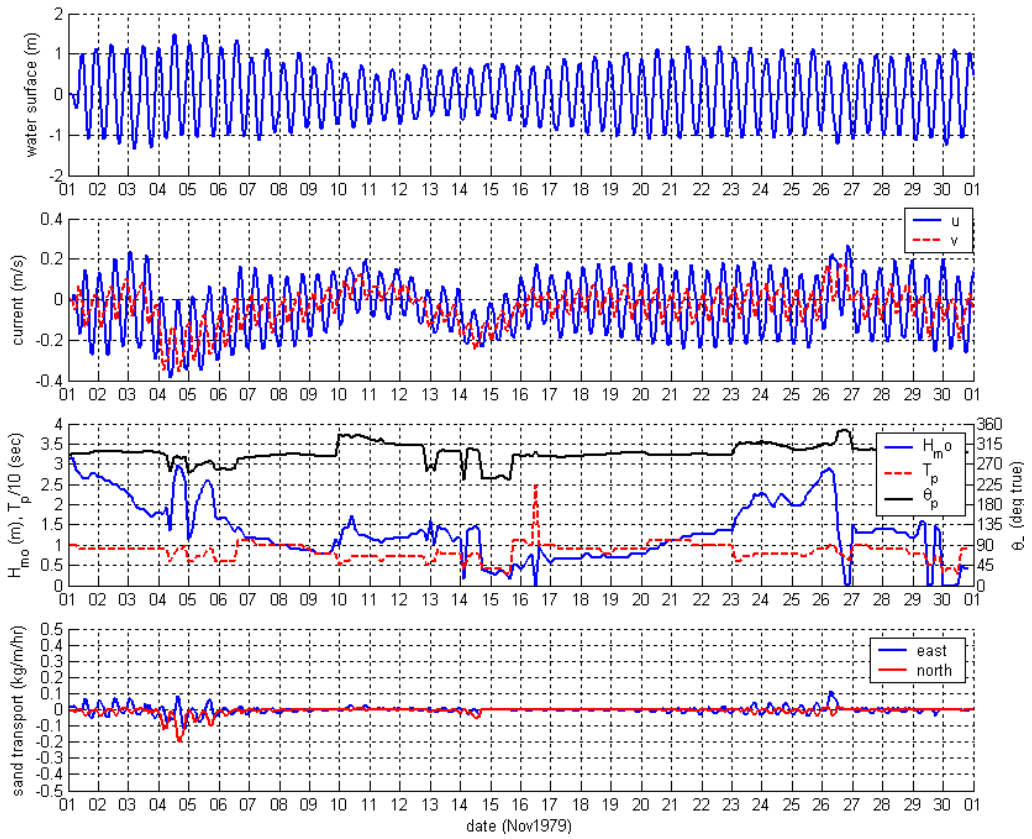

Figure 4-22 Time-series of water level, current, waves, and transport for November 1979 at existing offshore disposal site.

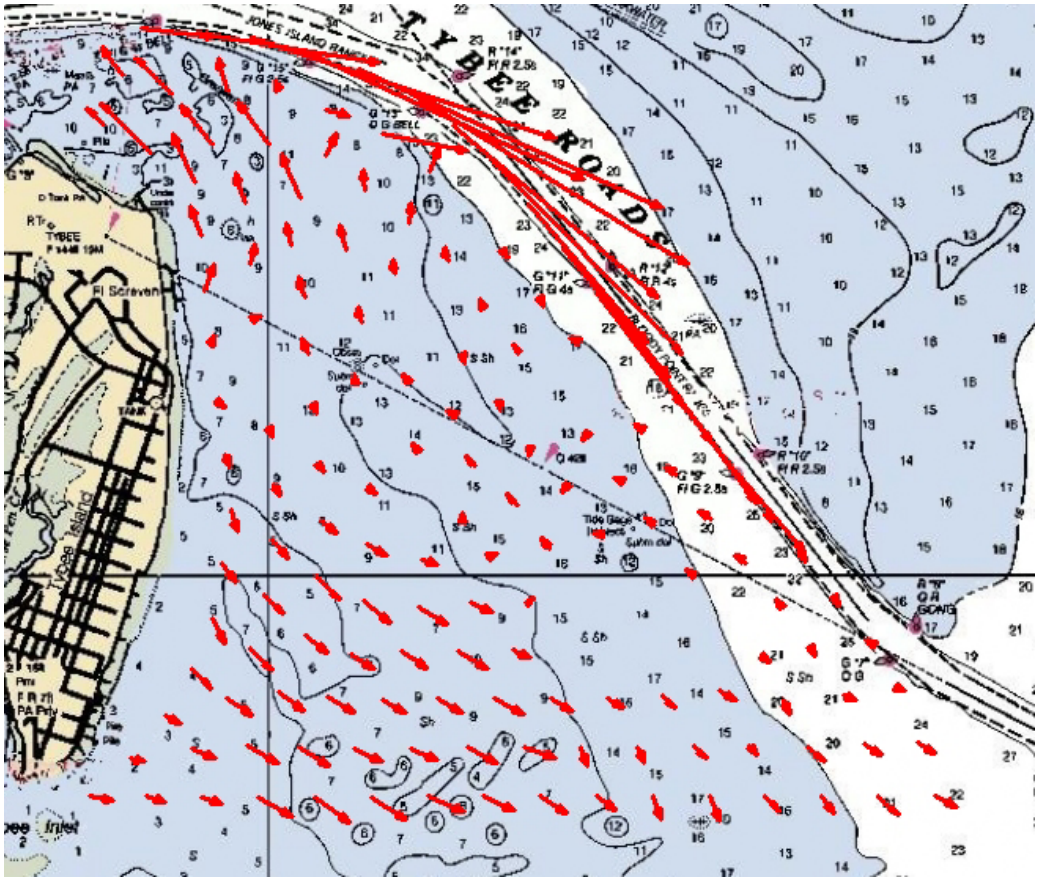

Figure 4-23. Net transport vectors for operational month (January 1992).

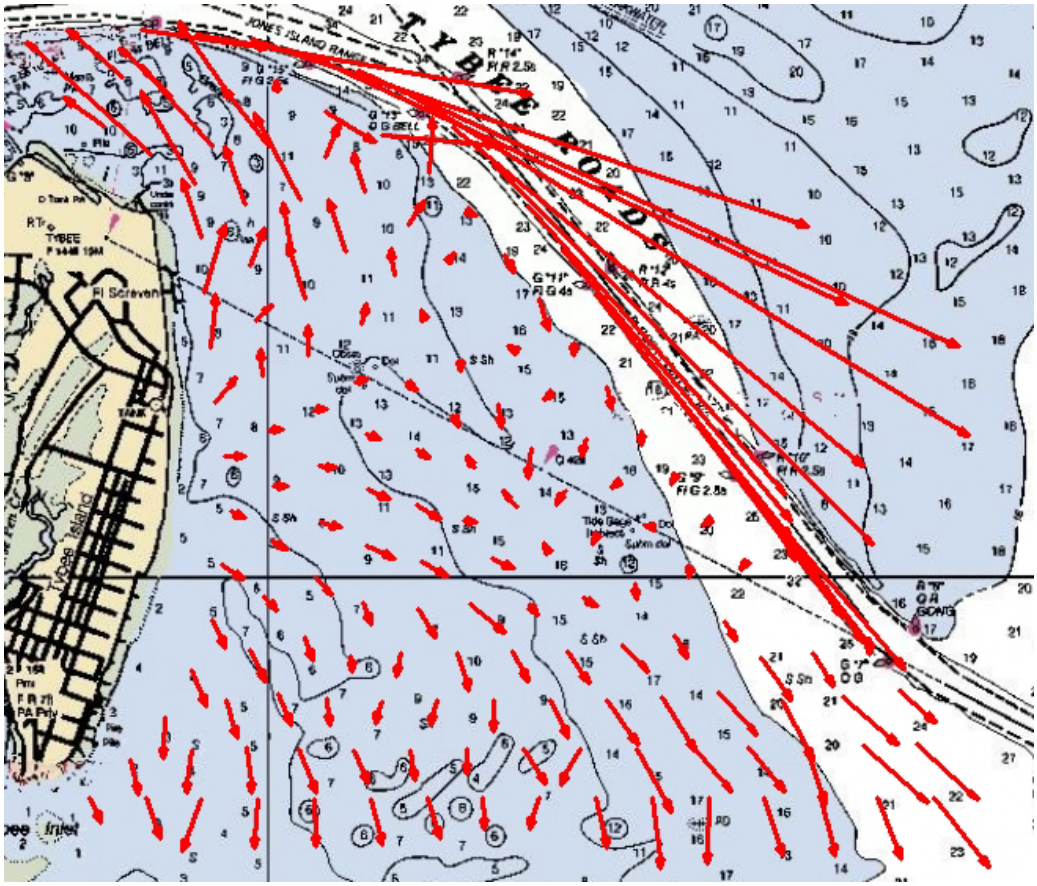

Figure 4-24. Net transport vectors for storm month (November 1979)

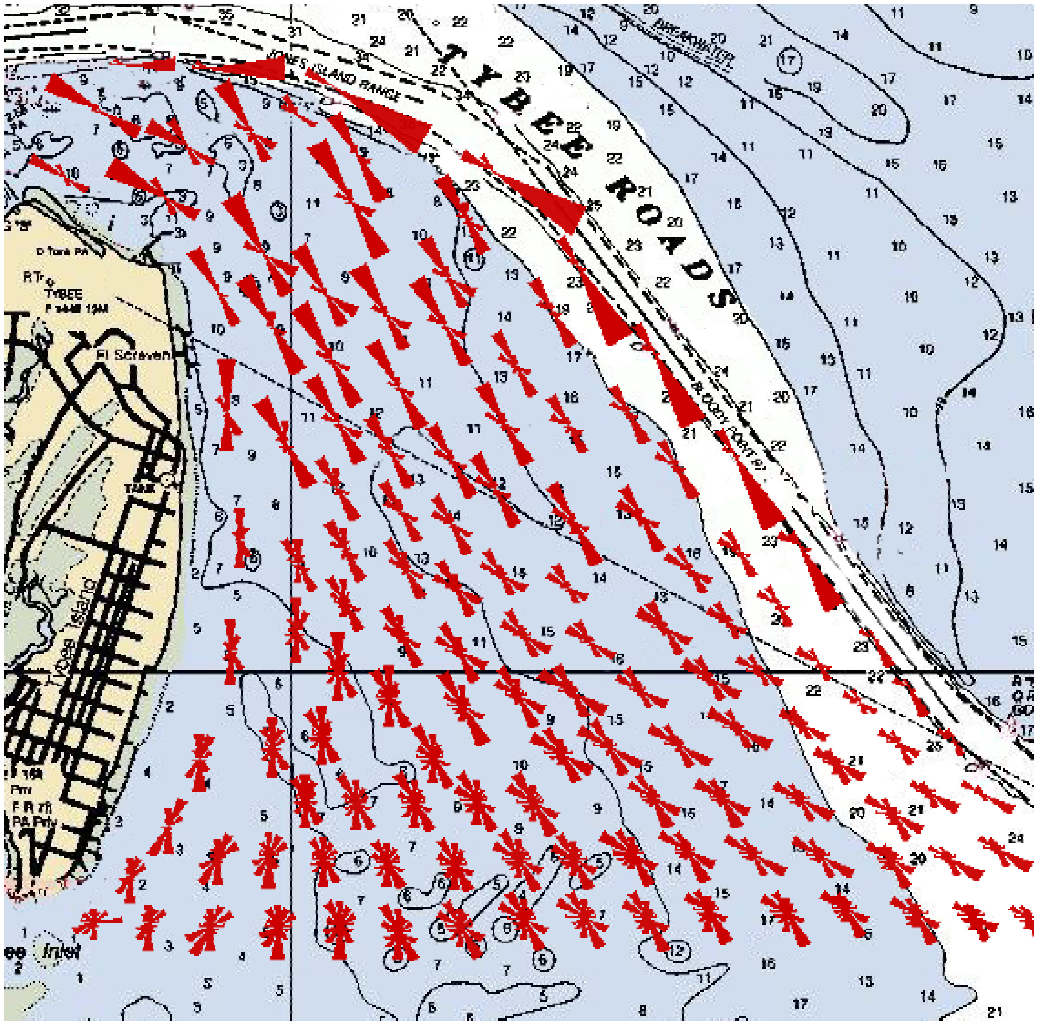

Figure 4-25 Transport roses at selected points for storm month (November 1979)

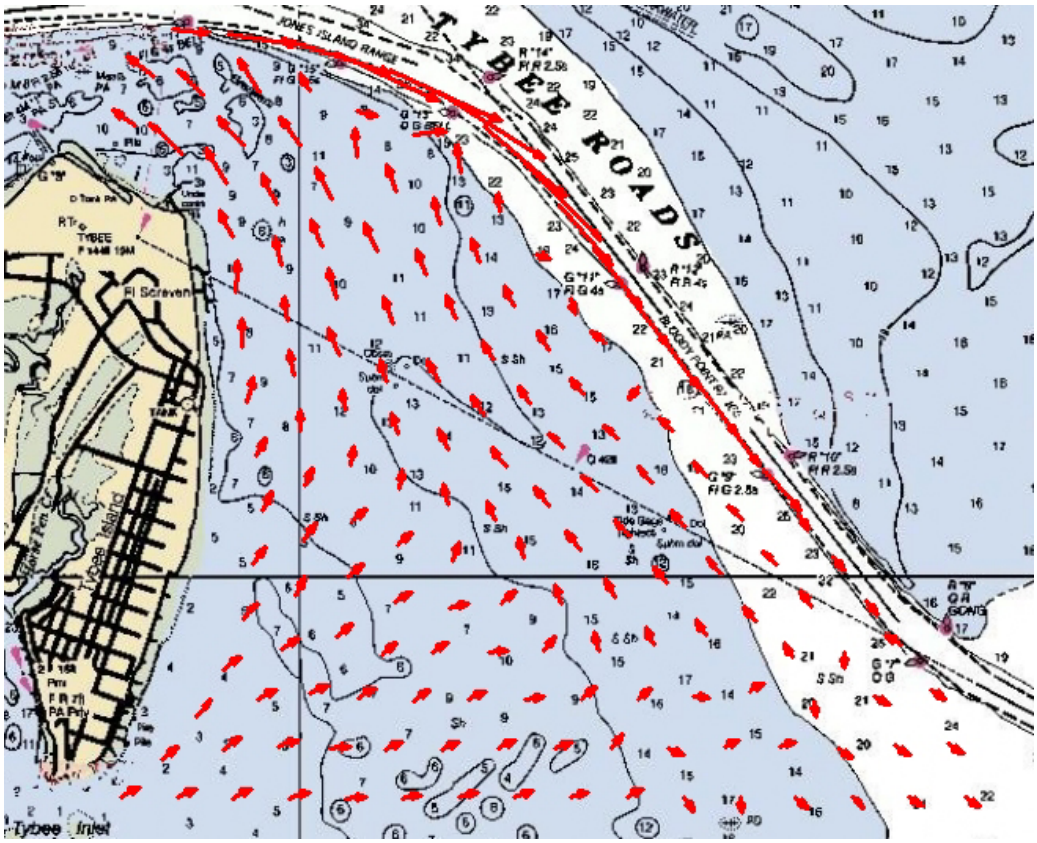

Figure 4-26. Net transport vectors for 24-year simulation (1976-1999). Note: not to same scale as presented in Figures 21 and 22.

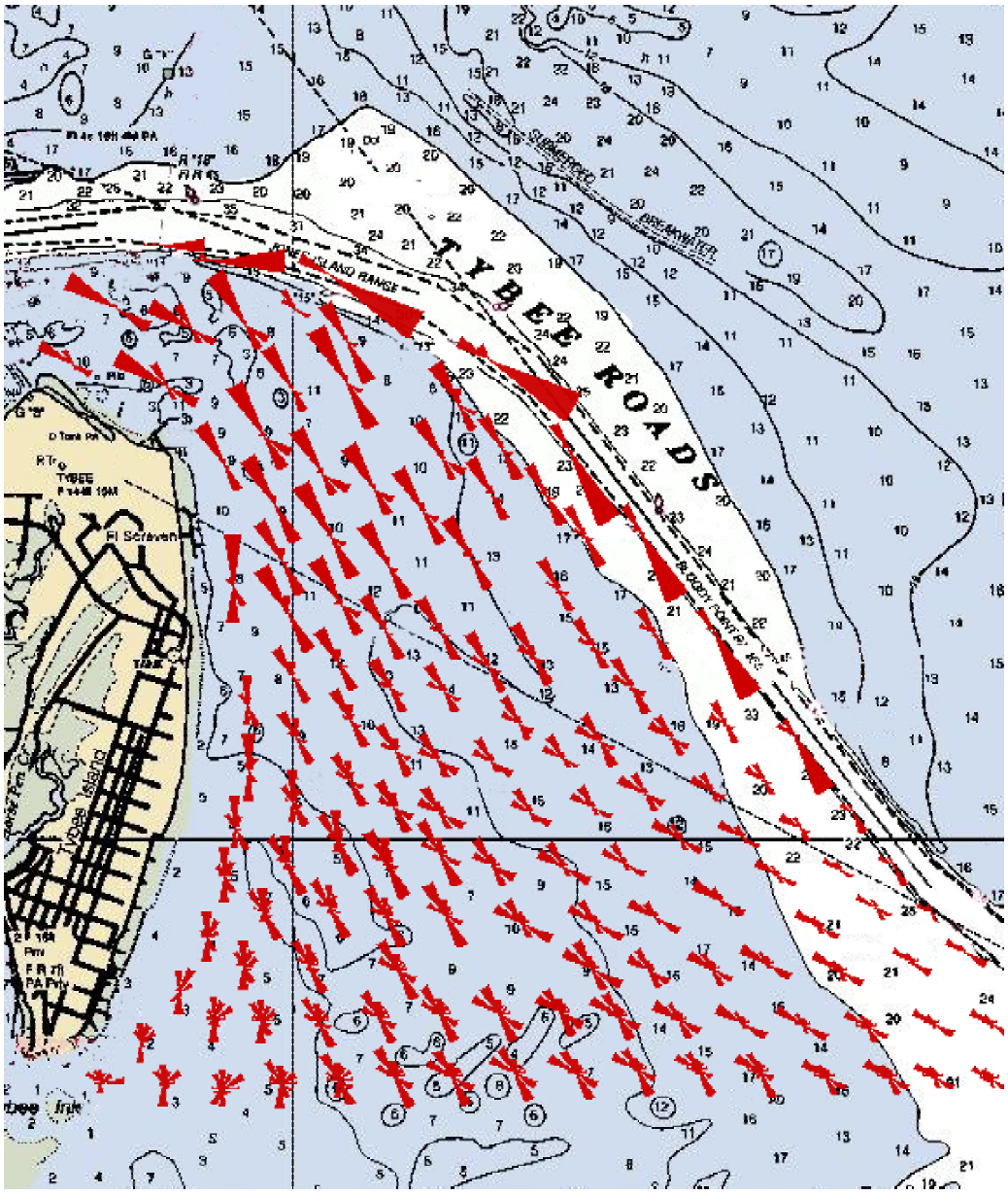

Figure 4-27. Transport rose at selected points for 24-year simulation (1976-1999).

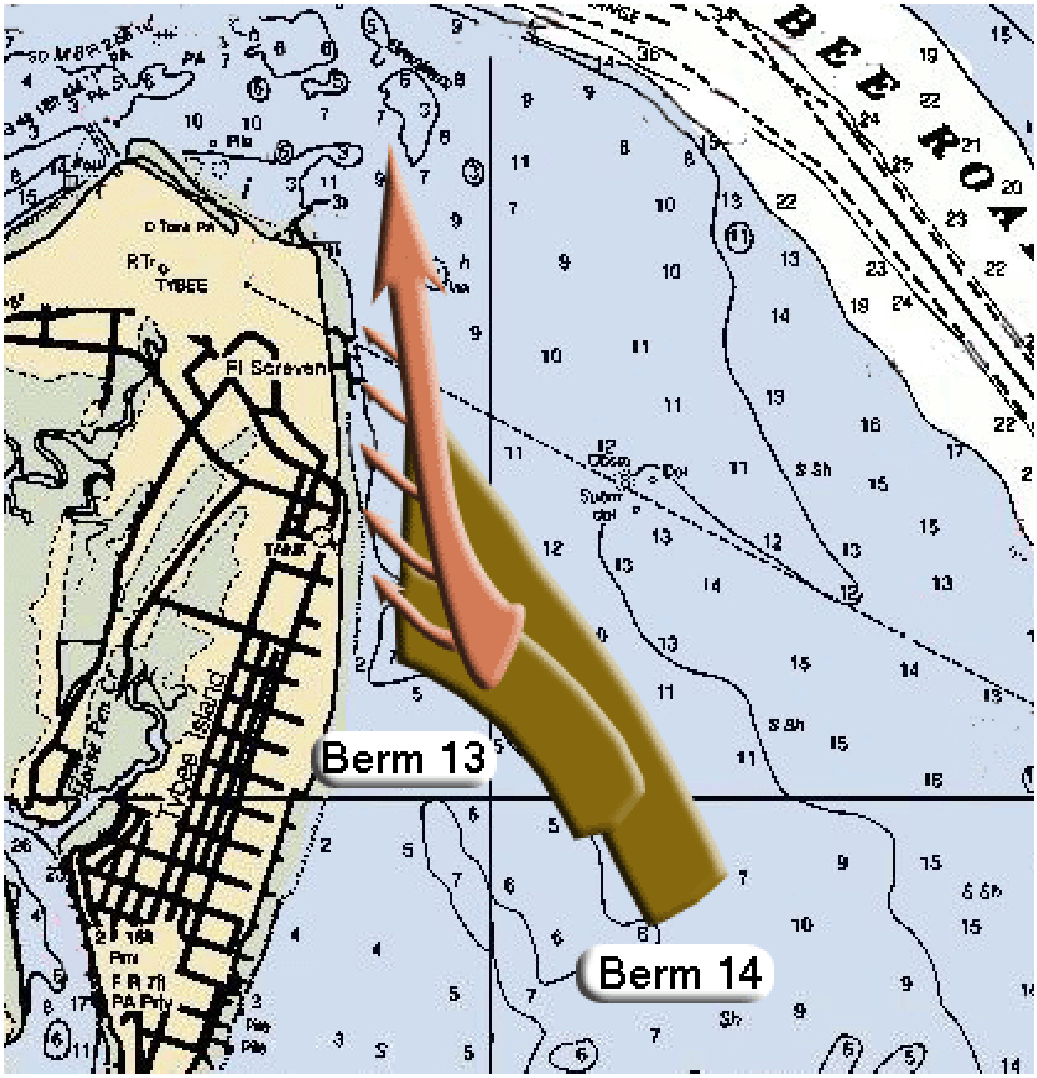

Figure 4-28. Net transport path for berms 13 and 14 (large arrow) with onshore transport component (small arrows). Note: other secondary transport directions are not included.

5 Sediment Suspension and Deposition During Dredging and Placement Operations

Plumes of suspended sediment generated during dredging and placement operations are of potential concern on the aquatic environment. Consequently, estimates of suspended sediment entrainment and transport during the dredging and placement operations are required to assess the potential impact to the environment. Chapter 5 describes model applications and analysis addressing sediment suspension, transport, and deposition during dredging and nearshore placement operations at the Savannah River entrance channel and adjacent waters. Two primary issues are 1) whether unsuitable levels of suspended sediment are present in the water column or suspended sediment in the water column or 2) do fines placed in suspension settle out in the nearshore zone. This chapter does not address the biological effects or risk to the environment, but presents suspended sediment concentrations from which those assessments may be made.

SSFATE Model and Input

The SSFATE (Suspended Sediment FATE) model was recently developed under the Dredging Operations and Environmental Research (DOER) Program of the US Army Corps of Engineers to address concerns related to sediment resuspension by the dredging process. The model is designed to predict spatial and temporal variations in suspended solids and re-deposition of dredged material. The model was originally intended for use in assessing environmental windows, but SSFATE is used for multiple purposes where dredge-generated turbidity is a concern. Model output includes three-dimensional temporal and spatial distribution of sediment concentration in the water column and thickness of deposition on the sea floor.

At the core of SSFATE is a computational, particle-based (Lagrangian) transport model with random-walk dispersion and settlement of material suspended during the dredging process. An integral component of the modeling system is the specification of the sediment source strength and the vertical distribution of the suspended material. Sediment sources in SSFATE represent the introduction of sediment into the water column as the result of a cutterhead dredge, a hopper dredge, or a clamshell dredge. The user specifies the source strength and the vertical distribution of the material released to the water column. This capability can be used to adapt the model input to simulate a wide range of dredging scenarios.

Model modifications

As a result of the complex hydrodynamics at the Savannah River Entrance and the surrounding coastal areas, limitations were encountered in the SSFATE model framework. In the

original SSFATE model, hydrodynamic and sediment transport simulations were performed on a rectangular grid. Data from a hydrodynamic model were imported and interpolated onto each cell in the rectangular SSFATE grid, or applied at specified points (for example, from current data measured in the field) and subsequently interpolated by the model to cover the entire grid. The rectangular grid was considered unacceptable for the Savannah application, where issues included both nearshore turbidity and far field concentrations in a complex estuarine/coastal ebb shoal environment for a wide area containing numerous dredging and placement locations. The original SSFATE model permits a maximum grid size of 100x100. The uniform, rectangular cell size is user specified. Adequate resolution of the complex nearshore/river areas in the Savannah River entrance required a small cell size, which coupled with the grid dimension limit, only allowed a small domain to be examined. Much of the suspended sediment in the fast-flowing Savannah River and ebb shoal channel exits this small grid domain within hours after release, long before most material is deposited. A larger domain requires larger grid cell size, thus resulting in lack of resolution in some areas of special interest such as the channel, nearshore regions, and near the jetties.

To address these model limitations, SSFATE was modified for application at Savannah to operate on an unstructured mesh with unlimited number of cells and variable, non-rectangular cell dimensions. In addition, SSFATE was modified to import the mesh, bathymetry, current time series, and water elevation time series directly from the ADCIRC simulations described in Chapter 3. Therefore, SSFATE transport simulations now include the same fine-scale resolution of river, coastal, and marsh areas as ADCIRC simulations. Cell spacing is as small as 30 m within the river and in the ebb shoal channel. Maximum resolution on the SSFATE grid is in the river and channel, where cell size is approximately 30x30 m. Vertical resolution is 2 m, resulting in approximately 6 vertical cells in the channel and less in nearshore regions. While permitting more flexibility in application, the new capabilities have two negative consequences. First, the computational requirements for unstructured grid SSFATE simulations are significantly increased. Savannah SSFATE simulations performed on the rectangular grid require approximately 1 hour to simulate 8 days. This same simulation now requires approximately 36 hours of computation time. The output files in the unstructured grid are also more cumbersome to manage (extract data and process results). The total number of simulations was reduced from original plans due to the increased CPU and processing requirements. The tradeoff between number of runs and grid resolution (simulation accuracy) is acceptable. The scenarios simulated provide substantial and adequate insight into dredge-generated total suspended solids (TSS) produced during dredging and placement operations at the Savannah River entrance.

Model input

SSFATE permits the user to specify local bathymetry, hydrodynamic conditions, dredging location, dredging processes and rates, and dredged material properties. Therefore, there are a large number of possible scenarios that can be simulated. Input variables used in the Savannah application of SSFATE are listed in Table 5-1. Dredging locations considered in SSFATE simulations are shown in Figure 5-1. User-specified input for each of the variables that are listed in Table 5-1 are described below.

Hydrodynamic conditions. As previously stated, the hydrodynamic conditions are imported directly from ADCIRC. All SSFATE simulations utilized the January 1992 operational period that was simulated using ADCIRC. Each simulation lasted for 8 or10 days, which included 4 or 5 days of dredging followed by 4-5 days of tracking plume movement and deposition. The simulation start date was always set to 12:00 PM on January 5. The SSFATE model treats sediment transport by current only, and therefore does not include the effects of wave-induced

nearshore currents or the impact of waves on the probability of deposition. In addition, the ADCIRC simulations did not include wave-generated longshore current in the simulations.

Dredging locations. The user specifies locations on the grid where dredging is simulated. These points represent initial source locations, i.e., locations where dredged material is released in SSFATE. Dredging simulations are specified either as a point source (all material released at the same location) or a line source (released evenly over a line of specified length and direction starting at the specified point). Four locations were selected for the Savannah River entrance simulations. These points, shown in Figure 5-1, include two locations in the river, one just seaward of the jetty, and one in the channel offshore of Tybee Island.

Dredging processes and rates. Savannah River entrance channel dredging utilizes both cutterhead and hopper dredges. SSFATE simulates either of these dredging processes. Hopper dredging was assumed for most offshore simulations (C and D in Figure 5-1), while riverine simulations (points A and B) exclusively used cutterhead dredging (Table 5-1). The user-specified production rates for these simulations were 500, 1000, and 2000 m^3/hr (Table 5-1). Loss rate for sediments during the dredging operation and distribution of this loss in the water column are also user-specified. Loss rates were set to 1, 3, or 5 percent, which correspond well with recent, yet unpublished, data based on monitoring at a dredge (John Land, personal communication; Donnie Hayes, personal communication). The majority of the sediment was assumed to be lost in the lower 25 percent of the water column. The user also specifies if the material is released at a single point over the entire dredging simulation or uniformly distributed along a line through the channel. River simulations (cutterhead) were designated as point sources. Simulations at Location C and D, offshore, (Figure 5-1) included both line and point sources.

Dredged material properties. The user specifies the fractions of the dredged material that are clumps, coarse sand, fine sand, silt, and clay. No clumps were assumed for Savannah simulations. This assumption is conservative in that it will overestimate far field TSS and deposition. Clumps would settle predominately immediately below the dredging source point. Fractions of sand, silt and clay were developed from the sediment samples used for Sedflume analysis and described in Chapter 4 (Table 4-2). All river location simulations used properties of sediment designated as 38N (Table 5-1). This material has the highest fine sediment fraction of all the locations that were sampled and analyzed. Sediments designated 17S and 33S (Table 5-1) were considered typical of sandy material dredged from the outer portion of the channel. Both of these sediment distributions was used for offshore SSFATE simulations.

SSFATE Simulations and Results

It should be noted here that the results of suspended sediment concentration calculations must be analyzed in perspective with the natural or background suspended solids concentrations in the river and nearshore. Because much of the suspended material in the river is fine-grained, both suspended solids and turbidity can be relatively high. In lieu of data from this region, it can be estimated that surface concentration would be approximately 5-10 mg/L in the river during non-storm periods and typically less than 1 mg/L concentration of fine-grained sediment in the Tybee nearshore region. The Savannah River concentration profile is generally highly stratified (Charles Dickerson, personal communication). Concentrations near the bottom in the channel are generally highest, because much of the sediment in this river moves in a near-bottom nephloid layer (Charles Dickerson, personal communication). SSFATE estimates concentration at 2-m vertical increments in the water column, and estimates are considered to be an average over this vertical increment. In addition, concentrations are averaged over the one-hour output interval of SSFATE. It should be noted that in most rivers, sediment concentrations often exceed 50-100 mg/L for several days during storm events. There is often a corresponding intrusion of fine material into the nearshore surf zone during storms (based on inspection of data acquired at the

CHL Field Research Facility in Duck, NC). However, high bottom shear stresses do not permit deposition of these fines near the beach and the material deposits offshore during the waning stages of the storm. Stratification is generally found only in the channel. Outside the channel (the area of most concern in these simulations), the water column concentrations are predominantly uniform with depth.

Location A

All dredging simulations at this river location assume a point-source discharge from a cutterhead dredge. Simulations were performed assuming 12% clay, 40% silt, 37% fine sand and 11% coarse sand. These values correspond to the Sedflume sediment sample extracted at location 38N. Production (m^3/hr) /loss rates (%) combinations simulated were: 500/1 (ex, 500 m^3/hr and 1% loss rate), 500/5, 1000/1, 2000/1, and 2000/5 (see Table 5-1). The 2000/5 combination is a worst-case scenario, from the perspective of introducing sediment into the water column, i.e., maximum production rate and maximum loss rate. Vertical dispersion is user specified and was set to 0.0001 m^2/sec, as recommended in the SSFATE users manual (Applied Science Associates, 2001). The 500/5 and 2000/5 simulations were re-run with vertical dispersion increased to 0.001 m^2/sec, and order of magnitude increase, to determine the sensitivity of results to this user input. Horizontal dispersion is calculated in the model and is a function of hydrodynamic conditions. There is no method for the user to modify horizontal dispersion in SSFATE. The simulation duration spanned 5 days of dredging and 5 days post-dredging.

Location B

Location B is also in the river, but closer to the mouth than Location A. Only two simulations were performed at this location because it was determined after these simulations that deposition and TSS patterns were similar to those calculated at Location A. The two simulations assumed a cutterhead dredge and point sources; with grain size distribution identical to those at Location A. Production/loss rates for the two simulations were 1000/3 and 2000/5.

Location C

Location C is just offshore of the north jetty and north of Tybee Island. Both cutterhead and hopper dredges were simulated. All hopper dredge simulations considered line sources approximately 1 km in length, originating at Location C. In addition, three cutterhead point sources and one line source were simulated. Hopper simulations assumed production/loss rates of 2000/1 and 2000/5. Cutterhead production/loss rates were 2000/1, 2000/3, and 2000/5. Sediment grain size distribution was based on Sedflume sample 17S, which was 3% clay, 8% silt, 70% fine sand, and 19% coarse sand.

Location D

Location D is east of the north end of Tybee Island. Two line source hopper dredge simulations and two point source cutterhead simulations were performed. Line sources were approximately 1 km long. Production/loss rates for the hopper dredge and cutterhead simulations were 2000/1 and 2000/3. Sediment was characterized as that from Sedflume sample 33S, which was 1% clay, 5% silt, 74% fine sand and 20% coarse sand.

Suspended Sediment

Due to strong tidal currents, dredging in the Savannah Harbor entrance channel produces a long, narrow plume that maintains its shape during the dredging period and moves upstream and downstream with the tidal current. Swift tidal currents rapidly spread the material released during dredging. This is seen in all SSFATE Savannah dredging scenarios. A large, relatively low concentration plume typifies high-current environments. Concentrations in low-current, low-convection regions (not typical of Savannah) can be much higher. Typical of the computed dredged material plumes associated with dredging at the bar channel, some shore-ward intrusion of fines occurred during flood tide, but the concentrations remain low (generally less than 1 mg/L) and are rapidly moved offshore during the ebb cycle. Some material enters the nearshore region, but virtually no sediment enters the surf zone at Tybee. None of the material, which moves into the nearshore region, deposits there due to the high shear stresses (even with wave-induced stresses neglected). The majority of the material remains near the channel, indicating the system is dominated by convective transport.

The convection-dominated transport is demonstrated in this paragraph. See Table 5-1 for specifics of the simulations that are discussed here. Calculated TSS time histories for simulation PACCAAA, the worst-case scenario (2000 m^3/hr production rate, 5% loss rate, increased vertical dispersion, 38N sediment), are provided in Figures 5-2a through 5-2e for Location A. Figure 5-2a shows depth-averaged TSS at the source, i.e. at the dredge. The concentration varies over several orders of magnitude during the dredging operation. Highest concentrations are observed during slack tide when velocities are low. Low concentrations are seen during maximum ebb and flood currents, when the high velocities rapidly move the material away from the source. The slack tide maximum concentrations also vary, depending on the effects of other conditions such as wind-driven currents and elevation changes at the river mouth. Maximum concentration at any cell at the source is approximately 600 mg/L. Concentrations over 100 mg/L last for two hours or less. Figures 5-2b and 5-2c show the time-series of average water column concentrations 50 m and 100 m from the source, respectively, in a direction perpendicular to the channel, heading toward the right (south) bank. It can be seen from these graphs that TSS concentration drops off rapidly with increasing cross-channel distance from the source. A depth-averaged concentration maximum of 320 mg/L is predicted at 50 m, and at 100 m from the source the maximum is about 110 mg/L. Figures 5-2d and 5-2e depict depth- averaged water column concentration time series at distances of 500 m and 2500 m in the down-channel direction from the source, respectively. These concentrations are higher than those calculated in the cross-channel direction due to high convective transport of sediment in the along-channel direction. Time variation in TSS is generally due to fluctuation in tidal velocities. These figures also demonstrate the rapid decrease in concentration away from the source. Similar time histories occurred upstream of the dredge, but with slightly lower concentrations in this ebb-dominated tidal environment. In addition, the TSS in Figures 5-2a-e indicate that dredging-induced increases in TSS are negligible within 12 to 24 hours after dredging operations cease on Day 10.5. Time- and depth-averaged concentrations at various cross-channel locations are provided in Table 5-2. From this table, it can be seen that concentration drops off rapidly from the source. At 100 m from the barge at Location A for the greatest loss rate, the concentration average is 5 mg/L.

TSS variation in the water column is also estimated using SSFATE. Generally, the highest water column concentrations were near the bottom. Surface TSS concentrations were lower than the depth-averaged values. As an example, time-varying, near-bottom concentration 500 m down-channel for simulation PACCAAA is provided in Figure 5-3. This can be compared to the depth-averaged concentration 500 m down-channel in Figure 5-2d. Concentrations near the bottom are generally a factor of 5 to 10 higher than depth-averaged values in high-concentration areas where

the sediment load is still stratified. The factor decreases as concentration decreases and distance from the disposal site increases.

Simulated plume concentrations at Location B are similar to those at Location A. Plume concentration from dredging at Location C and D are generally lower than those at Location A and B. This is due to the smaller fraction of fine sediment at the offshore dredging locations. Sand particles released during the dredging process quickly deposit near the dredge. Fine sediment does not deposit due to the lower settling speed and lower critical stress for deposition. Simulation PBCCAA, at Location B, and PCCCBA, at Location C, both reflect cutterhead dredging with 2000/5 production/loss rates (the worst case scenario). Table 5-2 indicates that the concentrations at Location C are significantly less due to the lower fine sediment content in the dredged material at this location. The concentrations away from the source are a factor of 2-4 lower for operations at Location C compared to Location B. This may be due in part to differences in hydrodynamic conditions, but is due predominately to the reduced fine fraction at Location C.

Water quality, habitat risk analysis, and turbidity analysis generally require that TSS remain below a certain level for a specified duration at various distances from the dredging location. Figures 5-4a-c quantify the percent of time TSS remain above various concentration levels during the period of dredging, for various dredging source term/location combinations. These values are for the largest dredging rate/loss rate combinations in Table 5-1. Figure 5-4a is for simulation PACCAA. It can be seen, for example, that depth- averaged water column concentration at a cross-shore distance of 50 m from the source (xs_50 in the figure legend) remains above 10 mg/L for approximately 28% of the 4-day dredging duration. Similarly, depth-averaged water column concentration in the 30x30 m cell around the dredge remains above 100 mg/L for approximately 6% of the 4-day dredging period. Comparison of Figure 5-4a to Figure 5-4c, which is at Location C, indicates the lower concentrations produced by dredging on the ebb shoal, where the fraction of fine sediment is much lower than at Location A or B.

The TSS at the source should be evaluated relative to the ambient concentrations in the river. This comparison, if data were available, would likely indicate that increased TSS from the dredging operation is lower than that experienced during natural events in the river (Chuck Dickerson, personal communication). In addition, storm-induced TSS in the river and nearshore remains high for several days. The dredge-induced TSS is highly variable (as seen in Figure 5-2) and concentrations above typical storm levels last for only a few hours at any one location.

The order-of-magnitude level of temporal variability in concentration between high and low values is in large part due to the strong tidal currents. The same suspended particle may cross a specified river cross section several times with the changing tidal currents. However, in this ebb-dominant channel region, most suspended material has moved permanently past Location A approximately two days after dredging ceases. It should be noted that increasing vertical dispersion by an order of magnitude beyond the SSFATE default value (simulation PACCAA vs. PACCAAA) did not significantly change the maximum near-bottom or near-surface concentration maxima or depth-averaged values.

For dredging in the coastal region, suspended solids concentrations are lower due to the reduced fraction of fine sediment and greater cross-channel dispersion. This cross-channel dispersion rapidly reduces concentration. Figures 5-5a to 5-5f show time series of depth-averaged concentration at the source, 50 m cross-channel, 100 m cross-channel, and 500 m cross-channel, 500 m down-channel, and 2500 m down-channel, for simulation PCCCBA at Location C (2000/5 production/loss rate, which is the worst case scenario). TSS concentrations associated with dredging at Location C are significantly less than those at corresponding distances from dredging at Location A. At a cross-channel position of 100 m from the dredging source, maximum depth-

averaged concentration is less than 11 mg/L and the time-averaged concentration over the dredging period was 0.5 mg/L (maximum near-bottom concentration remains below 50 mg/L). At 500 m cross-channel from the dredging location, maximum depth-averaged concentration was less than 5 mg/L; maximum near-bottom concentrations remain below 25 mg/L. The time- and depth-averaged water column concentration over the entire dredging cycle 500 m cross-channel from the source was 0.07 mg/L. Similar patterns of concentration were observed at location D, but maximum and average concentration values were even slightly lower than at Location C, due to the smaller fraction of fine material.

Deposition of suspended sediments

Another area of concern during dredging operations is deposition of material released during the dredging operation. This deposition can impact benthic communities near the channel. SSFATE estimates the deposition of material suspended during the dredging process (deposition of ambient sediments is neglected). The deposition thickness output is provided to quantify deposition away from the source. It is important to note that deposition computations right at the source are probably unrealistic because SSFATE assumes the dredge remains stationary for four days in point model simulations. The along-channel deposition patterns for simulation PBCCAA (Location B, 2000/5 production/loss rate) are shown in Figure 5-6. As expected, the greatest deposit thickness is immediately below the dredge and in the channel near the dredge. However, deposition quickly drops off away from this line, particularly in the cross-channel direction. Light blue and dark blue colors indicate less than 0.5 mm deposition thickness outside the channel. The deposited layer outside the channel is almost all silt and clay particles. These sediments are similar to ambient material outside the channel within the river.

Deposit thickness after four days of dredging for Location C (simulation PCCCBA) is provided in Figure 5-7 (missing this figure). Deposit thickness outside the channel for this simulation is less than at Location B. There are two reasons for this. First, dredging at Location B includes less fine sediment. Sand generally deposits in the channel soon after release from the dredge. Fine material is the only material that remains in suspension long enough to exit the channel. Second, high shear stress outside the channel on the ebb shoal does not permit fine material to deposit. This material will remain in suspension for longer periods of time until it is transported to lower-shear stress regions (offshore) where deposition is possible. Table 5-3 provides cross-channel bottom deposit thickness for several SSFATE simulations covering all four locations shown in Figure 5-1. The pattern described above is clear. Deposit thickness outside the channel (250-500 m in the cross-channel direction) is less than 0.06 cm for all conditions and is insufficient to significantly impact benthic communities. Deposition within the channel of several cm is expected as part of the dredging process.

D-CORMIX Model

The Continuous Dredge Cornell Mixing Zone Model (D-CORMIX) is a program for the analysis, prediction, and design of aqueous, dense-sediment-laden, pipeline discharges into coastal water bodies, with emphasis on the geometry and dilution characteristics of the initial mixing zone, and for evaluating compliance with regulatory requirements. D-CORMIX was developed as an extension to the CORMIX family of models for representing discharges and mixing zones of buoyant plumes (Donneker and Jirka, 1991). D-CORMIX gives water column predictions of suspended sediment concentrations. Predictions of bottom fluid mud movement, which is an important aspect of pipeline placement, are not included in this model. D-CORMIX was applied to both riverine and nearshore pipeline placement of dredged material at the Savannah River entrance channel to determine extent and density of the resulting plume. Initially, use of the PDFATE model was planned to examine the spread of fluid mud. However, testing

with PDFATE determined that this model is not applicable to high-sand-content mixtures found in the Savannah River entrance channel. No model or method available was considered to be an appropriate replacement for predicting bottom flow (fluid mud) movement of the types of mixed sand/silt/clay dredged material from the Savannah River entrance that were sampled.

D-CORMIX is a simplified, idealized, screening level model that is designed to simulate a highly complex process. Unlike SSFATE, D-CORMIX does not account for complex bathymetric or hydrodynamic variation. Input includes two zones, or model domains, one nearshore and one offshore. Each zone has a specified width, bottom slope, and time-invariant velocity. Zone 1 starts at the shoreline and requires a minimum 1-degree bottom slope and user defined domain width. Therefore, even relatively flat regions must be simulated using this modest slope. Zone 2 also requires a minimum 1-degree slope, begins at the deep-water end of Zone 1, and has an infinite width. The user also specifies sediment properties for the pipeline disposal including initial concentration, flux rate or velocity, fraction of various sediment classes, and pore water properties. User-specified pipeline characteristics include dimensions, orientation, and location. Since the bathymetry and velocity are highly idealized, the model does not apply to a specific location within the domain, but rather D-CORMIX is applied in a general manner with representative bathymetry/velocity conditions for the nearshore and river regions.

Two bathymetric conditions were simulated. The first was defined as the river condition, which included a 2-degree nearshore slope followed by a 5-degree slope in Zone 2. Zone 1 was 140-m wide. This bathymetry was designed to reflect the nearshore region and channel slope near river reach 38N. Pipeline placement was simulated at the divide between the zones, in 4.9-m water depth. The second bathymetry was assumed to reflect placement offshore of north Tybee Island. Zone 1 had a 1-degree slope and extended for 200 m. Zone 2 had a 2-degree slope. Placement was also at the boundary between zones, in 3.5-m water depth. Placement would not actually occur only 200 m from shore, but this distance was used so that a 1-degree slope would reflect the water depth at the placement location, 3.5 m, which does accurately reflect water depths for proposed nearshore placements. Table 5-4 shows the various river and north Tybee placement scenarios simulated using D-CORMIX. Variables included sediment type (chosen from various Sedflume sample analyses), discharge rate, and flow velocity. (Specifically define each of the parameters defined in the table.) The number of possible runs is quite extensive given the list of variables. The simulations listed in Table 5-4 provide sample results since exact specifications for dredging rates and dredge types are not yet determined.

Table 5-5 shows the gaussian half-width (BH) and centerline concentration (C) for each of the sample runs listed in Table 5-4. D-CORMIX assumes a gaussian distribution for the plume concentration. The centerline concentration is the highest concentration in the plume at the specified distance from the source. The concentration, C, at any cross-plume location from the centerline is estimated by:

$$C = C_{centerline} e^{(x/BH)^2}$$

where $C_{centerline}$ is the centerline concentration, BH is the gaussian half width, and x is the cross-plume distance. The gaussian half width, BH, is one-half the plume width that includes 68% of the mass in the plume at the specified distance downstream from the source. Concentration at the edges of the gaussian half width is equal to 0.6* $C_{centerline}$. Ninety-five percent of the suspended sediment mass is contained within two gaussian half-widths from the plume centerline. The concentration at the edges of this plume width is 0.4* $C_{centerline}$. Gaussian distribution of concentration within a plume is often utilized in environmental plume modeling. Figure 5-8 provides an example of how the suspended sediment concentrations would typically appear. Table 5-5 indicates that concentration drops off rapidly for pipeline placements of predominately sandy material (run tyb62s), while clays remain in suspension for silty/clay sediments (riverine

simulations). Centerline concentration for the riverine runs was 0.04 to 0.13 g/l (40-130 mg/L) for the riverine simulations. For sediments with higher sand content dredged offshore of Tybee, concentrations at 2 km from the source were 0-0.06 g/l (0-60 mg/L).

Centerline concentration of sand, silt and clay fractions (as a function of distance downstream from the pipeline) for three of the riverine simulations (riv10d, riv10h, and riv10j) is provided in Figure 5-9a-c. It can be seen that the only material with significant concentration remaining in suspension at distances greater than 500 m from the source is the clay material. Fine silt generally drops below 10 mg/L between 500-1000 m from the source. Figure 5-8c shows the concentration for simulation Riv10j, which is the 'worst-case' simulation. The dredging rate was set at 2000 m^3/hr in this simulation and the channel velocity was 0.5 m/s. This condition will carry the most material downstream, as shown in Table 5-5. Centerline concentration at 2 km from the source was approximately 130 mg/L. Figures 5-10a-c show gaussian half-width associated with the plume for the same river simulations. Similarly, Figures 5-11a-c show centerline concentration as a function of distance from the source for three Tybee offshore simulations (tyb25cms, tyb35cms, and tyb45cms). These figures indicate that centerline concentration decreases with increasing velocity because of increased mixing of the pipeline effluent with clean water.

One important factor missing in the Tybee nearshore simulations is wave action. Waves will act to dissipate the plume more rapidly. D-CORMIX does not include wave effects. Therefore, concentrations can be assumed to be lower than calculated in these simulations. In addition, the plume would probably be larger due to wave effects. It is not presently possible to quantify the effects of wave action in D-CORMIX, or in any other post-processing of results. Plume gaussian half-width is provided in Figure 5-12a-c for the same three Tybee nearshore simulations. These figures indicate that plume width decreases with increasing velocity.

Summary and Conclusions

Plumes of suspended sediment generated during dredging and placement operations are of potential concern to the aquatic environment. Consequently, estimates of suspended sediment entrainment and transport during the dredging and placement operations are required to assess the potential impact on the environment. Chapter 5 describes model applications and analysis addressing sediment suspension, transport, and deposition during dredging and nearshore placement operations at the Savannah River entrance channel and adjacent waters. Two primary issues are 1) whether unsuitable levels of suspended sediment are present in the water column or 2) do fines placed in suspension deposit in the nearshore zone. This chapter does not address the biological effects or risk to the environment, but presents suspended sediment concentrations from which those assessments may be made.

Two numerical models of dredged material resuspension and transport were applied to address the effects of suspended sediments at the dredge and the pipeline outfall. SSFATE was applied to quantify sediment suspension from the dredge, transport of the suspended sediment from the dredging site, and deposition of the suspended material. D-CORMIX was applied to quantify sediment entrainment and transport at the pipeline outfall.

Resuspension from dredging operations

Higher concentrations of resuspended sediments were predicted at riverine dredging sites, primarily attributed to the higher silt/clay content in the dredged sediments. Dredging in the coastal region (seaward of the Savannah River entrance) produced lower TSS concentrations because of the higher sand content, which more quickly settles out of suspension. SSFATE predicted that the resuspended dredged material was quickly advected in a net seaward direction

by the ebb-dominant tidal currents. Peak TSS concentrations from the resuspension plume were observed to coincide with near-slack currents. Suspended sediment concentrations also generally drop to negligible levels within 12-24 hours after cessation of dredging operations. Accumulation of resuspended dredged material ranged up to several centimeters within the navigation channel (as expected) and amounted to sub-millimeter thickness outside the navigation channel. Only small quantities of fine sediments were observed to pass within the nearshore region of the Atlantic shoreline of Tybee Island and suspended fine-grained sediments were not deposited in the nearshore because of the relatively large tidal-current-generated shear stresses in this region. The influence of waves on suspended material in the nearshore was not simulated. Agitation by waves would further prevent the deposition of fine-grained suspended sediments in the nearshore.

Resuspension from pipeline disposal

As experience would suggest, significantly higher suspended sediment concentrations are produced at pipeline outfalls than for resuspension at the dredging site. Plumes from pipeline outfalls are expected to be transported primarily in the direction of the tidal currents, with some lateral mixing. Sand and coarse silts were observed in the model simulations to settle out of suspension fairly close to the discharge location, while fine silts and clays remained in suspension to be transported further distances from the discharge point. Fine silts were found to settle out of suspension between 500-1000 m from the discharge point, and the clay fraction remained in concentrations of approximately 100 mg/L at a distance of 2000 m from the discharge point.

References

Doneker, R.L., and G.H. Jirka. 1991. An Expert System for Hydrodynamic Mixing Zone Analysis of Conventional and Toxic Submerged Single Port Discharges (CORMIX 1). EPA 600/3-90/012. DeFrees Hydraulics Laboratory, School of Civil and Environmental Engineering, Cornell University, Ithaca, NY (Prepared for US EPA Office of Research and Development).

Table 5-1: SSFATE simulations

Filename	Dredge Type	Line or Point Source	Location	Dredging Rate (m^3/hr)	Percent Loss	Dredged Sediment	Start Date	Dredging (Days)	Model Simulation (Days)	Vertical Dispersion (m^2/s)
PAAAAA	Cutterhead	Point	A	500	1%	38N	5th Jan 92	5	10	0.001
PAACAA	Cutterhead	Point	A	500	5%	38N	5th Jan 92	5	10	0.001
PAACAAA	Cutterhead	Point	A	500	5%	38N	5th Jan 92	5	10	0.0001
PABAAA	Cutterhead	Point	A	1000	1%	38N	5th Jan 92	5	10	0.001
PACAAA	Cutterhead	Point	A	2000	1%	38N	5th Jan 92	5	10	0.001
PACCAA	Cutterhead	Point	A	2000	5%	38N	5th Jan 92	5	10	0.001
PACCAAA	Cutterhead	Point	A	2000	5%	38N	5th Jan 92	5	10	0.0001
PBBBAA	Cutterhead	Point	B	1000	3%	38N	5th Jan 92	4	8	0.001
PBCCAA	Cutterhead	Point	B	2000	5%	38N	5th Jan 92	4	8	0.001
PCCABA	Cutterhead	Point	C	2000	1%	17S	5th Jan 92	4	8	0.001
PCCCBA	Cutterhead	Point	C	2000	5%	17S	5th Jan 92	4	8	0.001
PDCACA	Cutterhead	Point	D	2000	1%	33S	5th Jan 92	4	8	0.001
PDCBCA	Cutterhead	Point	D	2000	3%	33S	5th Jan 92	4	8	0.001
LCCABA	Hopper	Line	C	2000	1%	17S	5th Jan 92	4	8	0.001
LCCCBA	Hopper	Line	C	2000	5%	17S	5th Jan 92	4	8	0.001
LCCCBAA	Hopper	Line	C	2000	5%	17S	5th Jan 92	4	8	0.0001
LCCCBA-B	Cutterhead	Line	C	2000	5%	17S	5th Jan 92	4	8	0.001
LDCACA	Hopper	Line	D	2000	1%	33S	5th Jan 92	4	8	0.001
LDCBCA	Hopper	Line	D	2000	3%	33S	5th Jan 92	4	8	0.001

	PACCAA	PBCCAA	PCCCBA
Source	25	29	12
50-m	12	6.9	1.6
100-m	5	1.7	0.5
500-m	NA	NA	0.07

Table 5-2: Time-averaged, depth-integrated concentrations (mg/l) at various cross-channel locations during 2000 m^3/hr dredging rate, 5% loss rate simulations

Run	-500 m (cm)	-250 m (cm)	-100 m (cm)	-50 m (cm)	Source (cm)	50 m (cm)	100 m (cm)	250 m (cm)	500 m (cm)
LCCABA	5.16E-07	3.03E-04	1.71E-02	6.71E-01	2.13E+01	2.28E+00	1.30E-01	8.99E-06	0.00E+00
LCCCBA	1.56E-03	5.87E-05	1.52E-01	4.28E+00	1.14E+02	9.66E+00	5.55E-01	2.20E-06	0.00E+00
LDCACA	9.26E-04	1.77E-03	6.91E-01	7.06E+00	1.03E+01	6.59E+00	3.86E-01	4.02E-03	9.75E-06
PACAAA	NA	NA	1.24E+00	2.60E+01	4.90E+01	7.98E+00	7.98E+00	NA	NA
PAAAAA	NA	NA	2.46E-01	6.46E+00	1.20E+01	1.87E+00	1.87E+00	NA	NA
PBBBAA	NA	NA	1.18E-01	5.01E+00	1.11E+02	7.07E+00	5.34E-02	NA	NA
PBCCAA	NA	NA	3.56E-01	1.71E+01	3.85E+02	2.12E+01	2.46E-01	NA	NA
PCCCBA	3.14E-05	5.08E-03	7.38E-02	3.16E+01	7.37E+02	4.33E+01	6.90E-01	3.39E-04	1.09E-04
PDCACA	1.78E-05	3.69E-03	1.46E+00	2.13E+01	1.07E+02	1.83E+01	2.24E+00	9.02E-04	1.32E-03

Table 5-3: Deposition at various cross-channel locations from the source

Table 5-4: Sample D-CORMIX simulations

FILE Name	Sediment Type	slope1 (degrees)	slope2 (degrees)	u1 (m/s)	u2 (m/s)	ybreak (m)	zbreak (m)	slurry flux m3/hr	slurry flux m3/s	C total (g/l)	C sand (g/l)	C csilt (g/l)	C fsilt (g/l)	C clay (g/l)
riv10c	38N	2	5	0.1	0.15	140	4.89	1000	0.28	240	120	64.8	33.6	21.6
riv10d	38N	2	5	0.2	0.25	140	4.89	1000	0.28	240	120	64.8	33.6	21.6
riv10f	38N	2	5	0.2	0.25	140	4.89	500	0.14	240	120	64.8	33.6	21.6
riv10g	38N	2	5	0.3	0.4	140	4.89	500	0.14	240	120	64.8	33.6	21.6
riv10h	38N	2	5	0.4	0.5	140	4.89	1000	0.28	240	120	64.8	33.6	21.6
riv10i	38N	2	5	0.4	0.5	140	4.89	500	0.14	240	120	64.8	33.6	21.6
riv10j	38N	2	5	0.4	0.5	140	4.89	2000	0.56	240	120	64.8	33.6	21.6
tyb25cms	38N	1	2	0.25	0.35	200	3.49	1000	0.28	240	120	64.8	33.6	21.6
tyb35cms	17s	1	2	0.35	0.35	200	3.49	1000	0.28	240	144	48	36	12
tyb45cms	17s	1	2	0.45	0.45	200	3.49	1000	0.28	240	144	48	36	12
tyb62s	62s	1	2	0.14	0.1	200	3.49	1080	0.3	240	199.2	27.84	7.92	5.04
tyb78s	78s	1	2	0.14	0.1	200	3.49	1080	0.3	240	117.6	69.6	38.4	14.4

FILE Name	100m C (g/l)	100m BH (m)	500m C (g/l)	500m BH (m)	1000m C (g/l)	1000m BH (m)	2000m C (g/l)	2000m BH (m)
riv10c	1.98	140	0.71	249	0.26	347	0.05	517
riv10d	1.83	78	0.59	171	0.28	261	0.09	427
riv10f	1.62	33	0.35	98	0.08	167	0.03	313
riv10g	1.07	46	0.28	118	0.13	196	0.05	348
riv10h	1.41	47	0.39	122	0.18	200	0.07	354
riv10i	1.11	35	0.22	99	0.1	181	0.04	330
riv10j	1.95	60	0.63	146	0.3	229	0.13	385
tyb25cms	3.75	51	0.67	111	0.22	159	0.04	246
tyb35cms	3.3	37	0.49	84	0.14	129	0.03	207
tyb45cms	3.1	30	0.36	71	0.09	112	0.02	181
tyb62s	0.3	146	0.03	192	0.01	284		
tyb78s	2	168	0.2	235	0.11	358	0.06	554

Table 5-5: Centerline concentration and plume gaussian half width at 100, 500, 1000, and 2000 m from pipeline dredging source

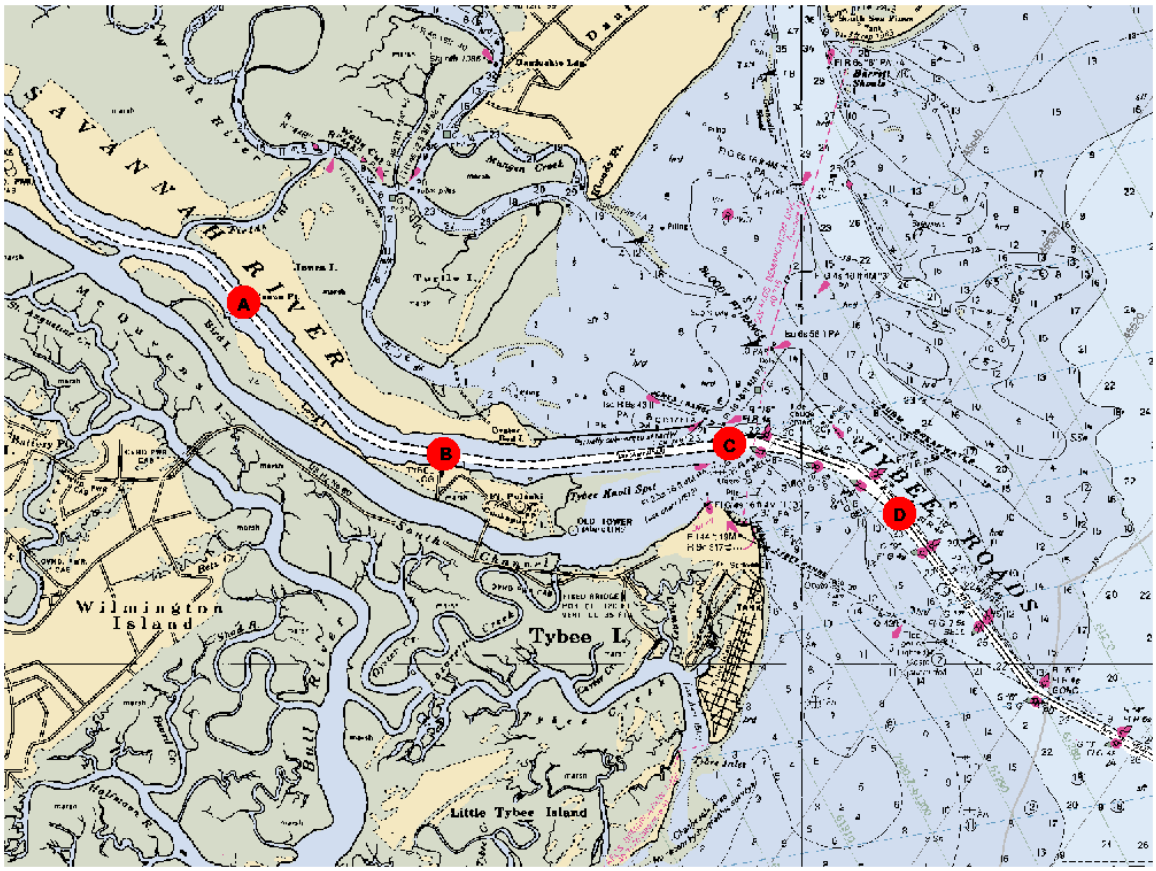

Figure 5-1: Locations of SSFATE simulations

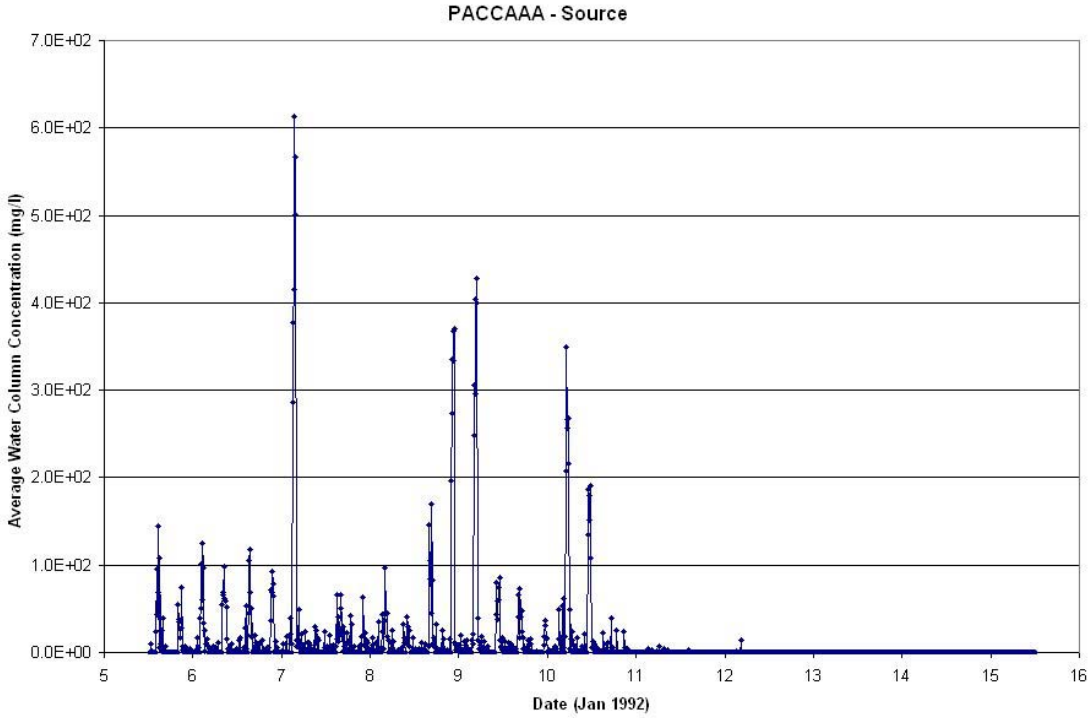

Figure 5-2a: SSFATE simulation PACCAAA, depth-averaged time-series concentration at the source

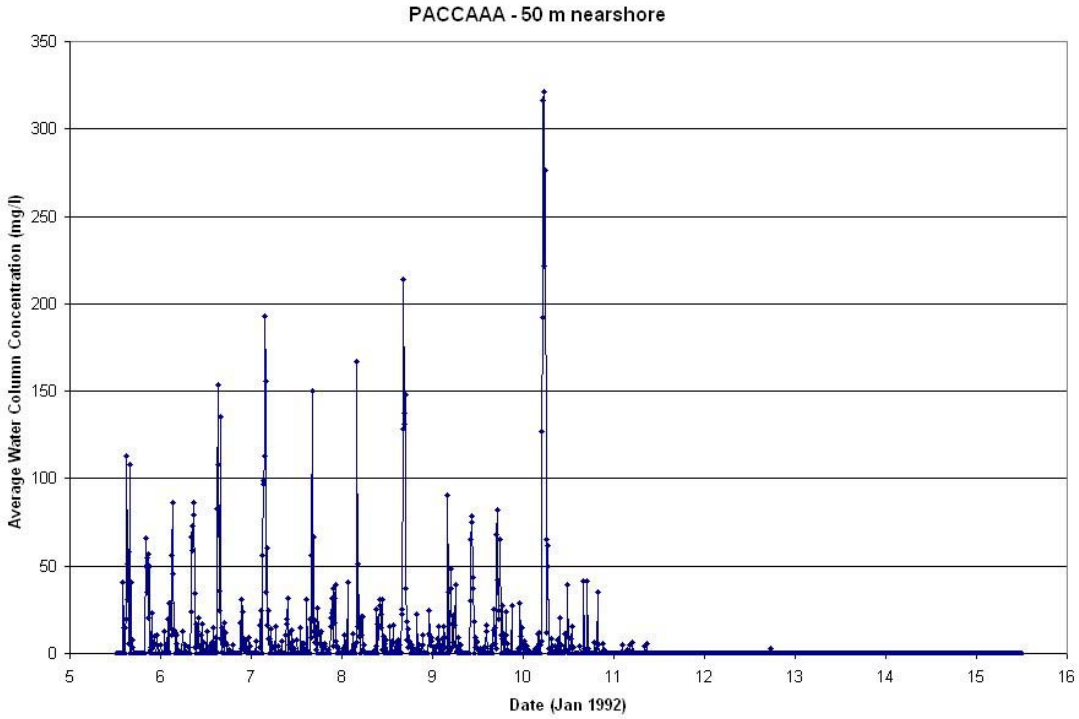

Figure 5-2b: SSFATE simulation PACCAAA, depth-averaged time-series concentration 50 m cross-channel from the source

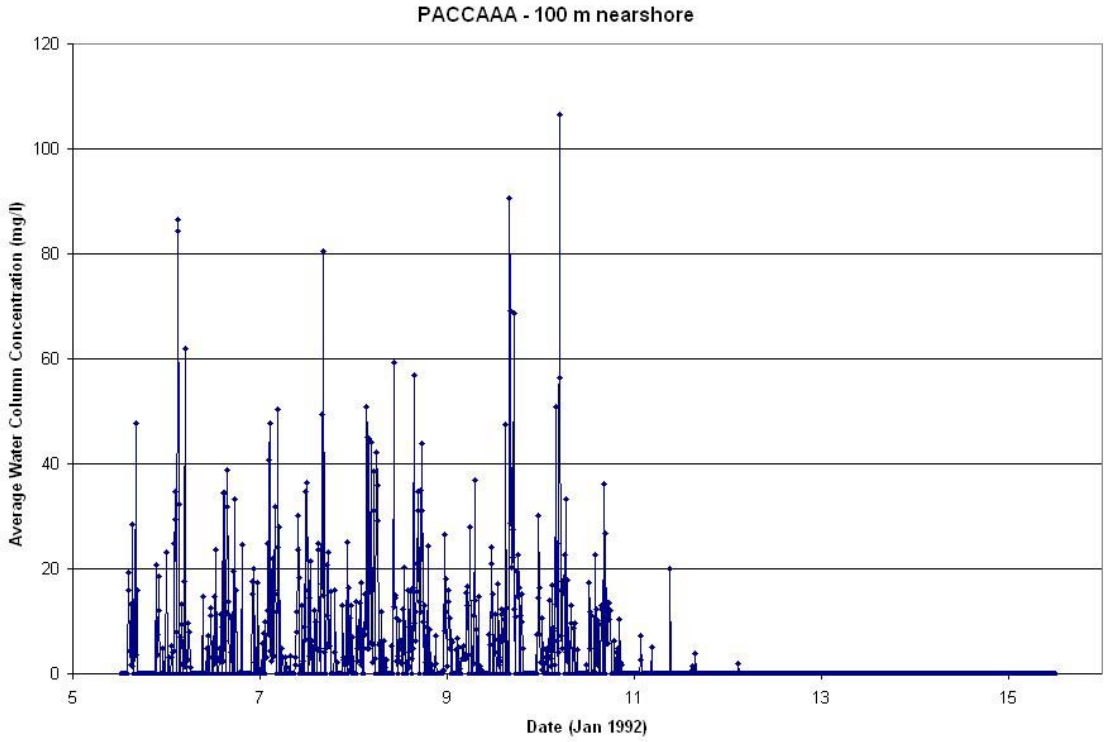

Figure 5-2c: SSFATE simulation PACCAAA, depth-averaged time-series concentration 100 m cross-channel from the source

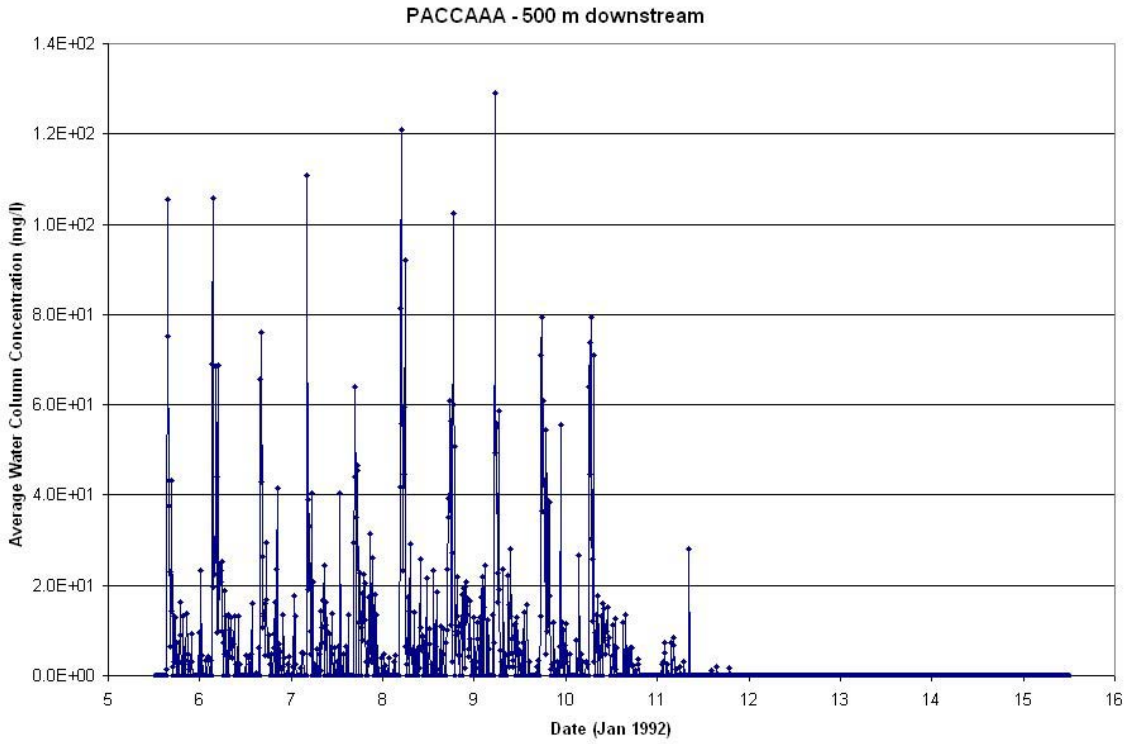

Figure 5-2d: SSFATE simulation PACCAAA, depth-averaged time-series concentration 500 m down-channel from the source

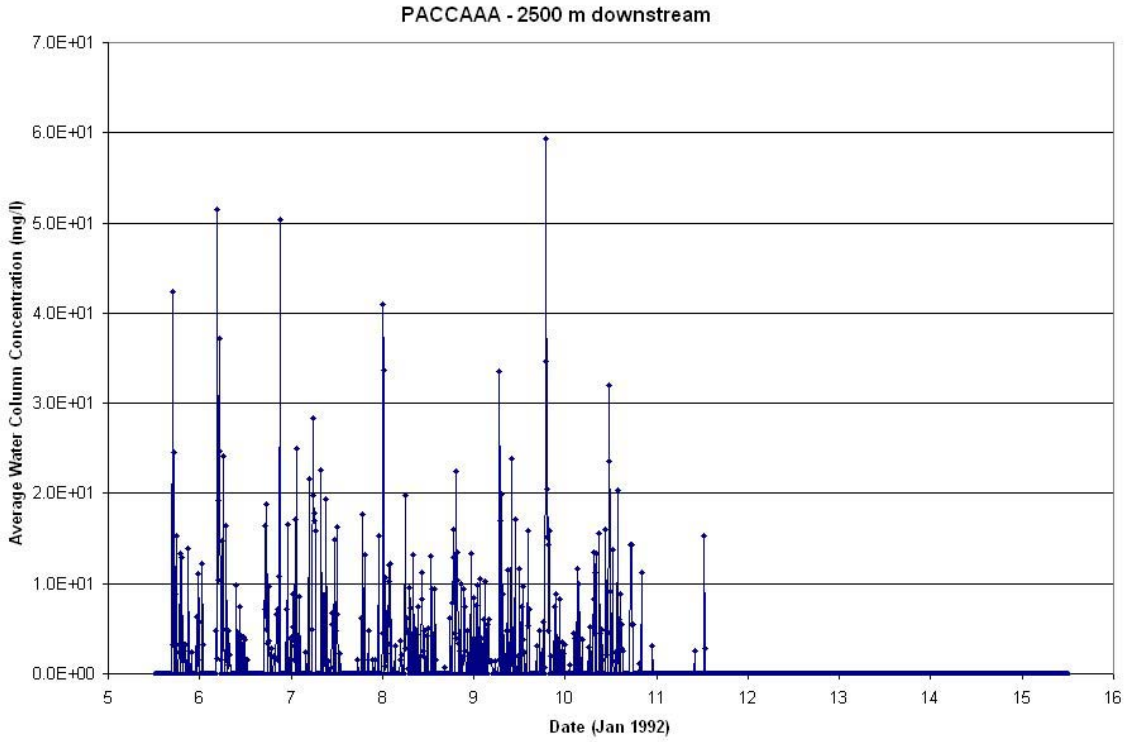

Figure 5-2e: SSFATE simulation PACCAAA, depth-averaged time-series concentration 2500 m down-channel from the source

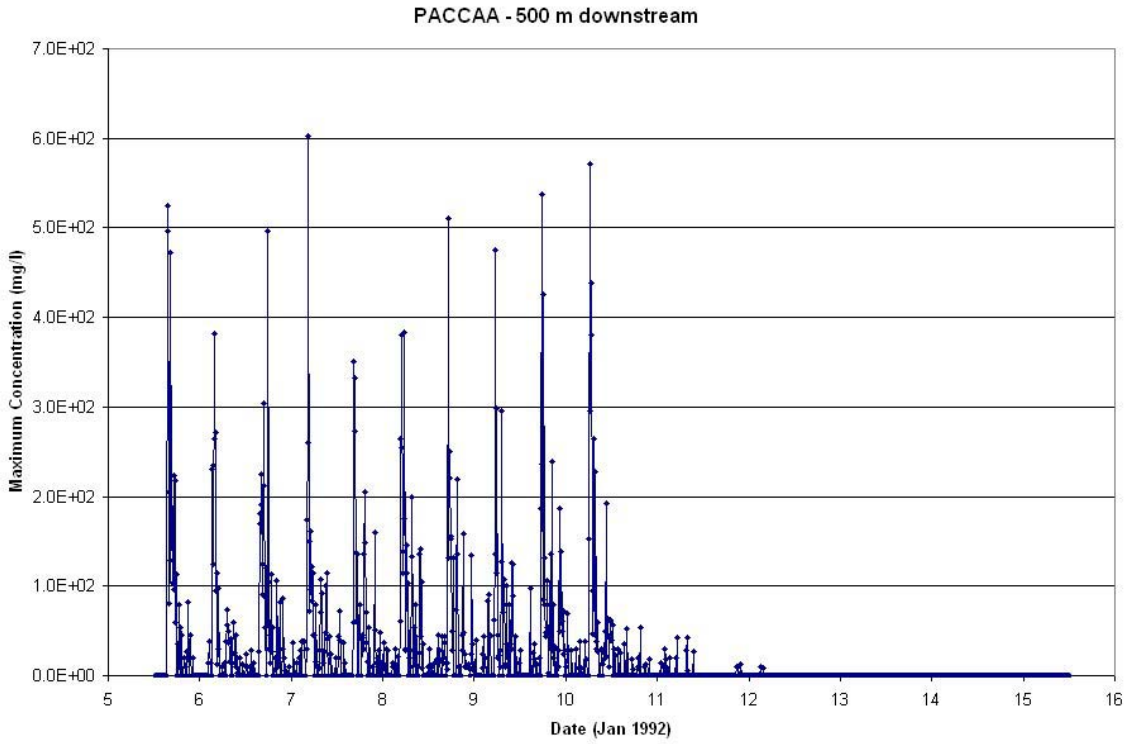

Figure 5-3: SSFATE simulation PACCAAA, near-bottom time-series concentration 500 m down-channel from the source

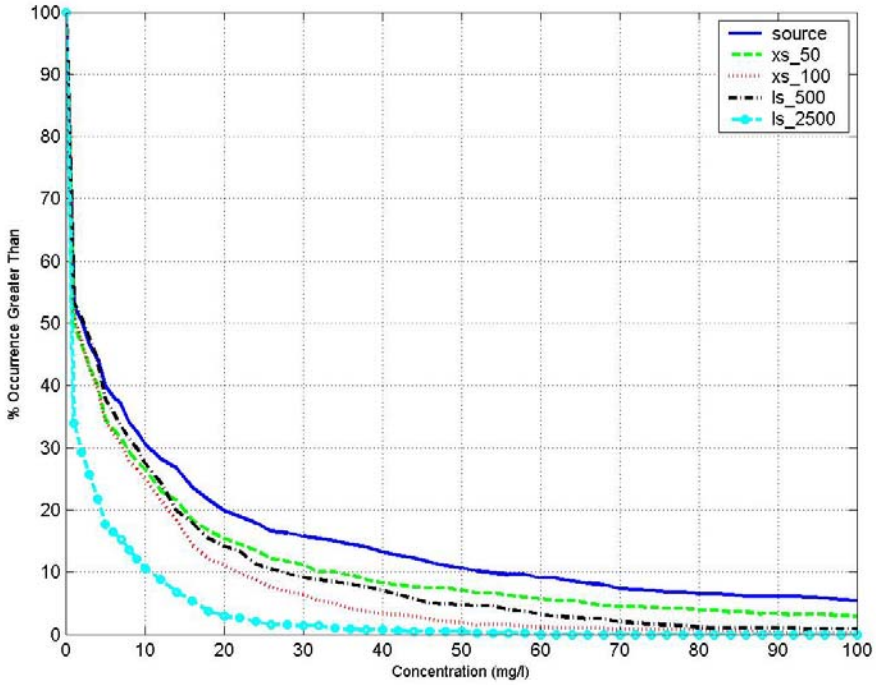

Figure 5-4a: Percent occurrence greater than specified depth-averaged concentration for simulation PACCAA

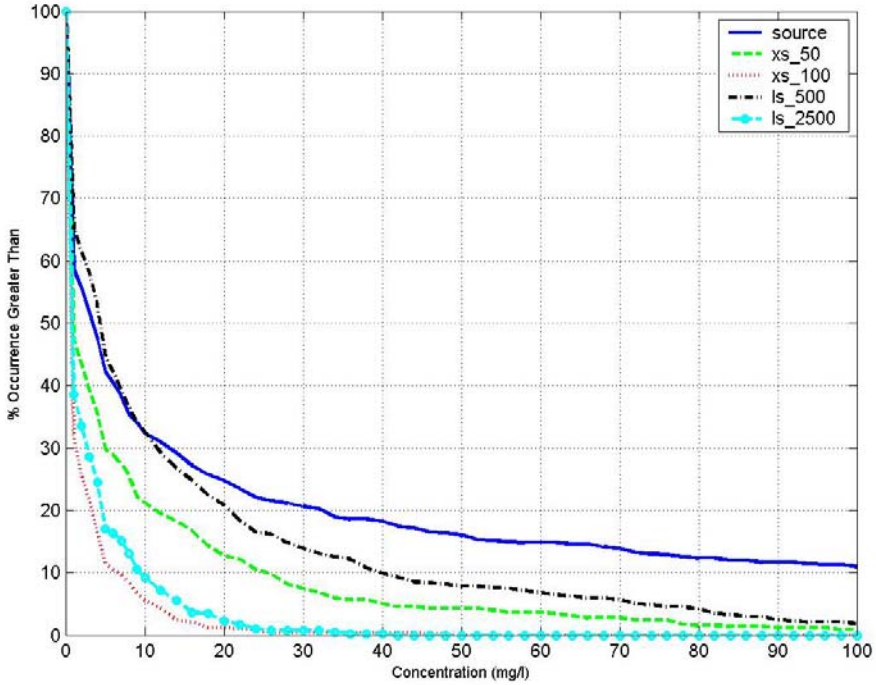

Figure 5-4b: Percent occurrence greater than specified depth-averaged concentration for simulation PBCCAA

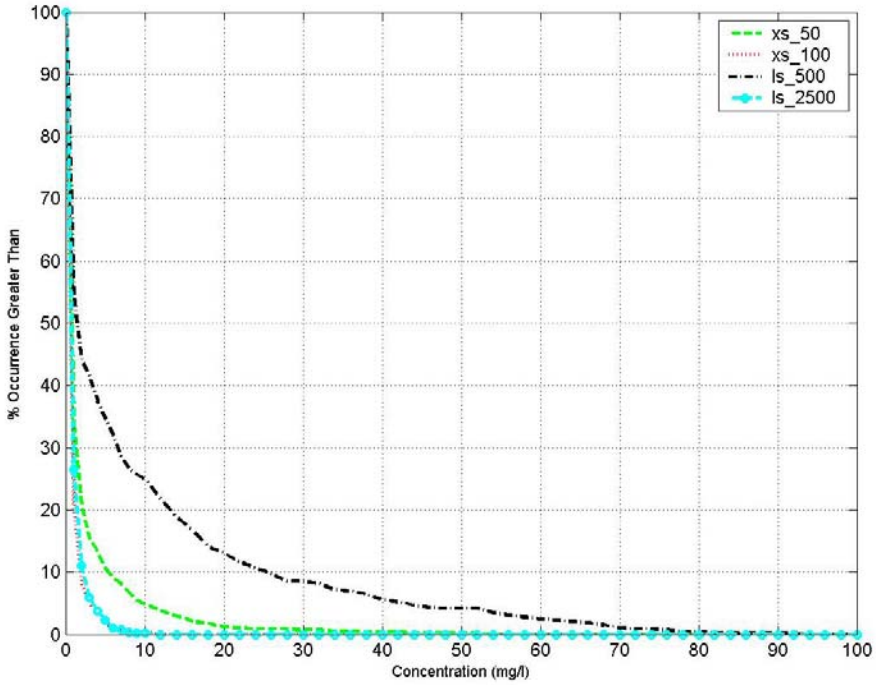

Figure 5-4c: Percent occurrence greater than specified depth-averaged concentration for simulation PCCCAA

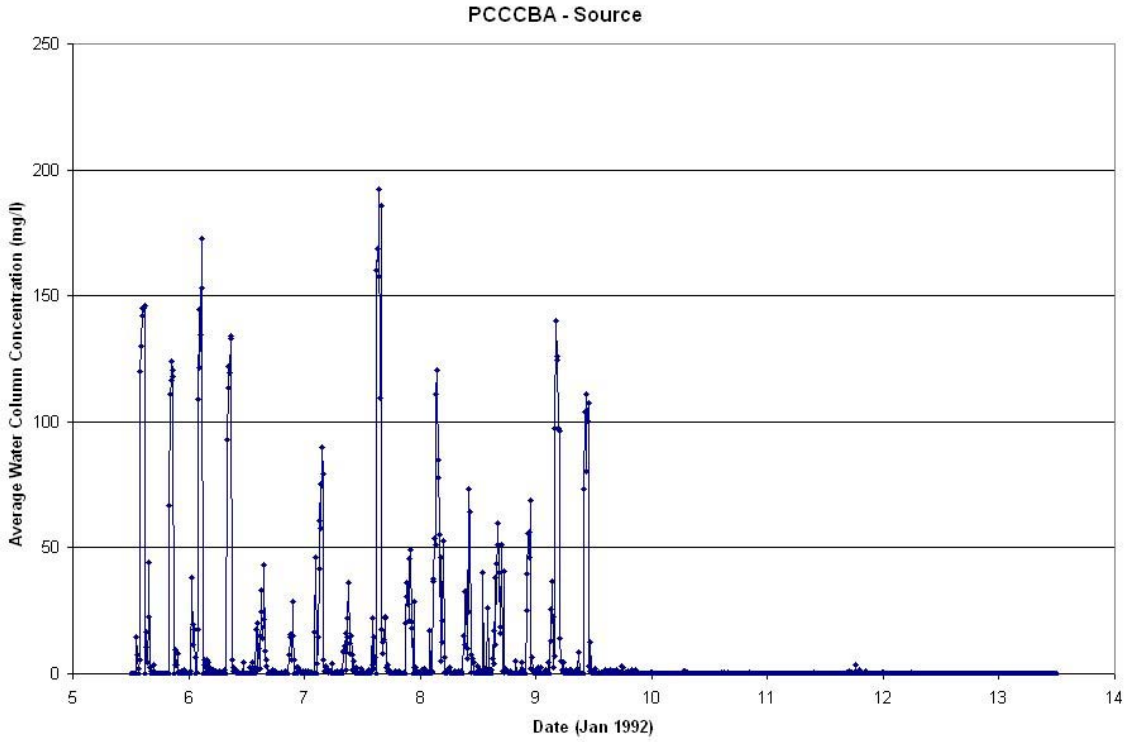

Figure 5-5a: SSFATE simulation PCCCAA, depth-averaged time-series concentration at the source

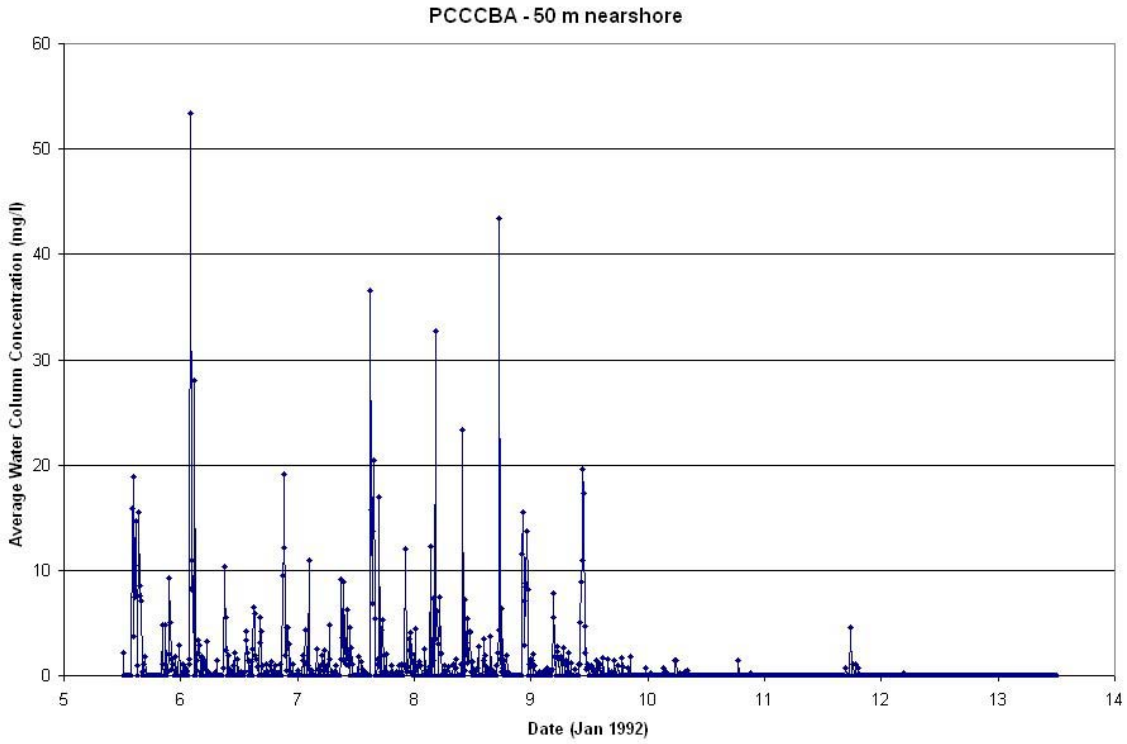

Figure 5-5b: SSFATE simulation PCCCAA, depth-averaged time-series concentration 50m toward shore from the source

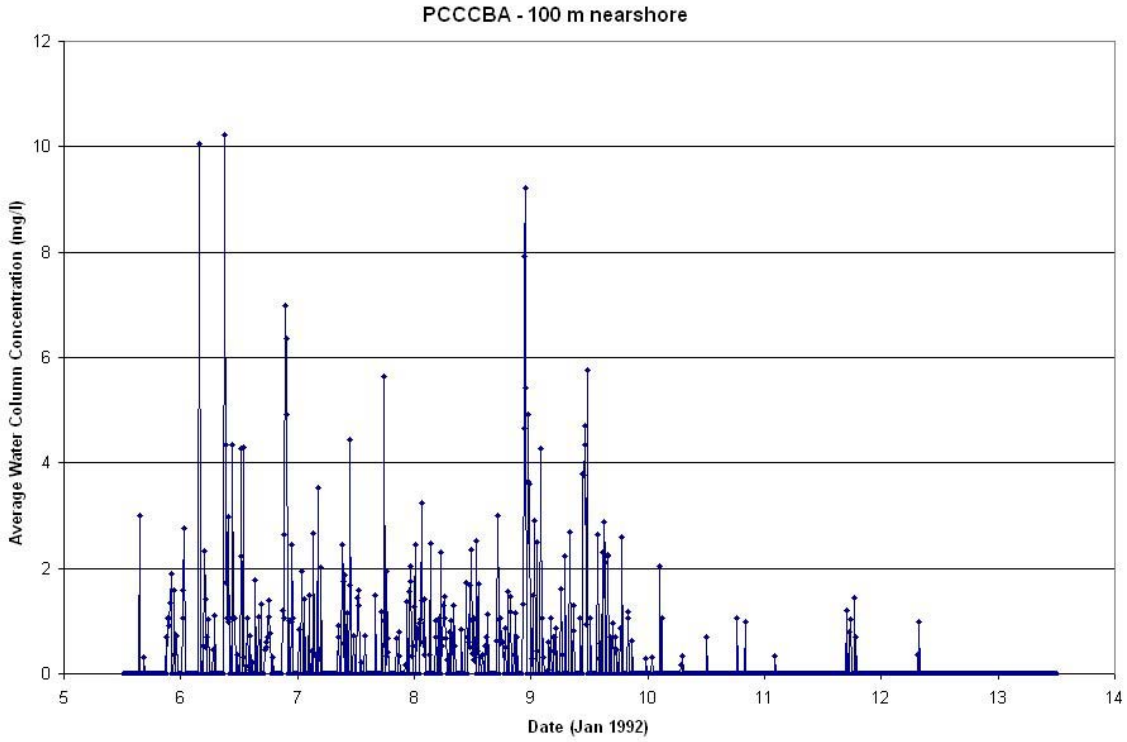

Figure 5-5c: SSFATE simulation PCCCAA, depth-averaged time-series concentration 100m toward shore from the source

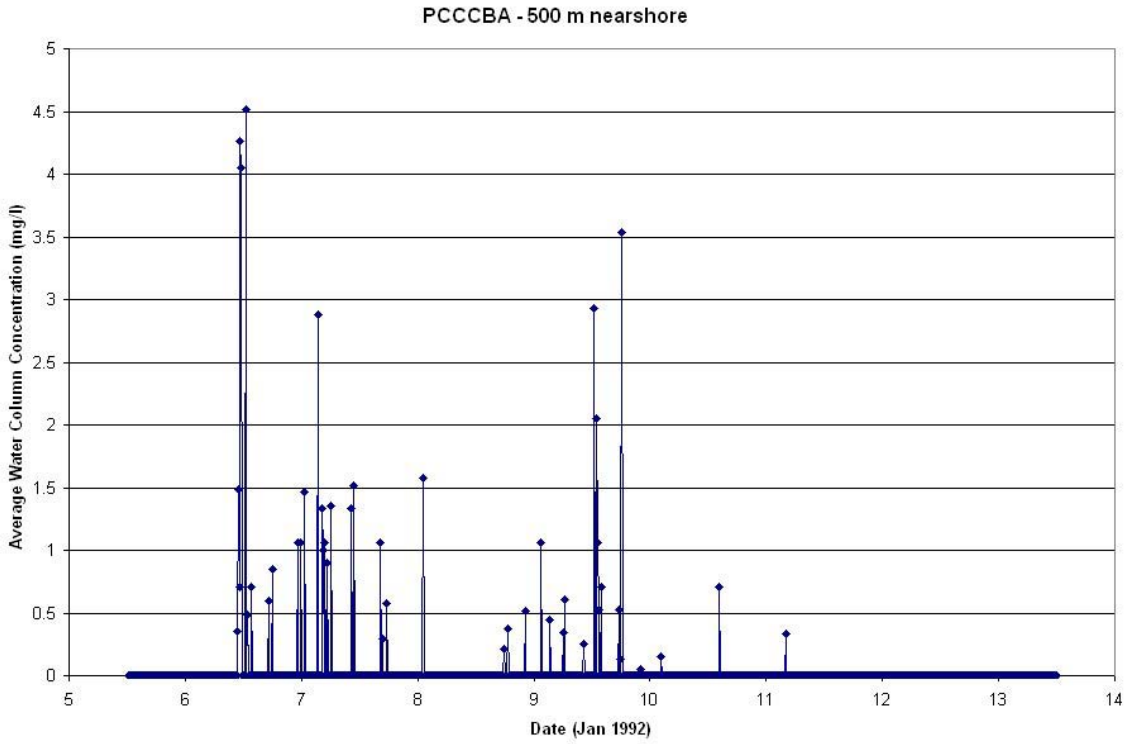

Figure 5-5d: SSFATE simulation PCCCAA, depth-averaged time-series concentration 500m toward shore from the source

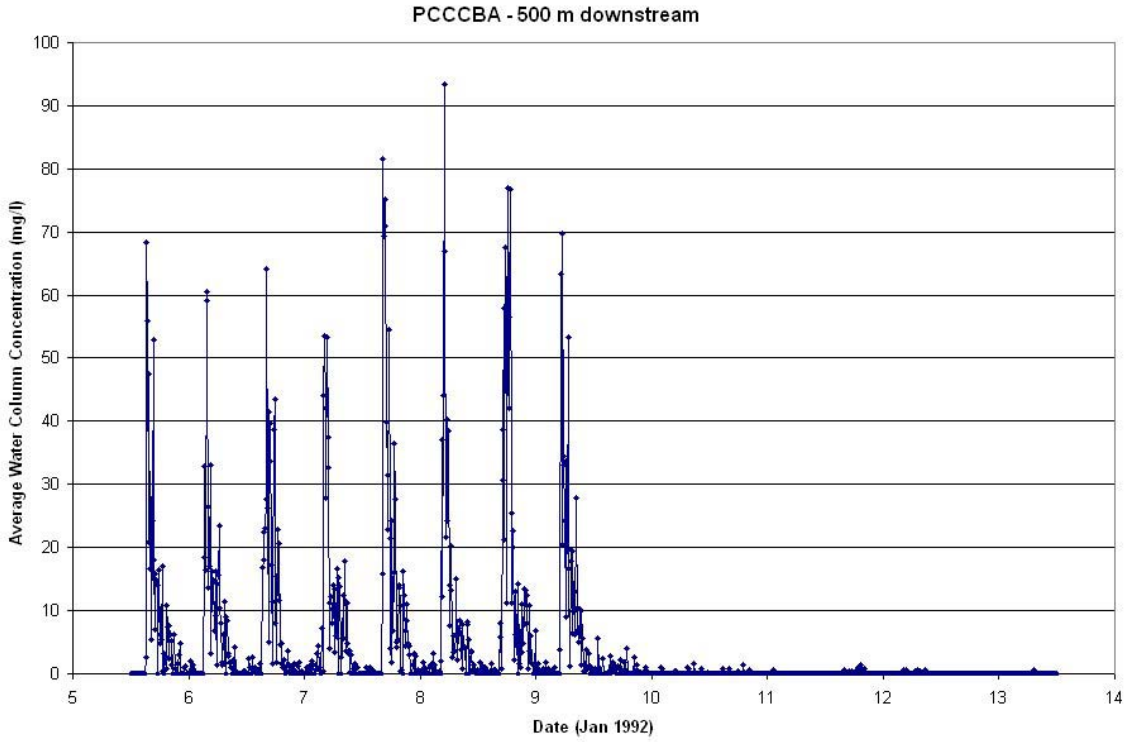

Figure 5-5e: SSFATE simulation PCCCAA, depth-averaged time-series concentration 500 m down-channel from the source

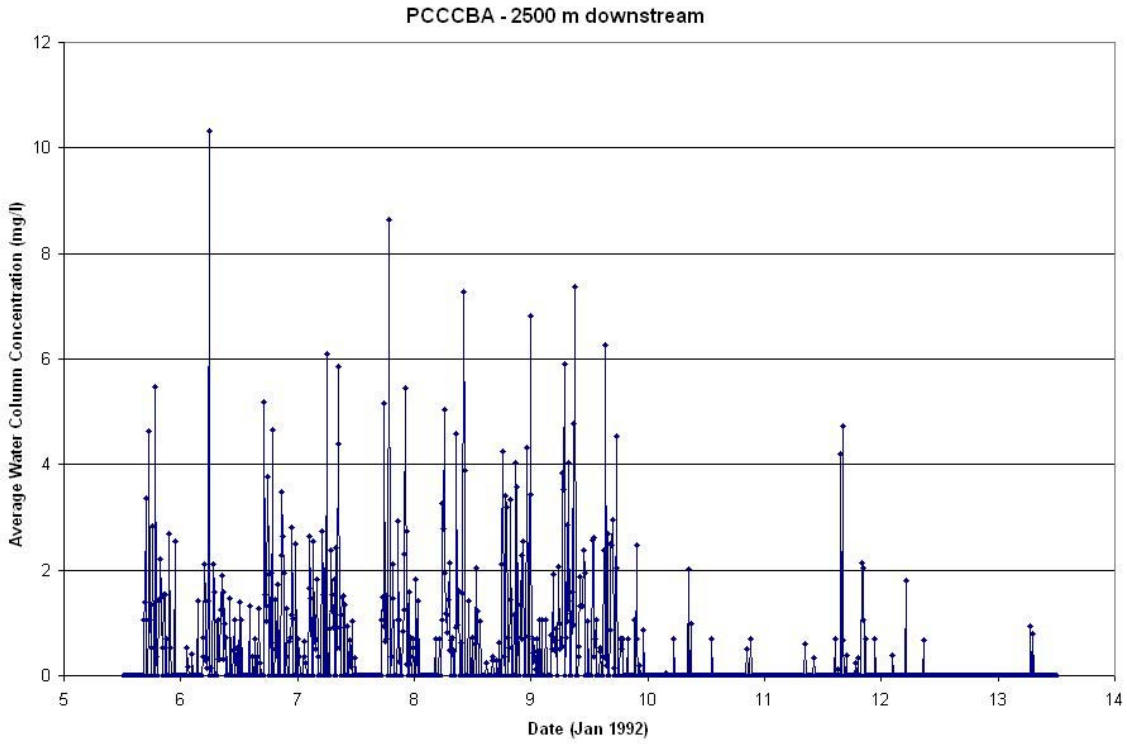

Figure 5-5f: SSFATE simulation PCCCAA, depth-averaged time-series concentration 2500m down-channel from the source

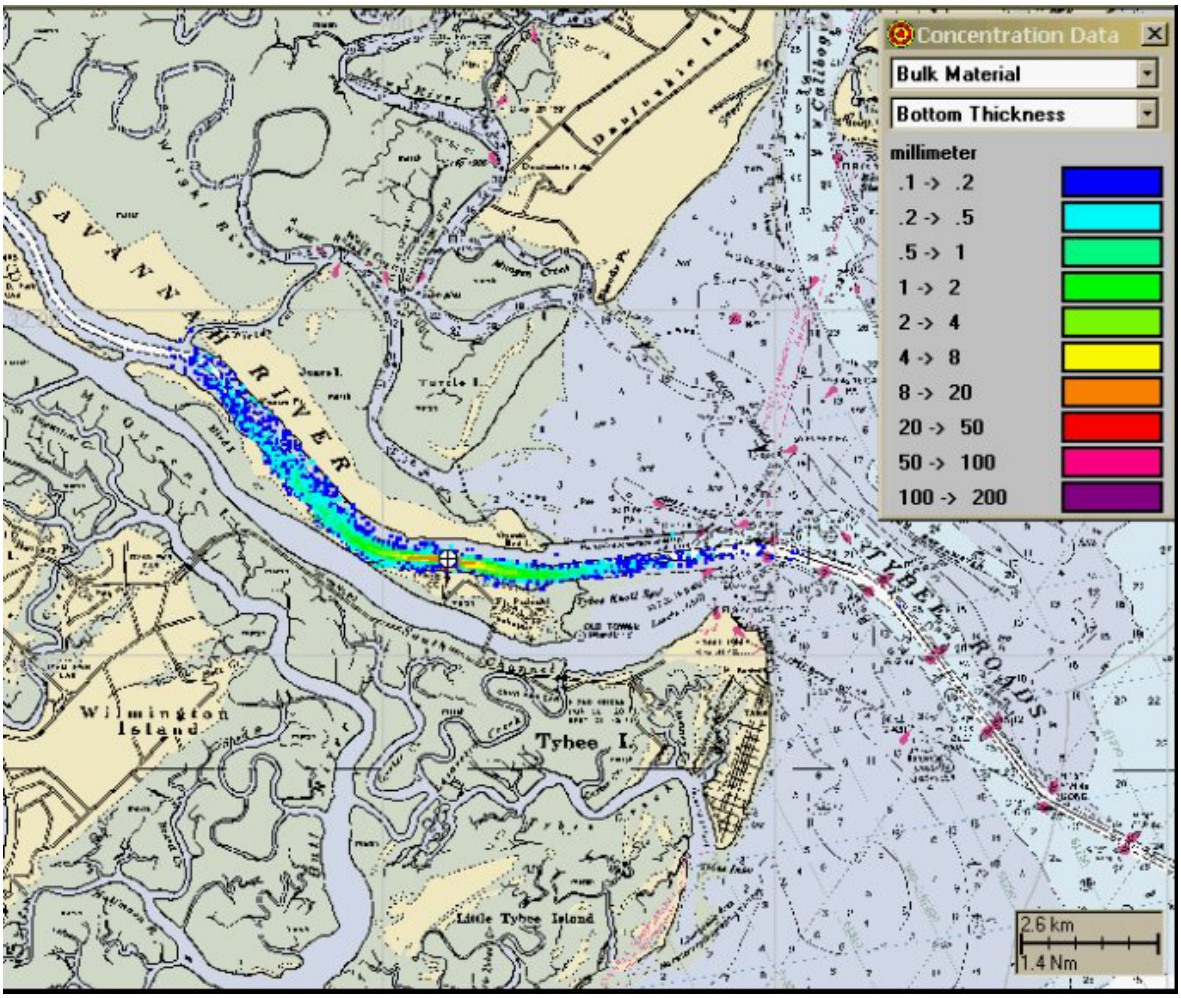

Figure 5-6: Bottom deposition after 4 days of dredging, simulation PBCCAA

<< Figure missing >>

Figure 5-7 Bottom deposition after 4 days of dredging, simulation PCCCBA

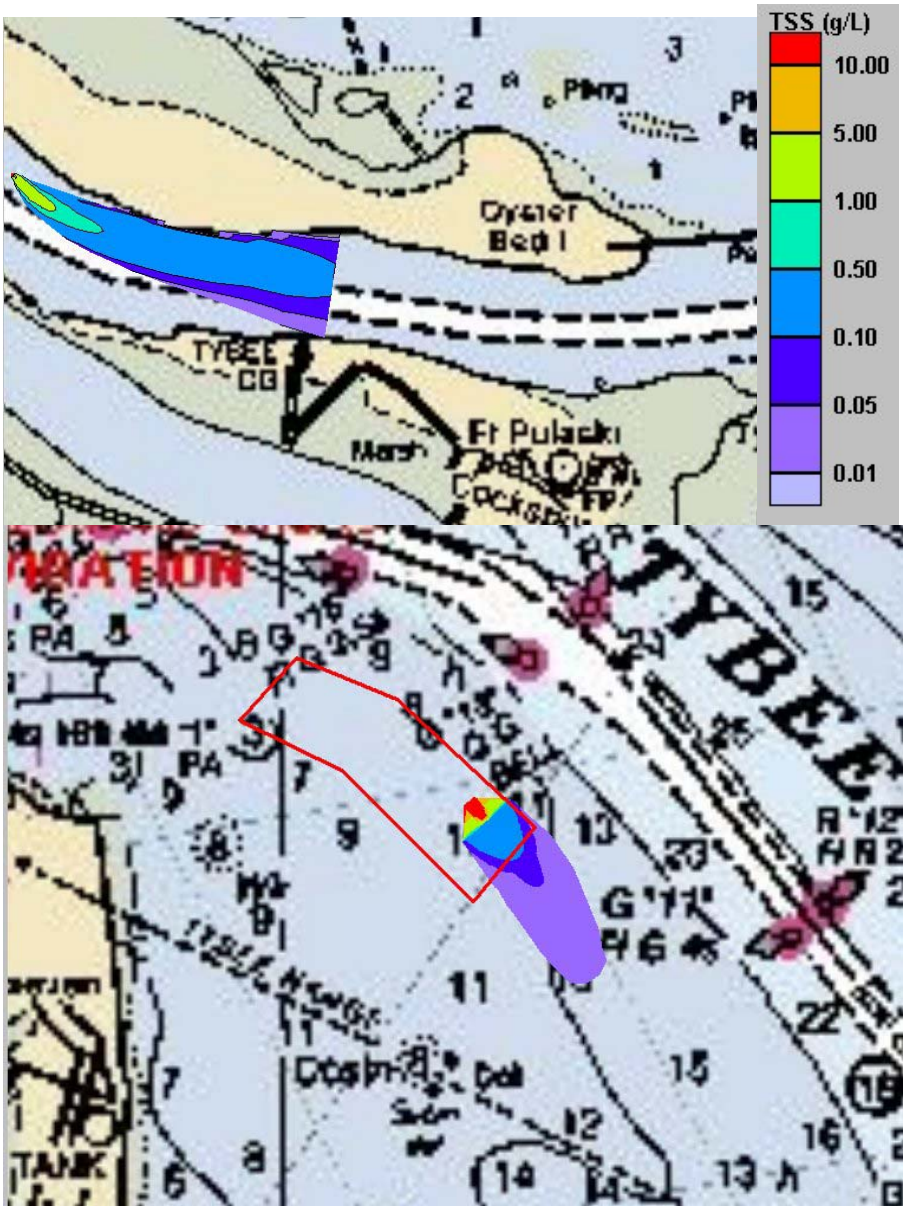

Figure 5-8: Pipeline placement: river plume at 40 cm/s velocity (upper panel); and offshore plume at 14 cm/s velocity (lower panel)

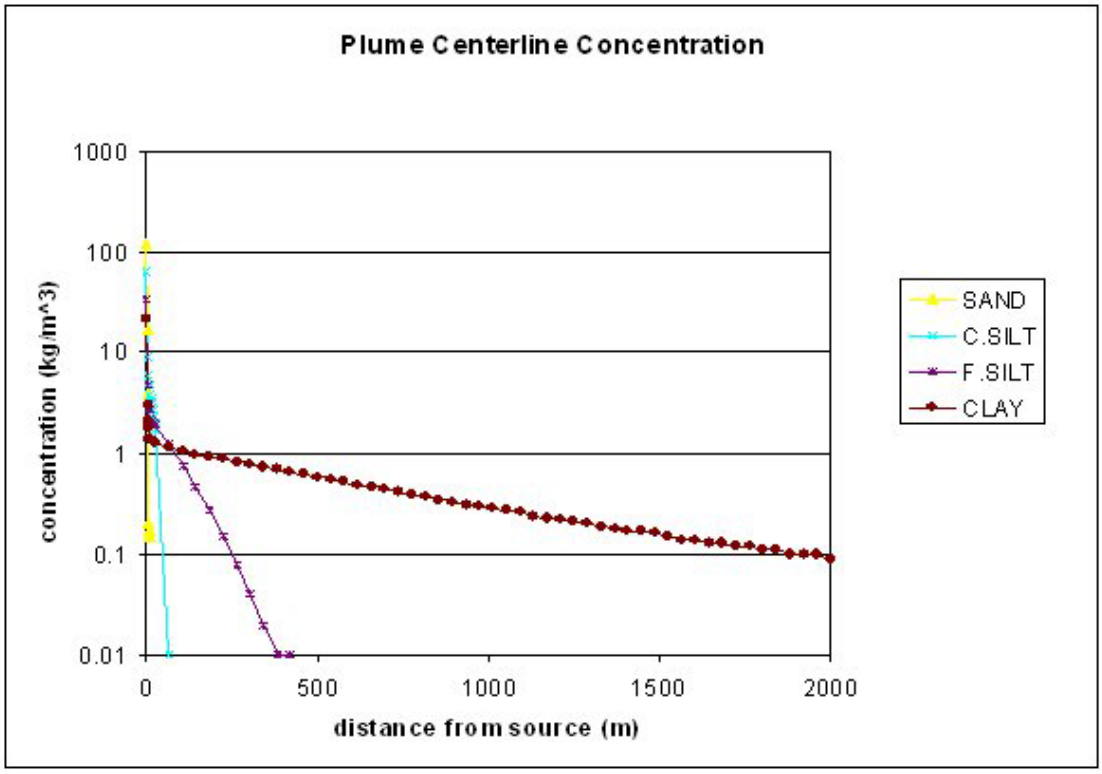

Figure 5-9a: Centerline concentration of sand, fine silt, coarse silt, and clay, simulation riv10d

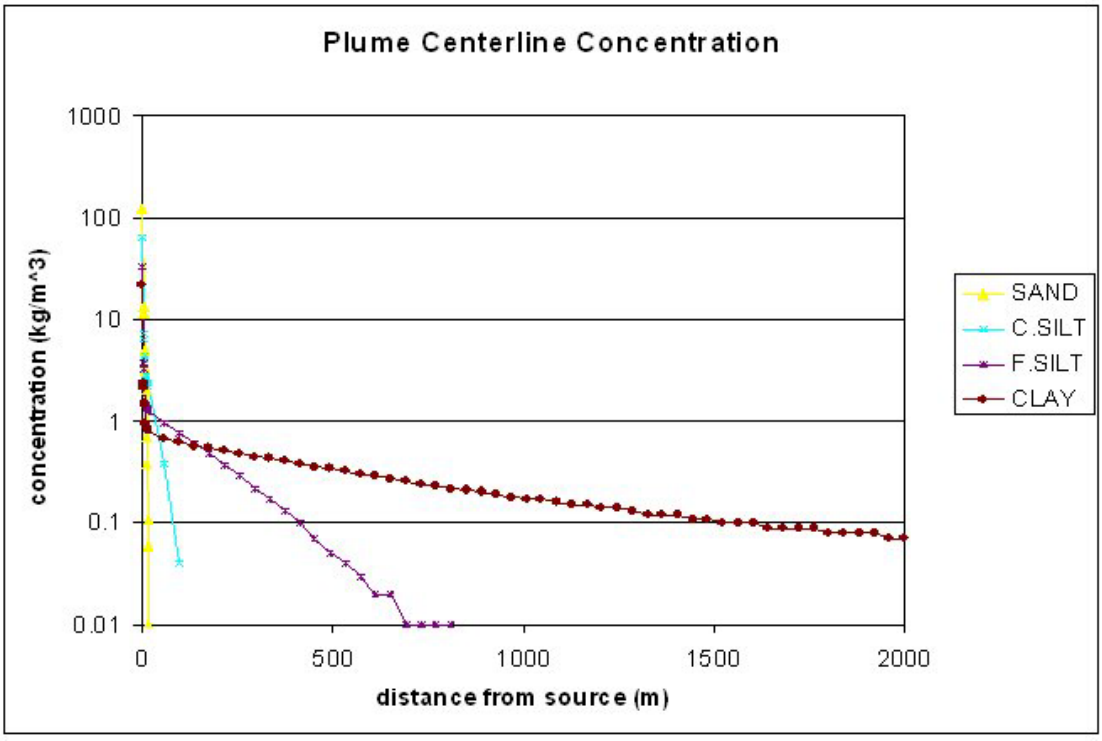

Figure 5-9b: Centerline concentration of sand, fine silt, coarse silt, and clay, simulation riv10h

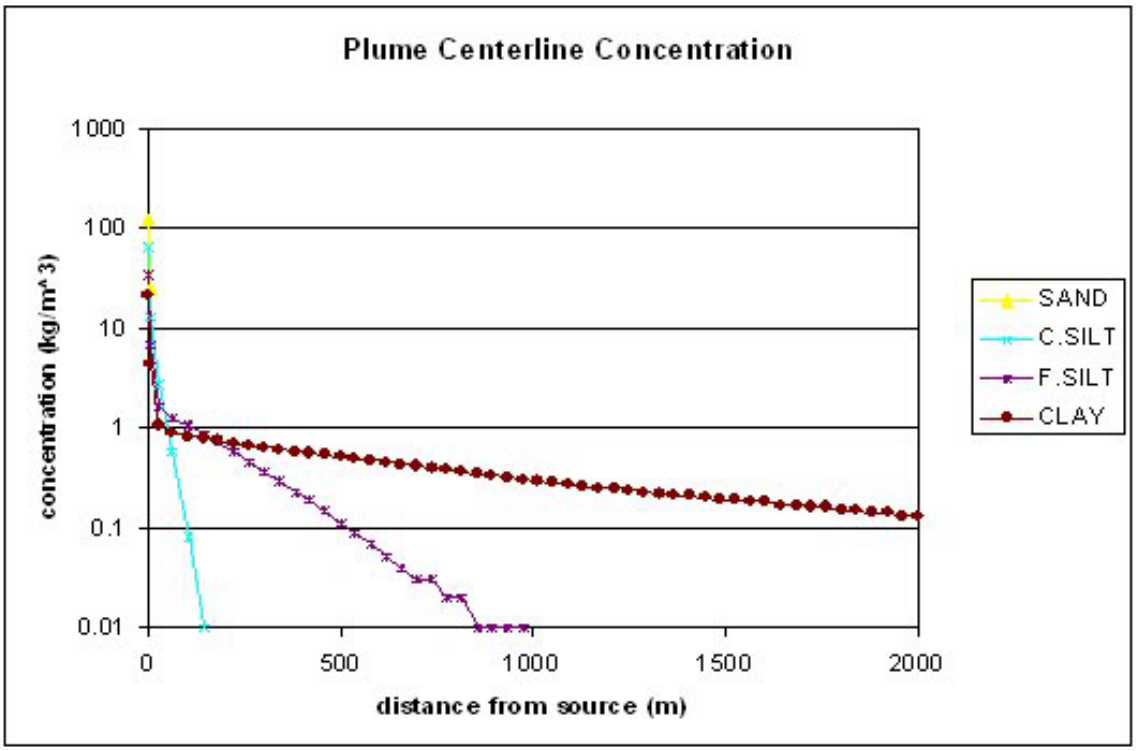

Figure 5-9c: Centerline concentration of sand, fine silt, coarse silt, and clay, simulation riv10j

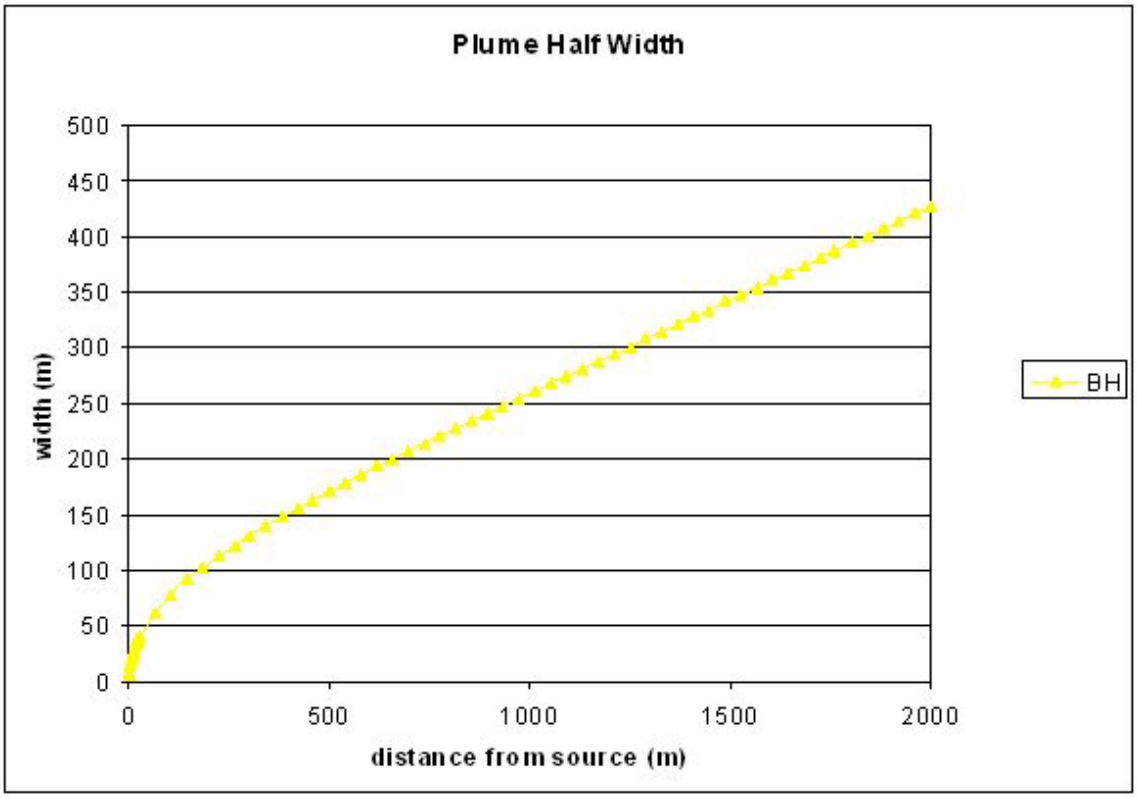

Figure 5-10a: Plume gaussian half width, simulation riv10d

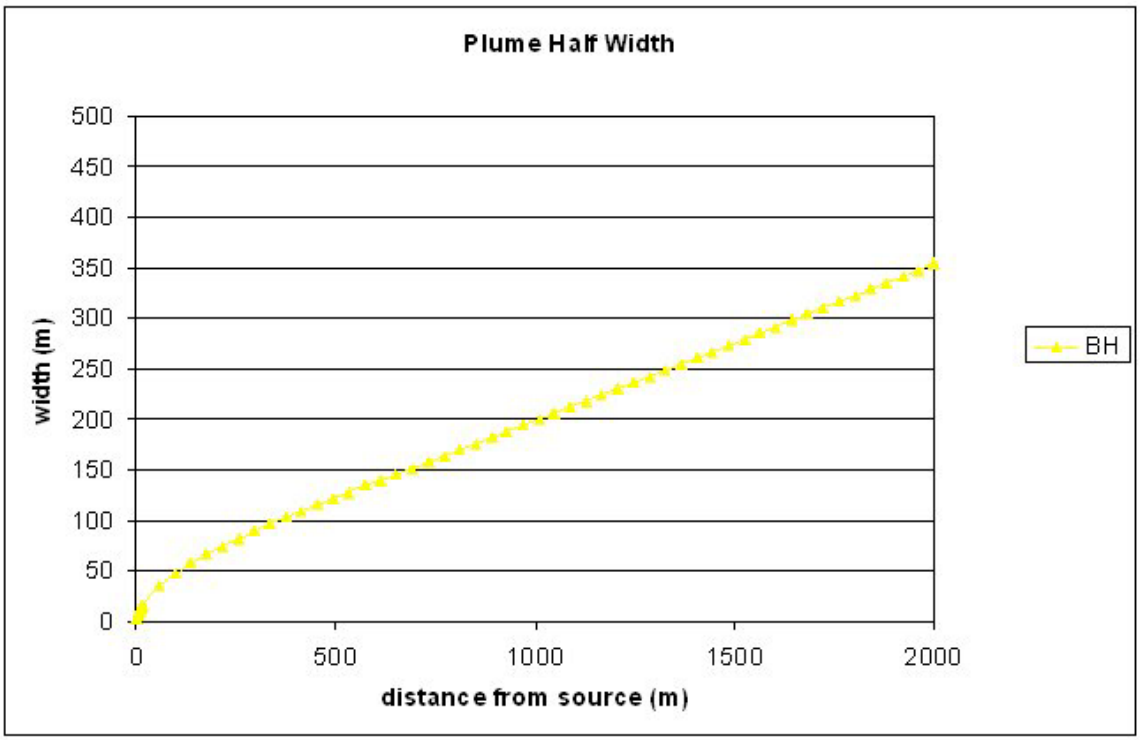

Figure 5-10b: Plume gaussian half width, simulation riv10h

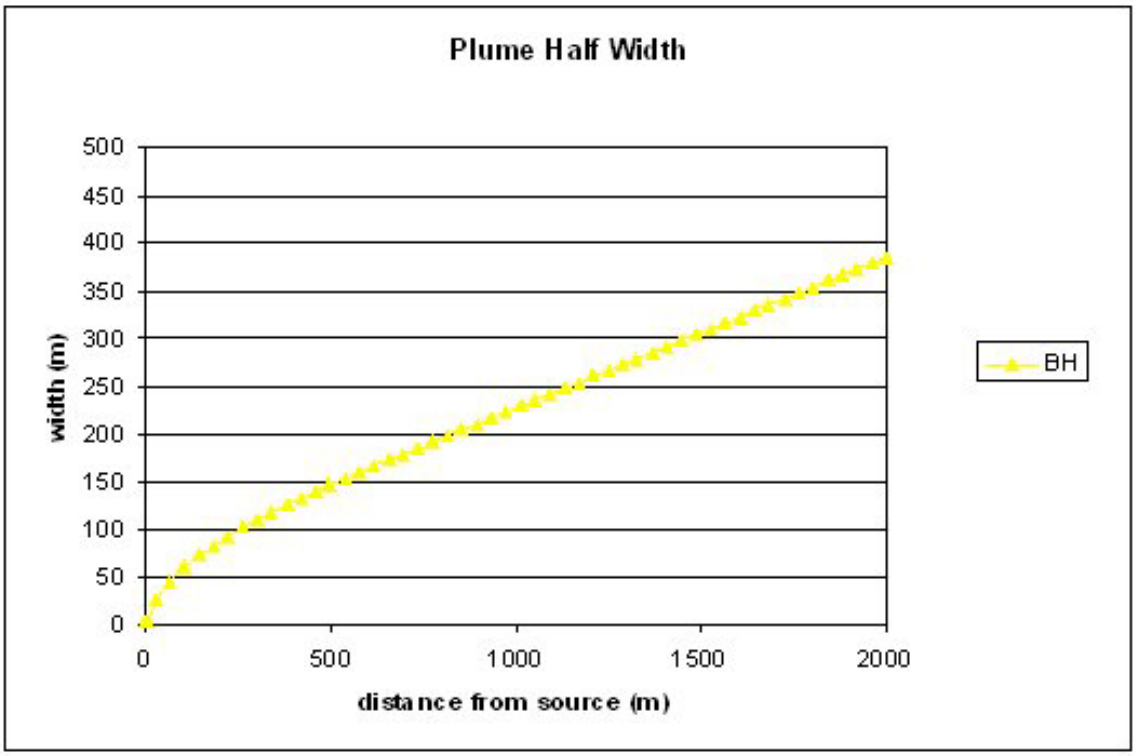

Figure 5-10c: Plume gaussian half width, simulation riv10j

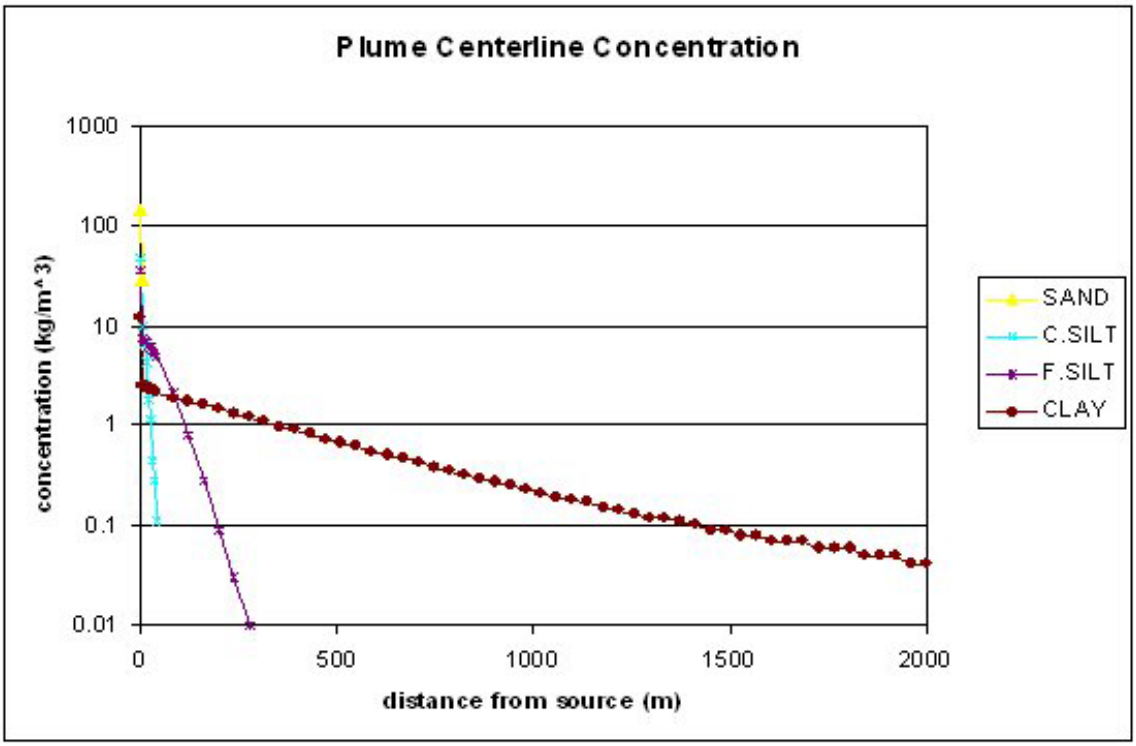

Figure 5-11a: Centerline concentration of sand, fine silt, coarse silt, and clay, simulation tyb25cms

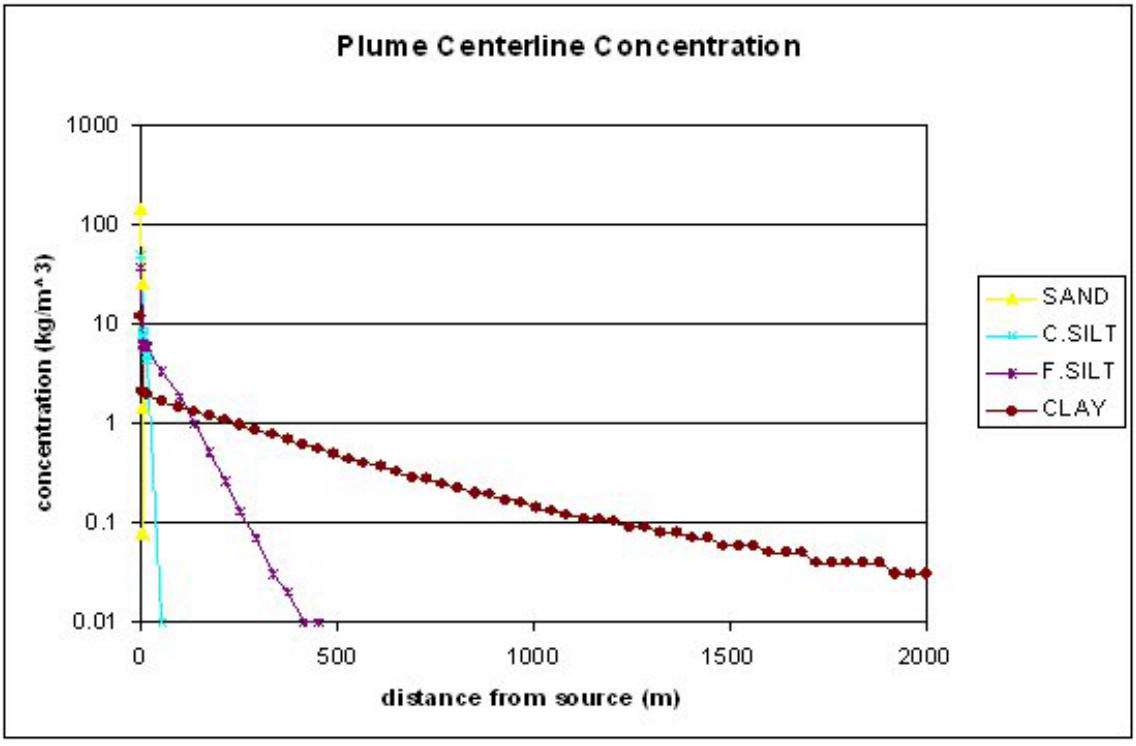

Figure 5-11b: Centerline concentration of sand, fine silt, coarse silt, and clay, simulation tyb35cms

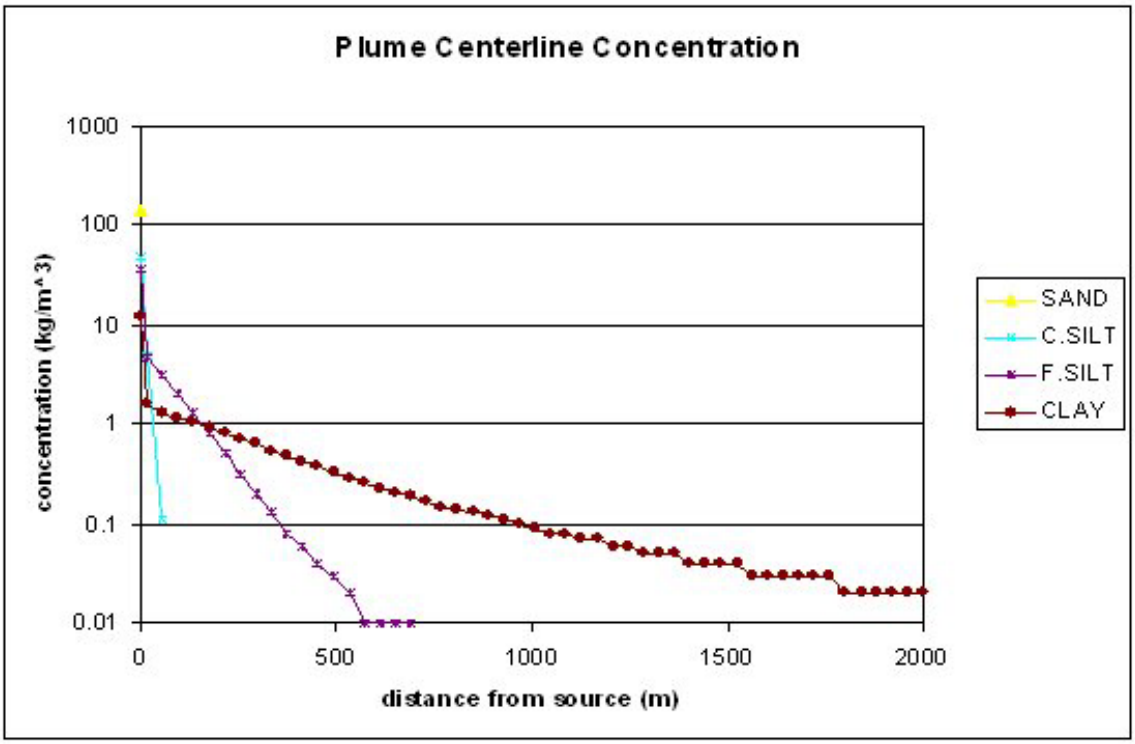

Figure 5-11c: Centerline concentration of sand, fine silt, coarse silt, and clay, simulation tyb45cms

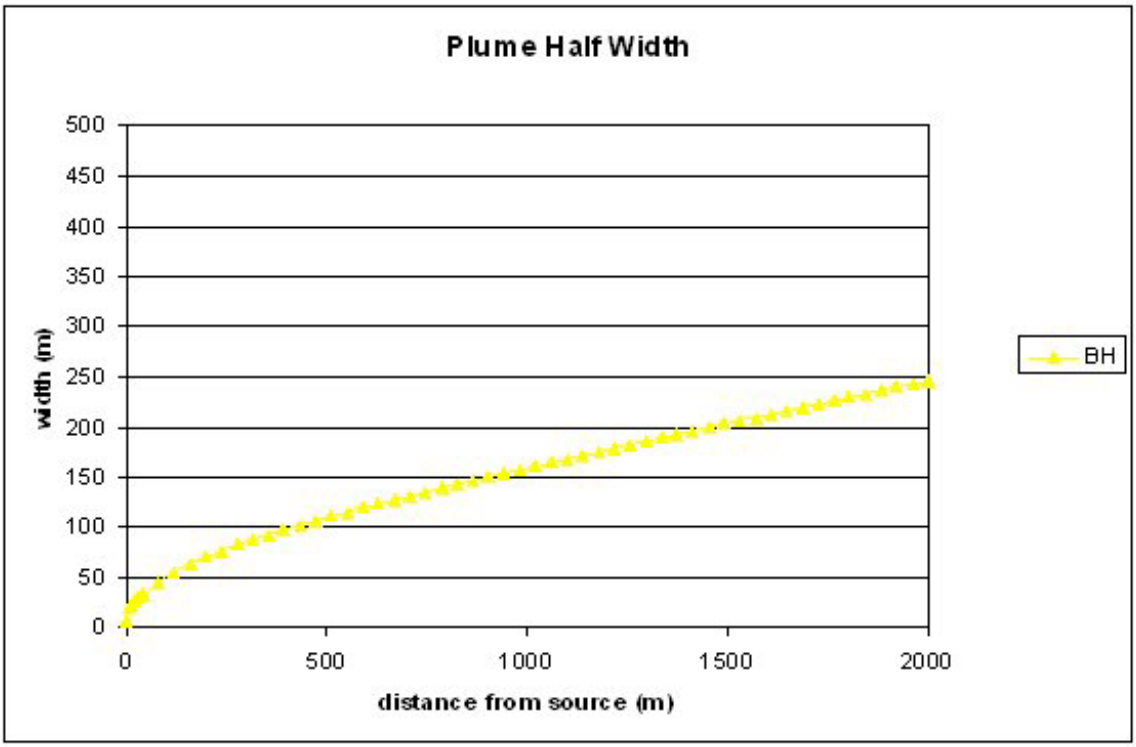

Figure 5-12a: Plume gaussian half-width, simulation tyb25cms

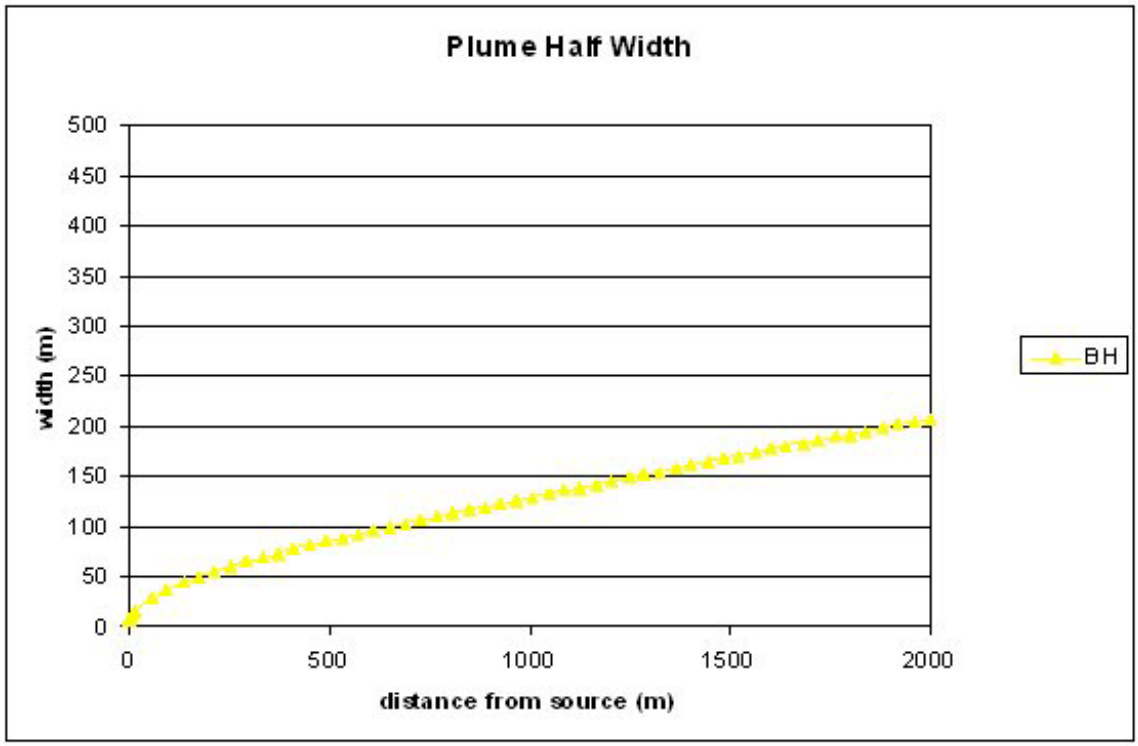

Figure 5-12b: Plume gaussian half-width, simulation tyb35cms

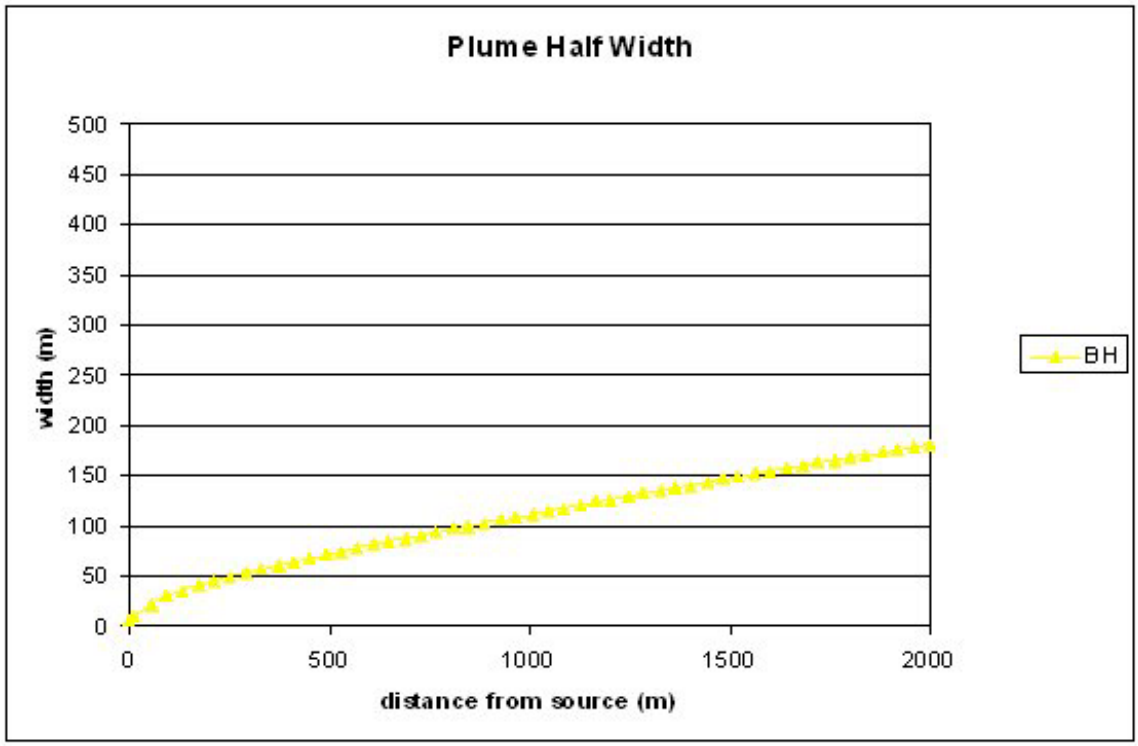

Figure 5-12c: Plume gaussian half-width, simulation tyb45cms

6 Summary and Conclusions

At the request of SAS, the U.S. Army Engineering Research and Development Center, Coastal and Hydraulics Laboratory (CHL) conducted studies that involved use of numerical models to characterize water level, current, and wave conditions in areas being considered for nearshore placement; and using the models, identified sediment pathways around the Savannah Harbor Entrance Channel and the surrounding ebb shoal. Specifically, CHL was tasked with preparing recommendations for nearshore placement of dredged material. Of specific interest is nearshore placement that maximizes benefit to the littoral system and the beaches along Tybee Island. Concerns with nearshore placement include increased nearshore turbidity during and after placement, movement of the dredged material back into the navigation channel, and influence of a nearshore berm on adjacent shorelines. The conclusions of this study will assist SAS in developing a Dredged Material Management Plan (DMMP) for the Savannah Harbor and River Federal Navigation channel and will assist the district in developing methods for utilizing dredged material beneficially within the context of a Regional Sediment Management (RSM) plan for the Savannah River/north Georgia coastline.

Study Objectives

The primary objectives of this study are:

1. Develop, calibrate, and apply a fine-grid hydrodynamic model of the Savannah River Entrance Channel and the surrounding ebb shoal and coast.
2. Develop and apply a fine-grid wave model to simulate transformation of offshore waves over the entire ebb shoal.
3. Simulate dredged material mound movement in the nearshore and lower river regions
4. Develop methods for assessing sediment pathways in the region between Tybee Island and the channel
5. Predict magnitude of turbidity during the dredging and placement operations
6. Provide guidance and recommendations for nearshore placement for feeding sand to the littoral system and beach, while minimizing re-handling (dredged material re-entering the channel), and minimizing any adverse impact on adjacent shorelines

Study Approach

Meetings between ERDC and SAS staff were used to develop project goals and an initial scope of work (SOW) covering areas of interest to the district. The original SOW included study of offshore placement sites and a few nearshore mound locations. As the study progressed, goals were modified to meet evolving questions and the focus was placed on nearshore placement for maintaining dredged material in the littoral zone/beach area.

Current and wave conditions expected during placement operations, i.e., typical non-storm wave and tidal conditions, and active high-energy (storm) periods are critical for dredged-material locations being considered for placement. Therefore, as part of this project, SAS requested a comprehensive review and modeling of current and wave conditions across the ebb shoal as well as current conditions in the river and around the jetties. In addition, sediment properties of the dredged material must be assessed for transport predictions. The dredged material is a mixture of sand, silt, and clay. Some of these mixed sediments will behave as non-cohesive sand, but some material will display cohesive properties. Erosion, transport and dispersion properties of cohesive material depends on multiple factors, including grain size distribution, mineralogy, pore water chemistry, organic content, bulk density, and other factors. Although these bulk properties are easily assessed, there are no theoretically valid methods available to accurately quantify sediment transport processes based on the sediment properties for mixed cohesive sediments. Therefore, a second part of this study was laboratory testing of sediments collected on site to quantify the erodability and transport characteristics of the dredged material (expected maintenance material). The third part of this study was assessing placement options for maintaining the material in the littoral system. The final part addresses turbidity due to dredging and placement operations.

The remainder of this section briefly describes each of the study components.

a. ADCIRC modeling of tidal circulation, wind-driven currents, and storm surge. The ADvanced CIRCulation (ADCIRC) model (Luettich et al, 1992) was used to generate tidal currents, wind driven currents and storm surges needed for the for the sediment transport and wave models. ADCIRC is a two-dimensional, depth-integrated, finite element, ocean circulation model that has been proven to accurately simulate tidal and storm conditions in near-shore regions. ADCIRC-predicted velocities and water levels were used to develop storm and non-storm hydrodynamic conditions in the river and on the ebb shoal. The ADCIRC modeling effort is described in Chapter 2. The accuracy of the model was evaluated using available tidal data at Fort Pulaski, in Tybee Creek, and offshore. In addition, current data provided by ATM, which were collected using an Acoustic Doppler Current Profiler (ADCP) (ENSR, 1999) were used to evaluate the model.

b. STWAVE modeling of wave transformation over the ebb shoal. Databases exist for offshore wave conditions near Savannah (Brooks and Brandon, 1995), produced by the U.S. Army Corps of Engineers Wave Information Studies (WIS). These data reflect conditions well offshore of Tybee Island, in deeper water, and do not accurately reflect conditions in shallower water. Also, wave transformation over a complex channel/ebb shoal region

cannot be predicted using simple refraction and shoaling equations because the bottom bathymetry is so irregular. Therefore, the STWAVE model was applied over the entire ebb shoal to predict wave refraction and shoaling, and to characterize wave conditions at the potential nearshore placement sites and along Tybee Island. The offshore WIS wave data were used to define the offshore boundary conditions needed as input by STWAVE. A two-step STWAVE modeling approach was adopted, using nested grids, in light of the wide shelf seaward of the ebb shoal and the complexity of the bathymetry. The STWAVE model was also used, along with the GENESIS shoreline change model, to investigate the potential impacts of a nearshore berm on local wave transformation, longshore sand transport processes, and shoreline change.

c. Sediment properties analysis. Historical data available from dredging records and previous studies were used to estimate grain size distributions, dredging volumes, and ebb shoal evolution. These data provide significant information on the ebb shoal and channel processes which can be used as input to transport models and to verify transport model results. As stated previously, site-specific cohesive sediment erosion tests were required to understand critical stresses for initiation of transport and transport rates of mixed dredged material. These experiments involved applying an erosion-testing flume, SEDFLUME (McNeil et al, 1996), to examine erodability of dredged material collected from various stretches of the channel. The erosion data are then used to develop site-specific erosion algorithms that are incorporated into the sediment transport models. The algorithms define sediment erosion rates as a function of bulk density, shear stress, and depth of burial. Algorithms were developed for each stretch of channel, for which sediments were acquired and tested.

d. Modeling of mound erosion and sediment pathways. The GTRAN model was used to simulate mound erosion at each proposed nearshore and riverine mound during storm and normal hydrodynamic conditions. The cohesive sediment erosion algorithms were incorporated into GTRAN and erosion from various mound configurations was simulated. In addition, a mesh of points was established between the channel and Tybee Island. Sand erosion magnitude and direction time series were developed at each point to assist in determining sediment pathways. This provided needed information for assessment of various nearshore placement locations. Hydrodynamic and wave time series required to estimate transport were developed from ADCIRC and STWAVE simulations.

e. Modeling of dispersion of material during dredging and placement operations. A significant amount of fine material is stripped from the sediment/water mixture during dredging and placement. This material is free to move through the water column. Transport of material released during the dredging process was modeled using the SSFATE model (Clarke ****). Various dredging methods, sediment types, dredging rates, and loss rates were simulated to provide a comprehensive understanding of sediment plume concentration and migration. In addition, the D-CORMIX model was used to predict loss of sediment during a pipeline placement operation. Placement is especially a concern in the nearshore where released sediment could migrate toward the beach.

Nearshore Placement of Dredged Material

Optimal location(s) of nearshore placement of dredged material is strongly dependent upon an understanding of coastal processes near the Savannah River Entrance and the Tybee Island littoral zone. Understanding of sediment transport patterns near the channel and ebb shoal gained from sediment transport modeling is presented followed by discussion of how the transport patterns influence selection of nearshore placement sites.

Channel and Ebb Shoal Sediment Transport Patterns

The modeling studies have revealed certain aspects of the coastal processes in and around the Savannah River Entrance, which provide valuable insight regarding the optimal location for nearshore placement. It is worthwhile to review some of these modeling results.

Sediment pathways at the entrance are influenced by many factors, which interact in a complex manner. These factors include: the relative strength of ebb and flood tidal currents, locally; spatial variability in the relative current strength throughout the entrance region, which is controlled by bathymetry and topography; local wave conditions which are dictated by many factors including incident deepwater conditions, tide stage, and bathymetry which influences refraction, shoaling, and wave asymmetry; and wave generated currents. For example, at a particular location, given the same wave conditions, ebb currents that are relatively stronger than flood currents will tend to produce ebb-directed sediment transport. The jetties and channel act to concentrate the ebb tidal jet, and influence the balance between ebb and flood flows at the entrance

Point sediment modeling results indicate that the navigation channel and areas in close proximity to it are dominated by sediment transport in the ebb direction (seaward). Ebb current speeds in the channel are greater than flood current speeds (the ebb jet is a little more concentrated), and this appears to create the ebb dominance in and near the channel. Model results for the computational points that were considered in the analysis (see Figure 6-1) indicate that in the channel section just to the north of Tybee Island, there is a pattern of increasing ebb-dominant transport. This gradient, increasing ebb-directed transport in the seaward direction, suggests an erosive pattern. This erosion tendency is consistent with the relatively low dredging requirement associated with the section of channel between stations 14S and 20S shown in Figure 6-2. Point model results in Figure 6-1 also indicate that there is a strong gradient in the ebb-dominant transport where the channel takes a more northwest/southeast orientation in the Tybee Roads area, but here the gradient is characterized by decreasing transport. This gradient suggests a tendency for sediment accretion; and, the region where the simulated gradient is strongest matches well with the outer portion of the channel that has experienced the highest shoaling rates, from stations 20S to 40S in Figure 6-2. Also, model results indicate a location well out in the channel where the ebb-directed transport decreases dramatically, indicating a zone where tidal current strengths have diminished to the point that sediment is less easily transported. Here, the transport gradient decreases too. This region corresponds to the location where the ebb bar, on the north side of the channel, impinges on the channel and where the ebb bar is shallowest. It appears that most of the sand-sized sediment carried

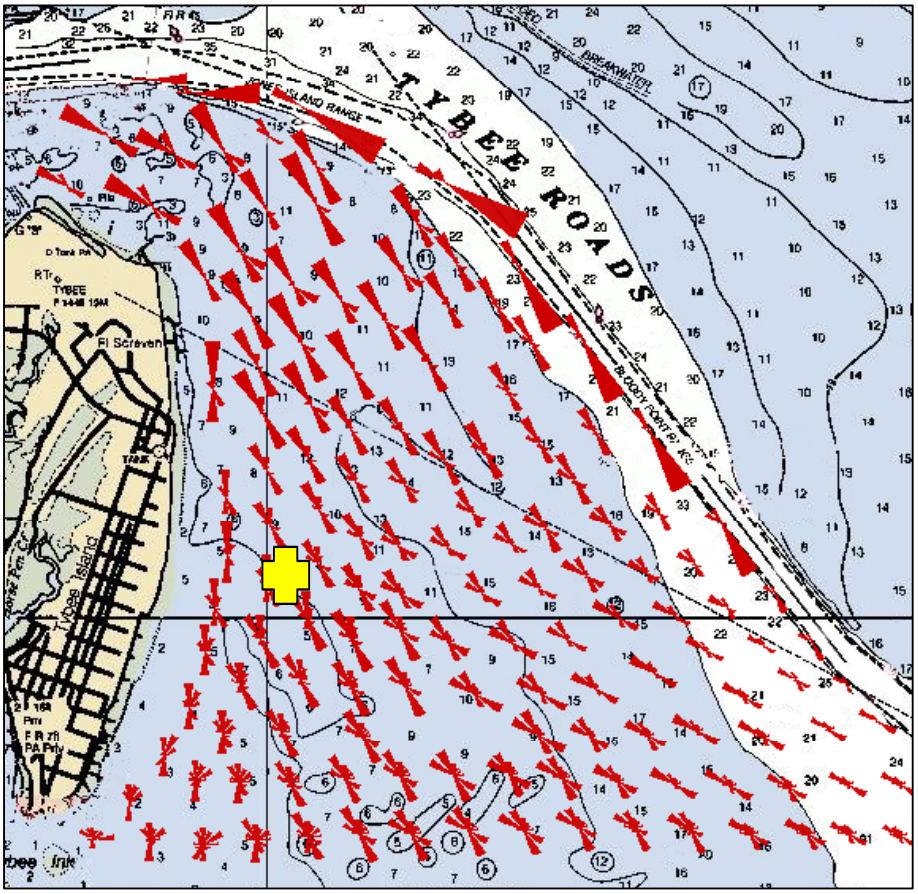

Figure 6-1. Sediment transport pattern at the Savannah River Entrance

out the channel is deposited in this vicinity, and landward of station 40S. Seaward of this point, dredging requirements are much smaller, which is also consistent with transport gradients evident in the model results.

The transport pattern to the south of the navigation channel, on the shallow tidal flats which are just offshore of the northern half of Tybee Island, is quite different according to the model results. Here, model results indicate a flood-dominant transport pattern. This different pattern, opposite of that computed in the channel region, is attributed to shallow water effects on the waves and the relative balance between flood and ebb tides on the tidal flats. Model results also suggest what seems to be an increasing gradient in flood-directed transport just offshore of north Tybee Island (evident in some of the calculation results; but less clear in others), in the region extending from the middle of the island to the north end of the island. An increasing gradient of flood-dominant transport would suggest an area of erosion. The tendency for erosion in this area is consistent with the recent historic pattern of tidal flat deflation identified by ATM in their analysis of bathymetric changes in this region of the ebb shoal. The presence of extensive shallow shoals off the northern end of Tybee Island, between Tybee Island and the navigation channel, are also consistent with the model-generated flood-dominant transport pattern. Model results suggest that the tidal flats off north Tybee are the probable sources for the sediment that is now resident in the shoals north of the island. Model results and evidence from

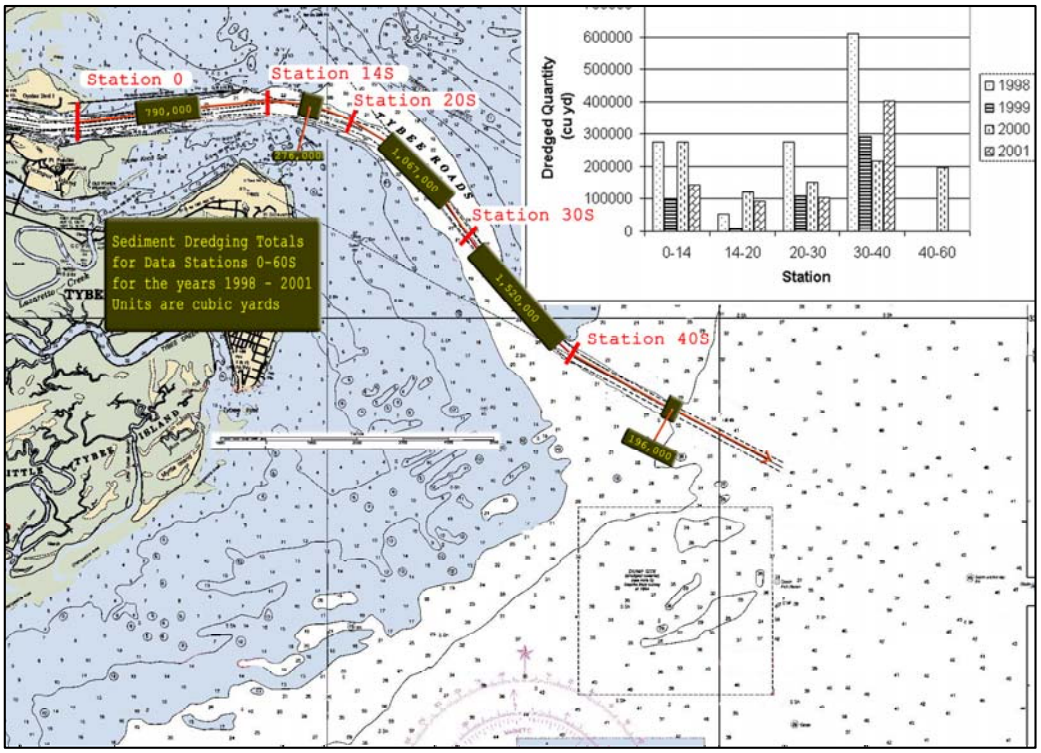

Figure 6-2. Recent pattern of channel maintenance dredging (length of the dark bars in the various channel sections indicate the magnitude of volume dredged)

sediment samples also suggest that if sand from these extensive flats and shoals is entering the navigation channel, it may be transported seaward and then deposited in the outer portions of the channel, in addition to sand being transported to the south along the outer ebb bar. Characteristics of these sediment transport patterns were a key factor in selecting an optimal location for nearshore placement.

Optimal Location for Nearshore Placement

Regional considerations of sediment management have expanded traditional viewpoints of dredged material handling to include nearshore placement of dredged material containing significant fractions of sand. The focus of this study was to identify favorable locations for nearshore placement of dredged material. Issues considered in the study include 1) the potential of nearshore-placed dredged material to provide sand to the littoral system of Tybee Island, 2) the likelihood that dredged material will re-enter the navigation channel and increase maintenance dredging volumes, and 3) the effects of nearshore berms of dredged material on wave refraction and consequently on shoreline change at Tybee Island.

Littoral Feeding Along North Tybee Island. The point sediment model results were used to assess the potential for benefits to the Tybee Island shoreline through feeding of sand to the littoral system. The balance of undertow and wave asymmetry were shown to play a strong role in shoreward sediment

transport. By placing dredged material in shallow water, the stronger influence of wave asymmetry allows sand to be transported toward shore. Sediment transport simulations at the offshore disposal site indicate that significantly lower transport rates occur there compared to the more energetic nearshore environment. Nearshore sediment transport simulations indicate that placement of dredged material near the central Tybee Island shoreline adjacent to the present transverse, shore-attached bar is most likely to introduce sand to the littoral system and provide the most benefit to the north Tybee shoreline. Trends in nearshore transport over the ebb shoal suggest that dredged material placed in deeper water near the navigation channel will either be transported back to the channel, or will re-enter the littoral system along the margins of the ebb shoal, providing little direct benefit to the north Tybee shoreline but possibly providing a benefit to south Tybee over the longer term. Transport offshore of the northern tip of Tybee Island is predominantly directed to the north due to both tidal and longshore transport influences. This predominant direction of transport is likely to produce little to no direct benefit to north Tybee, for material placed north of Tybee Island. Material placed here may simply re-enter the channel.

Maintenance Dredging Requirements. One issue of concern is an increase in maintenance dredging requirements resulting from the nearshore placement of dredged material. One conclusion from the sediment transport simulations is that placement of dredged material in the nearshore will likely lead to some increase in maintenance dredging requirements compared to placement of material in the offshore disposal site. But, placement offshore removes it from the littoral system, which is not desirable. Not all nearshore placement sites were equal in the likelihood of significant increases in maintenance dredging volumes. Simulated transport over the ebb shoal indicates that a significant portion of dredged material placed adjacent to the offshore channel, adjacent to the north jetty, and at the northeastern tip of Tybee Island is likely to re-enter the channel. Dredged material placed offshore of central Tybee Island is least likely to produce significant quantities of channel infilling. Model results suggest that material placed here will eventually work its way northward, eventually ending up in the shoals at the north end of Tybee Island, and possibly then entering the navigation channel. But during the northward movement, benefits to Tybee Island are likely to be maximized.

Impacts on Shoreline Change. Effects of nearshore berms of dredged material on wave refraction, longshore transport, and shoreline change were assessed through application of a shoreline change model, GENESIS. Nine nearshore berm scenarios were represented on the ambient bathymetry. Wave transformation simulations representing the long-term wave climate were preformed over the ambient bathymetry and each of the dredged material berm scenarios. The resulting nearshore wave climate was then passed to GENESIS to simulate changes in the shoreline change response of Tybee Island. Berms placed in deeper water and further from the shoreline produced little change in shoreline change trends. Berms placed closer to or immediately offshore produced moderate changes in the shoreline evolution trends. Berms 01 and 02, offshore of the northern tip of Tybee Island resulted in a decreased erosional trend at the northern tip of the island, but increased the erosional trend along the central portion of the shoreline. Berms 13 and 14, placed adjacent to the transverse bar attached to the central island shoreline produced a reduction in

erosion rates along the central third of the island and relatively weak erosional trends on the northern and southern thirds of the island. The influence of the sediment supply to the littoral zone and the influence of tidal currents were neglected in the GENESIS simulations. Because the positive influence of a sediment source to the beach system was not considered, negative impacts of berm placement on adjacent shoreline changes are likely overstated, particularly along north Tybee which is expected to benefit from placement of the dredged material. The beaches on the southern half of the island are reasonably healthy. Any negative impact on the beaches on south Tybee could be offset during the course of renourishment of the federal shore protection project on Tybee Island, or through alteration of the nearshore berm placement practice, i.e., periodically placing dredged material to the south side of the transverse bar off central Tybee, where model results suggest it will move to the south.

Recommendations. The recommended location for nearshore placement of dredged material is adjacent to the transverse, shore-attached bar just offshore of central Tybee Island (yellow cross shown Figure 6-1). Details of berms proposed for this location are provided in Chapter 4. The impacts to the shoreline by berms placed at this location are similar to those of other extreme-nearshore placement options, but these impacts are likely to be offset by the potential of sand to be transported shoreward to benefit the littoral system. This location has the least potential for increasing maintenance dredging while providing benefit to Tybee Island.

Impacts of Dredging and Placement Operations

Plumes of suspended sediment generated during dredging and placement operations are of potential concern to the aquatic environment. Consequently, estimates of suspended sediment entrainment and transport during the dredging and placement operations are required to assess the potential impact on the environment. Chapter 5 describes model applications and analysis addressing sediment suspension, transport, and deposition during dredging and nearshore placement operations at the Savannah River entrance channel and adjacent waters. Two primary issues are 1) whether unsuitable levels of suspended sediment are present in the water column or 2) do fines placed in suspension deposit in the nearshore zone. This chapter does not address the biological effects or risk to the environment, but presents suspended sediment concentrations from which those assessments may be made.

Two numerical models of dredged material resuspension and transport were applied to address the effects of suspended sediments at the dredge and the pipeline outfall. SSFATE was applied to quantify sediment suspension from the dredge, transport of the suspended sediment from the dredging site, and deposition of the suspended material. D-CORMIX was applied to quantify sediment entrainment and transport at the pipeline outfall.

Resuspension from dredging operations

Higher concentrations of resuspended sediments were predicted at riverine dredging sites, primarily attributed to the higher silt/clay content in the dredged sediments. Dredging in the coastal region (seaward of the Savannah River entrance) produced lower TSS concentrations because of the higher sand content,

which more quickly settles out of suspension. SSFATE predicted that the resuspended dredged material was quickly advected in a net seaward direction by the ebb-dominant tidal currents. Peak TSS concentrations from the resuspension plume were observed to coincide with near-slack currents. Suspended sediment concentrations also generally drop to negligible levels within 12-24 hours after cessation of dredging operations. Accumulation of resuspended dredged material ranged up to several centimeters within the navigation channel (as expected) and amounted to sub-millimeter thickness outside the navigation channel. Only small quantities of fine sediments were observed to pass within the nearshore region of the Atlantic shoreline of Tybee Island and suspended fine-grained sediments were not deposited in the nearshore because of the relatively large tidal-current-generated shear stresses in this region. The influence of waves on suspended material in the nearshore was not simulated. Agitation by waves would further prevent the deposition of fine-grained suspended sediments in the nearshore.

Resuspension from pipeline disposal

As experience would suggest, significantly higher suspended sediment concentrations are produced at pipeline outfalls than for resuspension at the dredging site. Plumes from pipeline outfalls are expected to be transported primarily in the direction of the tidal currents, with some lateral mixing. Sand and coarse silts were observed in the model simulations to settle out of suspension fairly close to the discharge location, while fine silts and clays remained in suspension to be transported further distances from the discharge point. Fine silts were found to settle out of suspension between 500-1000 m from the discharge point, and the clay fraction remained in concentrations of approximately 100 mg/L at a distance of 2000 m from the discharge point.

APPENDIX A: SEDFLUME/ASSET Flume Analysis

Description of ASSET Flume

The ASSET flume is a straight flume that has a test section with an open bottom through which a rectangular or circular cross-section coring tube containing sediment can be inserted (Figure A-1). Downstream of the test section is a bedload trap used to capture eroded sediment that rolls or moves by saltation along the bottom of the flume channel. The flume used in these experiments is a modified version of Sedflume, developed by researchers at the University of California at Santa Barbara (McNeil et al, 1996). The difference between the two flumes is the bedload trap section, which permits separation of suspended load and bed load in the ASSET flume. The main components of the flume are the coring tube; the test section; an inlet section for uniform, fully developed, turbulent flow; a bedload trap section, a flow exit section; a water storage tank; and a pump to force water through the system. The coring tube, test section, inlet section, bedload trap section, and exit section are made of clear polycarbonate so that the sediment-water interactions can be observed. The coring tubes, which are up to 80 cm in length, are 10 cm diameter.

Water is pumped through the system from a storage tank into a 5 cm diameter pipe, and then through a flow converter into the rectangular duct (Figure A-1). The duct is 2.5 cm in height, 10 cm in width, and 120 cm in length; it connects to the 15 cm long test section and 1 m long bedload trap section, which have the same cross-sectional area. The flow converter changes the shape of the cross-section from circular to the rectangular duct shape while maintaining a constant cross-sectional area. A three-way valve regulates the flow so that part of the flow goes into the duct while the remainder returns to the water source (tank or river). In addition, there is a small valve in the duct immediately downstream from the test section that is opened at higher flow rates to keep the pressure in the duct and over the test section at atmospheric conditions.

At the start of each test, the coring tube is filled with the reconstructed sediment core that was permitted to consolidate prior to erosion testing. Three consolidation times we used for each sediment type tested. Consolidation time and it's variation are important because bulk density, which changes with time for

cohesive sediments, is one of the key factors in cohesive sediment erosion potential. The procedure for preparing the reconstructed core sediments in the laboratory will be described later. The coring tube and the sediment it contains are then inserted into the bottom of the test section. The flume operator moves the sediment upward using the plunger, which is inside the coring tube and is connected to a jack (Figure A.2). The jack is driven by motor, which is regulated with a switch. By this means, the sediment surface is raised and made level with the bottom of the test and inlet sections. The speed of the jack movement can be controlled at a variable rate in measurable increments as small as 0.5 mm.

Water is forced through the duct and the test section over the surface of the sediments. The shear produced by this flow, if great enough, causes the sediments to erode. As the sediments in the core erode, the core surface is moved upwards by the operator as necessary so that the sediment-water interface remains level with the bottom of the test and inlet sections. The erosion rate is recorded as the upward movement of the sediments in the coring tube over time. Duration of each erosion test for a specified shear stress is dependent on the rate of erosion and generally is between 0.5 and 10 minutes.

Hydrodynamics

Fully developed turbulent flow exists in the test section for the flow rates of interest. Turbulent flow through pipes has been studied extensively, and empirical functions have been developed which relate the mean flow rate to the wall shear stress. In general, flow in circular cross-section pipes has been investigated. However, the relations developed for flow through circular pipes can be extended to non-circular cross-sections by means of a shape factor. An implicit formula relating the wall shear stress to the mean flow in a pipe of arbitrary cross-section can be obtained from Prandtl's Universal Law of Friction (Schlichting, 1979). For a pipe with a smooth surface, this formula is

$$\frac{1}{\sqrt{\lambda}} = 2.0 \log\left[\frac{UD\sqrt{\lambda}}{\nu}\right] - 0.8 \qquad \text{(A.1)}$$

where U is the mean flow speed, ν is the kinematic viscosity, λ is the friction factor, and D is the hydraulic diameter defined as the ratio of four times the cross-sectional area to the wetted perimeter. For a pipe with a rectangular cross-section, or duct, the hydraulic diameter is

$$D = 2hw/(h + w) \qquad \text{(A.2)}$$

where w is the duct width and h is the duct height. The friction factor is defined by

$$\lambda = \frac{8\tau}{\rho U^2} \qquad \text{(A.3)}$$

where ρ is the density of water and τ is the wall shear stress. Inserting Eqs. (2.2) and (2.3) into Eq. (2.1) then gives the wall shear stress τ as an implicit function of the mean flow speed U.

For shear stresses in the range of 0.1 to 10.0 N/m^2, the Reynolds numbers, UD/ν, are on the order of 10^4 to 10^5. These values for Reynolds numbers are sufficient for turbulent flow to exist for the stresses of interest in this study. For flow in a circular pipe, turbulent flow theory suggests that the transition from laminar to turbulent flow occurs within 25 to 40 diameters from the entrance to the pipe. Since the hydraulic diameter of the duct pipe is 4 cm, this suggests an entry length of 100 to 160 cm. The length of the duct leading to the test section is 120 cm and is preceded by a 20 cm flow converter and several meters of inlet pipe. These arguments along with direct observations indicate that the flow is fully turbulent in the test section.

Core Collection and Preparation

Approximately 50 gallons of sediment were collected from each of seven sites in the Savannah ship channel (Figure A-3). The sediment for each site was slurried immediately prior to creating cores for Sedflume analysis. This is done to assure that the sediments are well mixed and will be of similar grain size distribution.

Pouring the slurried sediment from each site into coring tubes created the sediment cores tested in Sedflume. This process was repeated for each of the six Sedflume analysis sites. Cores were consolidated for periods of 4, 20, and 120 days. The variation in consolidation times permits erosion analysis over a wide range of bulk density conditions. At the end of each consolidation period, two cores were extracted. One was used for bulk property analysis (including bulk density) and the other for Sedflume erosion analysis.

Measurements of Sediment Erosion Rates

The procedure for measuring the erosion rates of the sediments as a function of shear stress and depth is described in this section. The sediment cores were obtained as described above and then moved upward into the test section until the sediment surface was even with the bottom of the test section. A measurement was made of the depth to the bottom of the sediment in the core. The flume was then run at a specific flow rate corresponding to a particular shear stress. Erosion rates are estimated by measuring the remaining core length at different time intervals, taking the plunger height difference between each successive measurement, and dividing by the time interval.

In order to measure erosion rates at several different shear stresses using only one core, the following procedure was used. Starting at a low shear stress, the flume was run sequentially at higher shear stresses with each succeeding shear stress being twice the previous one. Generally about three shear stresses were run sequentially. Each shear stress was run until at least 0.5 mm but no more than 2 cm was eroded. The minimum 5 mm is required to obtain sufficient sample for bedload analysis The time interval was recorded for each run with a stopwatch and the bedload traps emptied and effluent saved for later analysis. The flow was then increased to the next shear stress, and so on until the highest shear stress was run. This cycle was repeated until all of the sediment had eroded from the core. If after two cycles a particular shear stress showed a rate of erosion less than 10^{-4}

cm/s, it was dropped from the cycle; if after many cycles the erosion rates decreased significantly, a higher shear stress was included in the cycle. A lower shear stress was sometimes re-introduced to the cycle if it became apparent that a more easily erodible layer was exposed. In general, erosion tests for each cycle were chosen from 1, 2.5, 5, 10, 20, and 40 dynes/cm^2. Sedflume can generate shear stress as great as 100 dynes/cm^2, but high values were not needed for these sediments

The previously described laboratory cores were developed so bulk properties other than bulk density, which affect erosion could be held constant and erosion rates could be related to bulk density. These data can then be fit to equations describing erosion as a function of bulk density and shear stress only. The equations are then used to develop algorithms for predictive models of sediment transport. Generally, with the other bulk properties held constant, erosion rates decrease exponentially as bulk density increases (Jepsen et al 1997a and 1997b; Roberts et al 1998) for natural sediments. In general, the data can be approximated by an equation of the form

$$E = A\tau^n \rho^m \qquad \text{(A.4)}$$

where E is the erosion rate (cm/s), τ is the shear stress (dynes/cm^2), ρ is the bulk density (g/cm^3), and n, m, and A are constants. The constants are shown in Table *** for the composite sediment from each site. For each shear stress, the erosion rate as a function of bulk density is shown as a straight line, which demonstrates that the above equation represents the data quite well and also that the erosion rate is a unique function of shear stress and bulk density. This relationship (with different constants) has been shown to successfully describe several other natural sediments (Jepsen et al, 1997a and 1997b; Jepsen et al 1998).

Measurements of Critical Shear Stress for Erosion

The value for critical shear stress, τ_c, is determined directly from the erosion rate equation developed from the laboratory SEDflume results, equation 2.4, which, after rearranging becomes

$$\tau_c = \left(\frac{E}{A}\right)^{1/n} \rho^{-m/n} \qquad \text{(A.5)}$$

where E, the erosion rate is defined here as E=1x10^{-4} and the constants A, n, and m are determined from the erosion experiments. Smaller values of E can also be used to define critical shear stress to develop a sensitivity analysis. For this study, sensitivity testing is performed by analyzing critical shear stress based on a minimum erosion rate of 1x10^{-5} cm/s. This value of E is significantly less than is measurable using SEDflume and corresponds to an erosion rate of 1 mm every 150 minutes.

Measurements of Sediment Bulk Properties

Bulk properties of the sediment and water in the core influence erosion rate. Cores were consolidated in water from the site of collection. One of the main

factors influencing erosion is bulk density. For each sediment, a core that was consolidated in the same conditions as the Sedflume core was analyzed for bulk density. In addition, several samples were analyzed for grain size distribution.

Bulk density measurements

In order to determine the bulk density of the sediments at a particular depth and consolidation time, the weight of the sediment analysis samples, including the cup, were measured immediately after extraction from the core. Weight of the cup (tare weight) was measured and recorded prior to sample extraction. Wet weight of the sample was calculated by subtracting tare weight from the weight of the sample. The samples were then dried in the oven at approximately 75°C for 2 days and weighed again. The dry weight of the sample was calculated as the tare weight subtracted from the weight after drying. The water content W is then given

$$W = \left(\frac{m_w - m_d}{m_w} \right) \tag{A.6}$$

where m_w and m_d are the wet and dry weights respectively. A volume of sediment, V, consists of both solid particles and water, and can be written as

$$V = V_s + V_w \tag{A.7}$$

where V_s is the volume of solid particles and V_w is the volume of water. If the sediment particles and water have density ρ_s and ρ_w respectively, the water content of the sediment can be written as

$$W = \frac{\rho_w V_w}{\rho V} \tag{A.8}$$

where ρ is the bulk density of the sediment sample. A mass balance of the volume of sediment gives

$$\rho V = \rho_s V_s + \rho_w V_w \tag{A.9}$$

By combining Eqs. (2.5), (2.6), and (2.7), an explicit expression can be determined for the bulk density of the sediment sample, ρ, as a function of the water content, W, and the densities of the sediment particles and water. This equation is

$$\rho = \frac{\rho_s \rho_w}{\rho_w + (\rho_s - \rho_w) W} \tag{A.10}$$

For the purpose of these calculations, it was assumed that $\rho_s = 2.6$ gm/cm^3 and $\rho_w = 1.0$ gm/cm^3.

Particle size distribution measurements

A Coulter LS Series100 was used to measure the size distributions of particles for each of the Sedflume sites. The LS100 measures particles from 0.4μm to 900 μm in size. The particle size for the material is measured by placing a small portion of the sample in the fluid module. The fluid module is a chamber that is

filled with water and is sonicated to break up the particles for measurement. Once the sample has been placed in the fluid module, the sample is pumped and recirculated through the system past the optical module. The optical module is a rigid frame containing the light sources, lenses, detectors and printed circuit cards. The optical module uses a spatial filter assembly containing a laser diode and laser beam collimator. The diffraction detector assembly contains a custom photodector array that is used for the measurement of the particle size. From these measurements, the distribution of grain sizes at each erosion analysis site is provided.

Analysis of bedload samples

After each shear stress erosion measurement, the bedload traps were evacuated before beginning the next erosion experiment. The evacuated water with sediment generally amounted to approximately 1 liter. The samples were labeled, and sediment allowed to settle for 24 hours. A pipette was then used to remove water overlying the deposited sediment. After removal of most of the water, the sediment samples were oven dried as described in the previous section. The dried sediments were weighed and a grain size distribution measured using the Coulter LS particle sizer described above.

Each bedload sample corresponded to a specific erosion test in the Sedflume for which a depth of erosion of the core was measured. The surface area of the core is known and the bulk density was measured from the duplicate core. These three parameters were used to calculate the mass of sediment eroded. This calculation, along with the measured mass of bedload provided the fractions moving in suspension and on the bed.

Results

Six sites were chosen for analysis from the river and bar channels at Savannah. Sediment sites were selected to attempt to collect samples that would behave cohesive and would be from a broad range of locations in the channel. The six sites are shown in Figure A-3. Site selection was based in part on grain size distributions collected from the bar channel in 2000 by Law Engineering (Table ***). Sites were chosen to represent various areas in the bar and river channel. In addition, samples were not collected in areas that were defined as sandy. The transport processes for sand are well known and Sedflume is not required for sand transport analysis. However, grain size distribution in the channel is temporally changing and Sedflume samples grain size distribution did not generally match those from the Law Engineering data set.

Two of the sites selected, 17S and 62S, were non-cohesive. A relatively constant bulk density characterized these sites in both consolidation time and depth from the surface. In addition, erosion rates did not vary with the small span of bulk density variation. The grain size distributions of these two sites demonstrate very little fine material (Figure A-4). Table A-1 provides the median and other relevant grain sizes in the distribution plotted in Figure A-4.

The other sites behaved as cohesive sediment. Erosion rate generally decreased with increasing bulk density. Table A-2 provides the equations and coefficients to Equation A-4 for each of the four cohesive sediments. Plots of bulk density verses shear stress for each of the four cohesive sediment samples are provided in Figure A-5a-d. The colored lines are the slopes for each of the corresponding shear stresses. The black lines are the slopes for each shear stress for all data. Greater values of m indicate increased sensitivity to bulk density. All of the cohesive samples from Savannah can be classified as moderately cohesive. The value of parameter m is often 40 or greater for strongly cohesive sediments. Outlying points that do not fit the trend are expected. These could be due to gas bubbles, an oxidized layer, or other aberrations in what is assumed to be a well mixed sediment. Sometimes this can lead to positive slopes in the bulk density/erosion relationship (see τ=4.0 in Figure A-5c), but this generally happens only when all bulk density points are near each other and only a few data points exist for the given shear stress. Despite these anomalies, the inverse relationship trend between bulk density and erosion is clear.

Plots of bulk density verses depth for the six sites are presented in Figure A-6. The consolidation with time between 4 and 120 days is seen. For the four cohesive sites, these plots indicate that the sediment bed becomes more consolidated and thus harder to erode as it ages. In addition, these plots indicate that the sediment becomes more consolidated with depth below the surface. This indicates that the sediment surface is more easily eroded than deeper layers. The two non-cohesive sites (17S and 62S) show a relatively vertical profile with depth when consolidated (except for the surficial layer, which is often a layer of fine sediment). The vertical profile is indicative of non-cohesive sediments, which generally do not have bulk density variation when consolidated There are other factors, such as thixotropic effects and increasing organic content that will also increase the erosion resistance, but bulk density has been determined to be one of the most important factors (Roberts et al, 1998). Also, the increase in bulk density with depth below the surface for most samples is seen in Figure A-6. This indicates that the bed will become more difficult to erode with depth below the original sediment surface. This is an important feature of cohesive sediment beds. Many previous experiments have been only on the surficial layer of sediment. Estimated erosion rates will be excessive if the mound is assumed homogeneous and surficial sediment erosion rates are applied throughout the mound.

The decrease in erosion with depth is also important when considering turbidity generated by release of fines from the bed. Generally, a plume will be created at the beginning of a storm, but the plume will decrease greatly as the storm progresses. This is due, in part, to the significantly decreased erosion rates of sediments below the surficial layer. Time histories of suspended solids concentrations during storms have demonstrated this trend. A model cannot match these time history data if it assumes a homogeneous erosion rate with depth (for example, see Gailani et al, 1991).

Bedload trap analysis indicated that material from the bar channel separated after erosion (Table A-3). The material collected from the bedload traps was

coarser than the core sediments. Therefore, the fine material was moving in suspension while the sand fraction moved as bedload. Figure *** shows the separation 1 m downstream from the core by providing grain size distribution for both the trap and core sediments. The 'tail' of fines in the original core (sediment smaller than 80 μm) is almost completely missing from the trap grain size distribution. Other river sediments showed similar distribution change. Site 38N, in the river, included a higher percent fines than the bar channel. This material eroded as aggregates and individual particles. The aggregates moved as bedload and were collected in the bedload trap. These aggregates had the same composition as the core and therefore there is little difference in median grain size between core and bedload trap (Table A-3).

The coefficients in Table A-2 were used as input to the cohesive portion of the GTRAN model as described in Chapter 4. These data permitted testing of mound erosion using various sediment types that may be placed in the nearshore. The bedload trap data were used to validate the hypothesis that mixed silt/sand placed in the nearshore will quickly separate. Fine-grained sediment not associated with aggregates will not deposit in the higher energy nearshore. It will eventually disperse and move, then deposit, offshore.

References

Gailani, J., C.K. Ziegler, and W. Lick, 1991. Transport of Suspended Solids in the Lower Fox River. Vol. 17, No. 4, pp. 479-494.

Jepsen, R., J. Roberts, and W. Lick, 1997a. Effects of Bulk Density on Sediment Erosion Rates, *Water, Air, and Soil Pollution*. Vol. 99, pp. 21-31.

Jepsen, R., J. Roberts, and W. Lick, 1997b. Long Beach Harbor Sediment Study, Report Submitted to U.S. Army Corps of Engineers, DACW09-97-M-0068

Jepsen, R., Roberts, J., W. Lick, Gotthard, D., and Trombino, C, 1998. New York Harbor Sediment Study, Report Submitted to the U.S. Army Corps of Engineers, New York District.

McNeil, J., C. Taylor, and W. Lick, 1996. Measurements of the Erosion of Undisturbed Bottom Sediments with Depth, *Journal of Hydraulic Engineering*. Vol. 122, No. 6, pp. 316-324.

Roberts, J., Jepsen, R., Gotthard, D., and Lick, W. 1998. Effects of Particle Size and Bulk Density on Erosion of Quartz Particles. *Journal of Hydraulic Engineering*. Vol. 124, No. 12, pp. 1261-1267.

Schlichting, H., 1979. *Boundary-Layer Theory*. Seventh ed, McGraw-Hill.

	38n	17s	33s	52s	62s	78s
Percent < 4 micron	8.9	1.5	1	2.7	2.5	7
Percent < 20 micron	23.1	4.8	2.5	10.3	6.1	20.5
Percent < 80 micron	47.7	14.3	8.2	35.9	23	50.7
Percent < 400 micron	96.3	63.2	55.7	98.4	100	99.1
D10 (micron)	5	52	96	20	45	7
D50 (micron)	90	290	350	115	120	80
D90 (micron)	280	1000	850	270	200	205

Table A-1 Sedflume sediment sample grain size distributions

Site	A	n	m
38N	9.3	2.07	-28.3
33S	5140	2.45	-27.7
54S	88.7	2.75	-40.1
78S	27.8	1.35	-26.0

Table A-2: Site-Specific coefficients and exponents for four cohesive sites

Site	Bedload	Mean Particle Size		Silt Component	
		Trap	Core	Trap	Core
	(%)	(mm)	(mm)	(%)	(%)
38N	70	0.136	0.136	37	40
17S	62	1.226	0.51	3.1	11
33S	65	0.868	0.584	1.8	6
52S	40	0.205	0.144	23	27
62S	20	0.19	0.147	1.8	14
78S	50	0.2	0.112	21	41

Table A-3: Example from one Sedflume erosion test: Percent bedload erosion, mean particle size in core and bedload trap, percent silt in core and bedload trap

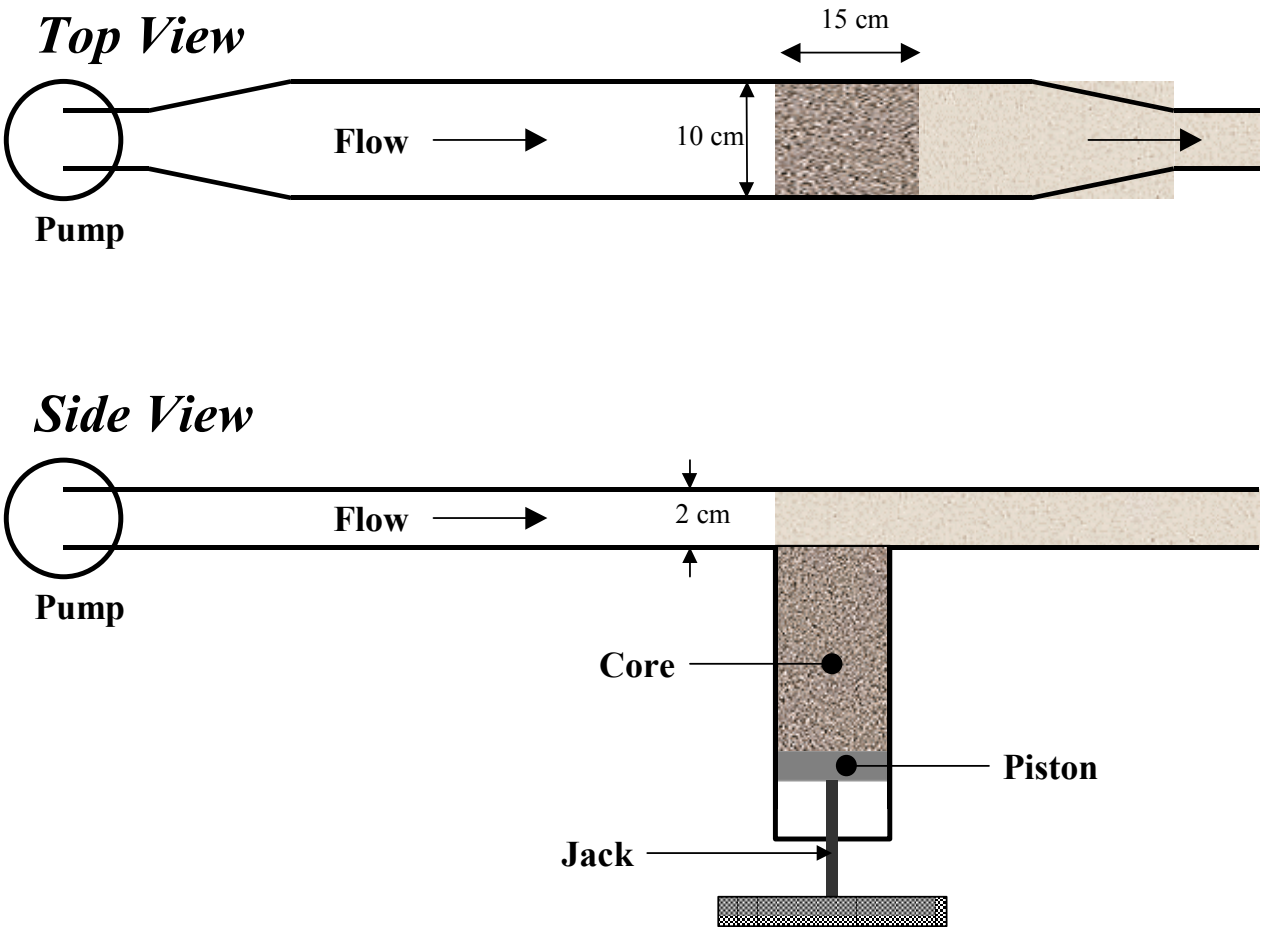

Figure 2.1: Schematic of Sedflume device

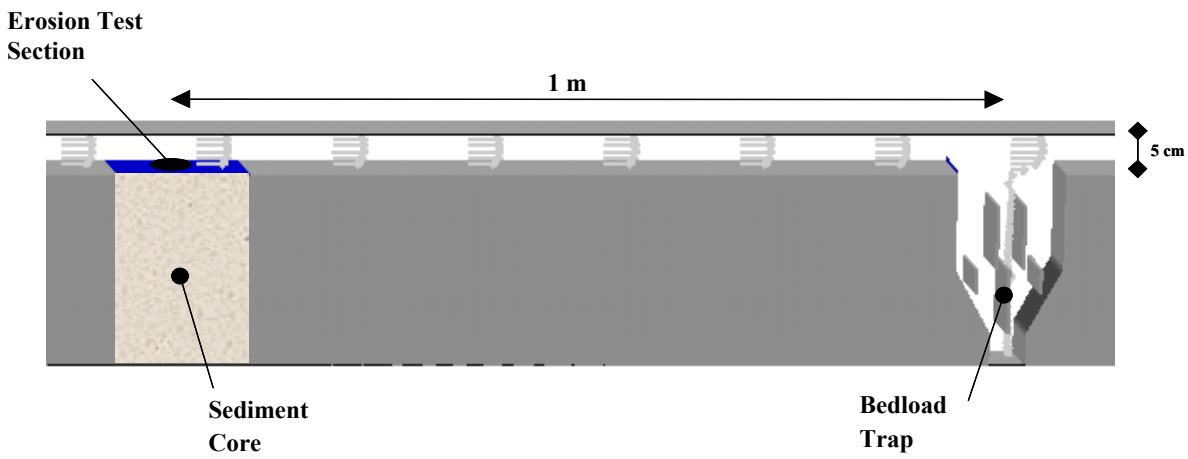

Figure 2.1: Schematic of ASSET flume, modified Sedflume

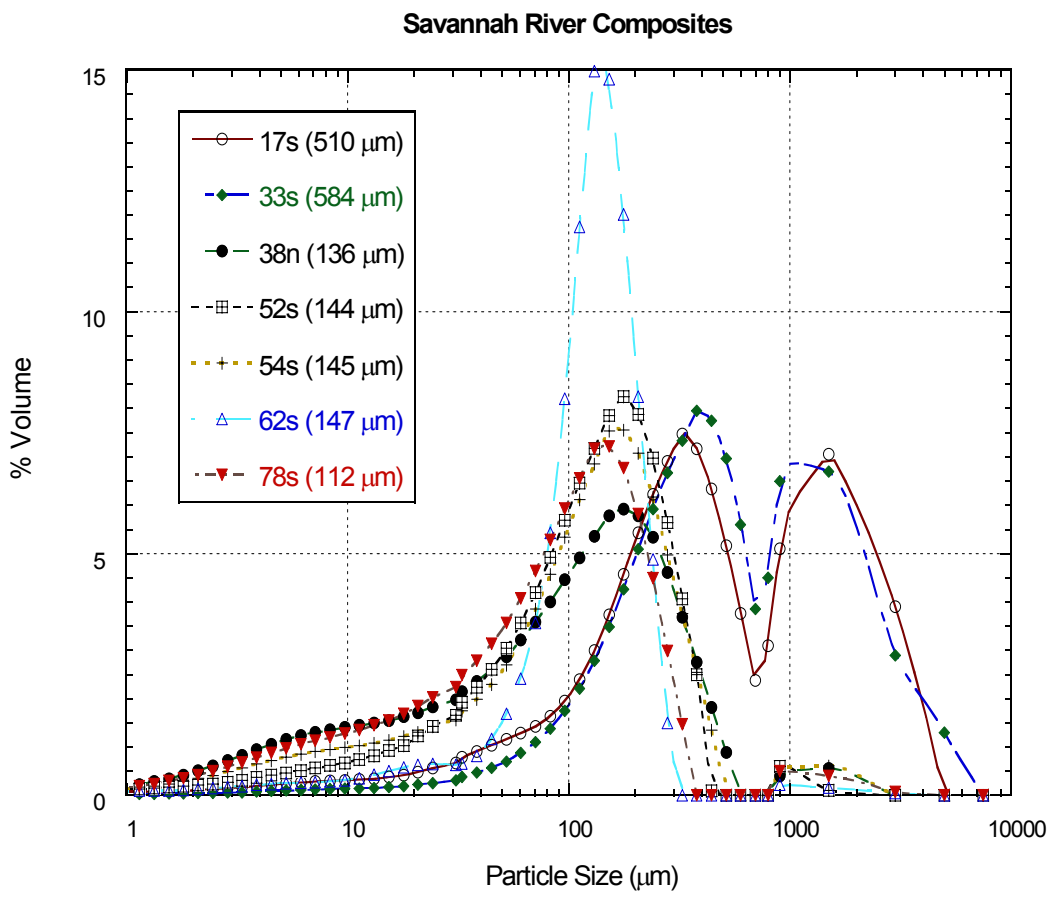

Figure A-4: Grain size distribution at six Sedlume analysis sites

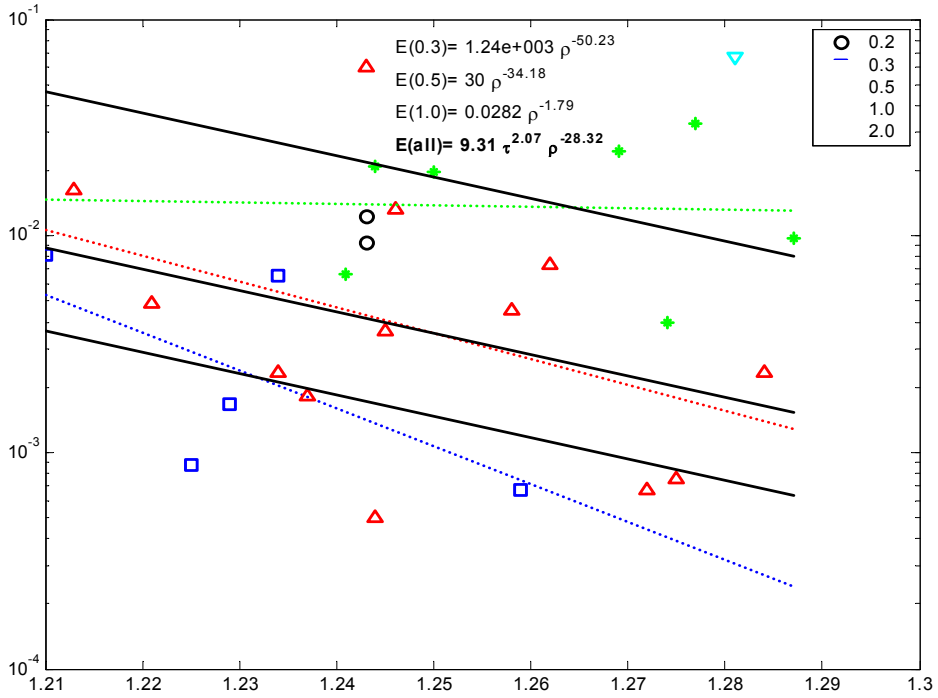

Figure A-5a: Erosion data for Site 38N

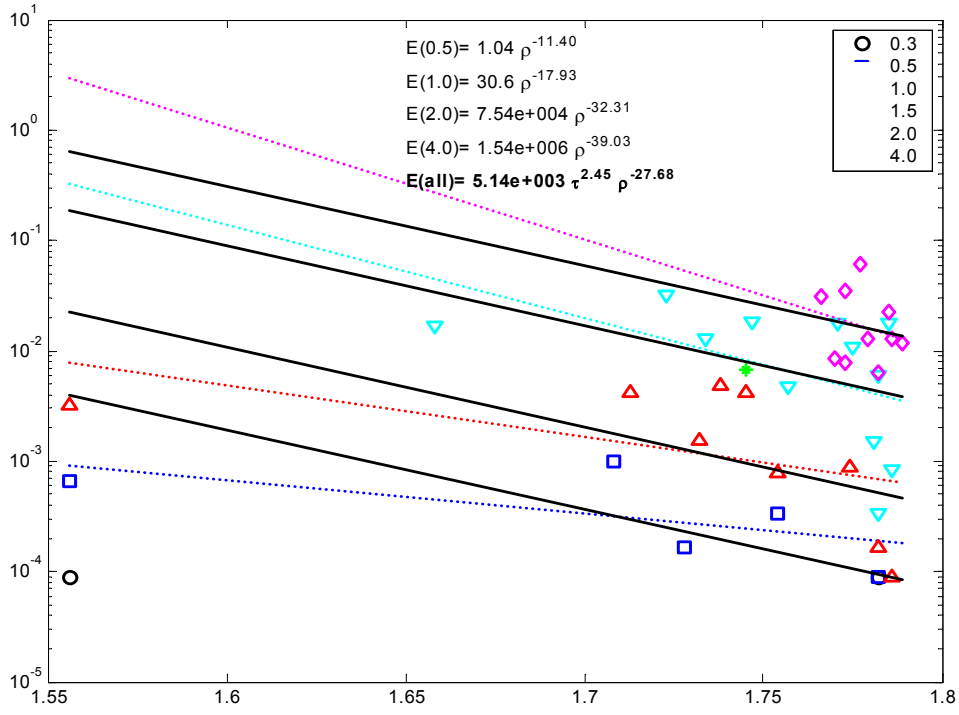

Figure A-5b: Erosion data for Site 33S

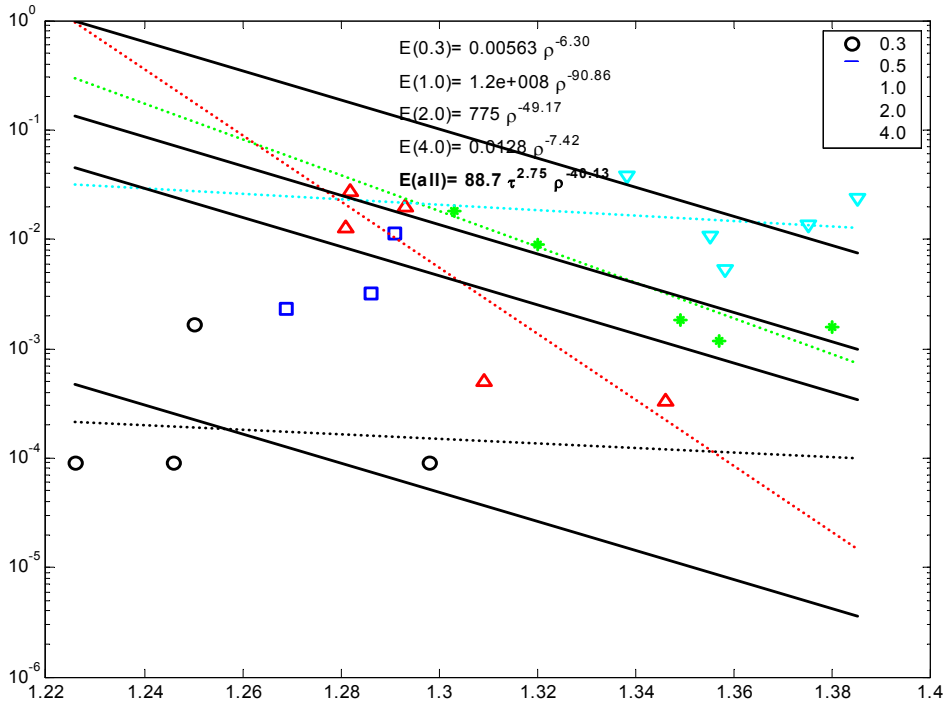

Figure A-5c: Erosion data for Site 52S

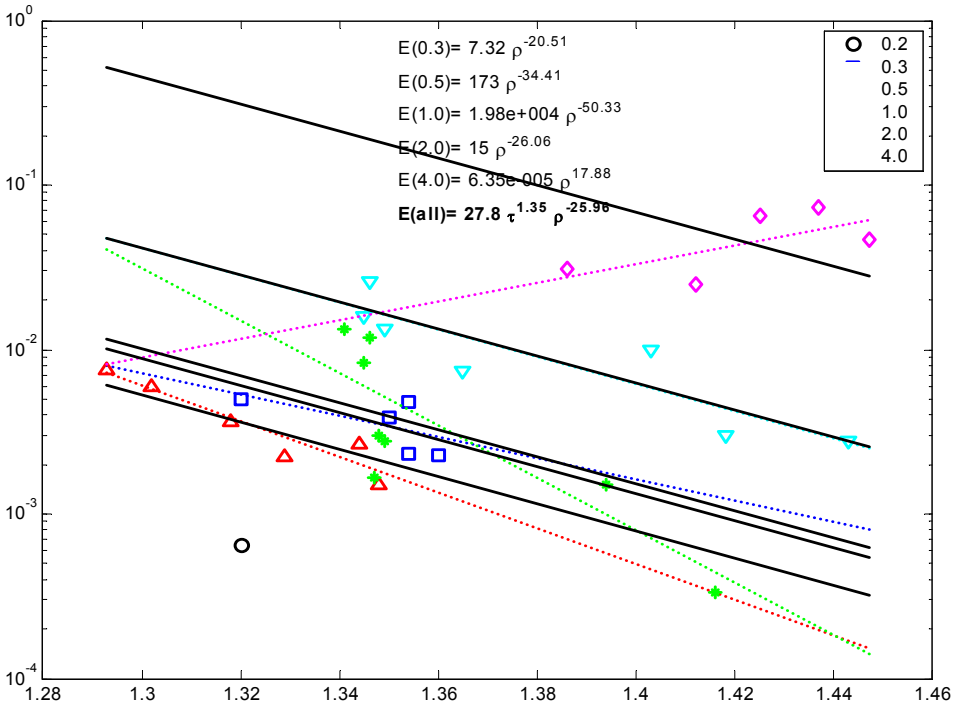

Figure A-5d: Erosion data for Site 78S

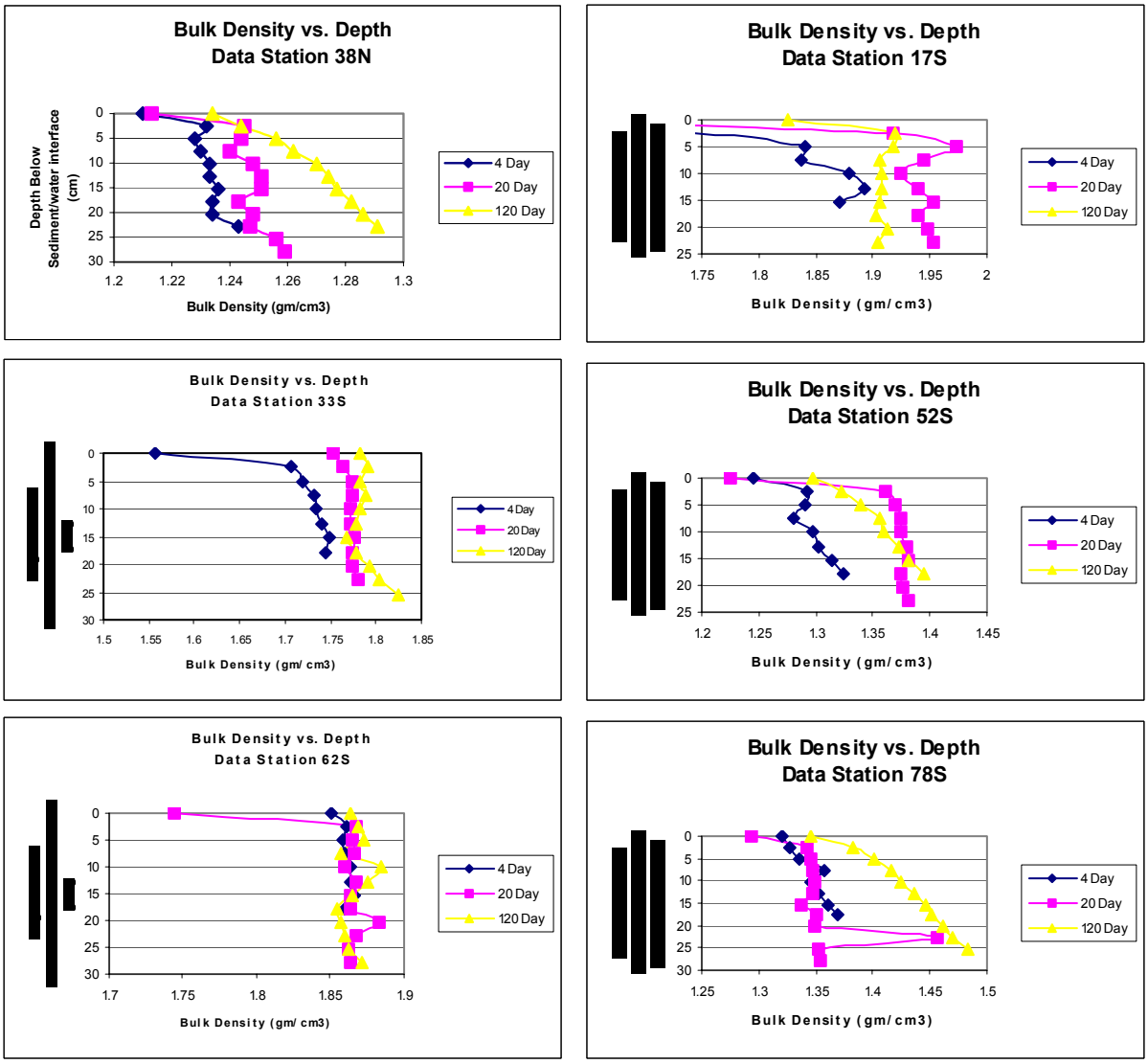

Figure A-6: Bulk density profiles for Sedflume cores consolidated 4, 20, and 120 days